

**Supporting Information
for
Acidic pH Modulated Photoswitching of Sulfur-bridged
Seven-membered Cyclic Azopyridines**

Fengying Lan,^a Cefei Zhang,^a Zhihao Liu,^a Sitong Li,^a Jinmeng Yan,^a Xiaohu Zhao*,^a Changwei Hu,^a Zhishan Su*,^a Pengchi Deng,^b and Zhipeng Yu*^a

^aKey Laboratory of Green Chemistry and Technology of Ministry of Education,
College of Chemistry, Sichuan University, 29 Wangjiang Road,
Chengdu 610064, P. R. China
E-mail: xhzhao@scu.edu.cn; suzhishan@scu.edu.cn; zhipeng@scu.edu.cn

^bAnalytical & Testing Center
Sichuan University, 29 Wangjiang Road, Chengdu 610064, P. R. China

Table of Contents

1. General methods	4
2. Synthesis	5
2.1 Synthesis procedures	5
2.2 NMR spectra	14
3. Analysis for the photophysical properties	26
3.1 UV-Vis absorbance spectra of DBTD and 1a-4a in pH gradients.....	26
3.2 UV-Vis absorbance spectra of DBTD and 1a-4a at different pH before irradiation or at the PSS under the continuous 445 nm laser stimulation.....	36
3.3 Determination of the pK_a values for cycloazopyridines, 2a and 4a.....	46
3.4 The PSD_E quantification by the <i>in-situ</i> photo-stationary ¹H NMR analysis	48
3.5 Theoretical calculations after the second protonation of DBTD and 1a-4a, the corresponding theoretical absorbance spectra	50
3.5.1 Theoretical calculations for after the second protonation of Z-DBTD-H⁺ and Z-1a-H⁺ to Z-4a-H⁺.....	50
3.5.2 Thermal free energy barriers for the transition state from the E-isomer to the Z-isomer of Z-DBTD, and Z-1a to Z-4a.	50
3.5.3 The possible macrocyclic hydrogen-bonding structures interacting with water molecules for the protonated forms of Z-1a, Z-3a, and Z-4a, versus Z-2a in MeCN:H₂O =1:1 solution in the photoswitching process.....	51
3.5.4 The converged theoretical macrocyclic structures with hydrogen-bonding with two water molecules calculated for both Z- and E- isomer of 1a-H⁺, 3a-H⁺, and 4a-H⁺.....	52
3.5.5 Theoretical predicted absorbance spectra of DBTD (left side), and DBTD-H⁺ (right side, protonation on the azo moiety).	54
3.5.6 Theoretical absorbance spectra of 1a, 1a-H⁺ (protonation on the pyridine moiety) and 1a-H2⁺ (protonation on the azo moiety closer to the pyridine).	54
3.5.7 Theoretical absorbance spectra of 2a, 2a-H⁺ (protonation on the pyridine moiety) and 2a-H2⁺ (protonation on the azo moiety closer to the pyridine).	55
3.5.8 Theoretical absorbance spectra of 3a, 3a-H⁺ (protonation on the pyridine moiety) and 3a-H2⁺ (protonation on the azo moiety closer to the pyridine).	55
3.5.9 Theoretical absorbance spectra of 4a, 4a-H⁺ (protonation on the pyridine moiety) and 4a-H2⁺ (protonation on the azo moiety).	56
3.6 The electronic transition characteristics of Z-1a to Z-4a by DFT calculation	57

3.7 Photo-antifatigue studies for DBTD, 1a, and 3a. And photo-switching kinetic studies for DBTD, and 1a-4a, under intermittent irradiation of 445 nm laser under various pH gradients.....	58
3.7.1 The anti-fatigue tests were conducted during the back-and-forth photo-switching tests at pH values of -0.33 and 7.46.....	59
3.7.2 Photo-switching kinetics studies for DBTD and 1a-4a, under intermittent irradiation of 445 nm laser in various pH environment.....	62
3.8 Temperature-dependent thermodynamic decaying kinetics at different pHs and corresponding Eyring plots for 1a, 3a, and DBTD.....	117
4. HPLC-MS analysis to monitor the stability of DBTD and 1a-4a under neutral and acidic conditions.....	124
5. DFT calculation details.....	128
6. References	145

1. General methods

General Information – Chemical Synthesis

Unless specified otherwise, all solvents and raw materials were acquired from commercial suppliers, including Bide Pharmatech Ltd, Leyan Shanghai, Haoyuan Chemexpress Co. Ltd, Adamas-beta® Shanghai Titan Technology Ltd, Acros Organics, Aldrich Chemical Co., Alfa Aesar, and TCI. The ¹H and ¹³C NMR spectra were recorded on a Brüker Avance 400 or 600 spectrometer (¹H: 400 or 600 MHz, ¹³C: 101 or 150 MHz). The chemical shifts (δ) for both ¹H and ¹³C NMR are reported in ppm, referenced to TMS. The solvent signals present in the spectra served as internal references, and the chemical shifts were adjusted to the TMS scale: CDCl₃ 7.26 ppm for ¹H NMR and 77.16 ppm for ¹³C NMR; CD₃OD 3.31 ppm for ¹H NMR and 49.05 ppm for ¹³C NMR; DMSO-*d*₆, 2.50 ppm for ¹H NMR and 39.5 ppm for ¹³C NMR; CD₃CN-*d*₃, 1.940 ppm for ¹H NMR and 118.260 ppm for ¹³C NMR. Shifts multiplicity was reported as follows: s = singlet, d = doublet, t = triplet, td = doublet triplet, q = quartet, m = multiplet, brs. = broad.

General Information – Spectra Acquisition

UV-Vis absorption spectra were measured using 1.0 cm × 1.0 cm quartz cuvettes on a Thermo NANODROP 2000C Spectrophotometer. Exact ESI mass spectra were recorded on a SHIMADZU LCMS-IT-TOF. LC-ESI-MS were obtained on a Thermo LTQ-XL mass spectrometer.

The kinetics of isomerization were studied using a Sarspec STD UV-Vis spectrophotometer, which was linked to a cuvette holder equipped with a programmable thermostatic controller (Qpod 2eTM, American Quantum Northwest Ltd).

General Information – Light Sources

The photo-irradiation power density of light sources in photo-chemical transformation experiments were measured by an optical power meter produced by Thorlabs. An adjustable optical-fiber solid-state 445 nm laser was used for *in-situ* in cuvette stimulation (P_{max} = 1000 mW) and an optical fiber (1.0 mm diameter, quartz) guided 445 nm laser source for *in-situ* photo-stationary state NMR study at the PSS (P_{max} = 1000 mW at the fiber output port).

General Information – Preparation of the buffer solutions with designated pH value

A diluted sulfuric acid water solution (H₂SO₄/H₂O, v/v = 1/1) was added dropwise using a syringe to a phosphate-buffered saline (PBS) solution with an initial pH of 7.46. The pH of the resulting mixture was adjusted to a desired level within the specified range of -0.33 to 7.46, with the titration process being monitored using a pH meter. Subsequently, a stock solution of DBTD and **1a-4a** (1.0

mM in MeCN) was added to a solvent mixture of the pH-adjusted PBS and MeCN (v/v = 2/1), yielding a final concentration of 50 micromolar (μ M) for the solution with designated pH value.

2. Synthesis

2.1 Synthesis procedures

In the early stages of synthesizing the sulfur-bridged seven-member cyclic azopyridines, we attempted classical methods that had previously been successful in our research group for synthesizing cyclic azobenzenes, including the zinc(0)-barium(II) reductive cyclization approach and the Smiles rearrangement ring-closure method. However, both attempts were unsuccessful. The specific rationales for these failures are analysed as follows:

i) The zinc(0)-barium(II) method:

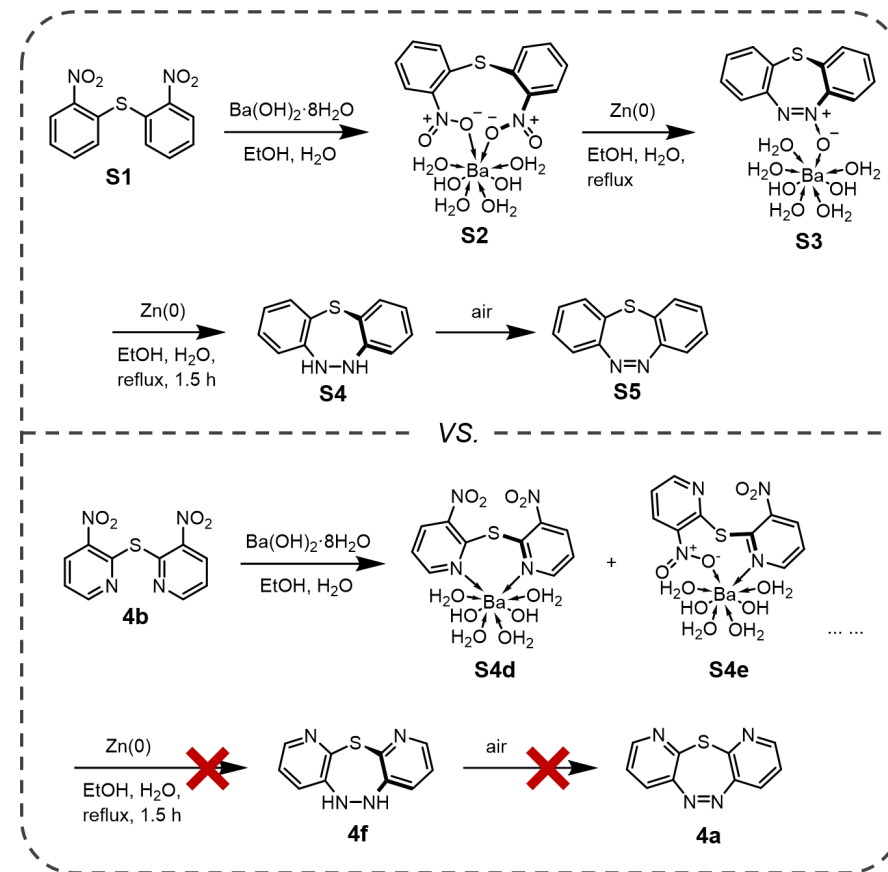


Figure S1. A plausible mechanism for the reductive cyclization of bis(2-nitrophenyl) sulfide to form a seven-membered cyclic azobenzene, and a possible reaction scheme for rationalize of the unsuccessful reductive cyclization of bis(3-nitropyridin-2-yl) sulfide to form a seven-membered cyclic azopyridine **4a**.

As shown in Figure S1, the bis(2-nitrophenyl) sulfide (**S1**) undergoes Zn(0)-mediated reductive

cyclization under the assistance of coordination with $\text{Ba(OH)}_2 \cdot 8\text{H}_2\text{O}$ to form a cyclic azo-*N*-oxide intermediate and over reduced to a dihydribenzothiazepine intermediate (**S4**),^[1-3] which subsequently oxidize in air in the presence of base to yield the seven-membered cyclic azobenzene (DBTD). In this mechanism, barium(II) ions function to spatially preorganize the two nitro groups into a proximal geometry favourable for intramolecular reductive cyclization (forming potential complexes, **S2** and **S3**, upper panel in Figure S1). Although we have attempted to synthesize cyclic azodipyridine (**4a**) using this method. Unfortunately, we did not detect any desired product in the resulting reaction mixture by TLC, HPLC-MS and NMR spectra analysis. We, therefore, speculate that the nitrogen atoms on the pyridine rings might prefer to coordinate with barium(II) ions (please see the molecular complexes, **S4d** and **S4e**, lower panel in Figure S1), which would alter the spatial distance of the two nitro groups within the molecular complex and can be detrimental to the coordinative arrangement where the nitro groups face to the same side. Consequently, it is failure to proceed the desired intramolecular reduction and ring-closure process.

ii) The Smiles rearrangement route:

The Smiles rearrangement is a crucial swapping cyclization step employed in another multi-step synthesis of the seven-membered cyclic azobenzenes from commercially available reagents. The complete synthesis of the seven-membered cyclic azobenzenes with various substituents requires the following five steps showing below (Figure 2):

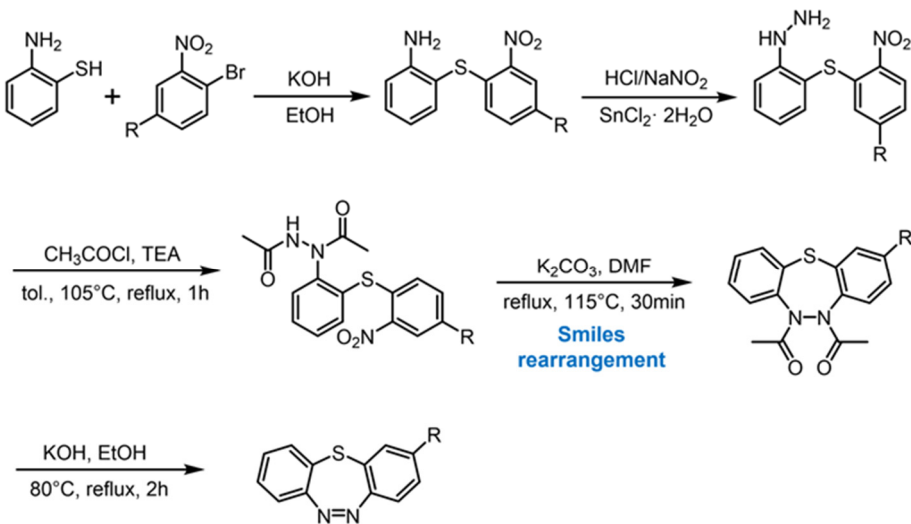


Figure S2. The multi-step synthetic route via the Smiles rearrangement reaction to establish the seven-membered azobenzenes.

However, during our attempts to synthesize unilateral pyridyl azobenzene (**2a**) via the Smiles synthetic route, we faced challenges in the second transformation step. This step entailed

diazotization and reduction of aminopyridine to form the pyridinyl hydrazine substructure. These difficulties hindered our ability to obtain the target hydrazinyl-pyridinyl phenyl sulfide. Despite proceeding to the subsequent acylation step in an effort to possibly isolate a more stable acetylated hydrazine intermediate, our attempts were also unsuccessful.

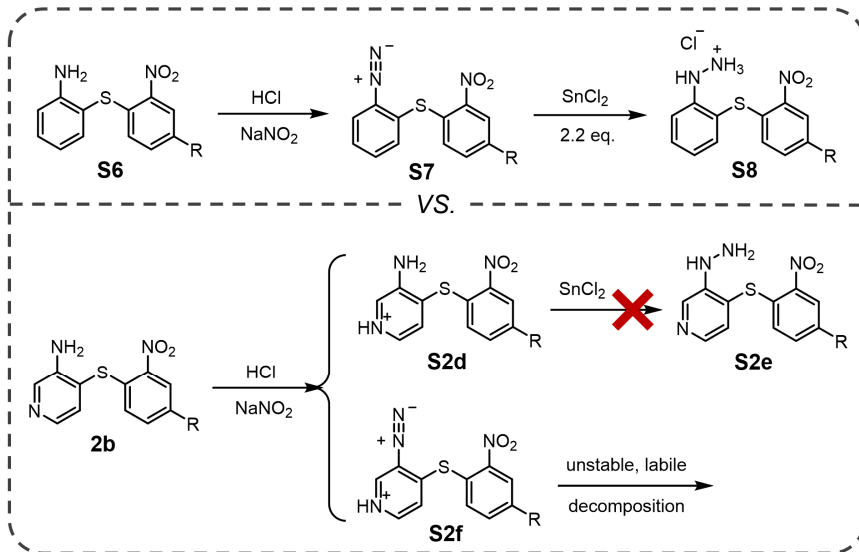


Figure S3. The process of generating a diazonium salt and a study on the mechanism of a possible unreactive reaction.

As shown in Figure S3, during the step for generating the hydrazine, we first added concentrated hydrochloric acid to acidify diphenyl sulfide amine (**S6**) at low temperature (0–5°C). Subsequently, sodium nitrite was added to convert aniline into a diazonium salt structure (**S7**) for 2 hours, followed by the addition of stannous(II) chloride (2.2 eq.) hydrochloric acid solution to in-situ reduce the intermediate, diazobenzene salt, and form diphenyl sulfide hydrazine salt (**S8**). The diazonium salt is actually a precipitate formed in the mixture that can be further dissolved by reduction with SnCl₂. However, in the case of pyridinylamine sulfide containing a pyridine moiety (**2b**), the addition of hydrochloric acid may preferentially lead to the formation of a pyridinium salt (**S2d**). This might hinder the process of generating the diazonium salt due to the electron deficiency of the pyridinium salt. Even after the subsequent addition of stannous chloride, the reduction reaction does not proceed further.

It is also possible that the electron-withdrawing effect of the pyridinium salt significantly weakens the stability of the corresponding diazonium salt. Even if a diazonium salt on a pyridine structure (**S2f**) is generated in situ, it is more unstable (especially at high temperatures or high acidity) and decomposes into free radicals before proceeding to the next step of in-situ reduction, triggering

polymerization or the formation of by-products, thereby preventing the subsequent reduction to pyridinyl hydrazine.

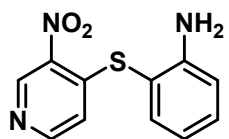
Experimental Procedures:

General procedure 1 (GP1): The selected 2-aminobenzenethiol compound (1.0 equiv.) and potassium carbonate (1.0 equiv.) were added to the solution of selected chloronitropyridine compound (1.0 equiv.) in acetonitrile (25 mL/mmol) while stirring, the mixture was stirred at room temperature for about 24 h. After full consumption of the starting material observed by TLC, the mixture was filtered and the precipitate was collected as desired product. Then, the filtered liquid was purified on silica gel by using a chromatography column and a mixture of petroleum ether/ethyl acetate (4:1) as eluant to obtain the desired product.

General procedure 2 (GP2): Synthesis of the corresponding amine compounds by reference to the method of reducing nitro group in Min Su Han's group.^[4] To a solution of DMF (5.0 mL) containing B₂(OH)₄ (3.0 equiv.) is added a quantity of 4,4'-bipyridine (0.5 equiv.). When 4,4'-bipyridine was added to the clear tetrahydroxydiboron solution, the solution immediately turned dark purple, at this point, the nitropyridine compound was added, and the reaction was carried out for 5-10 min, with the solution gradually changing from purple to yellow, and the reaction was monitored by TLC. At the end of the reaction, the solution was extracted with ethyl acetate 5 to 10 times and dried with anhydrous sodium sulfate. Then, the extracted liquid was purified on silica gel using a chromatography column and dichloromethane containing 10% methanol as the eluent to obtain the desired product.

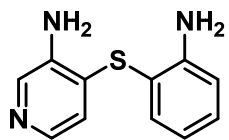
General procedure 3 (GP3): Synthesis of the corresponding seven-membered heterocyclic azobenzene by reference to the intramolecular ring-closing method of Angeles Castro's group.^[5] A mixture of bis(amido)compound (0.09 g) and (diacetoxido)benzene (0.013 g) in dry THF (15 mL) was stirred at 25 °C for 2 days. The solvent was removed under reduced pressure. The product was loaded onto silica gel and then chromatographed with ether/ethyl acetate (2:1) as eluent to obtain the desired product.

2-((3-nitropyridin-4-yl) thio) aniline (2b)



Following the **GP1**, this product was obtained (45%) as a yellow solid. $R_f = 0.3$ (petroleum ether/ethyl acetate = 4:1). ^1H NMR (400 MHz, Methanol- d_4) δ 9.28 (d, $J = 0.5$ Hz, 1H), 8.36 (d, $J = 5.6$ Hz, 1H), 7.38 – 7.30 (m, 2H), 6.91 (ddd, $J = 8.2, 1.3, 0.5$ Hz, 1H), 6.84 (dd, $J = 5.6, 0.5$ Hz, 1H), 6.76 (ddd, $J = 7.7, 7.3, 1.3$ Hz, 1H). ^{13}C NMR (101 MHz, CD₃OD) δ 152.55, 152.16, 150.79, 147.67, 143.38, 138.35, 133.99, 122.52, 119.25, 116.92, 109.94. HRMS (ESI) calcd. For C₁₁H₁₀N₃O₂S⁺ 248.0488 [M+H⁺], found 248.0489.

4-((2-aminophenyl) thio) pyridin-3-amine (2c)



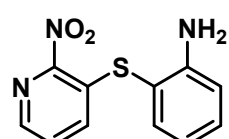
Following the **GP2**, this product was obtained (23%) as a white solid. $R_f = 0.5$ (dichloromethane/methanol = 9:1). ^1H NMR (400 MHz, DMSO- d_6) δ 7.93 (s, 1H), 7.59 (d, $J = 5.1$ Hz, 1H), 7.28 (dd, $J = 7.7, 1.6$ Hz, 1H), 7.18 (ddd, $J = 8.1, 7.2, 1.6$ Hz, 1H), 6.81 (dd, $J = 8.1, 1.3$ Hz, 1H), 6.60 (td, $J = 7.4, 1.4$ Hz, 1H), 6.46 (d, $J = 5.1$ Hz, 1H), 5.41 (s, 2H), 5.28 (s, 2H). ^{13}C NMR (101 MHz, DMSO- d_6) δ 150.35, 142.03, 137.69, 136.80, 136.08, 131.19, 128.22, 120.90, 116.92, 115.03, 109.92. HRMS (ESI) calcd. For C₁₁H₁₂N₃S⁺ 218.0746 [M+H⁺], found 218.0749.

benzo[*b*]pyrido[3,4-*f*] [1,4,5] thiadiazepine (3-BPTD, 2a):



Following the **GP3**, this product was obtained (8%) as a yellow solid. $R_f = 0.3$ (petroleum ether/ethyl acetate = 2:1). ^1H NMR (400 MHz, Chloroform- d) δ 8.85 (s, 1H), 8.47 (d, $J = 5.2$ Hz, 1H), 7.71 – 7.64 (m, 1H), 7.55 – 7.47 (m, 1H), 7.36 – 7.30 (m, 2H), 7.25 (d, $J = 4.4$ Hz, 1H). ^{13}C NMR (101 MHz, CDCl₃) δ 151.86, 150.19, 149.09, 147.22, 141.15, 132.40, 130.60, 130.00, 129.31, 128.55, 125.70. HRMS (ESI) calcd. For C₁₁H₈N₃S⁺ 214.0433 [M+H⁺], found 214.0432.

2-((2-nitropyridin-3-yl) thio) aniline (1b)



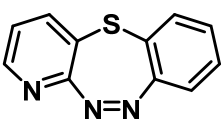
Following the **GP1**, this product was obtained (40%) as a tangerine yellow solid. $R_f = 0.5$ (petroleum ether/ethyl acetate = 4:1). ^1H NMR (400 MHz, Chloroform- d) δ 8.32 (dd, $J = 4.3, 1.6$ Hz, 1H), 7.47 – 7.20 (m, 4H), 6.89 – 6.77 (m, 2H), 4.33 (s, 2H). ^{13}C NMR (101 MHz, CDCl₃) δ 152.74, 149.54, 144.30, 137.85, 137.82, 133.47, 132.94, 128.41, 119.53, 115.90, 110.88. HRMS (ESI) calcd. For C₁₁H₁₀N₃O₂S⁺ 248.0488 [M+H⁺], found 248.0490.

3-((2-aminophenyl) thio) pyridin-2-amine (**1c**)



Following the **GP2**, this product was obtained (25%) as a white solid. $R_f = 0.4$ (dichloromethane/methanol = 9:1). ^1H NMR (400 MHz, Chloroform- d) δ 7.90 (dd, $J = 4.9, 1.7$ Hz, 1H), 7.26 (s, 1H), 7.23 – 7.19 (m, 1H), 7.09 (ddd, $J = 8.0, 7.3, 1.5$ Hz, 1H), 6.70 – 6.63 (m, 2H), 6.52 (dd, $J = 7.6, 4.9$ Hz, 1H), 4.95 (s, 2H), 4.20 (s, 2H). ^{13}C NMR (101 MHz, CDCl_3) δ 157.24, 147.55, 147.13, 139.80, 134.98, 130.40, 119.28, 115.71, 114.87, 113.89. HRMS (ESI) calcd. For $\text{C}_{11}\text{H}_{12}\text{N}_3\text{S}^+$ 218.0746 [M+H $^+$], found 218.0749.

benzo[*b*]pyrido[2,3-*f*] [1,4,5] thiadiazepine (4-BPTD, **1a**)



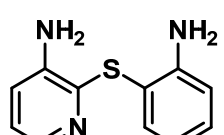
Following the **GP3**, this product was obtained (10%) as a yellow solid. $R_f = 0.3$ (petroleum ether/ethyl acetate = 2:1). ^1H NMR (400 MHz, Chloroform- d) δ 8.58 (dd, $J = 4.7, 1.6$ Hz, 1H), 7.71 (dd, $J = 7.8, 1.6$ Hz, 1H), 7.65 (ddd, $J = 7.9, 1.4, 0.4$ Hz, 1H), 7.47 (ddd, $J = 7.9, 7.3, 1.4$ Hz, 1H), 7.36 (ddd, $J = 7.8, 1.5, 0.4$ Hz, 1H), 7.30 – 7.27 (m, 1H), 7.22 (dd, $J = 7.8, 4.7$ Hz, 1H). ^{13}C NMR (101 MHz, CDCl_3) δ 160.05, 152.24, 149.61, 140.72, 131.90, 130.40, 129.93, 129.90, 128.68, 127.59, 124.31. HRMS (ESI) calcd. For $\text{C}_{11}\text{H}_8\text{N}_3\text{S}^+$ 214.0433 [M+H $^+$], found 214.0432.

2-((3-nitropyridin-4-yl) thio)aniline (3b)



Following the **GP1**, this product was obtained (50%) as a yellow solid. $R_f = 0.5$ (petroleum ether/ethyl acetate = 4:1). ^1H NMR (400 MHz, Methanol- d_4) δ 8.55 (dd, $J = 8.2, 1.6$ Hz, 1H), 8.48 (dd, $J = 4.6, 1.6$ Hz, 1H), 7.30 (ddd, $J = 8.4, 5.3, 3.1$ Hz, 2H), 7.23 (ddd, $J = 8.1, 7.2, 1.6$ Hz, 1H), 6.85 (dd, $J = 8.1, 1.2$ Hz, 1H), 6.70 (td, $J = 7.5, 1.3$ Hz, 1H). ^{13}C NMR (101 MHz, CD_3OD) δ 157.98, 154.59, 152.12, 143.83, 138.58, 134.94, 132.61, 120.99, 119.02, 116.80, 113.42. HRMS (ESI) calcd. For $\text{C}_{11}\text{H}_{10}\text{N}_3\text{O}_2\text{S}^+$ 248.0488 [M+H $^+$], found 248.0487.

2-((2-aminophenyl) thio) pyridin-3-amine (3c)



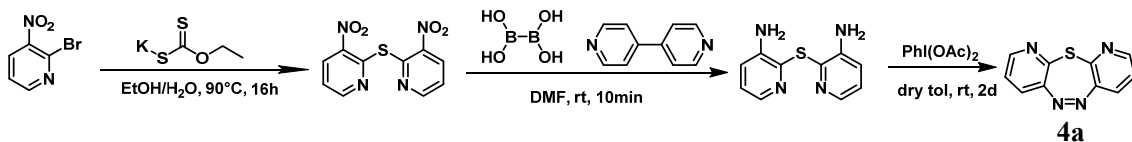
Following the **GP2**, this product was obtained (30%) as a white solid. $R_f = 0.3$ (dichloromethane/methanol = 9:1). ^1H NMR (400 MHz, Chloroform- d) δ 7.91 (dd, $J = 4.5, 1.7$ Hz, 1H), 7.42 (dd, $J = 7.7, 1.6$ Hz, 1H), 7.15 (ddd, $J = 8.0, 7.3, 1.6$ Hz, 1H), 6.94 (dtd, $J = 16.6, 10.3, 9.1, 6.5$ Hz, 2H), 6.77 – 6.67 (m, 2H), 4.46 – 3.85 (m, 4H). ^{13}C NMR (101 MHz, CDCl_3) δ 149.01, 143.06, 140.69, 140.00,

135.97, 130.55, 123.33, 122.01, 118.76, 115.91, 114.61. HRMS (ESI) calcd. For $C_{11}H_{12}N_3S^+$ 218.0746 [M+H $^+$], found 218.0747.

benzo[*b*]pyrido[3,2-*f*] [1,4,5] thiadiazepine (1-BPTD, 3a)

Following the **GP3**, this product was obtained (15%) as a yellow solid. $R_f = 0.3$ (petroleum ether/ethyl acetate = 2:1). 1H NMR (400 MHz, Chloroform- d) δ 8.43 (dd, $J = 4.8, 1.7$ Hz, 1H), 7.96 (dd, $J = 7.9, 1.7$ Hz, 1H), 7.66 (dd, $J = 7.8, 1.5$ Hz, 1H), 7.51 – 7.40 (m, 2H), 7.39 – 7.32 (m, 2H). ^{13}C NMR (101 MHz, CDCl $_3$) δ 151.63, 150.33, 148.78, 147.66, 135.67, 133.07, 130.58, 129.50, 128.70, 127.73, 124.27. HRMS (ESI) calcd. For $C_{11}H_8N_3S^+$ 214.0433 [M+H $^+$], found 214.0435.

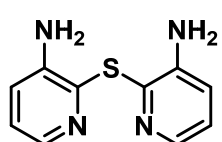
The synthesis of 1,10-DPTD (4a)



bis(3-nitropyridin-2-yl) sulfane (4b)^[6]

2-bromo-3-nitropyridine (2.03 g, 10 mmol), potassium ethylxanthate (1.6 g, 10 mmol) were charged in a 150 mL pressure-resistant tube, 95% ethanol (50 mL) was added to the mixture at room temperature, and the reaction mixture was heated at 90 °C for 24 h. After full consumption of the starting material observed by TLC, the mixture was dried directly by spinning under reduced pressure and was purified on silica gel by using a chromatography column and a mixture of petroleum ether/ethyl acetate (4:1) as eluent to obtain more desired product. This product was obtained (43%) as a tangerine yellow solid. $R_f = 0.4$ (petroleum ether/ethyl acetate = 4:1). 1H NMR (400 MHz, DMSO- d_6) δ 8.73 (dh, $J = 4.7, 1.5$ Hz, 2H), 8.63 (dh, $J = 6.4, 1.6$ Hz, 2H), 7.69 – 7.63 (m, 2H). ^{13}C NMR (101 MHz, DMSO- d_6) δ 153.63, 149.90, 145.63, 134.22, 123.71. HRMS (ESI) calcd. For $C_{10}H_7N_4O_4S^+$ 279.0183 [M+H $^+$], found 279.0187.

2,2'-thiobis(pyridin-3-amine) (4c)



Following the **GP2**, this product was obtained (30%) as a red liquid. $R_f = 0.4$ (dichloromethane/methanol = 9:1). 1H NMR (400 MHz, DMSO- d_6) δ 7.70 (dd, $J = 3.7, 2.4$ Hz, 2H), 7.05 – 6.99 (m, 4H), 5.39 (s, 4H). ^{13}C NMR

(101 MHz, DMSO-*d*₆) δ 145.62, 137.59, 137.07, 123.80, 121.09. HRMS (ESI) calcd. For C₁₀H₁₁N₄S⁺ 219.0699 [M+H⁺], found 279.0701.

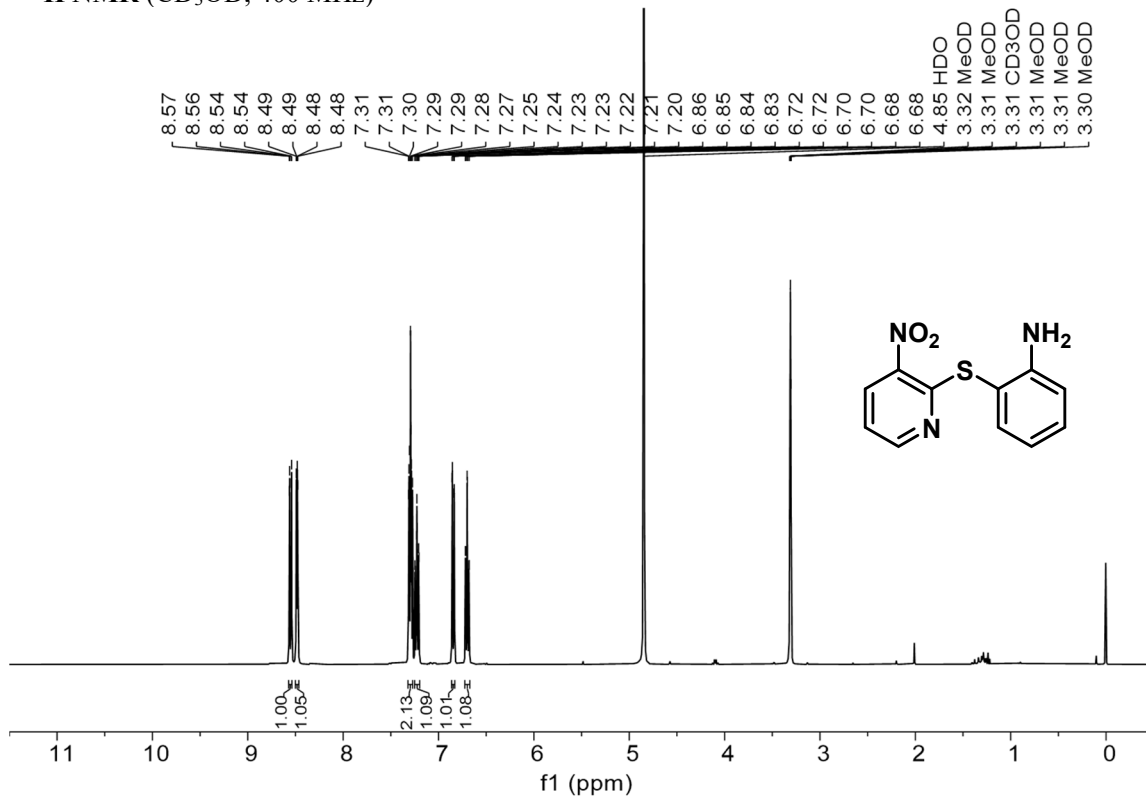
dipyrido[2,3-*b*:3',2'-*f*] [1,4,5] thiadiazepine (1,10-DPTD, 4a)

Following the **GP3**, this product was obtained (10%) as a yellow solid. R_f = 0.3 (petroleum ether/ethyl acetate = 1:1). ¹H NMR (400 MHz, Chloroform-*d*) δ 8.53 (dd, *J* = 4.7, 1.7 Hz, 2H), 8.01 (dd, *J* = 7.9, 1.7 Hz, 2H), 7.45 (dd, *J* = 7.9, 4.7 Hz, 2H). ¹³C NMR (101 MHz, CDCl₃) δ 151.31, 147.54, 146.61, 135.82, 124.05. HRMS (ESI) calcd. For C₁₀H₇N₄S⁺ 215.0386 [M+H⁺], found 215.0384.

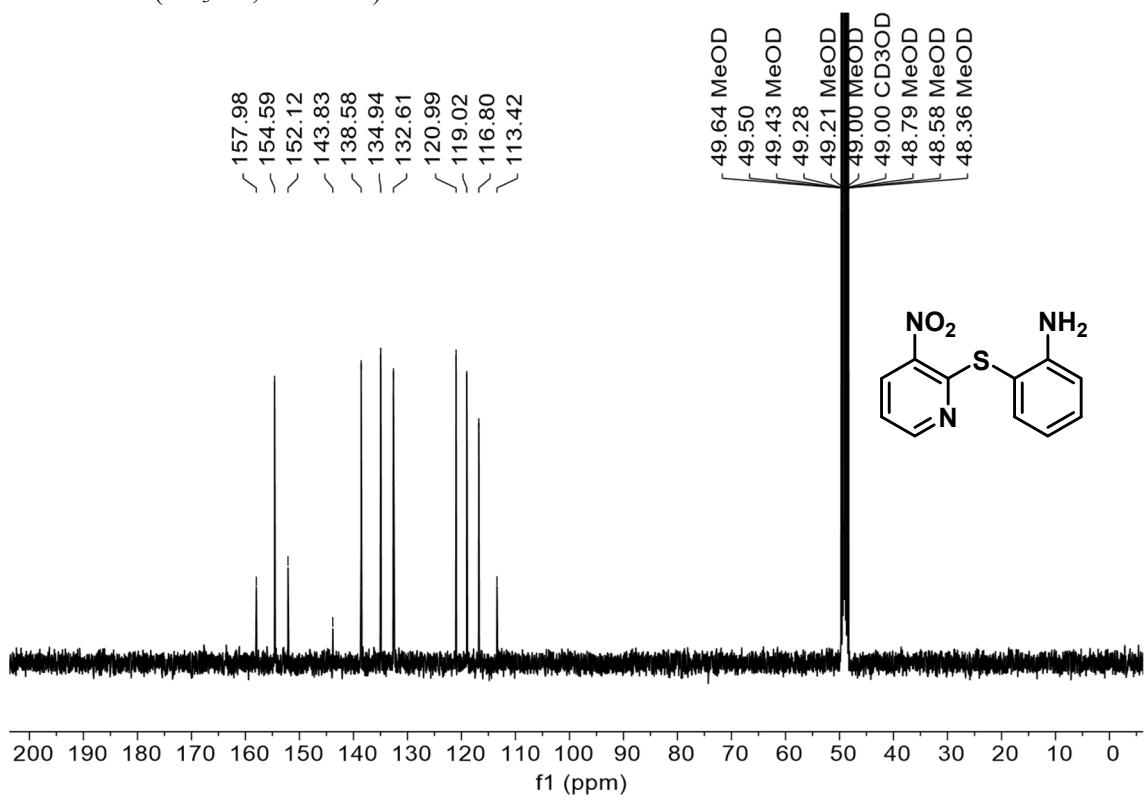
2.2 NMR spectra

2-((3-nitropyridin-2-yl) thio)aniline

¹H NMR (CD₃OD, 400 MHz)

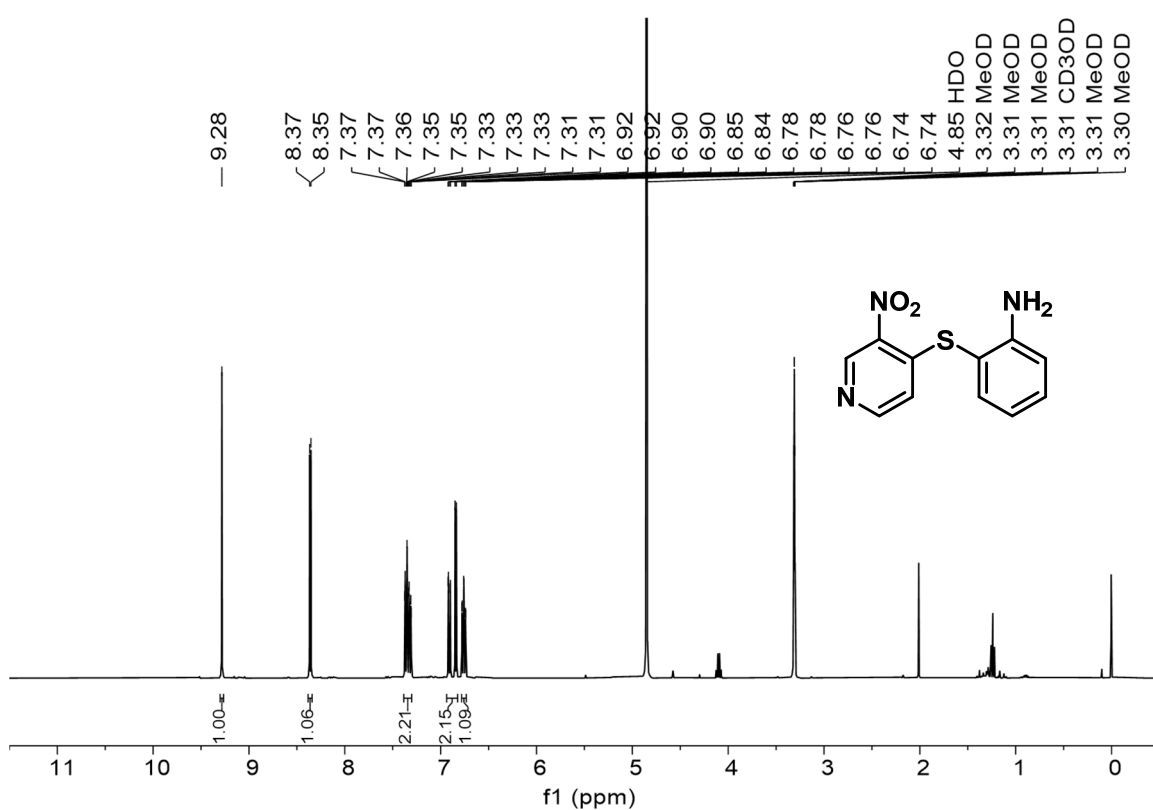


¹³C NMR (CD₃OD, 101 MHz)

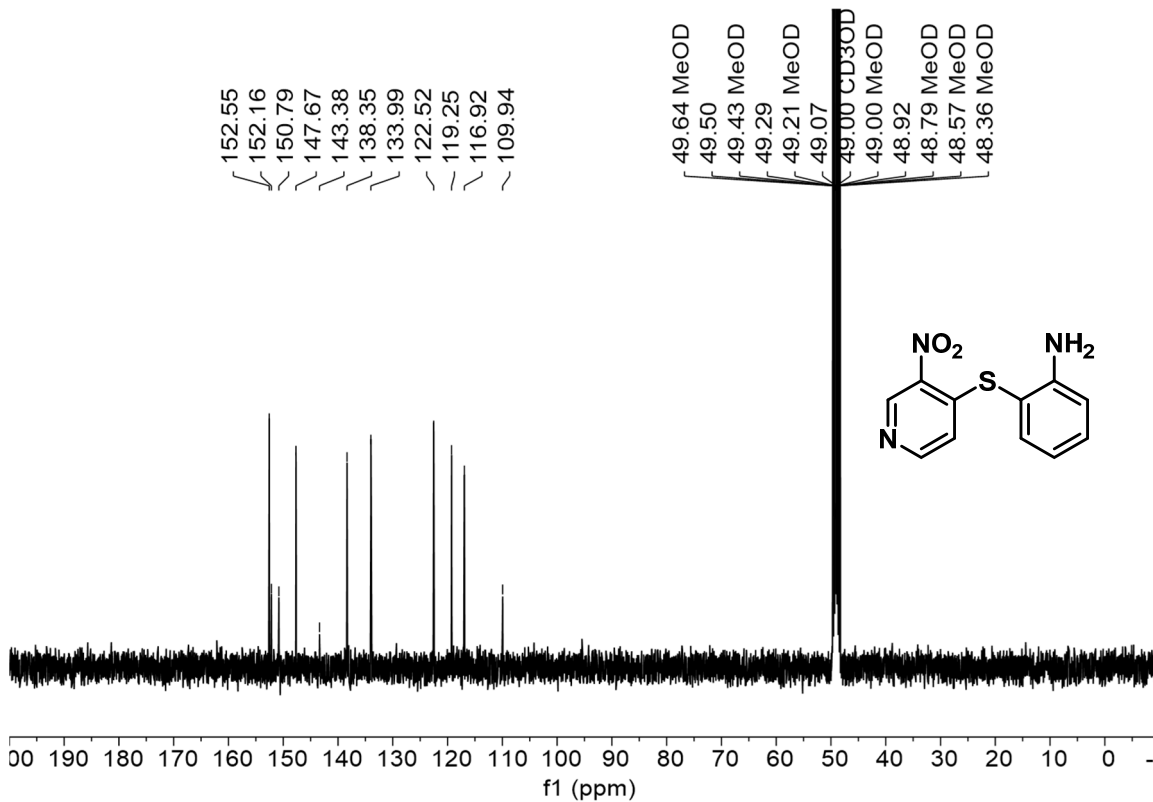


2-((3-nitropyridin-4-yl) thio)aniline

¹H NMR (CD₃OD, 400 MHz)

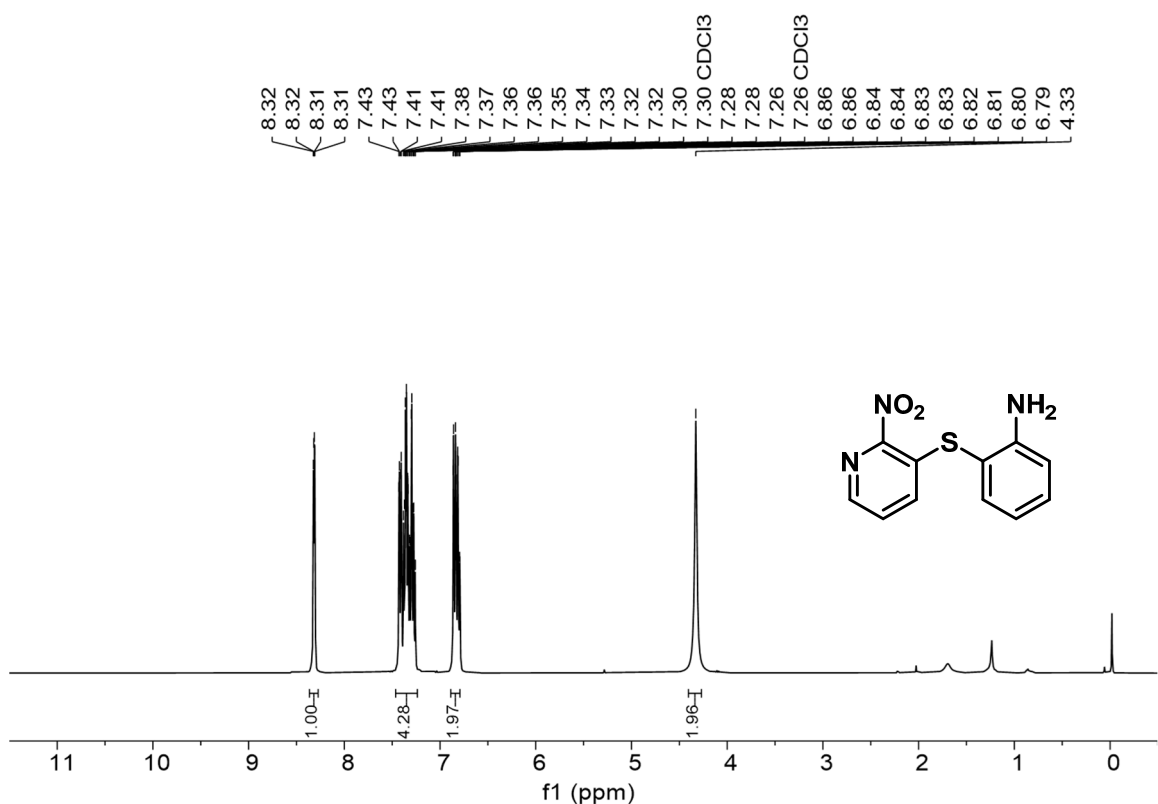


¹³C NMR (CD₃OD, 101 MHz)

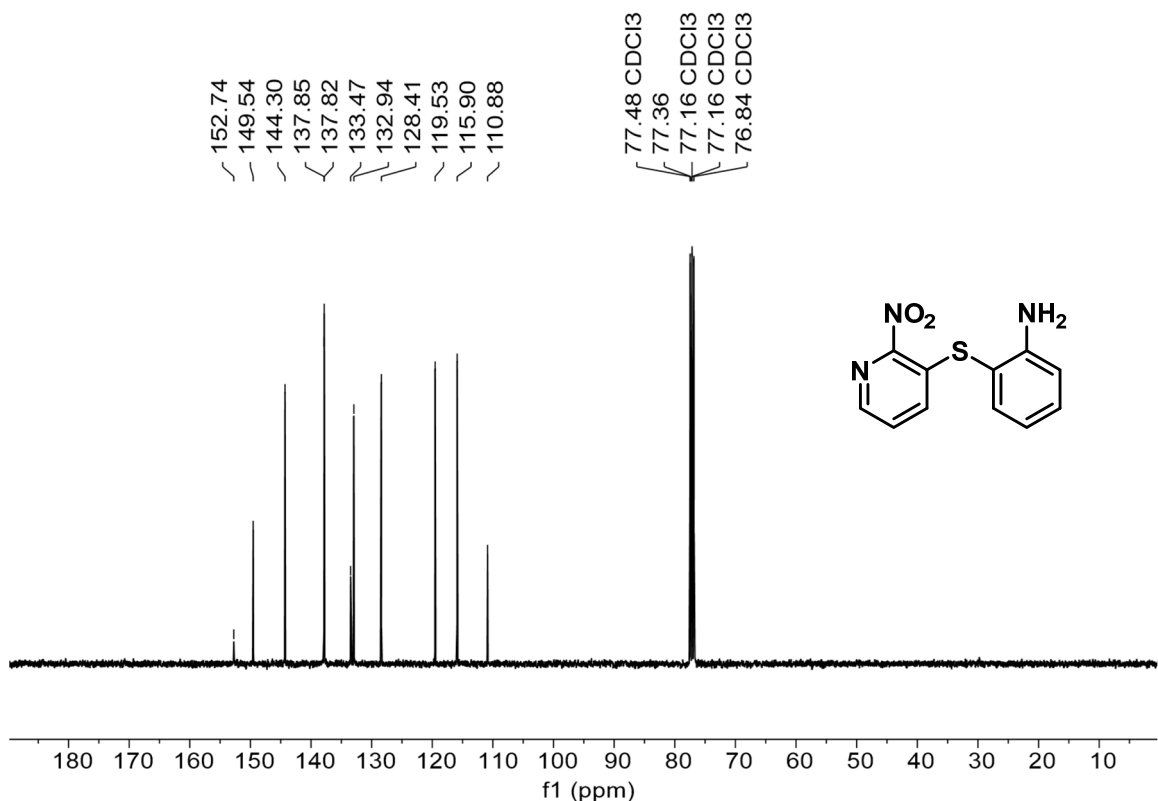


2-((2-nitropyridin-3-yl) thio)aniline

¹H NMR (CDCl₃, 400 MHz)

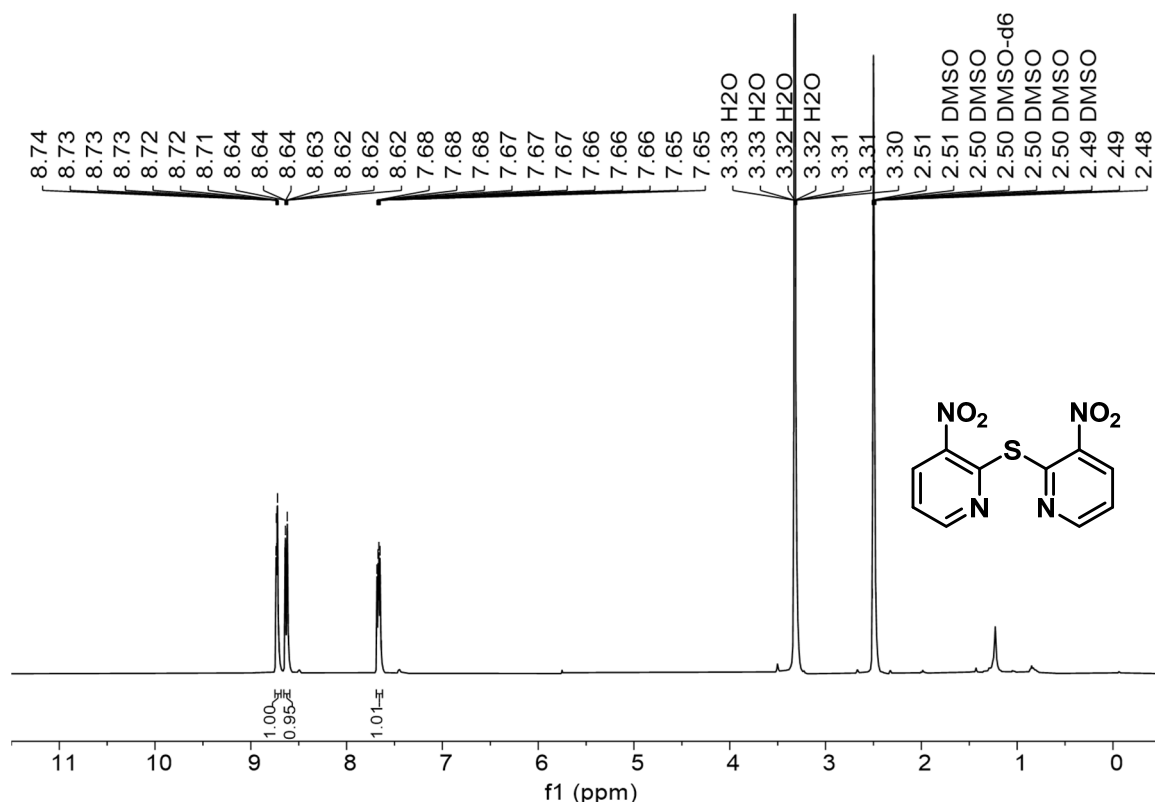


¹³C NMR (CDCl₃, 101 MHz)

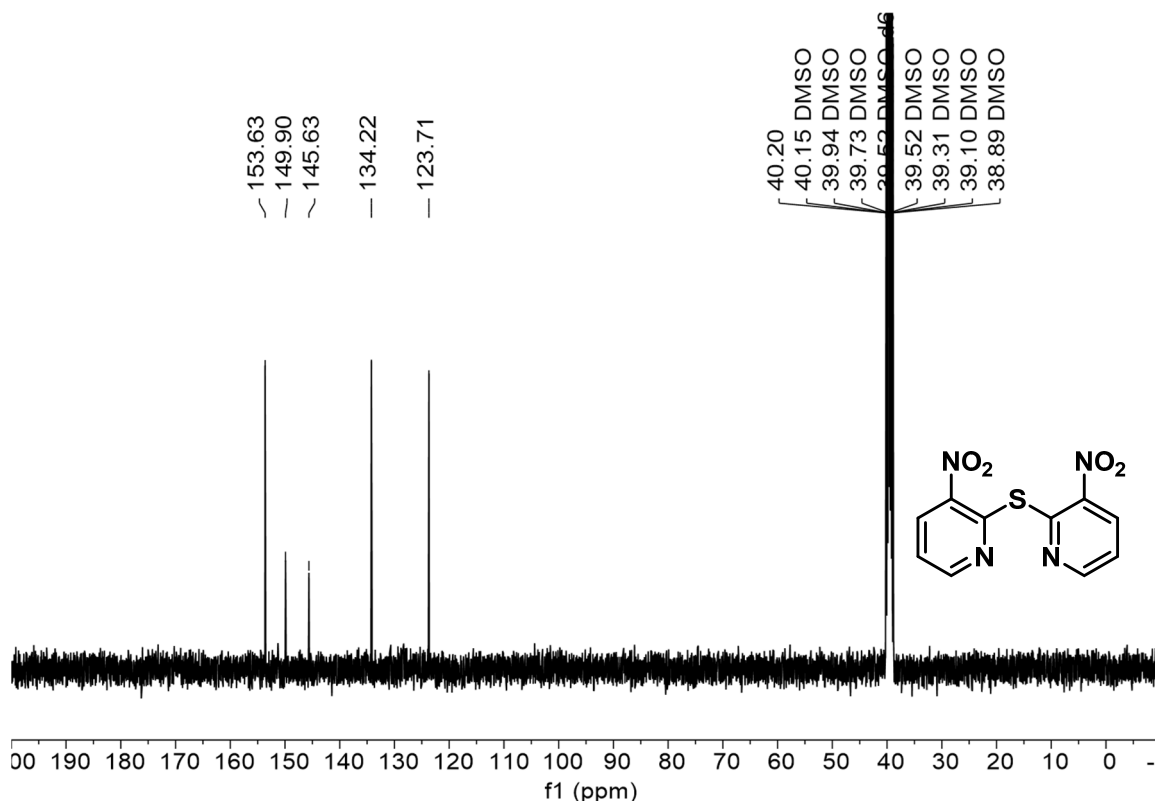


bis(3-nitropyridin-2-yl)sulfane

¹H NMR (DMSO-*d*₆, 400 MHz)

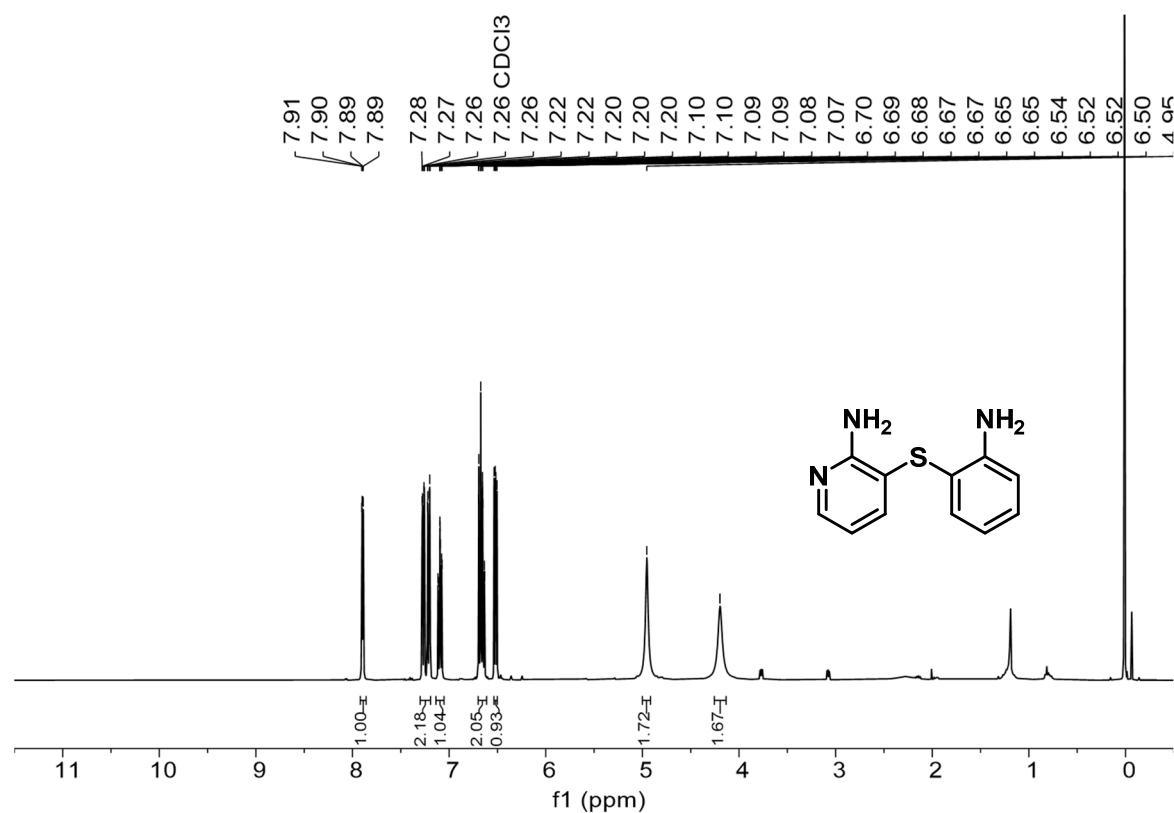


¹³C NMR (DMSO-*d*₆, 101 MHz)

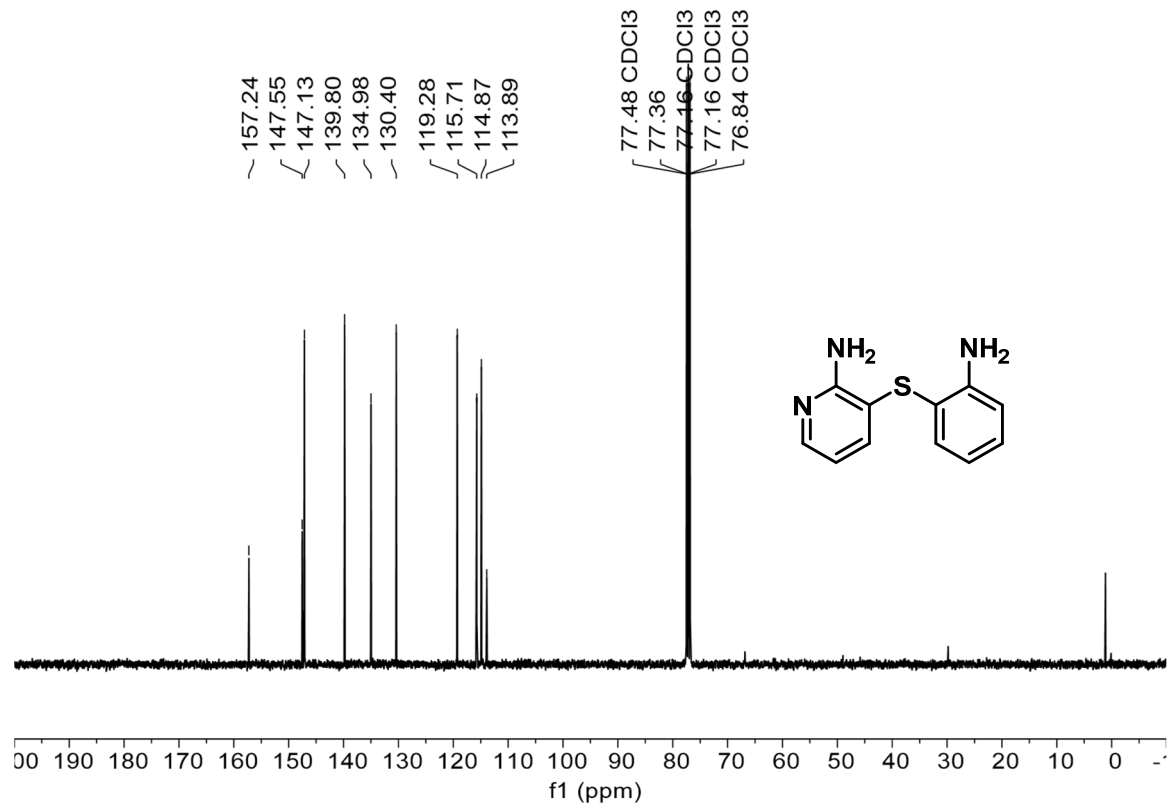


3-((2-aminophenyl)thio)pyridin-2-amine

¹H NMR (CDCl₃, 400 MHz)

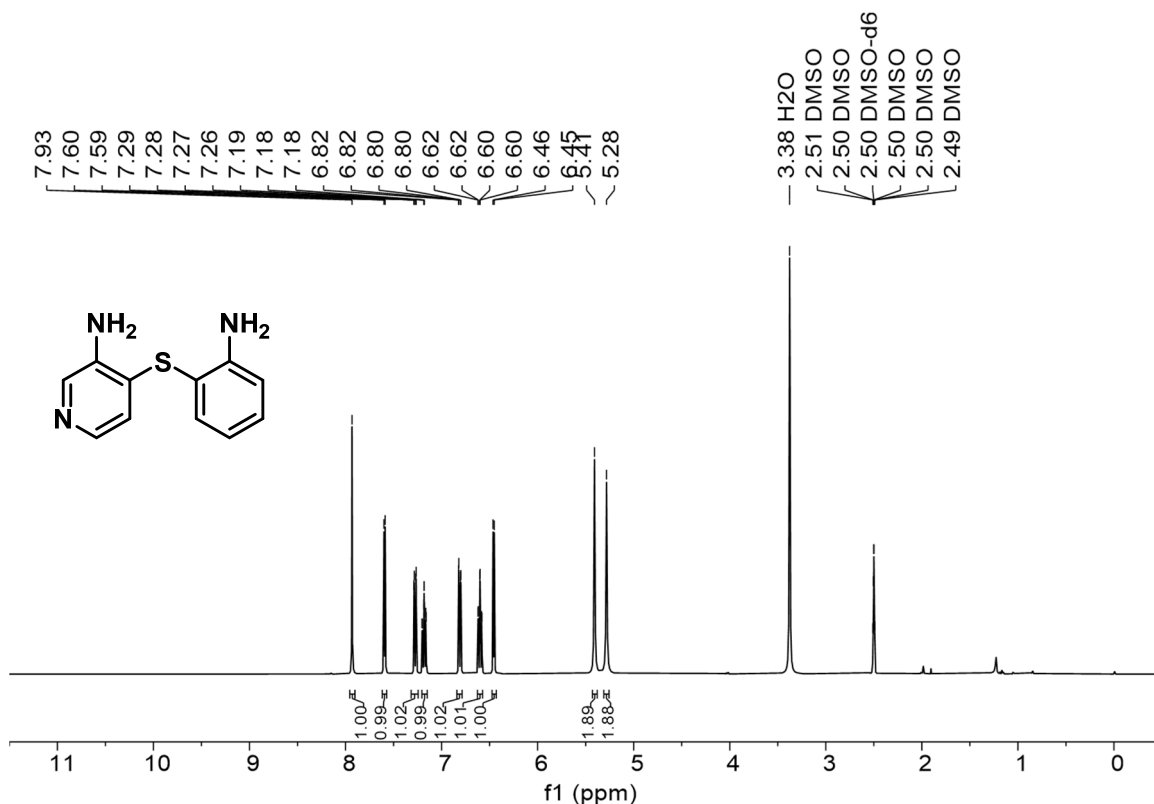


¹³C NMR (CDCl₃, 101 MHz)

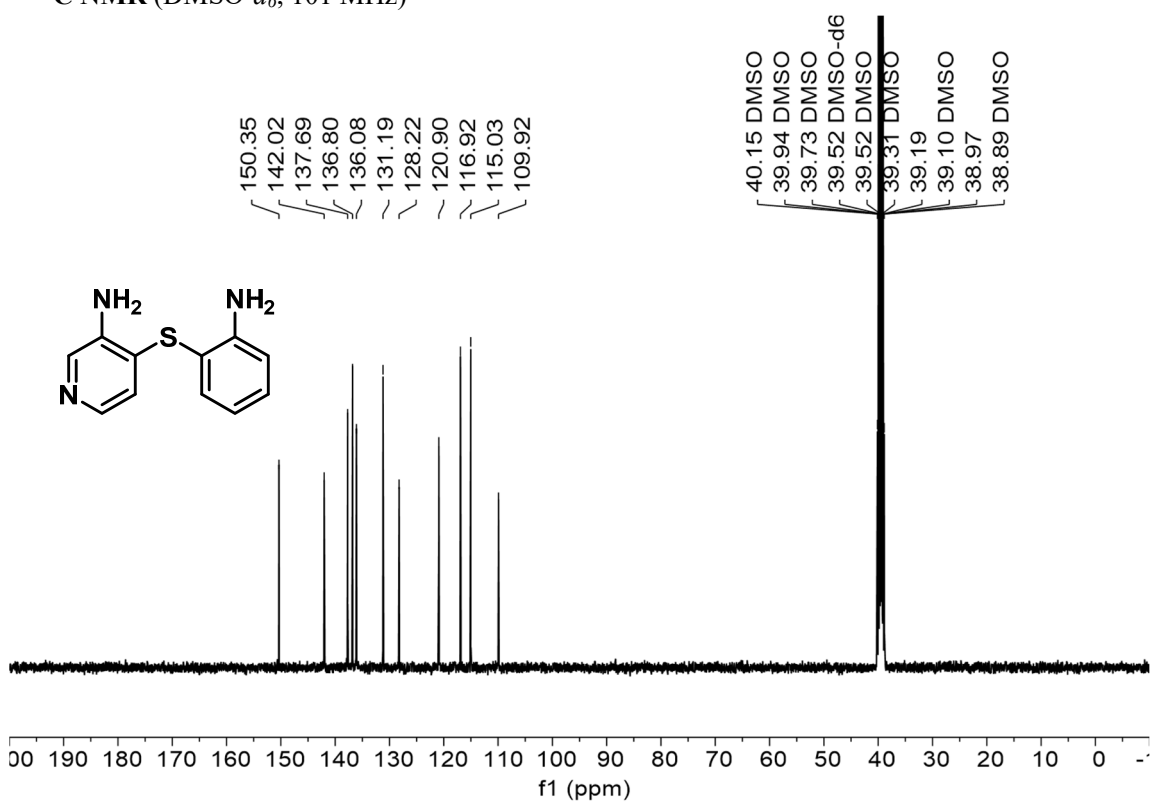


4-((2-aminophenyl) thio)pyridine-3-amine

¹H NMR (DMSO-*d*₆, 400 MHz)

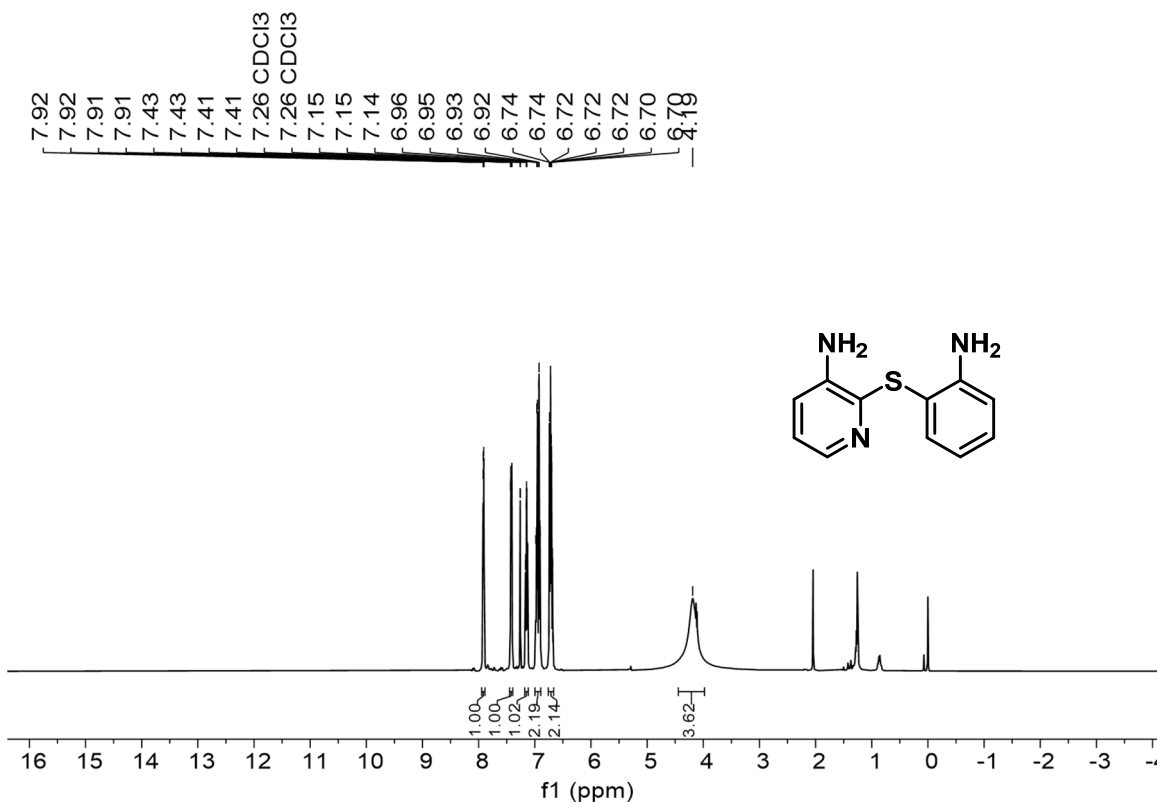


¹³C NMR (DMSO-*d*₆, 101 MHz)

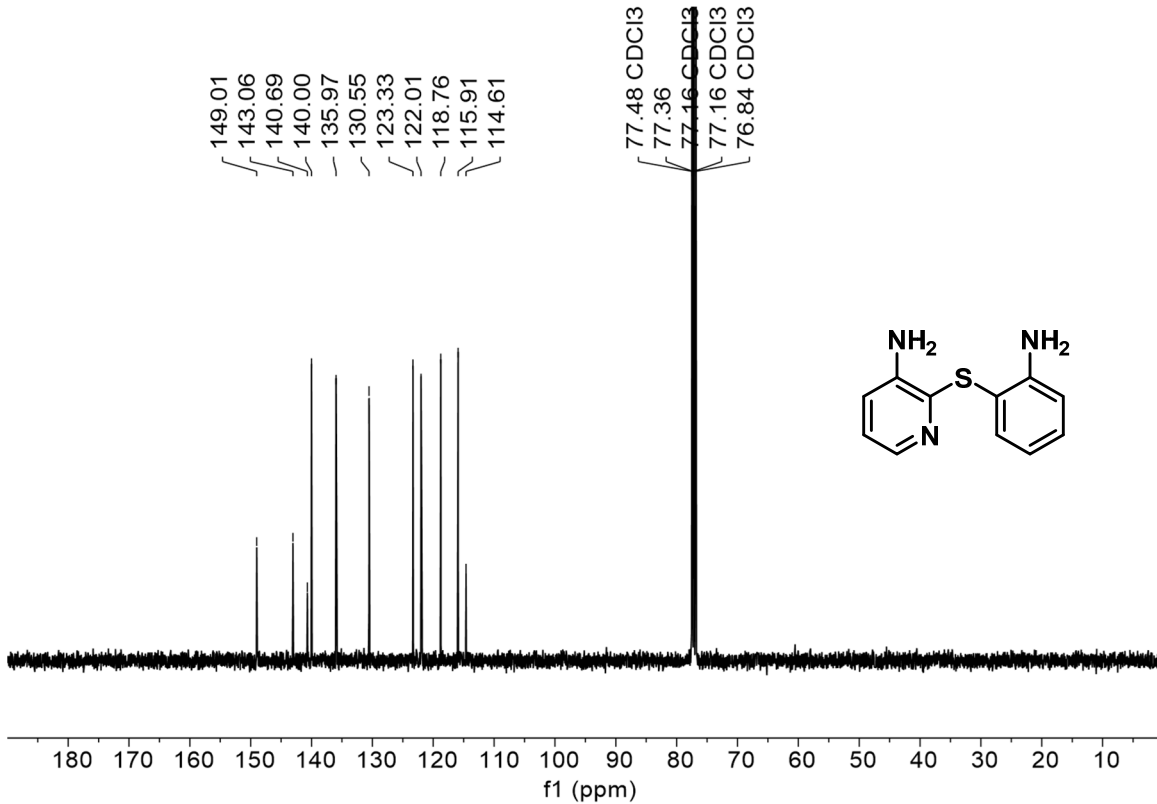


2-((2-aminophenyl)thio)pyridin-3-amine

¹H NMR (CDCl₃, 400 MHz)

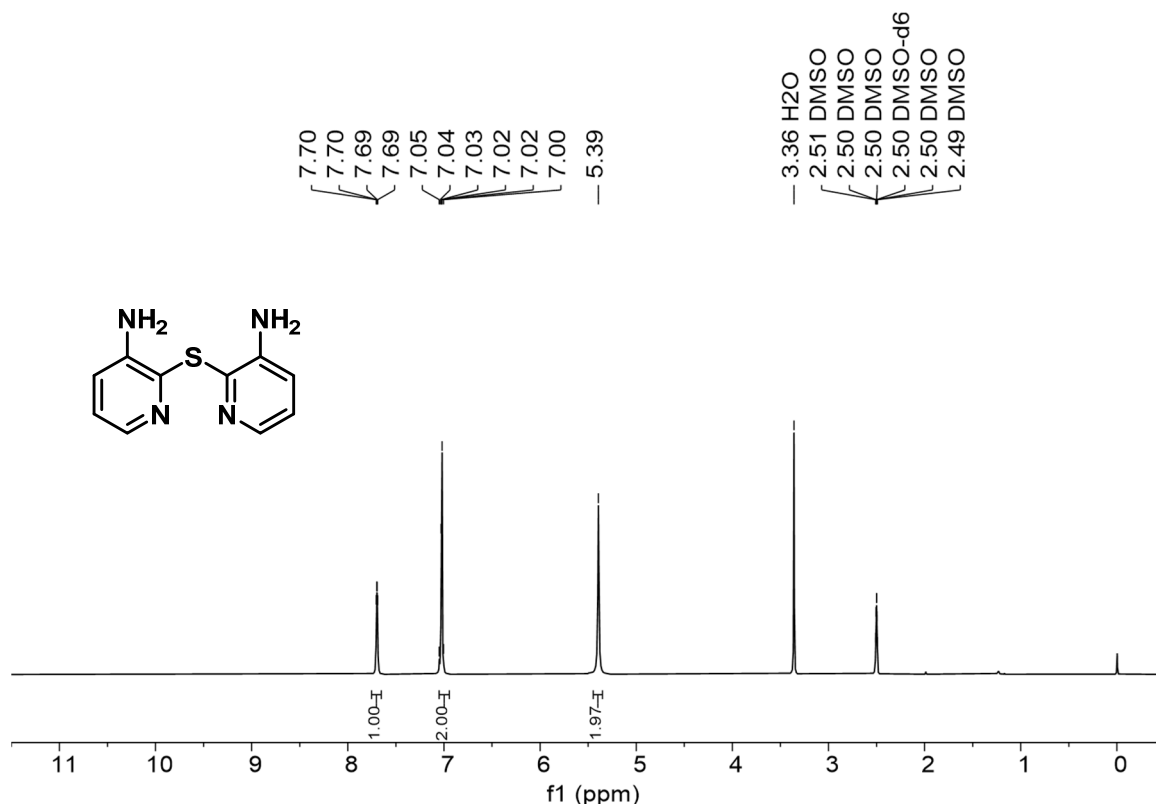


¹³C NMR (CDCl₃, 101 MHz)

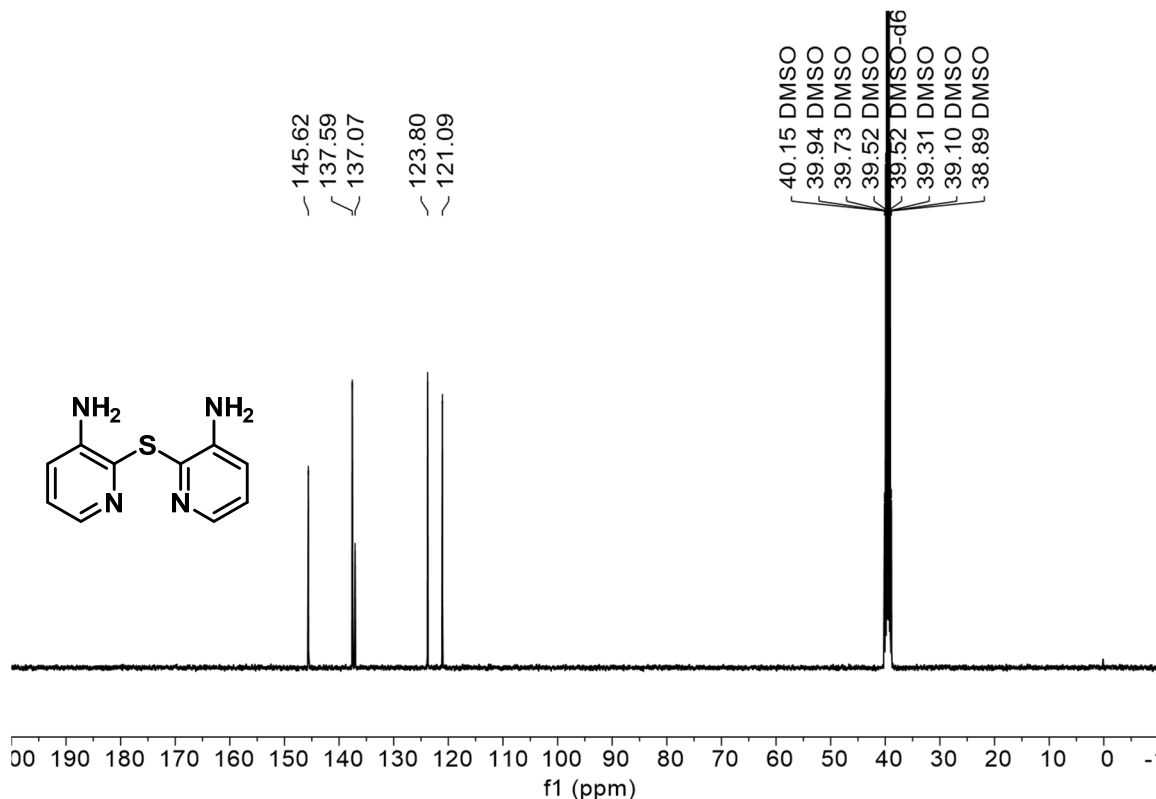


2,2'-thiobis(pyridin-3-amine)

¹H NMR (DMSO-*d*₆, 400 MHz)

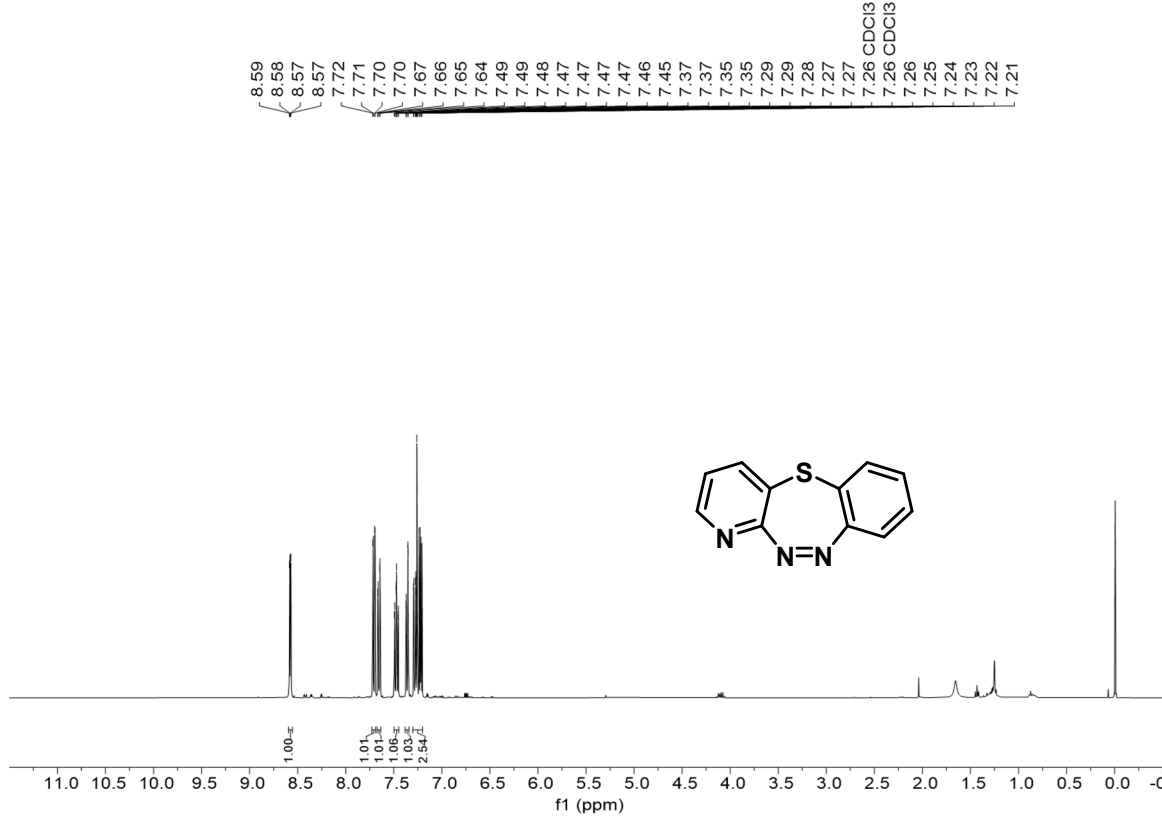


¹³C NMR (DMSO-*d*₆, 101 MHz)

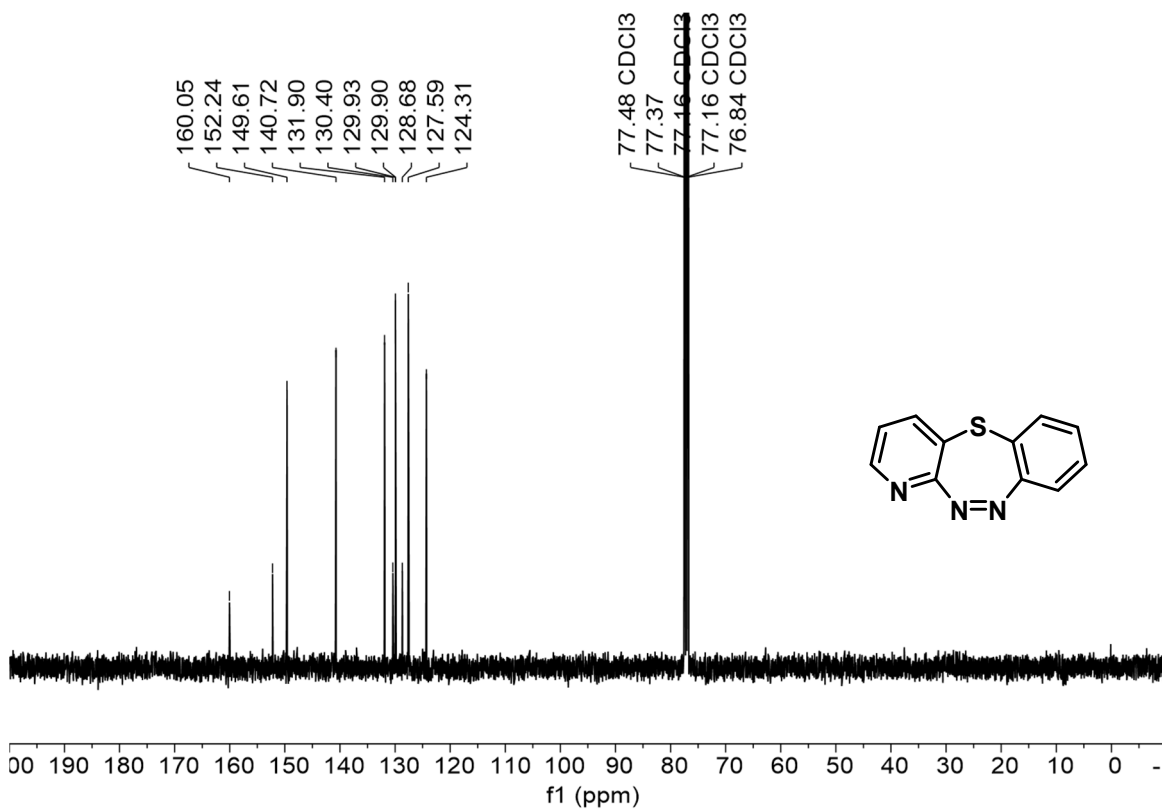


benzo[*b*]pyrido[2,3-*f*][1,4,5]thiadiazepine

¹H NMR (CDCl₃, 400 MHz)

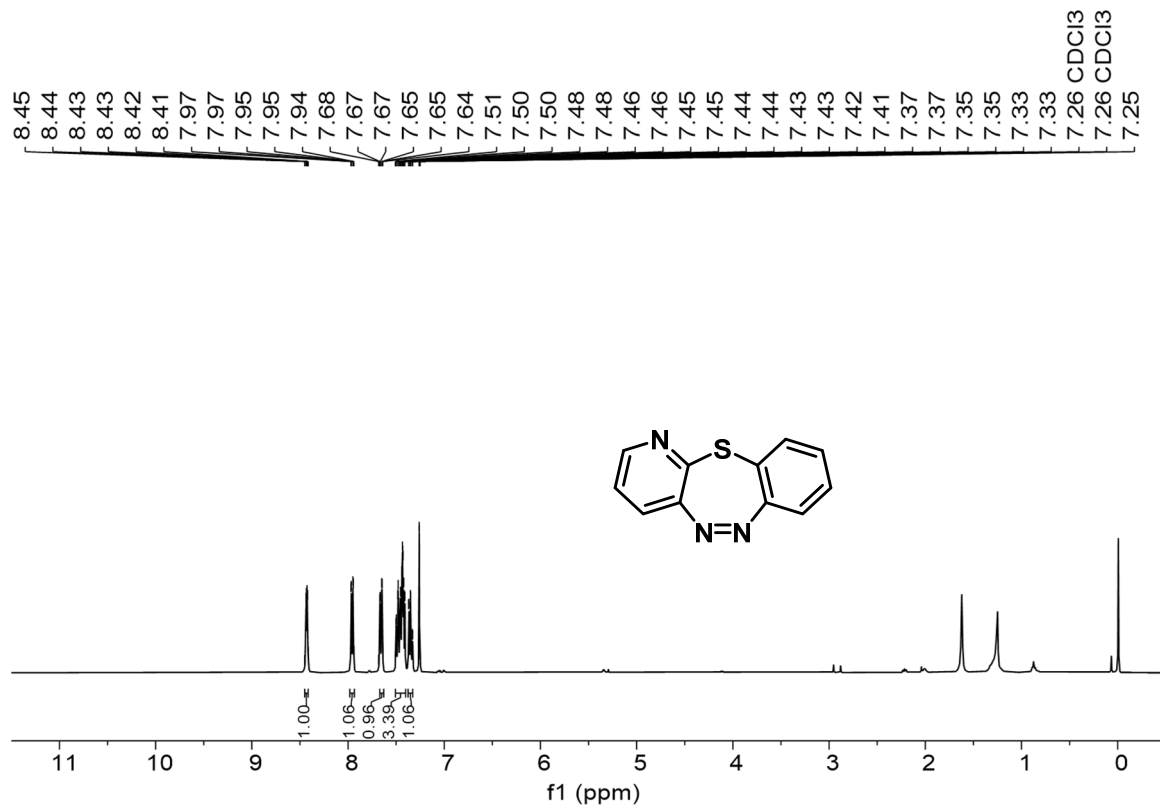


¹³C NMR (CDCl₃, 101 MHz)

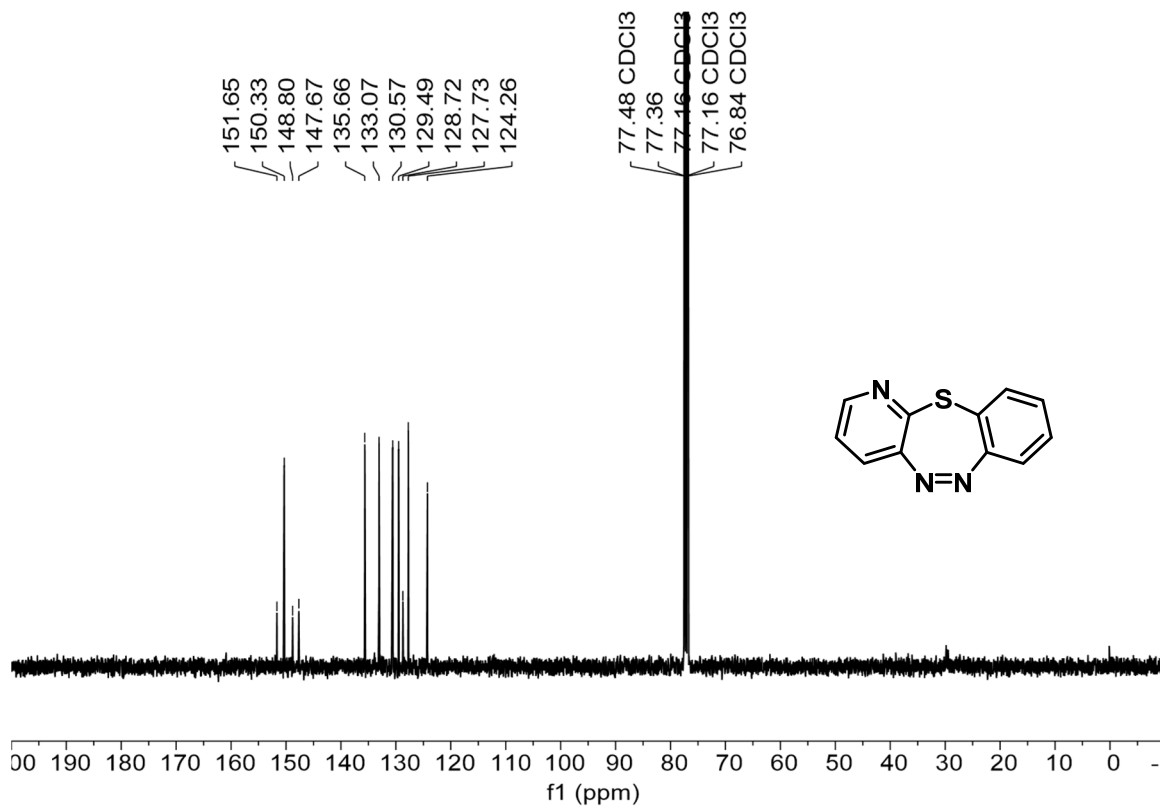


benzo[*b*]pyrido[3,2-*f*] [1,4,5] thiadiazepine

¹H NMR (CDCl₃, 400 MHz)

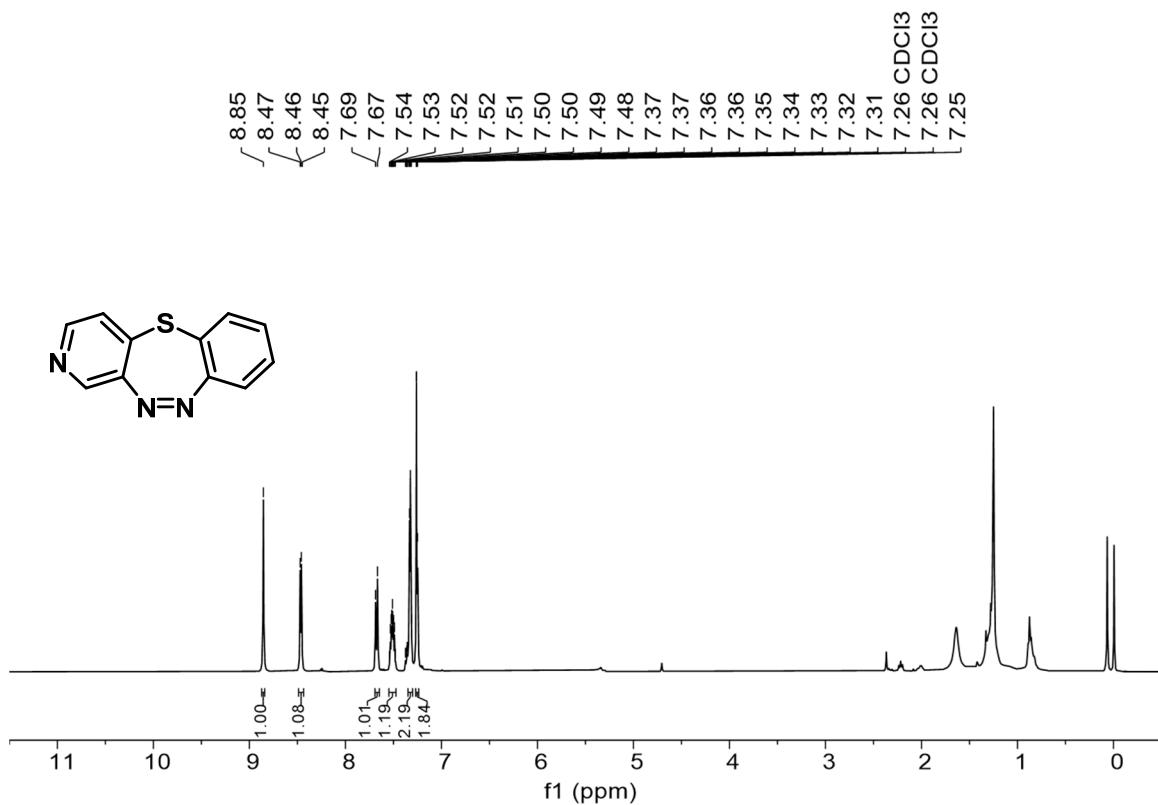


¹³C NMR (CDCl₃, 101 MHz)

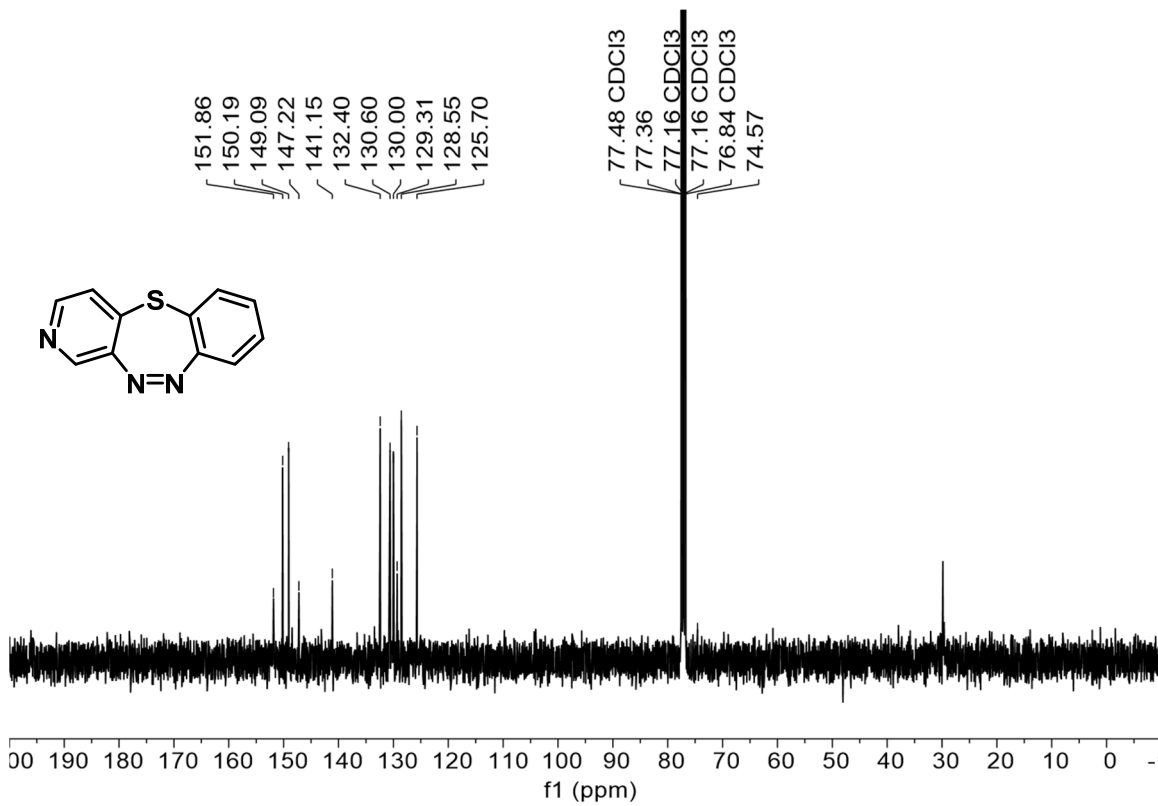


benzo[*b*]pyrido[3,4-*f*] [1,4,5] thiadiazepine

¹H NMR (CDCl₃, 400 MHz)

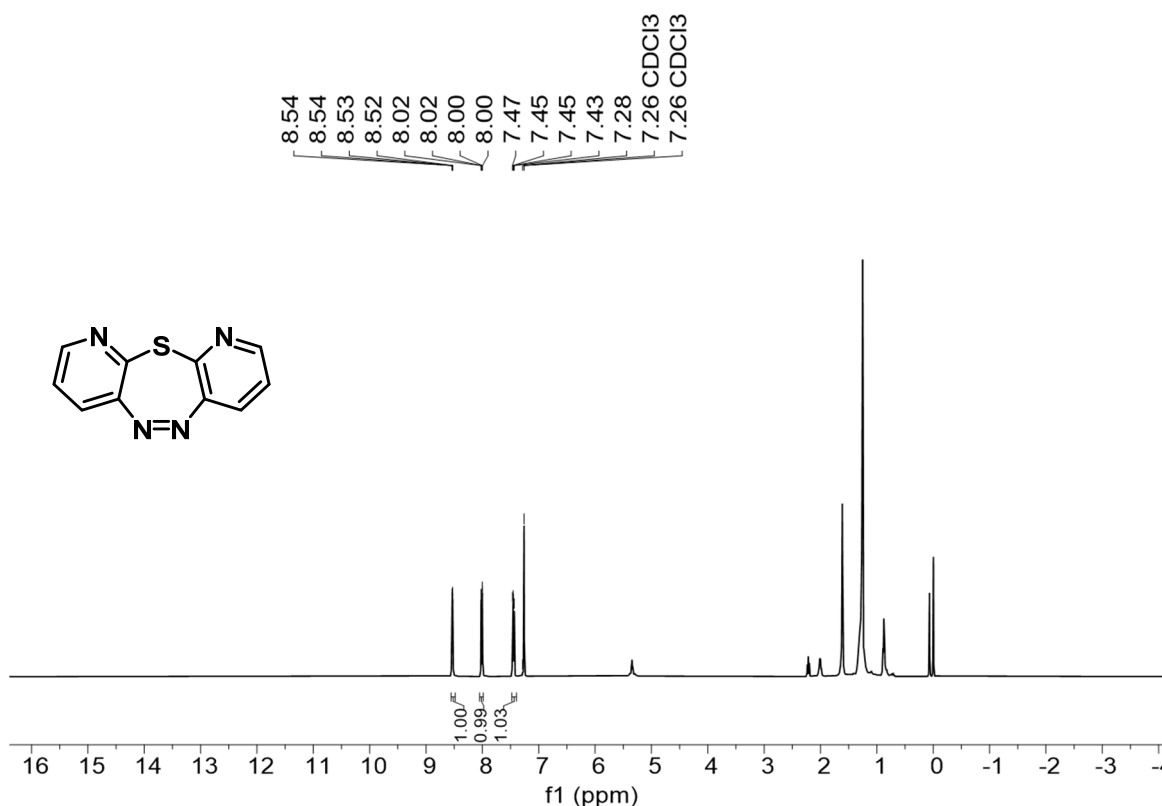


¹³C NMR (CDCl₃, 101 MHz)

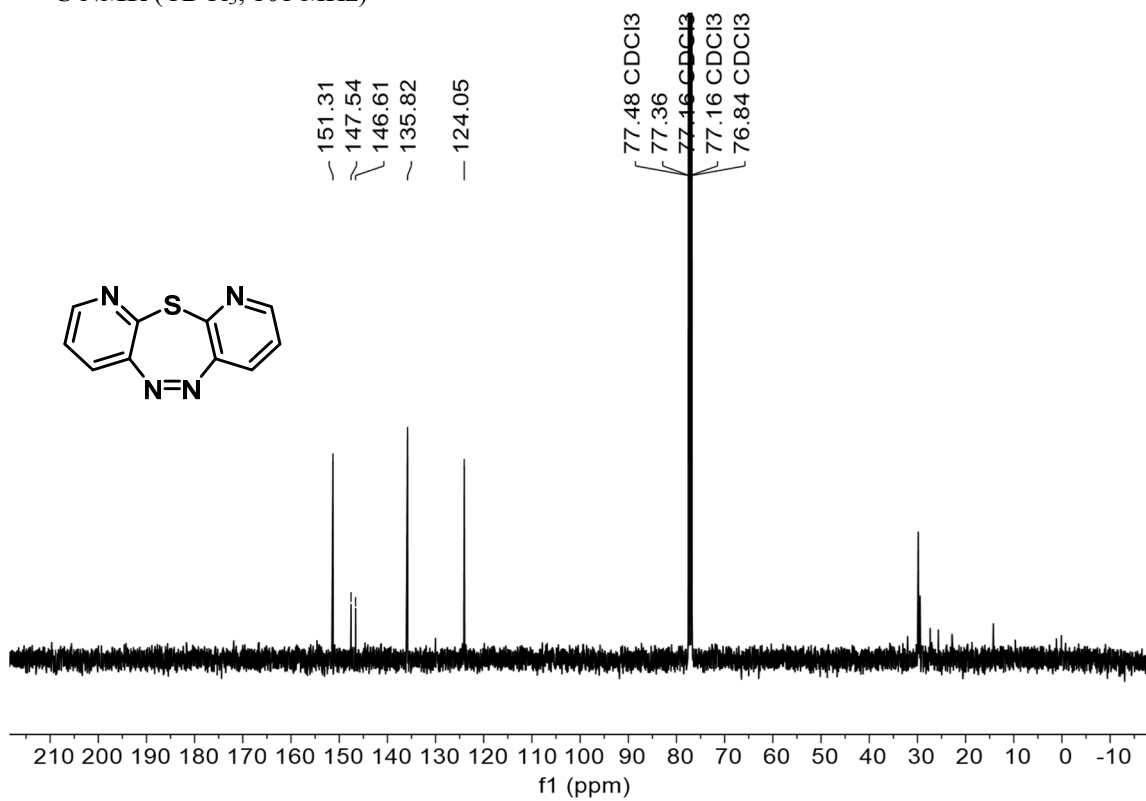


dipyrido[2,3-*b*:3',2'-*f*] [1,4,5] thiadiazepine

¹H NMR (CDCl₃, 400 MHz)

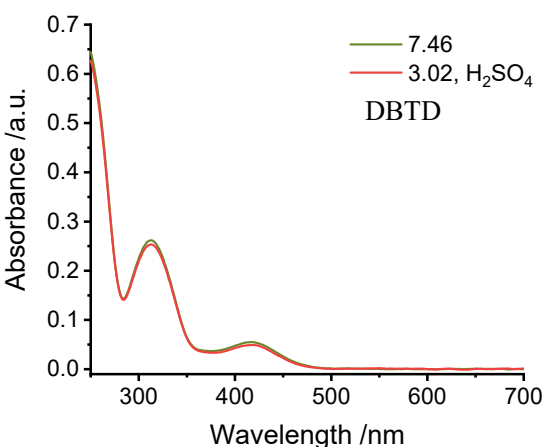
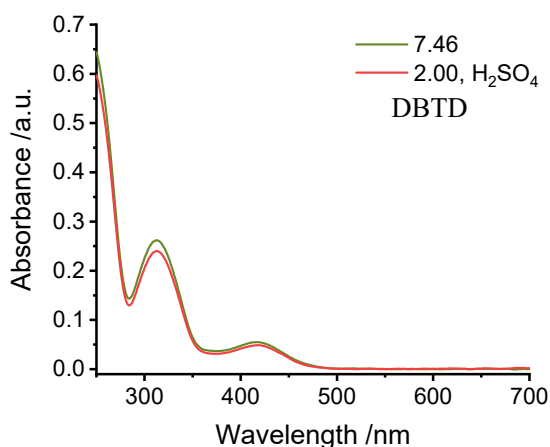
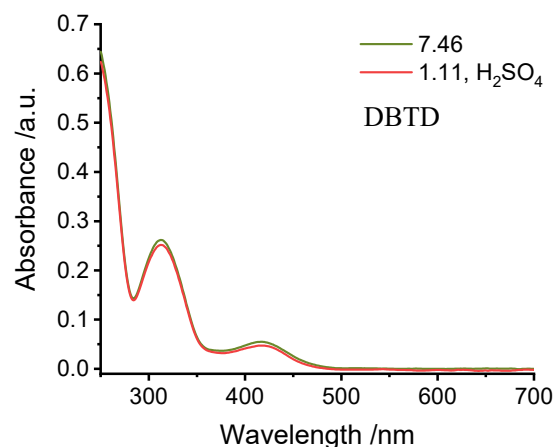
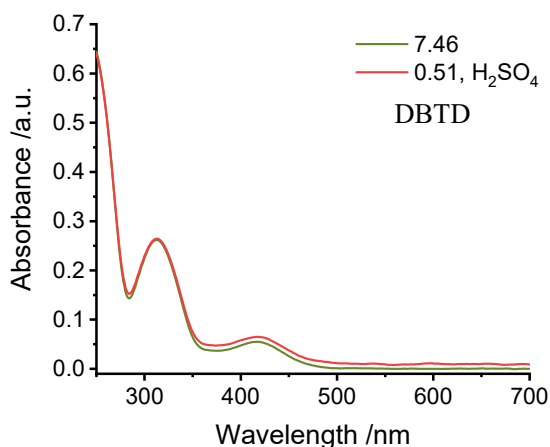
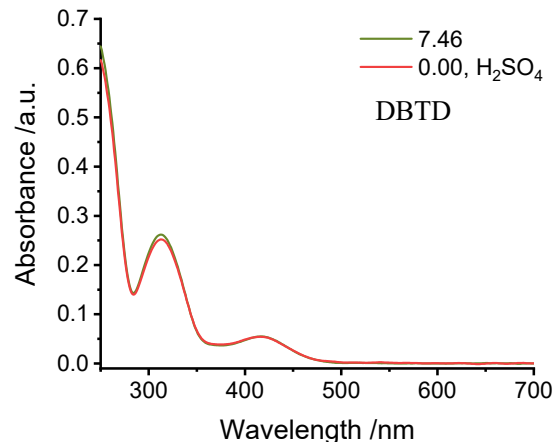
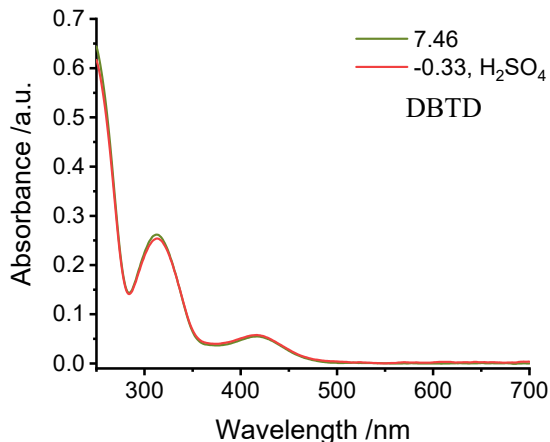


¹³C NMR (CDCl₃, 101 MHz)



3. Analysis for the photophysical properties

3.1 UV-Vis absorbance spectra of DBTD and 1a-4a in various pH gradients



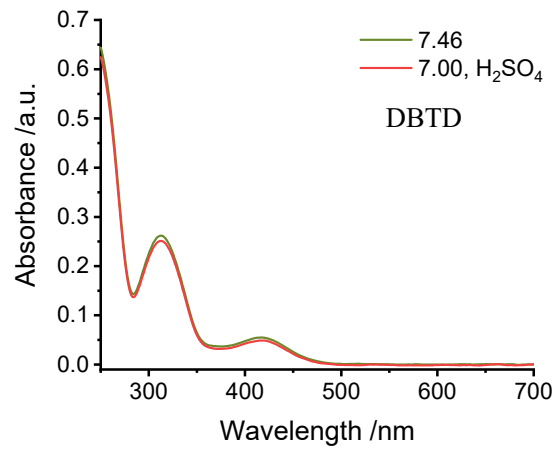
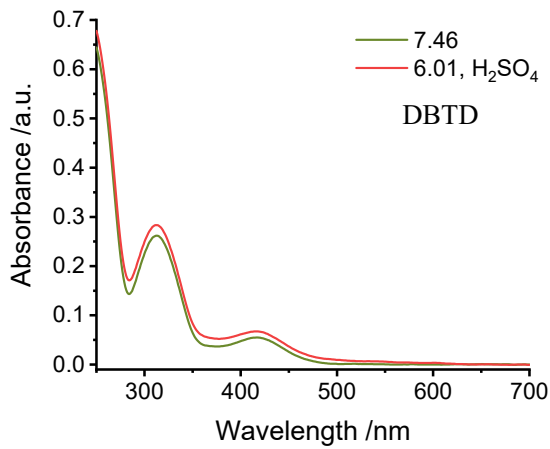
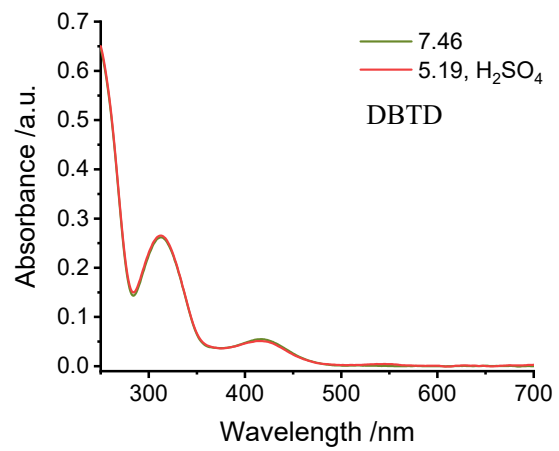
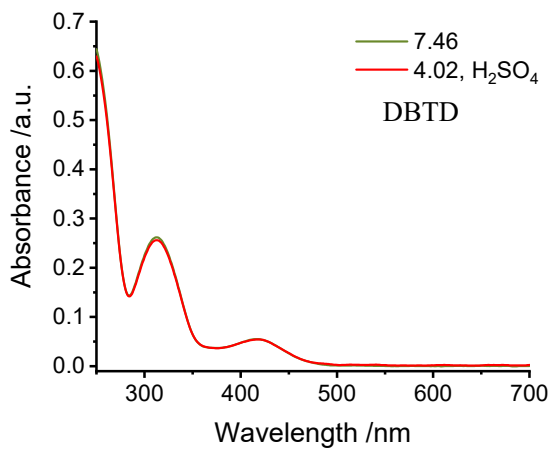
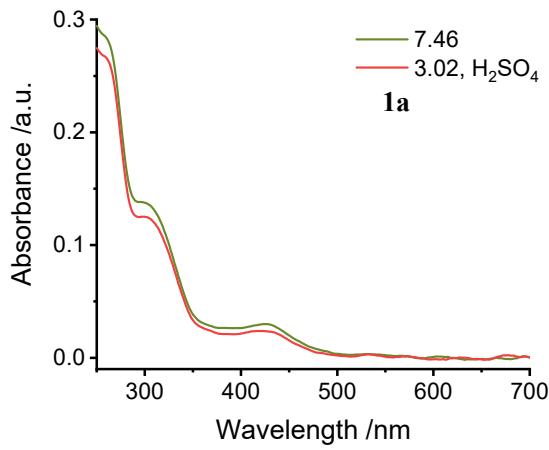
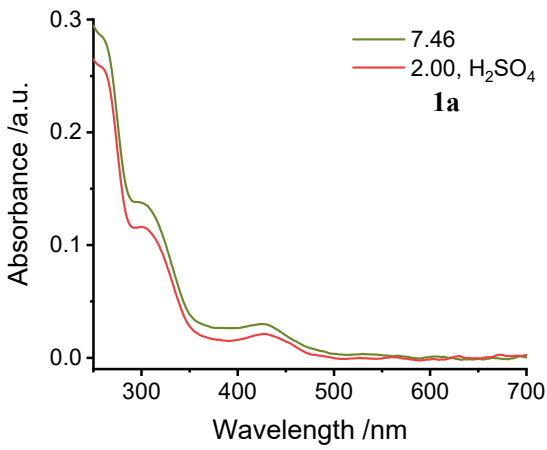
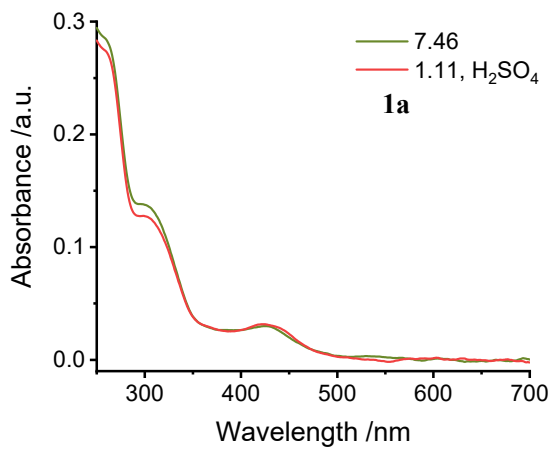
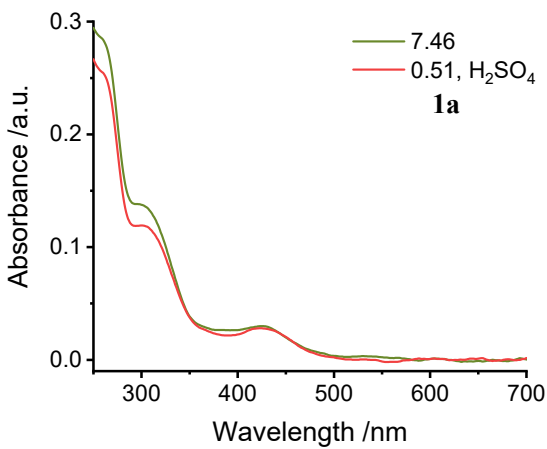
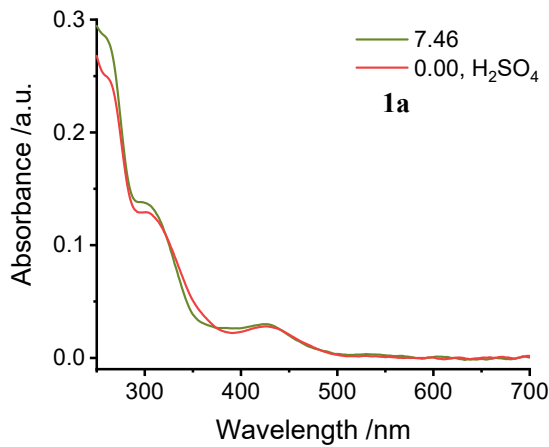
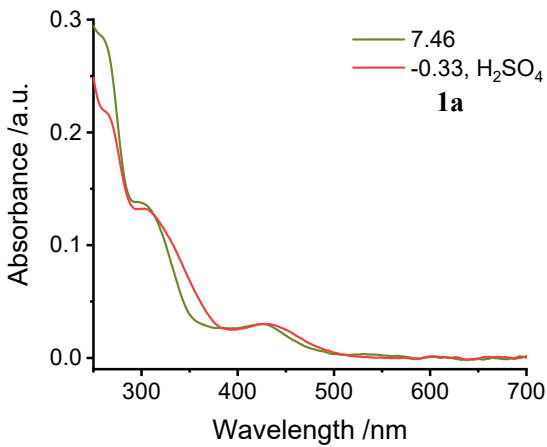


Figure S4. UV-Vis absorbance spectra of DBTD at $\text{pH} = -0.33$ to 7.46 in PBS/MeCN = 2/1, PBS = phosphate buffer saline at specified pH, $T = 298$ K, conc. = 50 μM .



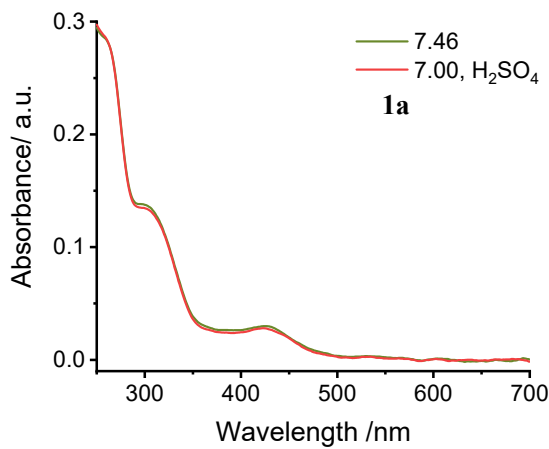
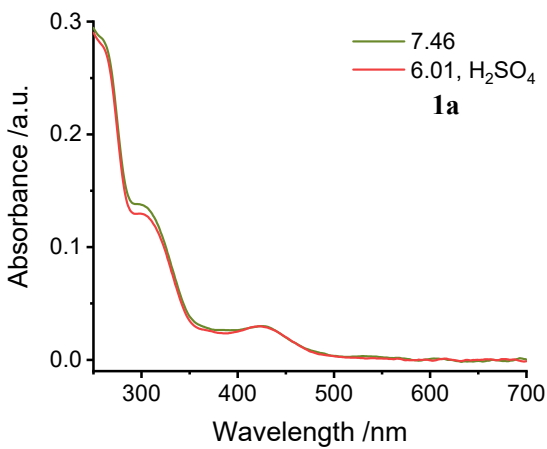
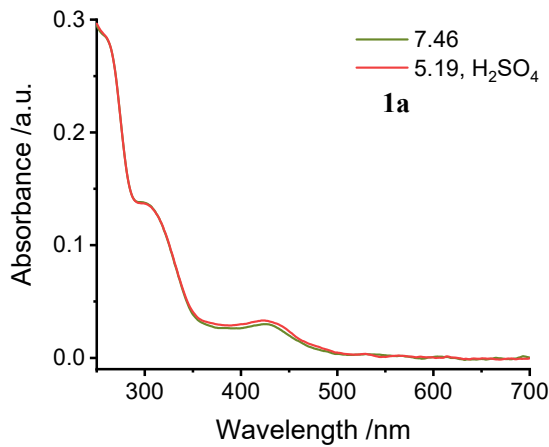
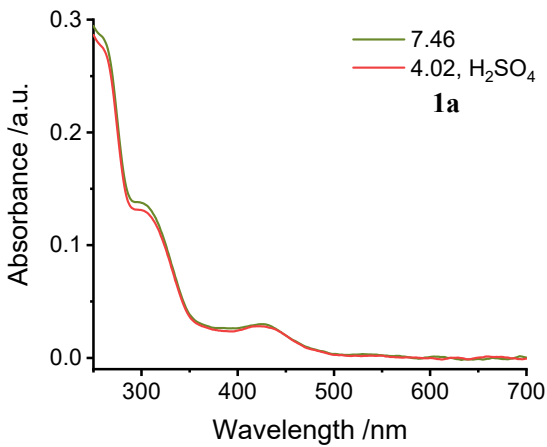
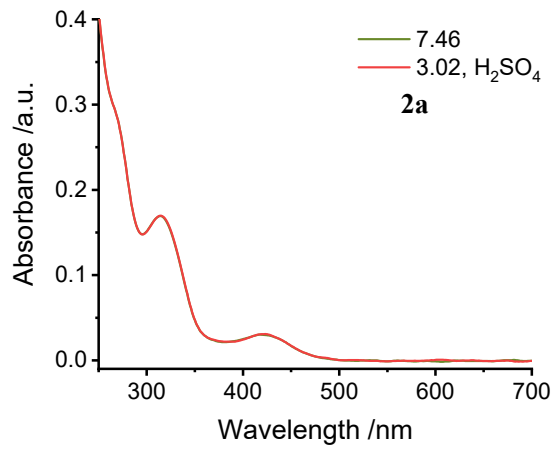
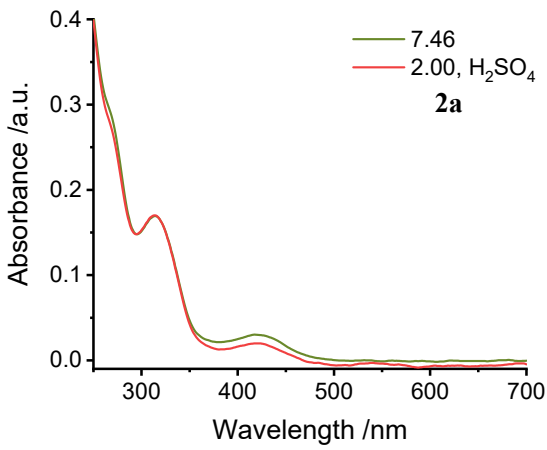
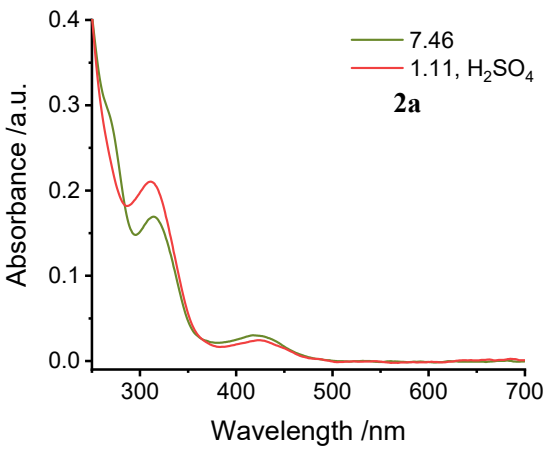
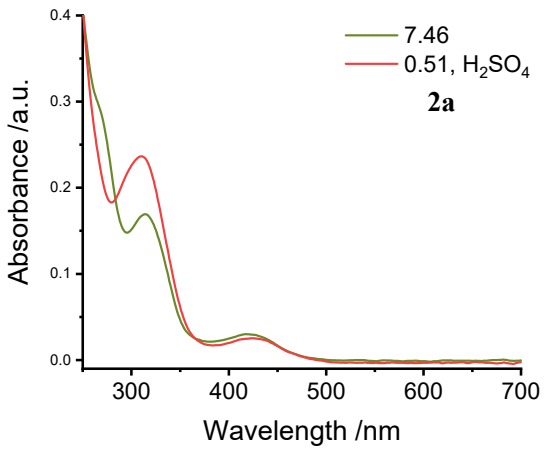
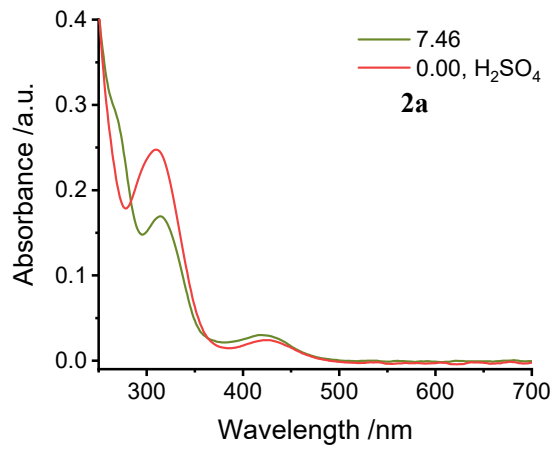
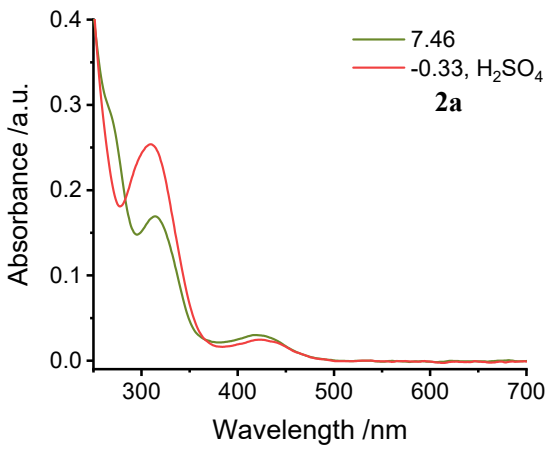


Figure S5. UV-Vis absorbance spectra of **1a** at pH = -0.33 to 7.46 in PBS/MeCN = 2/1, PBS = phosphate buffer saline at specified pH, T = 298 K, conc. = 50 μM .



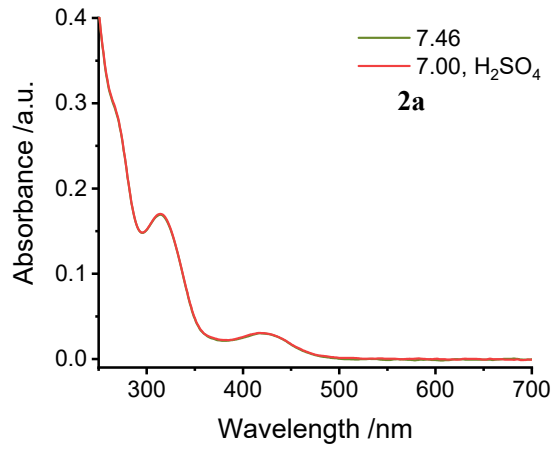
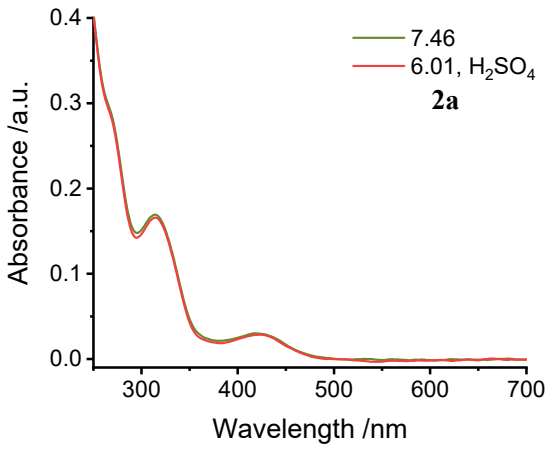
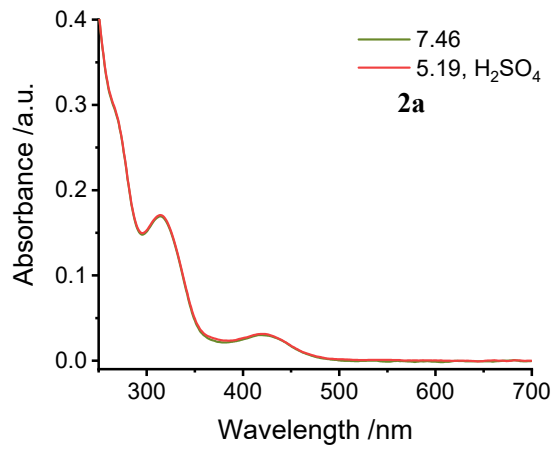
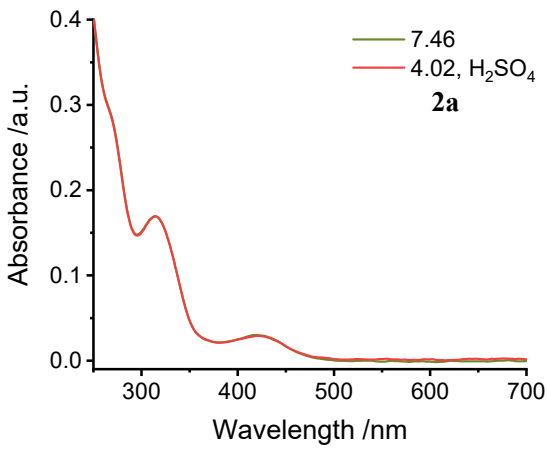
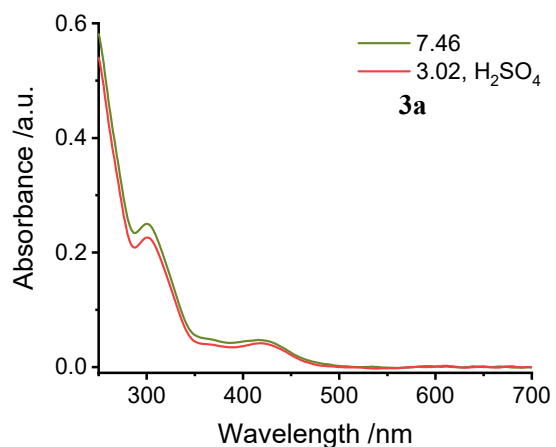
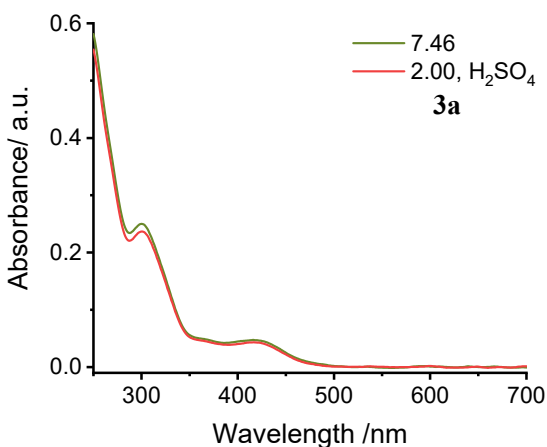
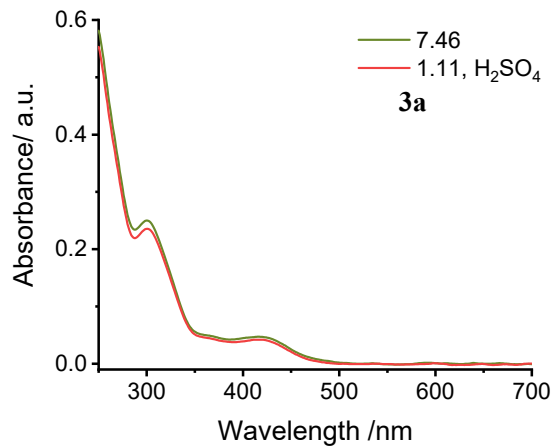
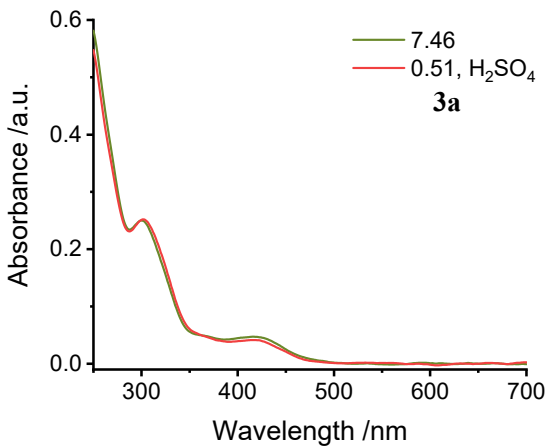
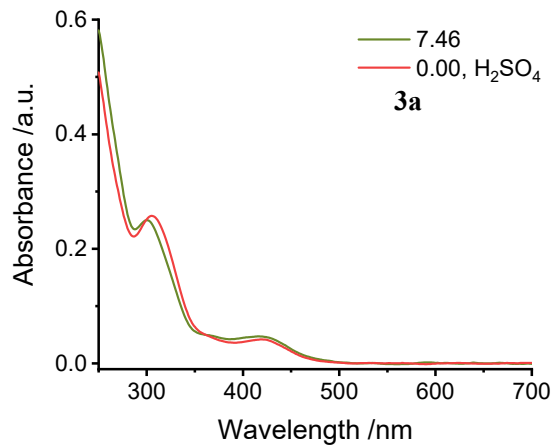
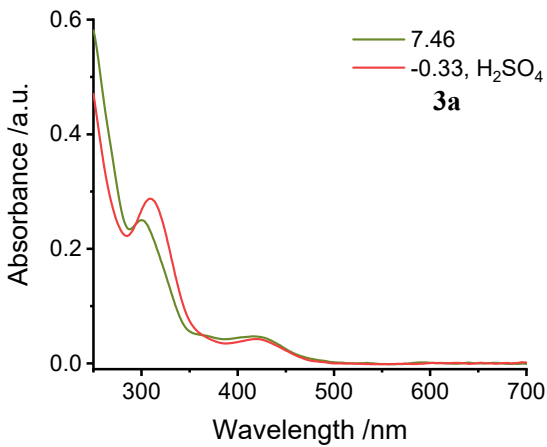


Figure S6. UV-Vis absorbance spectra of **2a** at pH = -0.33 to 7.00 in PBS/MeCN = 2/1, PBS = phosphate buffer saline at specified pH, T = 298 K, conc. = 50 μ M.



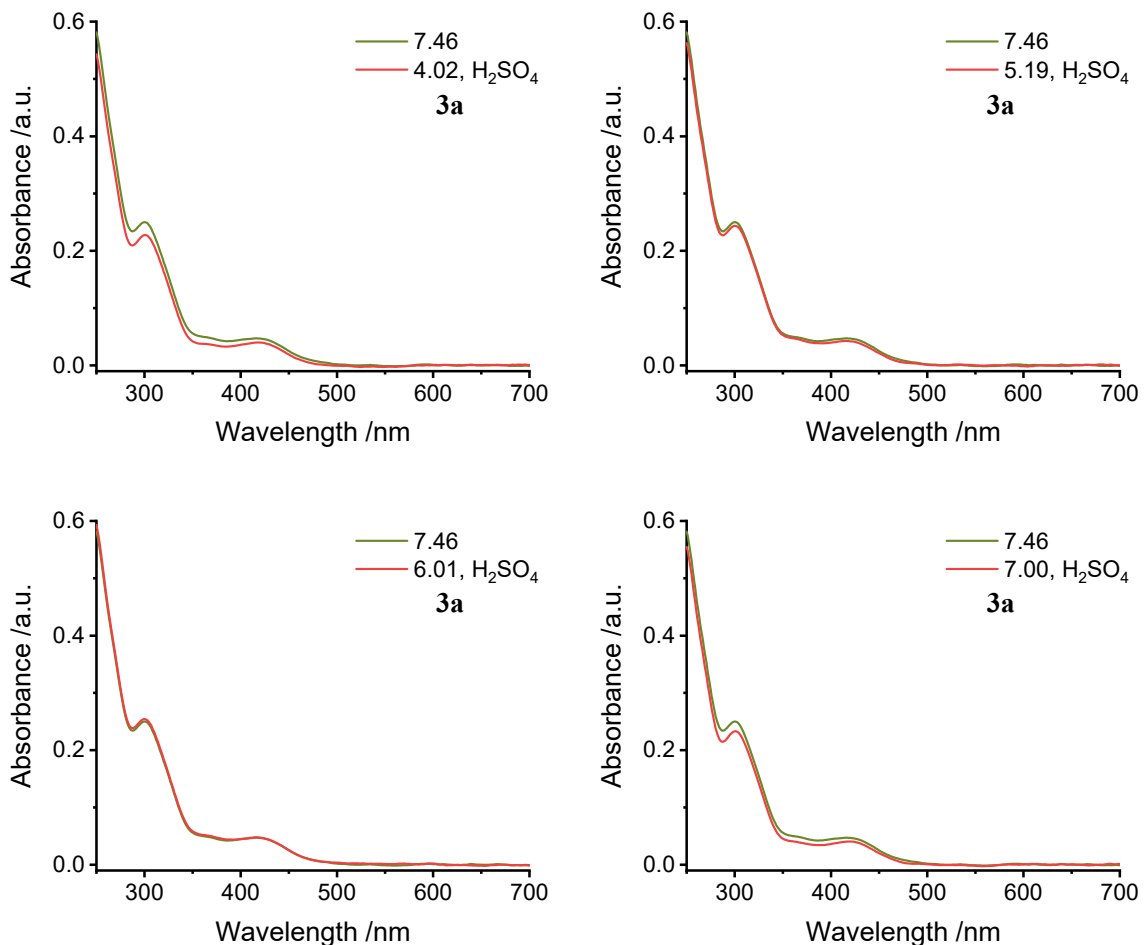
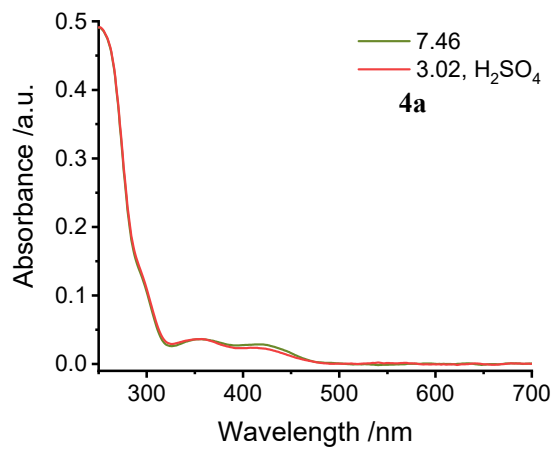
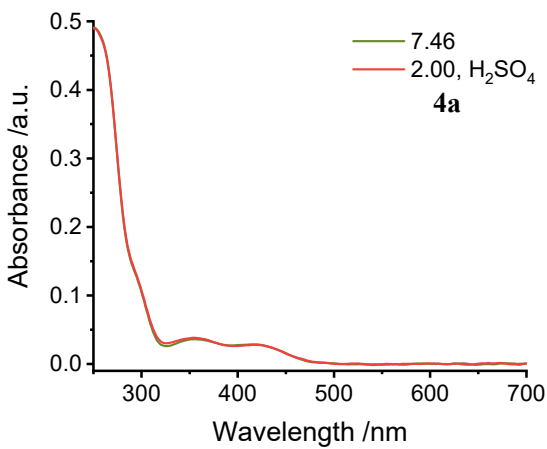
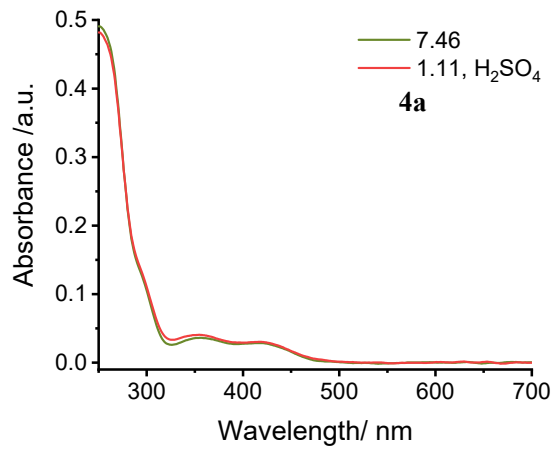
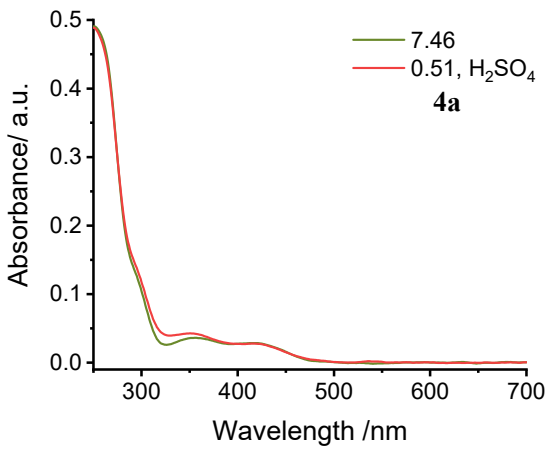
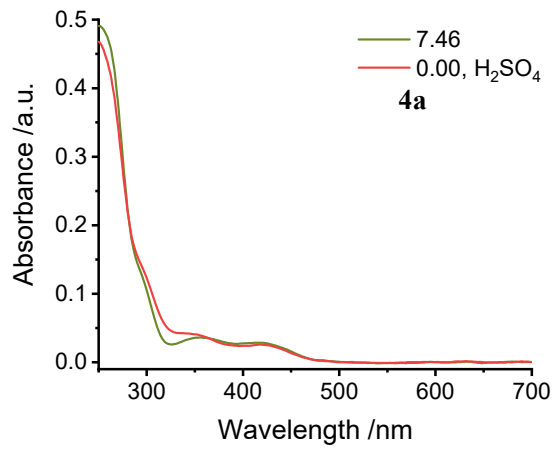
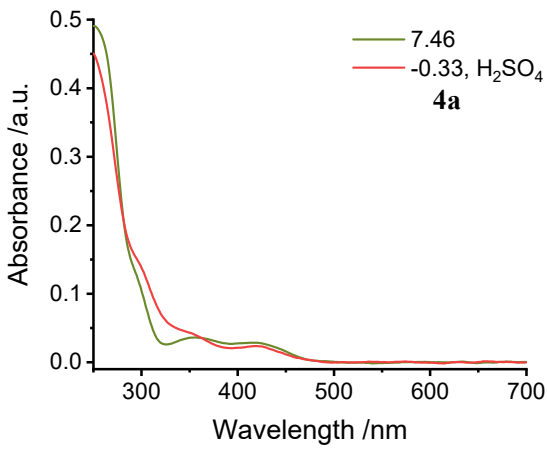


Figure S7. UV-Vis absorbance spectra of **3a** at pH = -0.33 to 7.00 in PBS/MeCN = 2/1, PBS = phosphate buffer saline at specified pH, T = 298 K, conc. = 50 μ M.



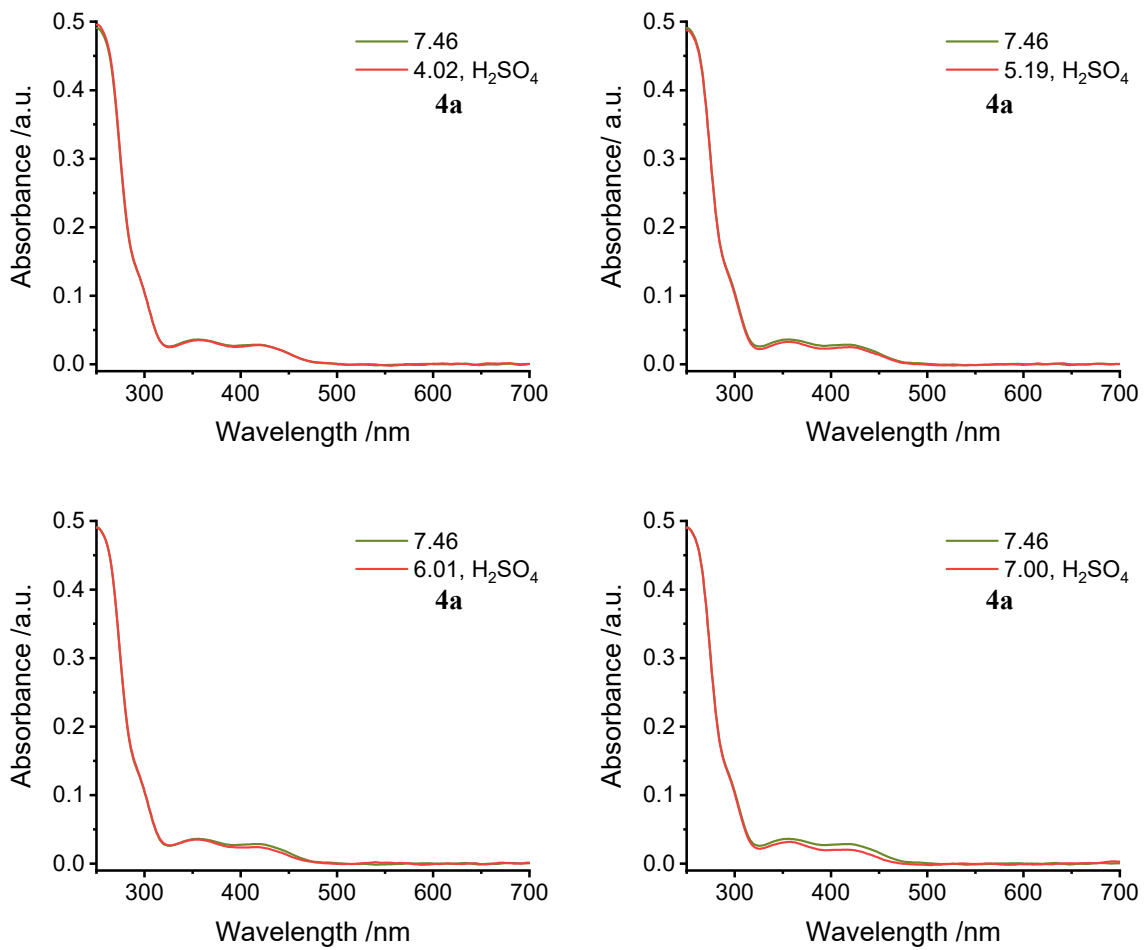
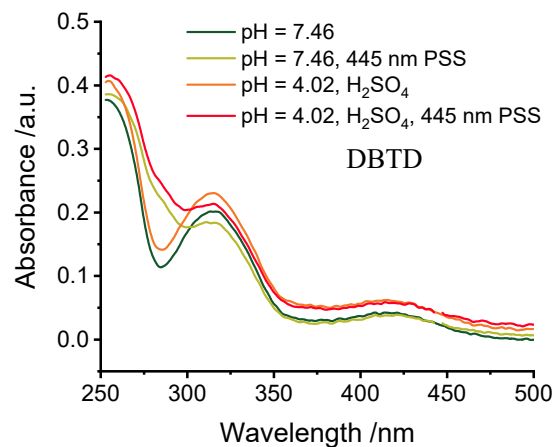
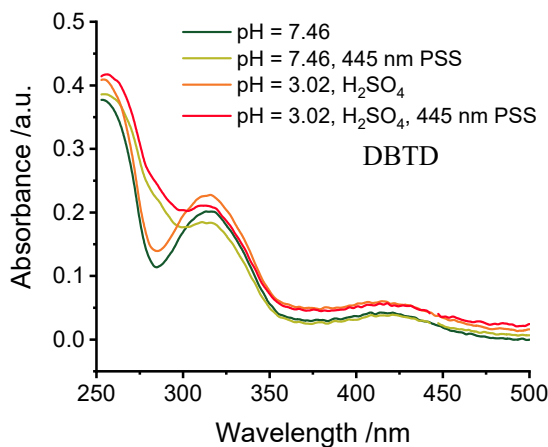
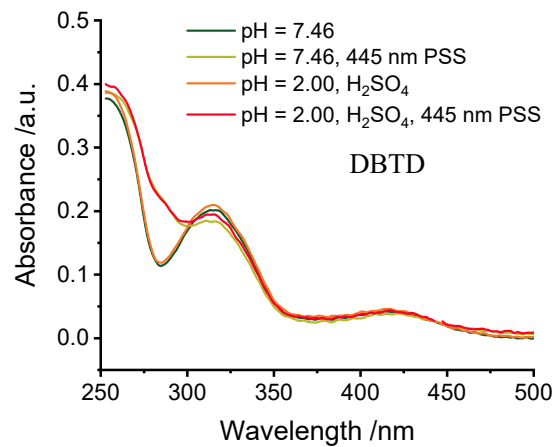
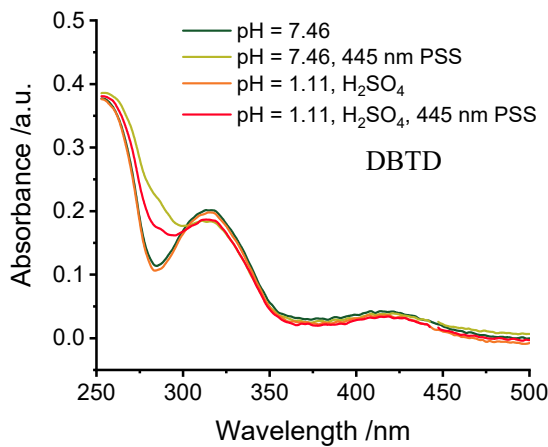
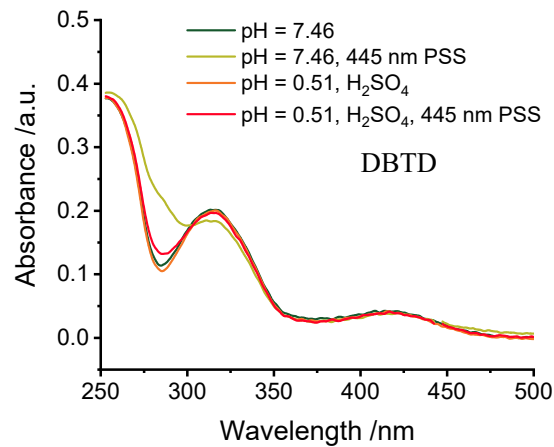
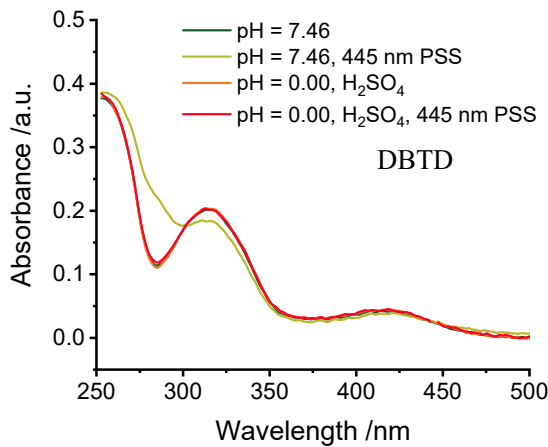


Figure S8. UV-Vis absorbance spectra of **4a** at pH = -0.33 to 7.00 in PBS/MeCN = 2/1, PBS = phosphate buffer saline at specified pH, T = 298 K, conc. = 50 μ M.

3.2 UV-Vis absorbance spectra of DBTD and 1a-4a at different pH before irradiation or at the PSS under the continuous 445 nm laser stimulation



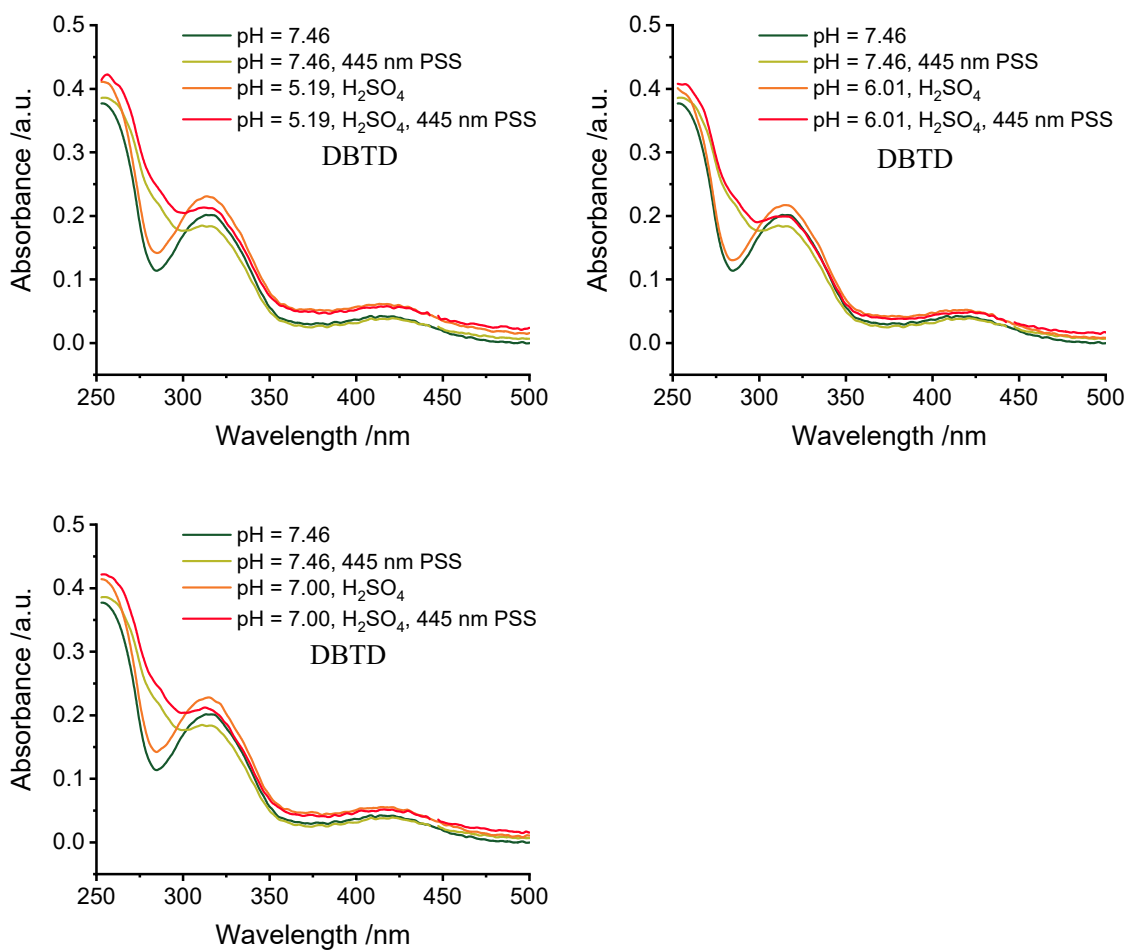
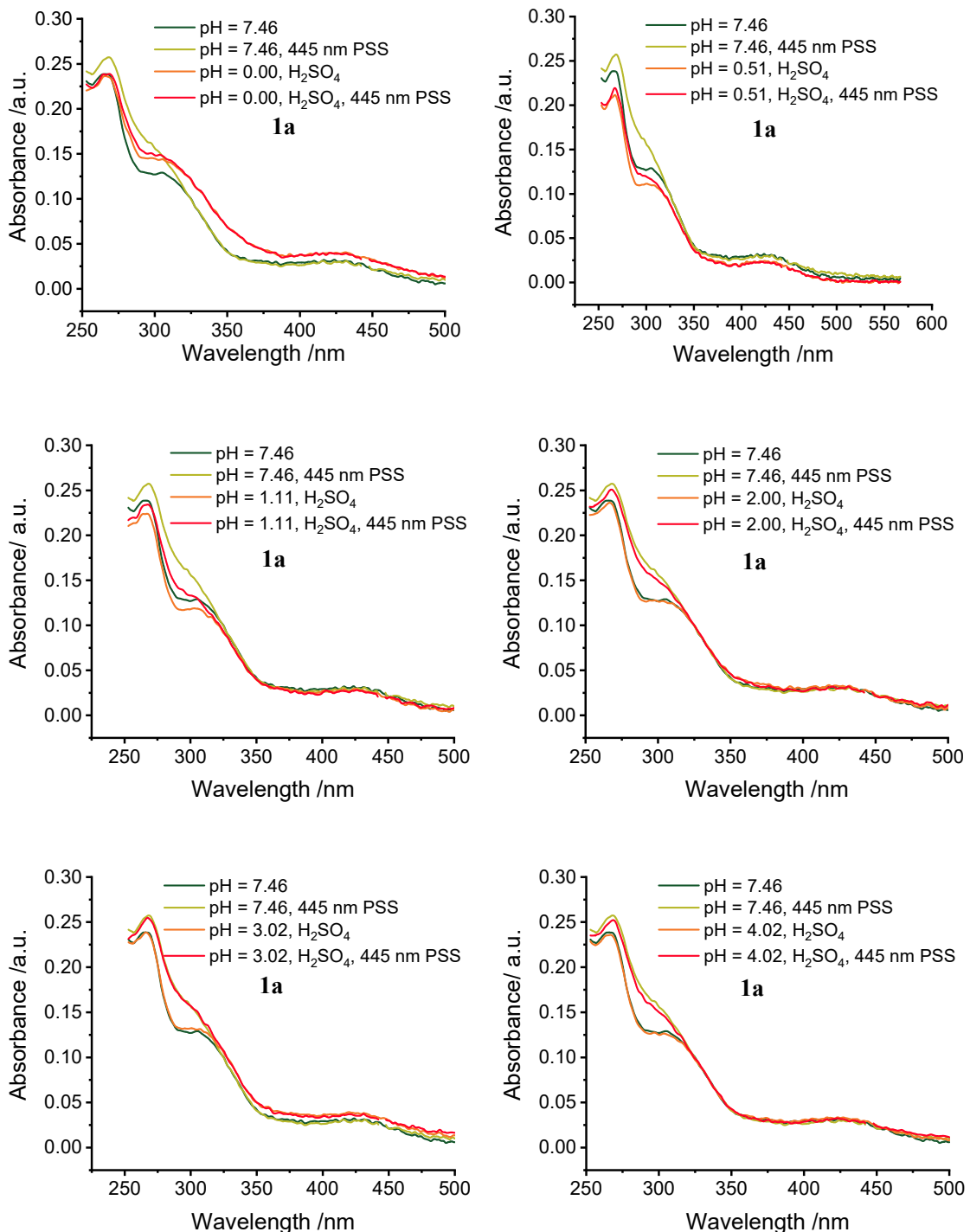


Figure S9. UV-Vis absorbance spectra of DBTD at pH = 0.00-7.00 *versus* at pH = 7.46, before photo-stimulation and at the PSS (in the dark *vs.* under the 445 nm laser irradiation at 391 mW cm⁻²), T = 298 K, conc. = 50 μM, in PBS/MeCN = 2/1, PBS = phosphate buffer saline at specified pH.



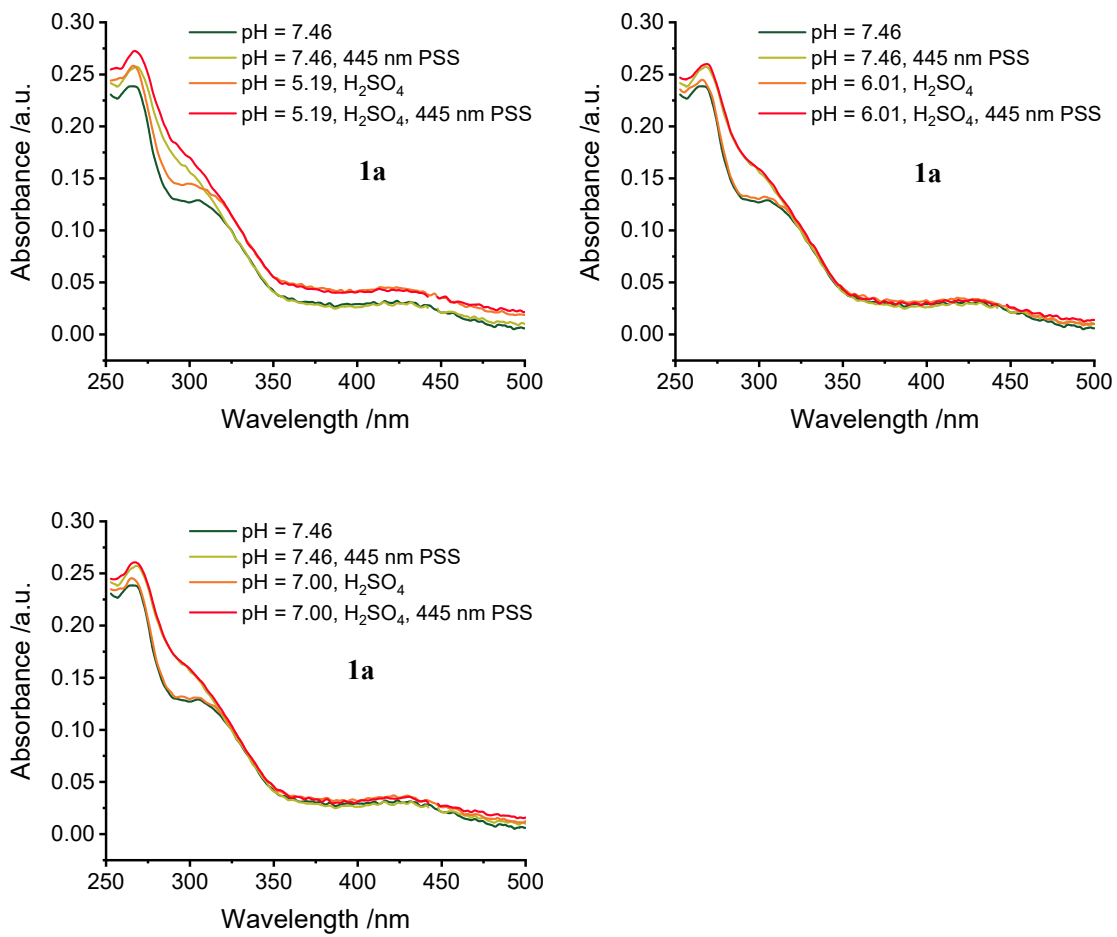
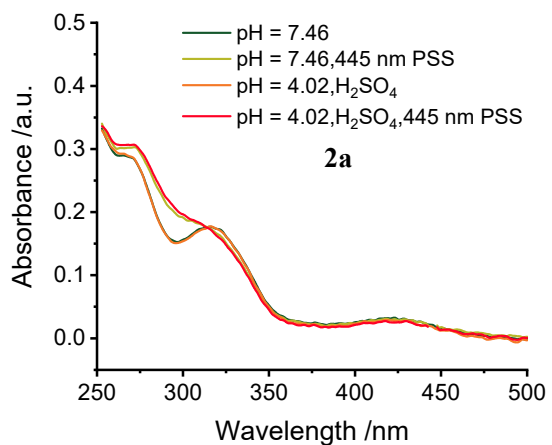
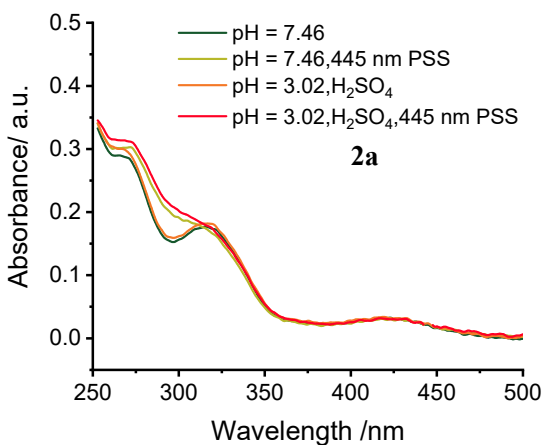
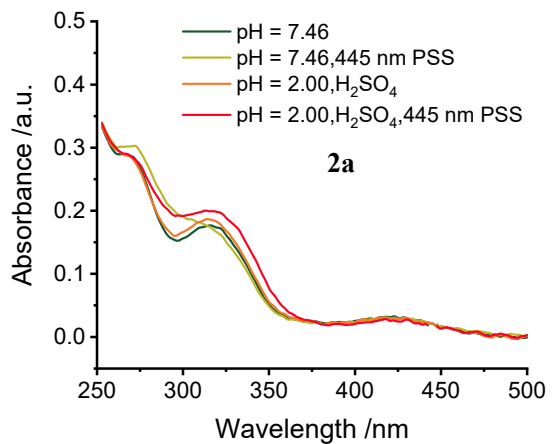
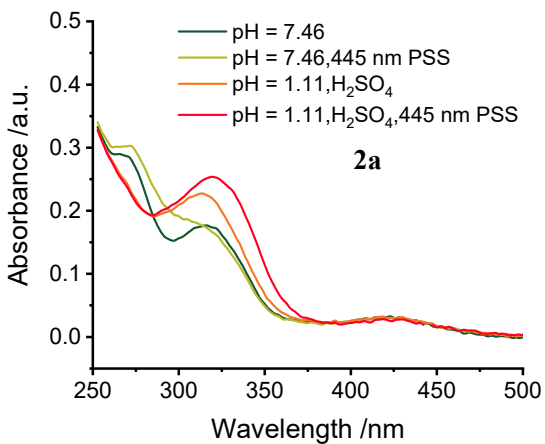
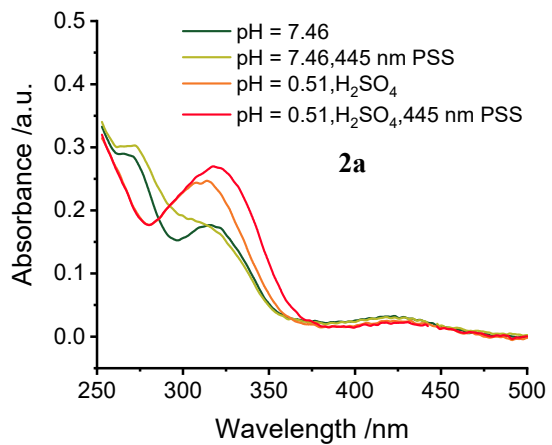
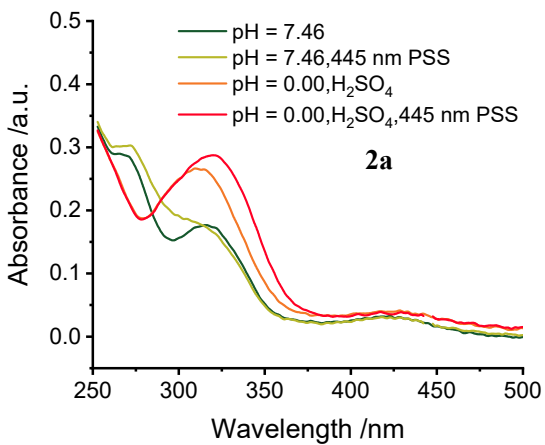


Figure S10. UV-Vis absorbance spectra of **1a** at pH = 0.00-7.00 versus at pH = 7.46, before photo-stimulation and at the PSS (in the dark vs. under the 445 nm laser irradiation at 391 mW cm⁻²), T = 298 K, conc. = 50 μM, in PBS/MeCN = 2/1, PBS = phosphate buffer saline at specified pH.



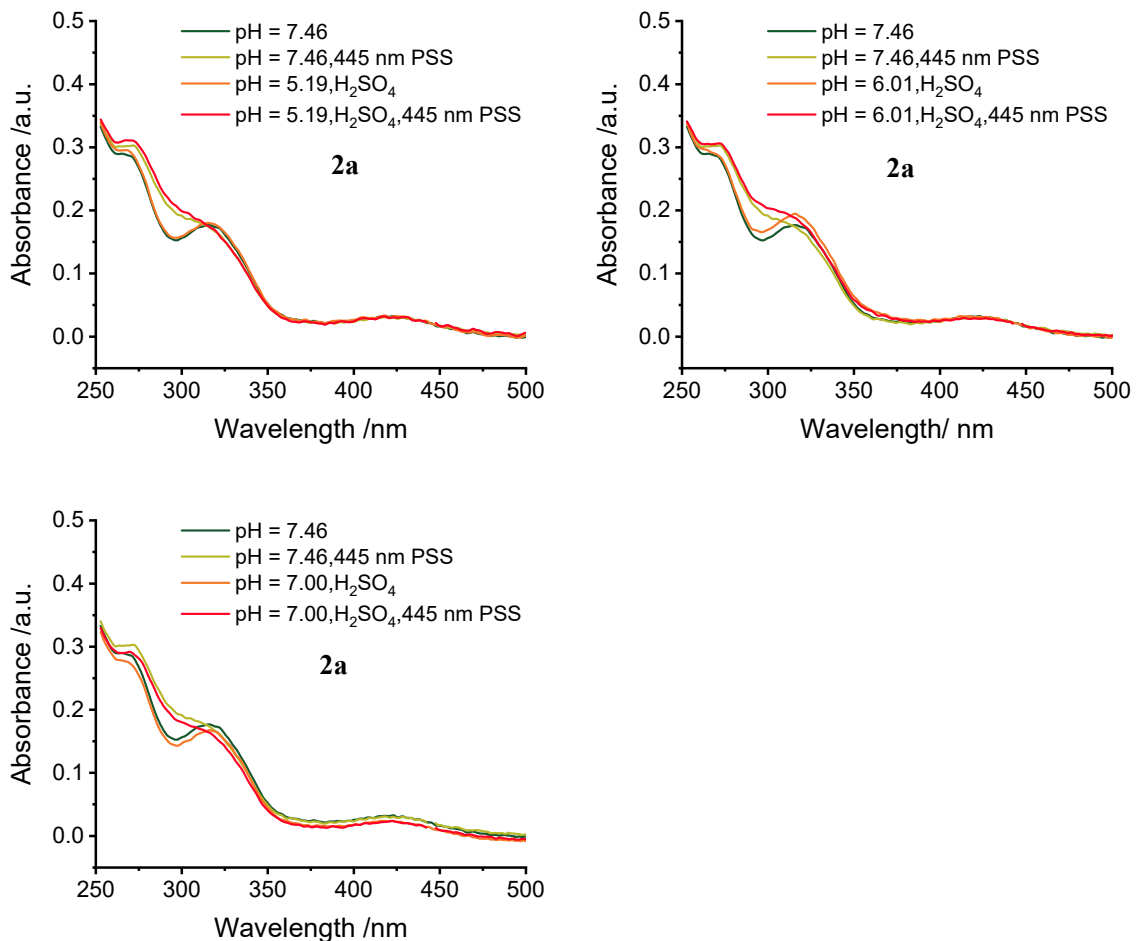
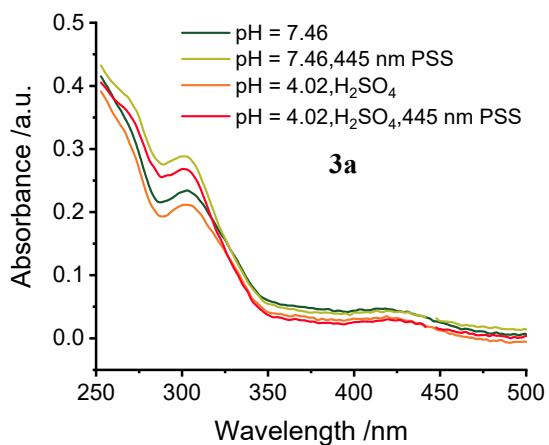
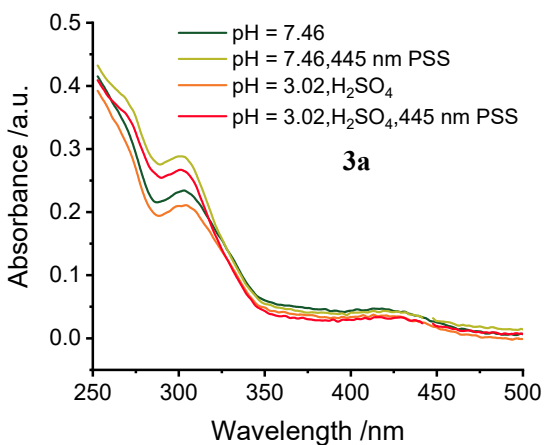
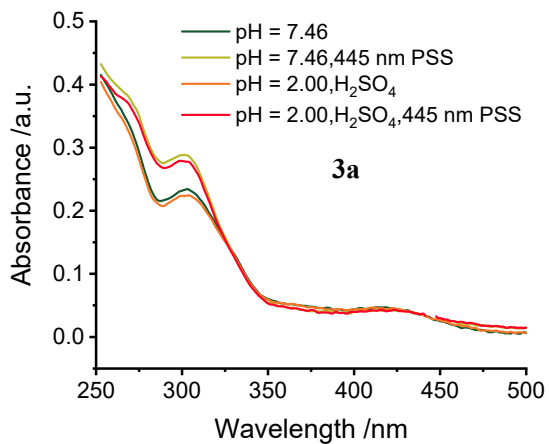
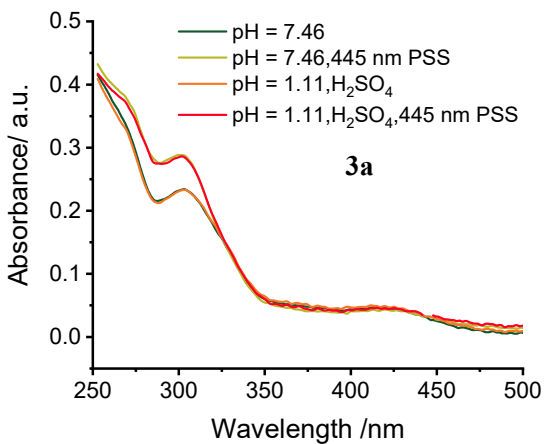
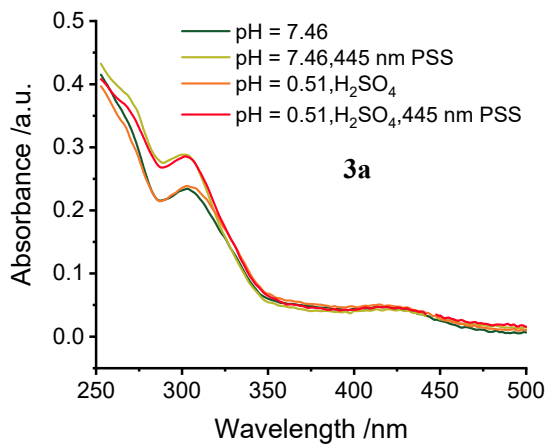
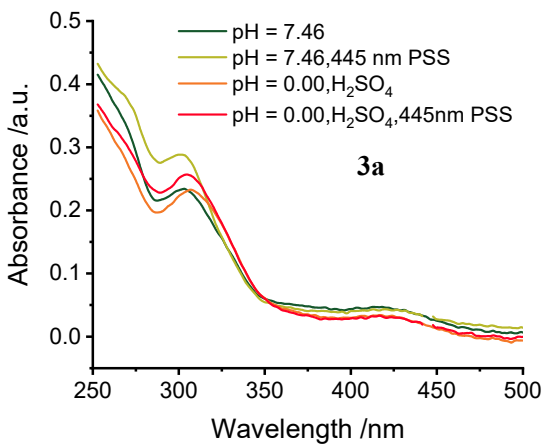


Figure S11. UV-Vis absorbance spectra of **2a** at pH = 0.00-7.00 *versus* at pH = 7.46, before photo-stimulation and at the PSS (in the dark *vs.* under the 445 nm laser irradiation at 391 mW cm⁻²), T = 298 K, conc. = 50 μ M, in PBS/MeCN = 2/1, PBS = phosphate buffer saline at specified pH.



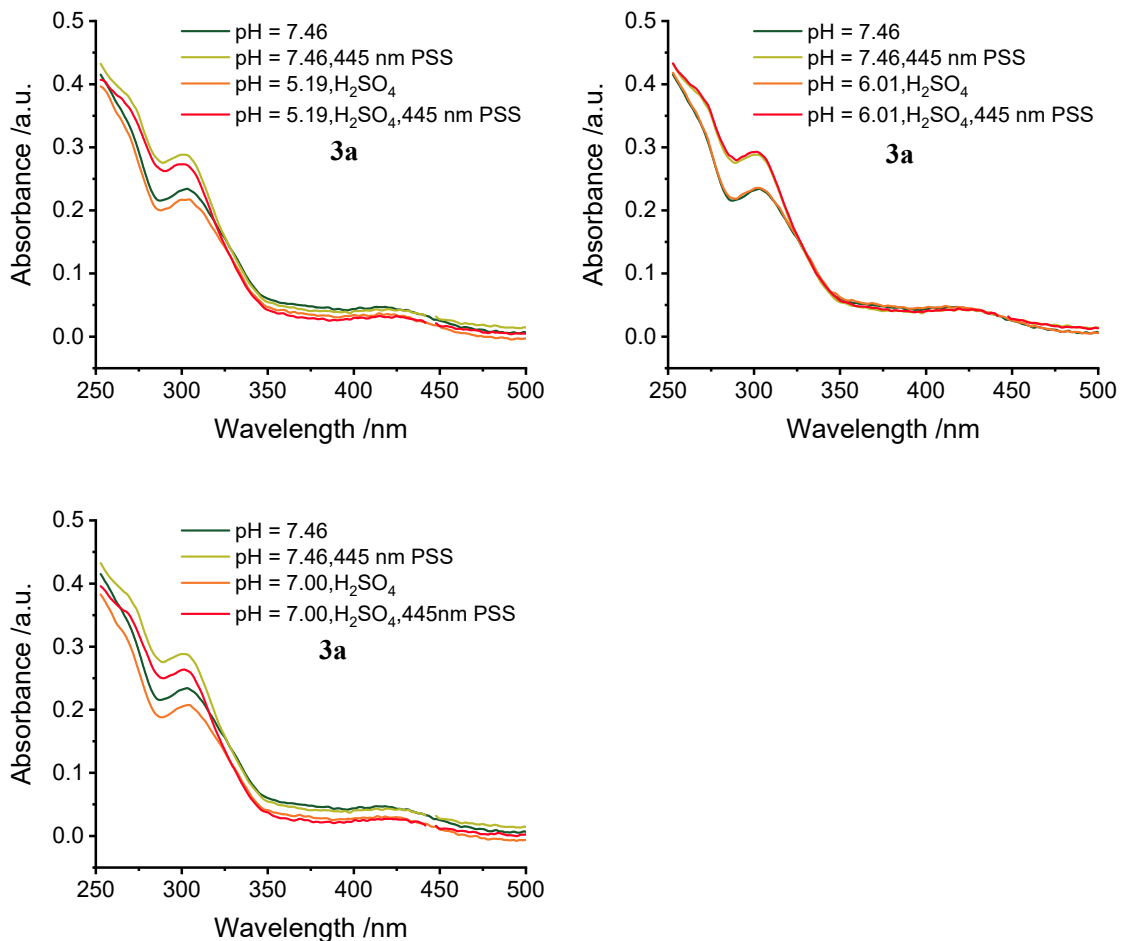
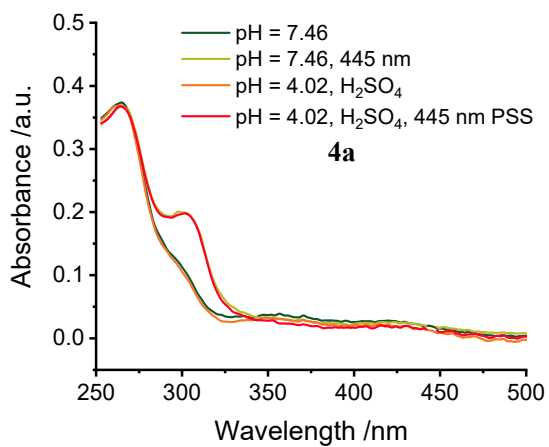
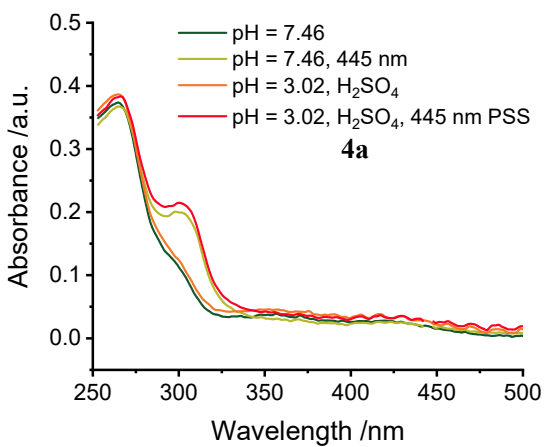
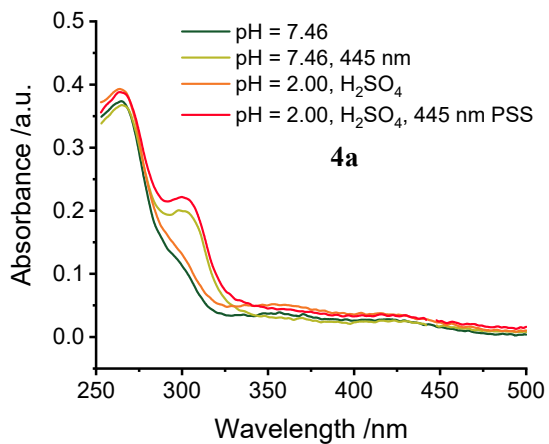
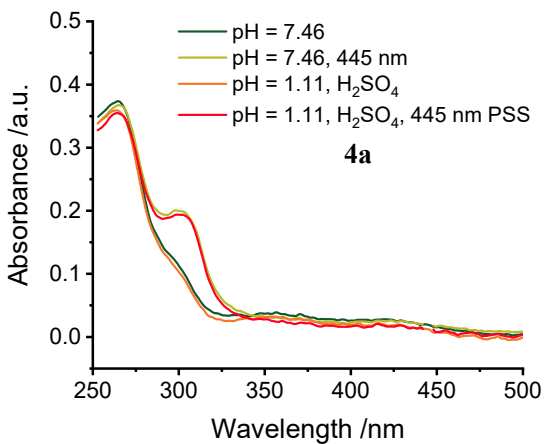
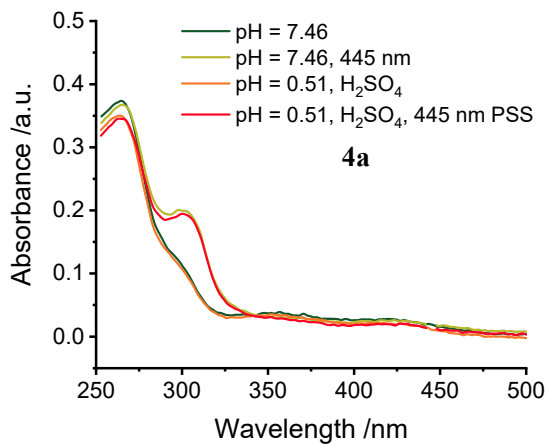
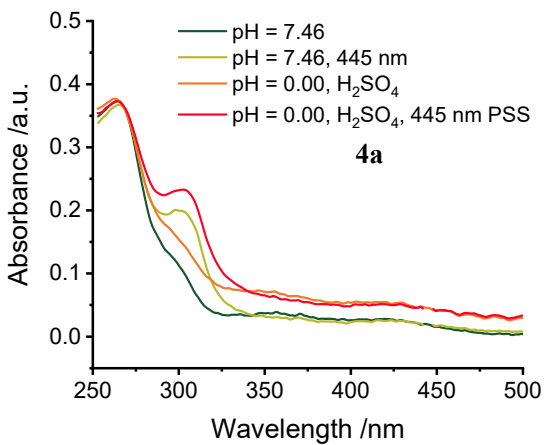


Figure S12. UV-Vis absorbance spectra of **3a** at pH = 0.00-7.00 *versus* at pH = 7.46, before photo-stimulation and at the PSS (in the dark *vs.* under the 445 nm laser irradiation at 391 mW cm^{-2}), T = 298 K, conc. = 50 μM , in PBS/MeCN = 2/1, PBS = phosphate buffer saline at specified pH.



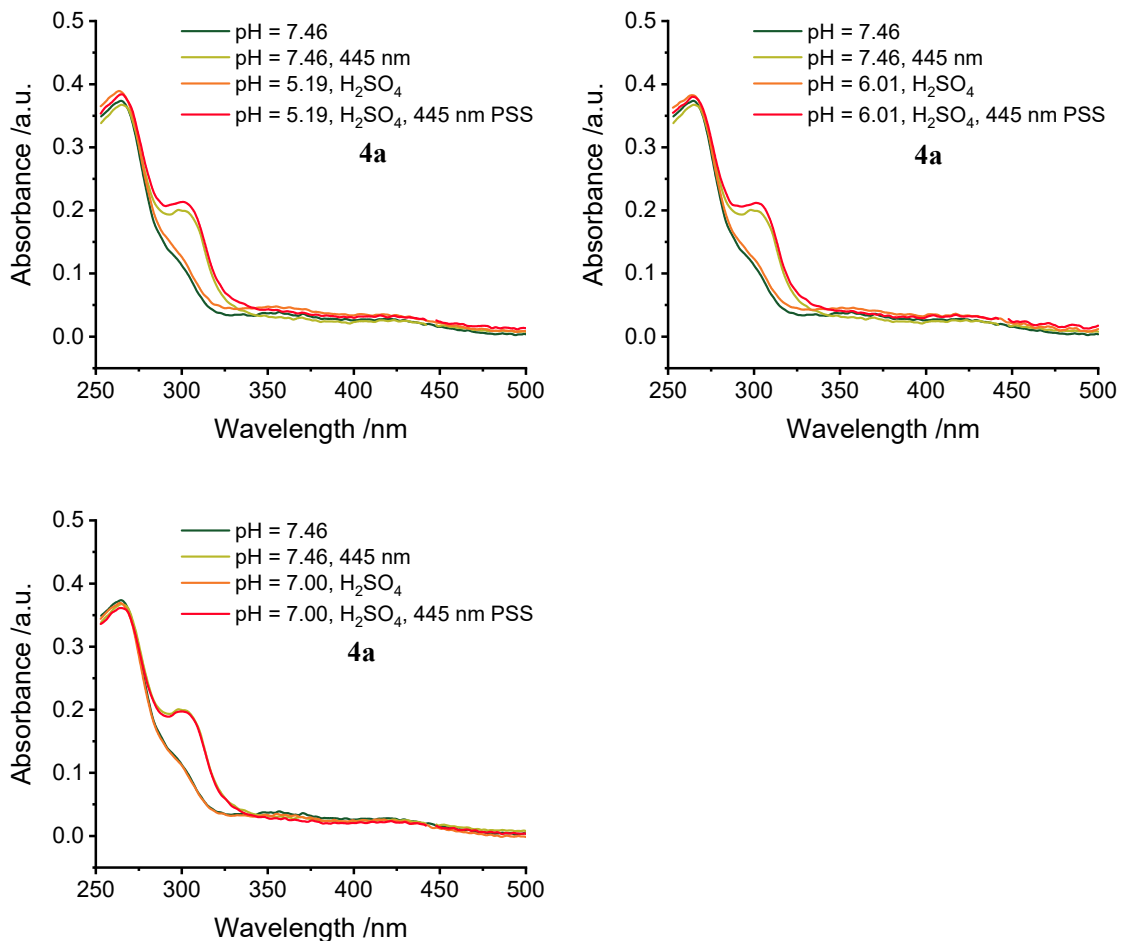


Figure S13. UV-Vis absorbance spectra of **4a** at pH = 0.00-7.00 *versus* at pH = 7.46, before photo-stimulation and at the PSS (in the dark *vs.* under the 445 nm laser irradiation at 391 mW cm⁻²), T = 298 K, conc. = 50 μM, in PBS/MeCN = 2/1, PBS = phosphate buffer saline at specified pH.

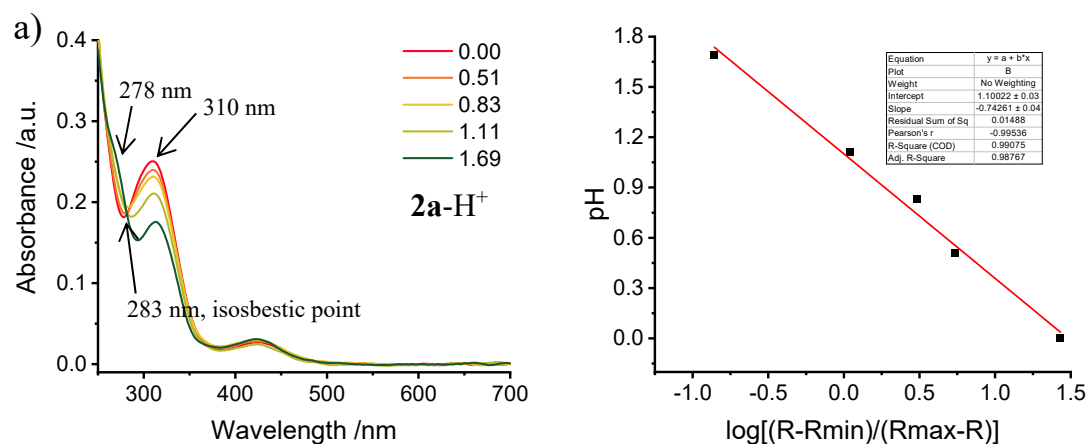
3.3 Determination of the pK_a values for cycloazopyridines, **2a** and **4a**.

A 100-microliter aliquot of the stock solution of **2a** in acetonitrile (MeCN), with a concentration of 1.0 mM, was added to a vial containing 1.9 mL of mixed buffer solution (PBS/MeCN = 2/1, PBS = phosphate buffer at indicated pH) using a micro syringe to prepare a 50 μ M solution of **2a**. Subsequently, the solution was transferred to a quartz cuvette ($l = 1.0$ cm), and the evolution in the absorbance spectrum were recorded within a pH range of 0.00 to 1.69. The pK_a value of **2a**-H⁺ was calculated by performing linear regression analysis on the absorbance data according to eq. 1.^[7] The calculation method for **4a** was consistent with that for **2a**.

$$pH = pK_a + c[\log \frac{R - R_{min}}{R_{max} - R}] \quad \text{eq. 1}$$

where R is the observed intensity ratios of the absorbance at characteristic wavelength point (For **2a**-H⁺, the maximum change of absorbance was observed at 278 nm and 310 nm. For **4a**-H⁺, the maximum change of absorbance was observed 326 nm) versus the absorbance at the isosbestic point (For **2a**-H⁺, the isosbestic absorbance was at 283 nm. For **4a**-H⁺, the isosbestic absorbance was at 281 nm.) at a given pH. R_{max} and R_{min} are the maximum and minimum limiting value of R , respectively, and c is the slope of the linear fitting curves. Finally, by fitting with the Henderson-Hasselbach equation with an intercept of the Y-axis, we were able to determine the pK_a value of **2a**-H⁺ to be 1.11, and the pK_a value of **4a**-H⁺ to be 0.42.

$$R_{max} = \frac{A_{max}}{A_{average}}, \quad R_{min} = \frac{A_{min}}{A_{average}}, \quad R = \frac{A}{A_{average}}.$$



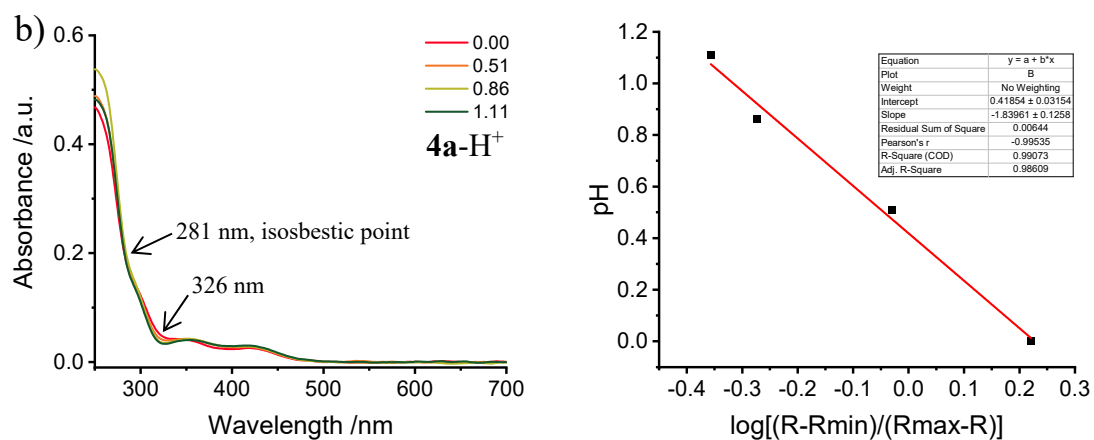


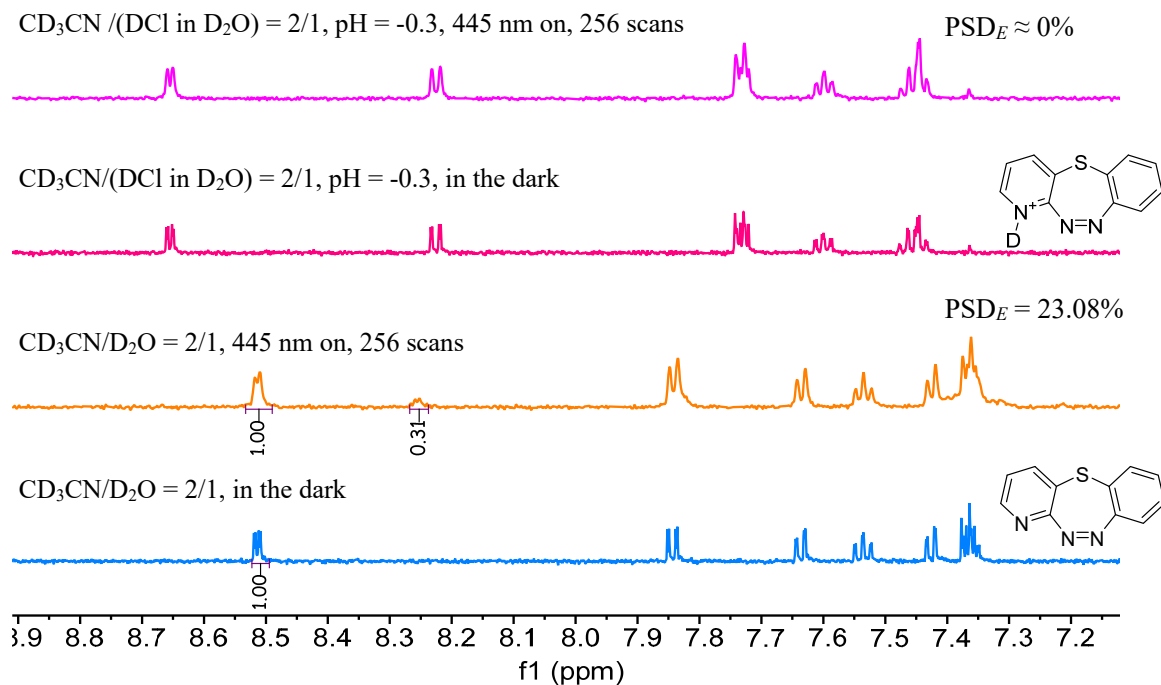
Figure S14. pH-dependent UV-Vis absorbance spectra variations of **2a** and **4a**. a) Absorbance spectra of **2a** in (50 μ M) solution in PBS/MeCN = 2/1, PBS = phosphate buffer saline at specified pH (pH ranging from 0.00 to 1.69). The Henderson-Hasselbach plot, the pH of the **2a** solution versus $\log[(R-R_{min})/(R_{max}-R)]$ with a linear fitting curve. b) Absorbance spectra of **4a** in (50 μ M) solution in PBS/MeCN = 2/1, PBS = phosphate buffer saline at specified pH (pH ranging from 0.00 to 1.11). The Henderson-Hasselbach plot, the pH of the **4a** solution versus $\log[(R-R_{min})/(R_{max}-R)]$ with a linear fitting curve.

3.4 The PSD_E quantification by the *in-situ* photo-stationary ^1H NMR analysis

^1H NMR spectrum was recorded on Brüker Avance 600 spectrometers at 600 MHz. Due to the light filtering (blocking) effect of BPTDS and DPTD as well as the photothermal effect of the T-type photoswitch, the concentration of the DPTD and BPTD samples in the NMR tube should be as low as possible for an even irradiation of light (1.0 mM in $\text{CD}_3\text{CN}/\text{D}_2\text{O}$ or in $\text{CD}_3\text{CN}/\text{D}_2\text{O}/\text{DCl}$) and an accurate determination of PSD_E (photo-stationary distribution for the *E*-isomer) at the photostationary state (PSS), while maintaining a reasonable ^1H NMR signal intensity, strong enough for better signal/noise ratio within a limited number of repetitions (scans). Because of the fast thermal $E \rightarrow Z$ isomerization rate of the *E*-BPTDs and *E*-DPTD, *in-situ* photo-stationary state was achieved via an optical-fiber guided laser stimulation into the NMR acquisition chamber of the NMR instrument. Adjusting the power of the 445 nm laser and thermostatic control in the NMR chamber is also necessary for determining the ratio of *E*-/*Z*-isomer at the PSS. Then the PSD_E values were quantified by integrating the areas corresponding signal peaks for *E*- and *Z*-isomers and derived by using the following equation.

$$\text{PSD}_E = \text{integrated area of } E\text{-isomer} / (\text{integrated areas of } Z + E\text{-isomers}).$$

1a:



3a:

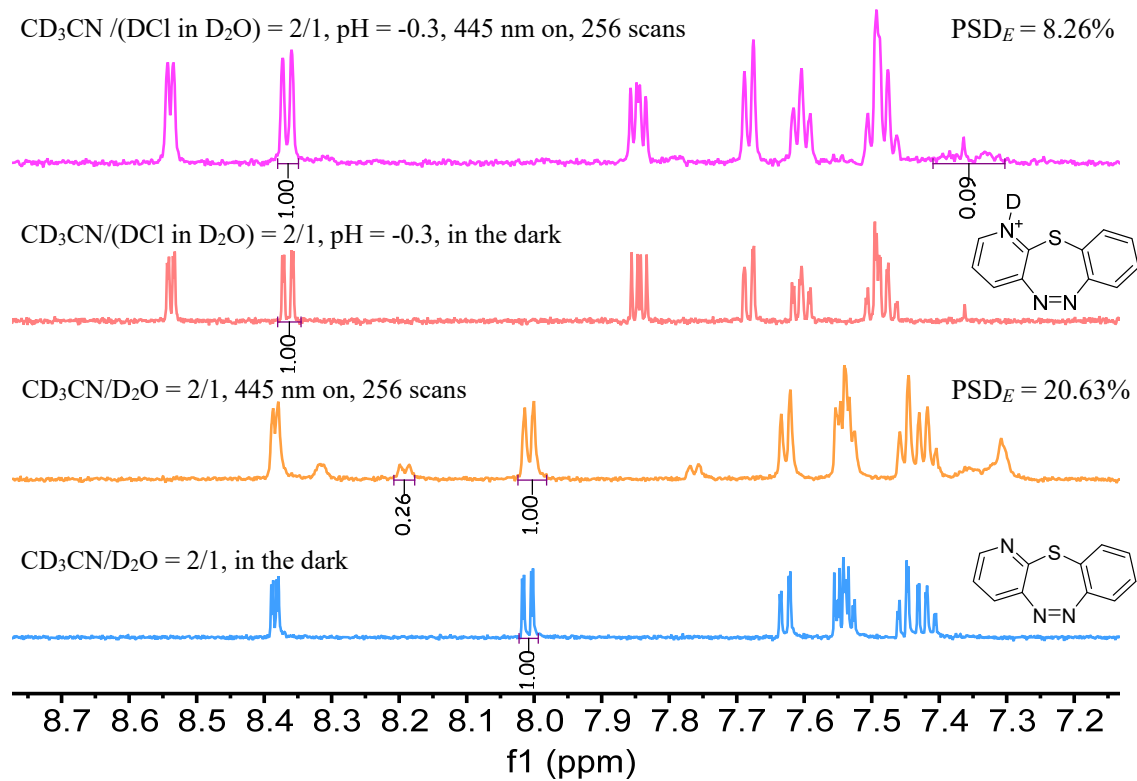
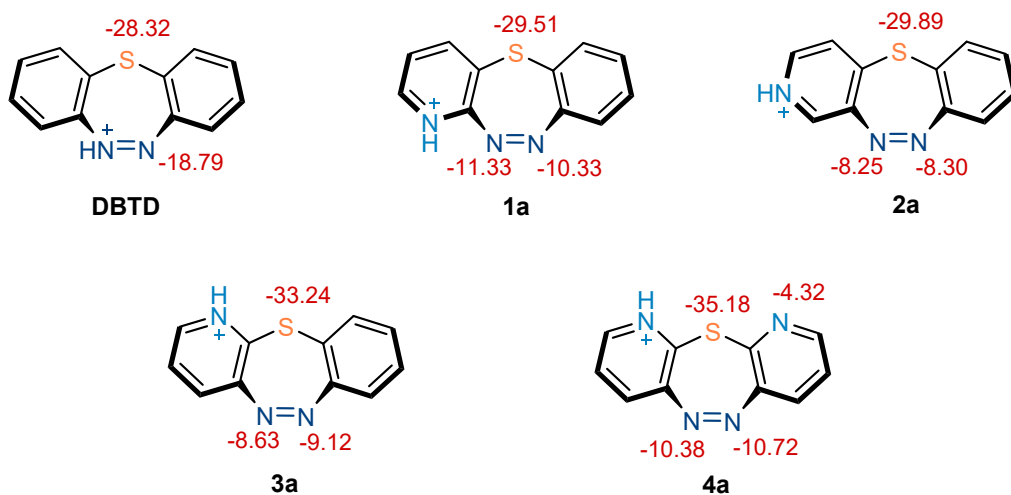


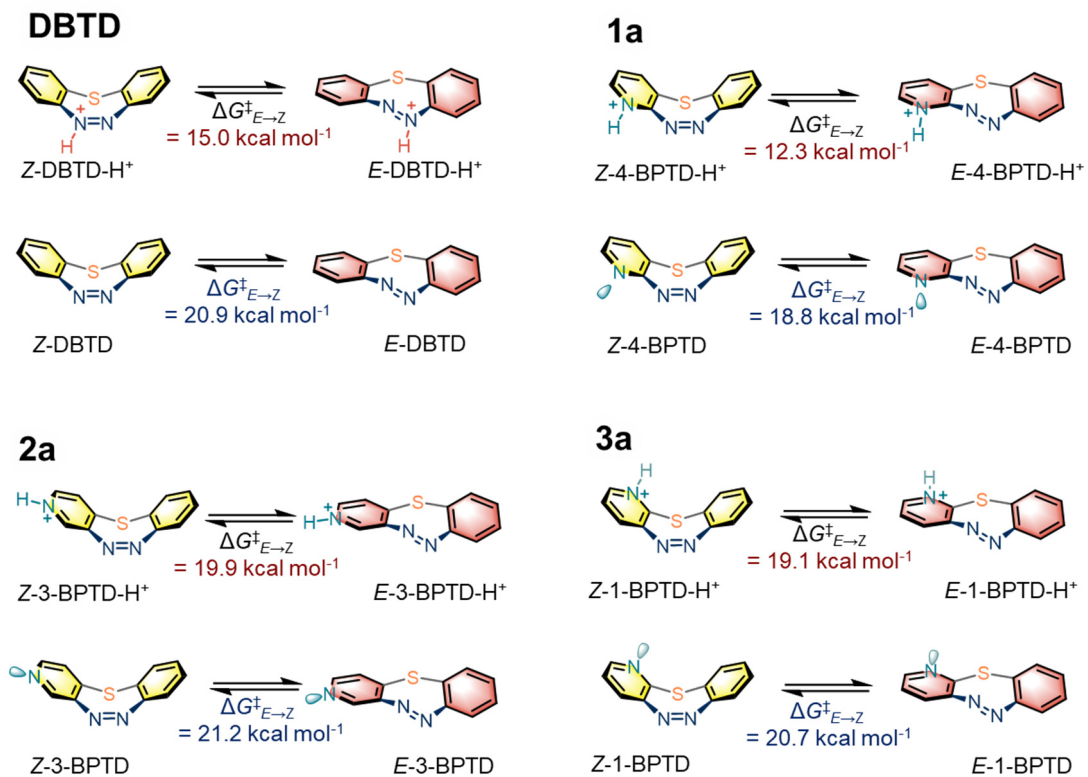
Figure S15. *In-situ* photo-stationary state ¹H NMR spectra for **1a** and **3a** for determination of the PSD_E values before and after protonation. ¹H NMR spectra before and under continuous exposure of 445 nm laser in CD₃CN/D₂O (v/v = 2/1) versus CD₃CN/DCl (35% in D₂O) (v/v = 2/1) as solvent, pH = -0.33, at 298K, Conc. = 1.0 mM. Power density for the 445 nm laser = 391 mW cm⁻².

3.5 Theoretical calculations after the second protonation of DBTD and 1a-4a, the corresponding theoretical absorbance spectra

3.5.1 Theoretical calculations for after the second protonation of Z-DBTD-H⁺ and Z-1a-H⁺ to Z-4a-H⁺.



3.5.2 Thermal free energy barriers for the transition state from the *E*-isomer to the *Z*-isomer of Z-DBTD, and Z-1a to Z-4a before and after protonation.



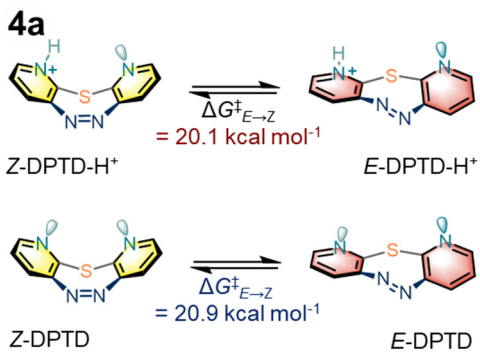


Figure S16. The free energy barriers of the $E \rightarrow Z$ isomerization for DBTD *vs.* DBTD- H^+ , **1a** *vs.* **1a-H** $^+$, **2a** *vs.* **2a-H** $^+$, **3a** *vs.* **3a-H** $^+$, and **4a** *vs.* **4a-H** $^+$.

3.5.3 The possible macrocyclic hydrogen-bonding structures interacting with water molecules for the protonated forms of **Z-1a**, **Z-3a**, and **Z-4a**, versus **Z-2a** in MeCN:H₂O =1:1 solution in the photoswitching process.

We preliminarily hypothesize that BPTD **1a-H** $^+$, BPTD **3a-H** $^+$, and DPTD **4a-H** $^+$, due to the *ortho*-position of the pyridine-N atom relative to the sulfur atom or to the azo-nitrogen atom (Figure S17, below), could form relatively rigid cyclic complexes with at least two water molecules via hydrogen bonding. We have obtained the optimized structures of the complexes formed between BPTD **1a-H** $^+$, BPTD **3a-H** $^+$, DPTD **4a-H** $^+$ with water molecules at the B3LYP(D3BJ)/def2-SVP/IEFPCM (MeCN:H₂O=1:1) theoretical level (Figure S18, below), confirming the rationality of such hydrogen-bonded macrocyclic interactions. Specifically, upon protonation of the pyridine nitrogen at the 4-position of BPTD **1a**, it converged into a hydrogen-bonded cyclic structure with the N atom on the azo through the bridging with two water molecules. This hydrogen-bonding formation reduces the energy gap of the $\pi \rightarrow \pi^*$ transition, leading to a red-shift of absorption wavelength of related transition bands. Similar cyclic hydrogen-bonding structures might also be available for BPTD **3a-H** $^+$ and DPTD **4a-H** $^+$ (Figure S18).

In contrast, due to the larger spatial distance between the pyridinyl-N atom and the S atom (*para*-position) or the azo-N atom (*meta*-position) in BPTD **2a-H** $^+$, it is unlikely to form such a rigid hydrogen-bonded macrocycle (Figure S17, below). Attempts to optimize the structure with the interactions between BPTD **2a-H** $^+$ and H₂O also did not yield a convergent result akin to that of **1a-H** $^+$. Additionally, the electron-withdrawing group (EWG) effect of the pyridinium ion may restrict the delocalization of π -orbital electrons, potentially increasing the energy gap of the $\pi \rightarrow \pi^*$ transition and thus resulting in a slightly blue-shift of the absorbance band.

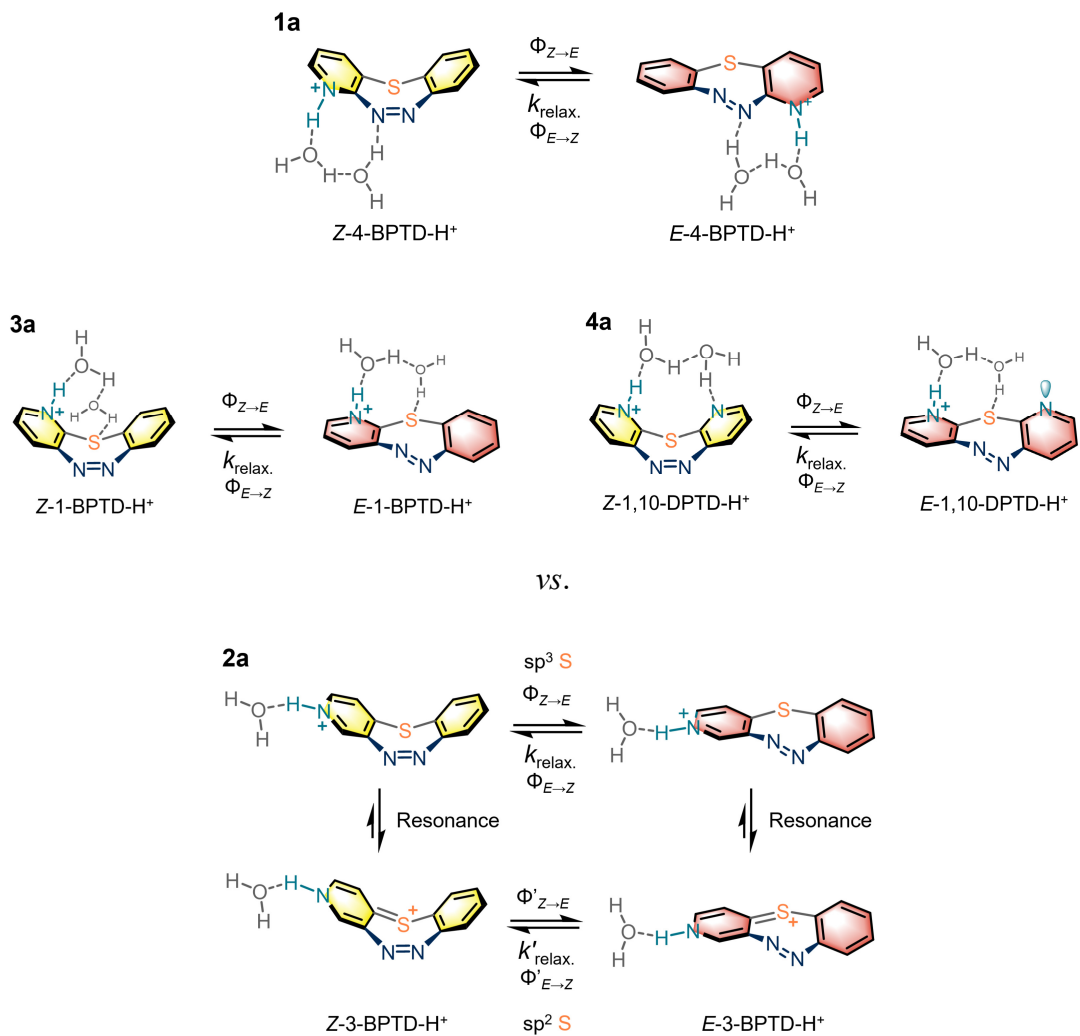


Figure S17. Possible macrocyclic hydrogen-bonding structures interacting with water molecules for the protonated forms of Z-1a-H⁺, Z-3a-H⁺, and Z-4a-H⁺, versus Z-2a-H⁺ in MeCN:H₂O = 1:1 solution in the T-type photoswitching cycles.

3.5.4 The converged theoretical macrocyclic structures with hydrogen-bonding with two water molecules calculated for both Z- and E- isomer of 1a-H⁺, 3a-H⁺, and 4a-H⁺.

We propose several structural models for **1a**, **3a** and **4a** in acidic aqueous solutions. Through structural comparative analysis, we hypothesize that protonation of the *ortho*-position pyridine nitrogen in 4-BPTD (**1a**), 1-BPTD (**3a**), and DPTD (**4a**) (relative to the sulfur atom) may facilitate the formation of hydrogen-bonded macrocyclic structures with water molecules, thereby accelerating the thermal relaxation rate. We have obtained the optimized structures of the complexes formed between BPTD **1a**-H⁺, BPTD **3a**-H⁺, DPTD **4a**-H⁺ with two water molecules in both Z- and E-configuration at the B3LYP(D3BJ)/def2-SVP/IEFPCM (MeCN:H₂O=1:1) theoretical level (Figure S18, below), confirming the rationality of such hydrogen-bonded macrocyclic interactions.

In contrast, as shown in the Figure S17, the *para*-position pyridine nitrogen (relative to the sulfur atom) in 3-BPTD (**2a**) presents a spatial distance range that precludes such macrocyclic

hydrogen bonding interaction with high rigidity. Moreover, protonation-induced positive charge on the pyridine of 3-BPTD-H⁺ (**2a**-H⁺) can be delocalized to the sulfur atom via resonance, forming possible an sp² hybridized sulfonium ion. This unique electronic configuration may stabilize the *E*-3-BPTD-H⁺ conformer via sp² bond angle optimization, prolonging its isomer lifetime and resulting in the observed apparent relaxation deceleration.

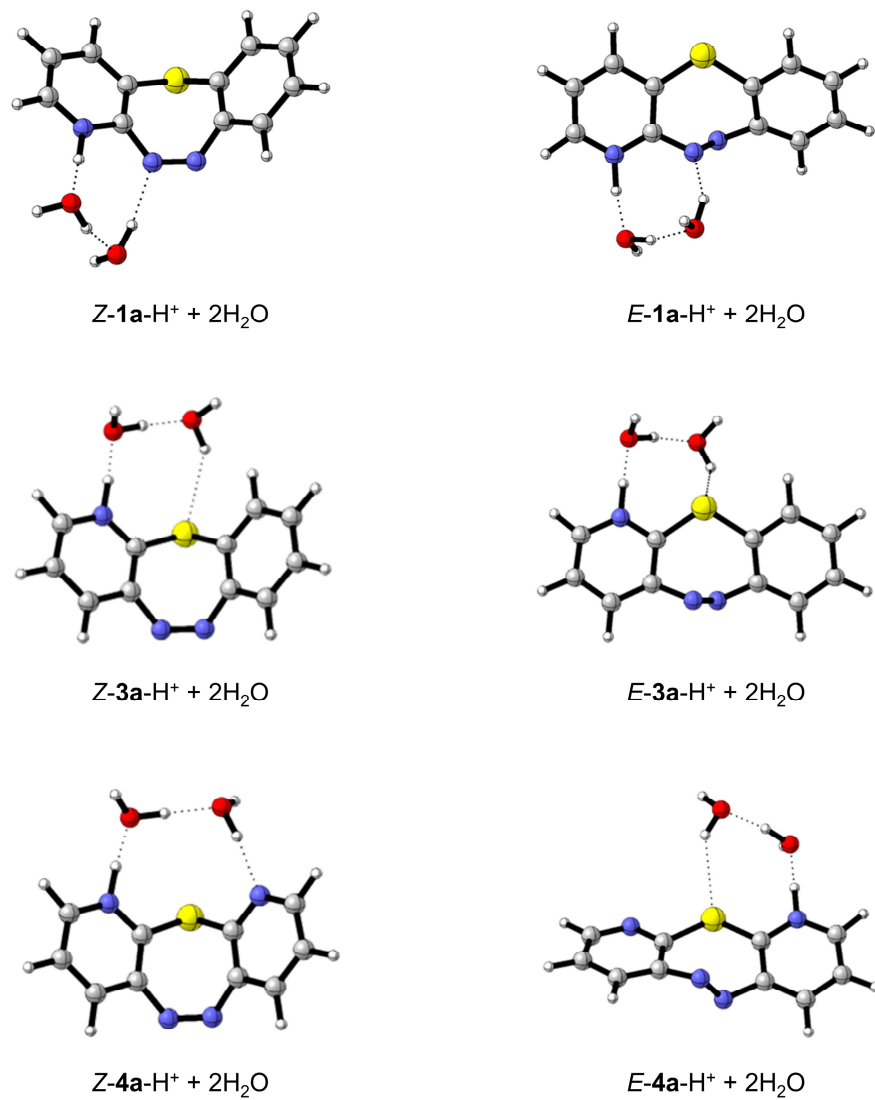
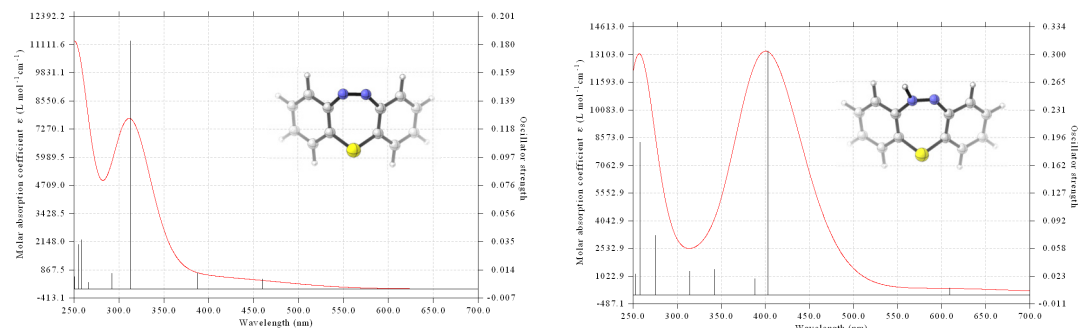


Figure S18. The hydrogen-bonded macrocyclic structure of both *Z*- and *E*- isomer of **1a**-H⁺, **3a**-H⁺, and **4a**-H⁺ calculated at the B3LYP(D3BJ)/def2-SVP/IEFPCM(MeCN:H₂O = 1:1) theoretical level.

3.5.5 Theoretical predicted absorbance spectra of DBTD (left side), and DBTD-H⁺ (right side, protonation on the azo moiety).



3.5.6 Theoretical absorbance spectra of **1a**, **1a**-H⁺ (protonation on the pyridine moiety) and **1a**-H2⁺ (protonation on the azo moiety closer to the pyridine).

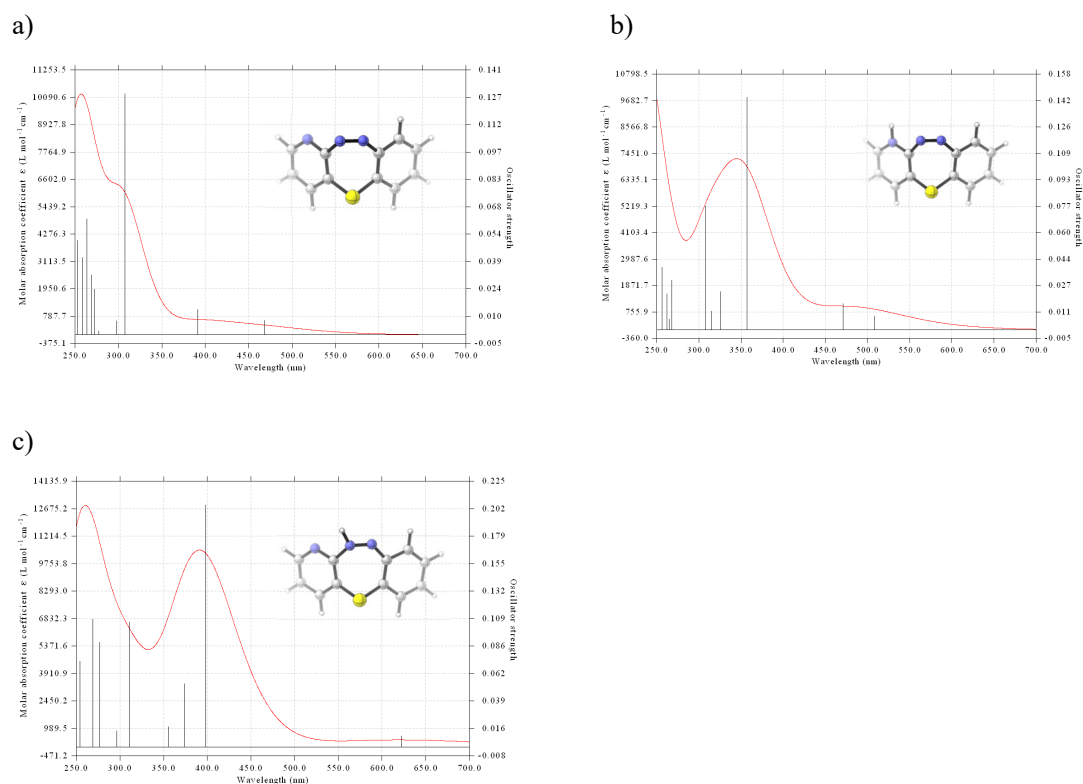


Figure S19. a) Theoretical absorbance spectra of **1a**, b) Theoretical absorbance spectra of **1a**-H⁺ (protonation on the pyridine moiety), c) Theoretical absorbance spectra of **1a**-H2⁺ (protonation on the azo moiety closer to the pyridine).

3.5.7 Theoretical absorbance spectra of **2a, **2a-H⁺** (protonation on the pyridine moiety) and **2a-H2⁺** (protonation on the azo moiety closer to the pyridine).**

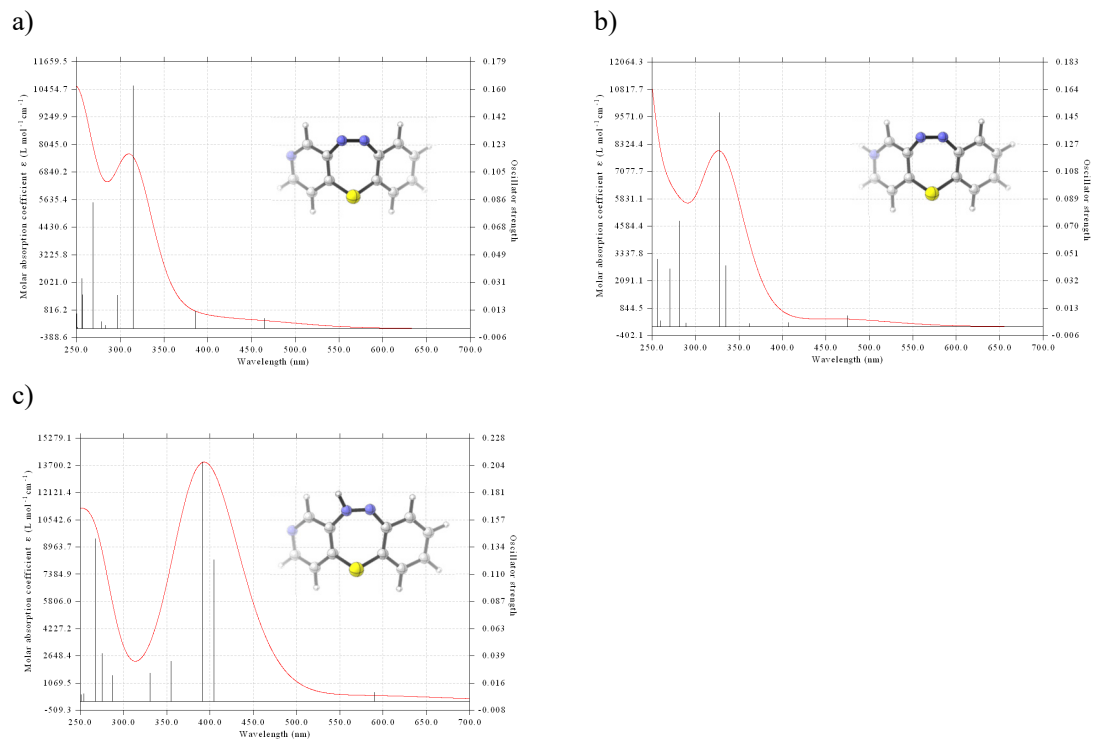
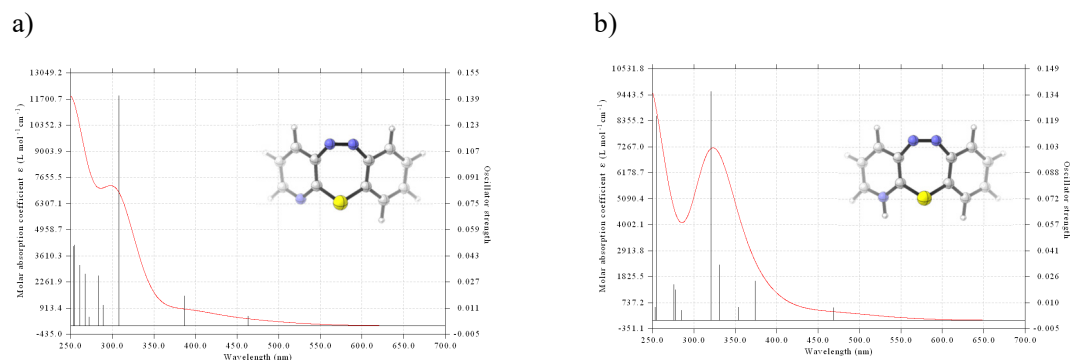


Figure S20. a) Theoretical absorbance spectra of **2a**, b) Theoretical absorbance spectra of **2a-H⁺** (protonation on the pyridine moiety), c) Theoretical absorbance spectra of **2a-H2⁺** (protonation on the azo moiety closer to the pyridine).

3.5.8 Theoretical absorbance spectra of **3a, **3a-H⁺** (protonation on the pyridine moiety) and **3a-H2⁺** (protonation on the azo moiety closer to the pyridine).**



c)

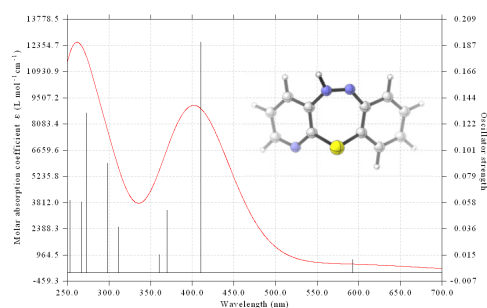
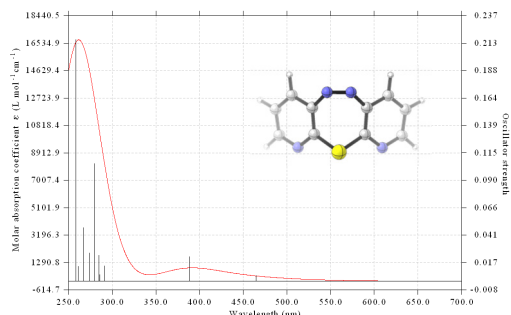


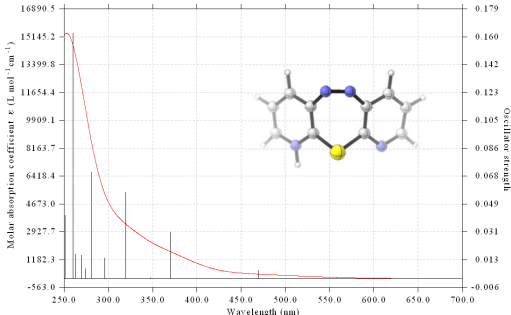
Figure S21. a) Theoretical absorbance spectra of **3a**, b) Theoretical absorbance spectra of **3a**-H⁺ (protonation on the pyridine moiety), c) Theoretical absorbance spectra of **3a**-H2⁺ (protonation on the azo moiety closer to the pyridine).

3.5.9 Theoretical absorbance spectra of **4a**, **4a**-H⁺ (protonation on the pyridine moiety) and **4a**-H2⁺ (protonation on the azo moiety).

a)



b)



c)

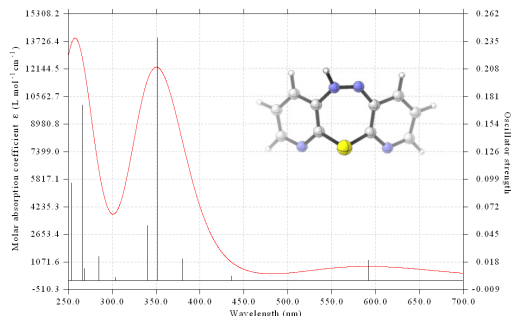


Figure S22. a) Theoretical absorbance spectra of **4a**, b) Theoretical absorbance spectra of **4a**-H⁺ (protonation on the pyridine moiety), c) Theoretical absorbance spectra of **4a**-H2⁺ (protonation on the azo moiety).

3.6 The electronic transition characteristics of Z-1a to Z-4a by DFT calculation

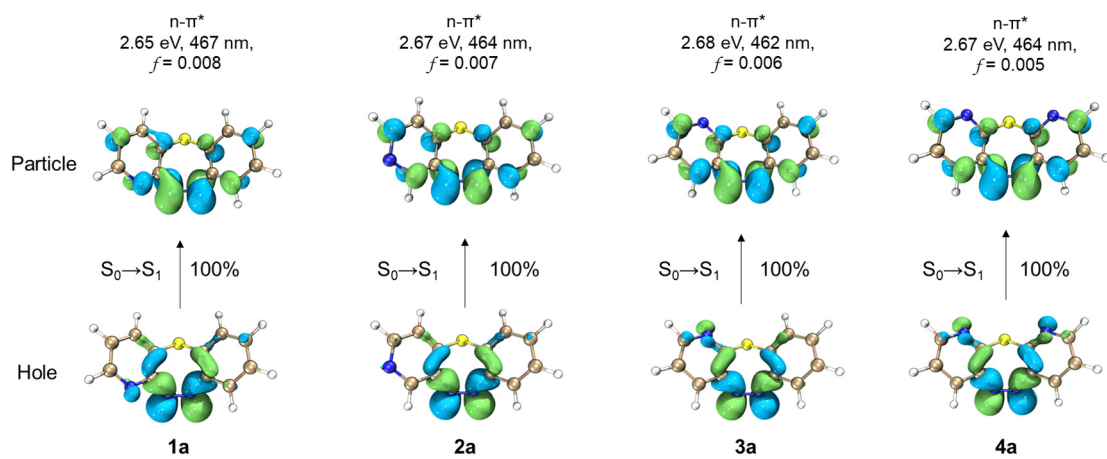


Figure S23. Vertical excitation energies and NTOs of the $S_0 \rightarrow S_1$ transition for Z-BPTDs and Z-DPTD (**1a-4a**) in Z-isomers, calculated at the TD-PBE0/def2-TZVP/IEFPCM (MeCN:H₂O = 1:1) level of theory. The oscillator strength (f) and eigenvalue of each NTO pair were shown. The isosurface (isovalue = 0.04) plots of NTO were performed with VMD1.9.3.

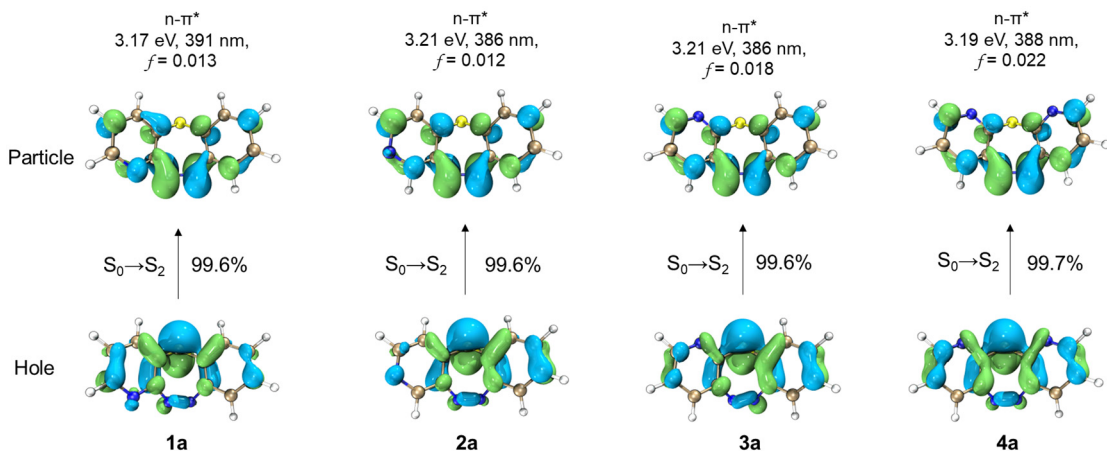


Figure S24. Vertical excitation energies and NTOs of the $S_0 \rightarrow S_2$ transition for BPTDs and DPTD (**1a-4a**) in Z-isomers, calculated at the TD-PBE0/def2-TZVP/IEFPCM (MeCN:H₂O = 1:1) level of theory. The oscillator strength (f) and eigenvalue of each NTO pair were shown. The isosurface (isovalue = 0.04) plots of NTO were performed with VMD1.9.3.

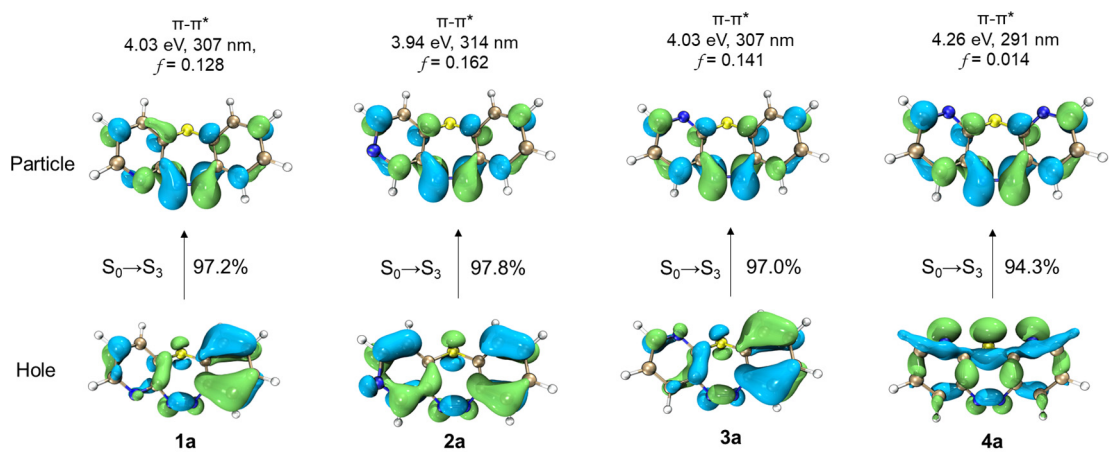


Figure S25. Vertical excitation energies and NTOs of the $S_0 \rightarrow S_3$ transition for BPTDs and DPTD (**1a-4a**) in Z-isomers, calculated at the TD-PBE0/def2-TZVP/IEFPCM (MeCN:H₂O = 1:1) level of theory. The oscillator strength (f) and eigenvalue of each NTO pair were shown. The isosurface (isovalue = 0.04) plots of NTO were performed with VMD1.9.3.

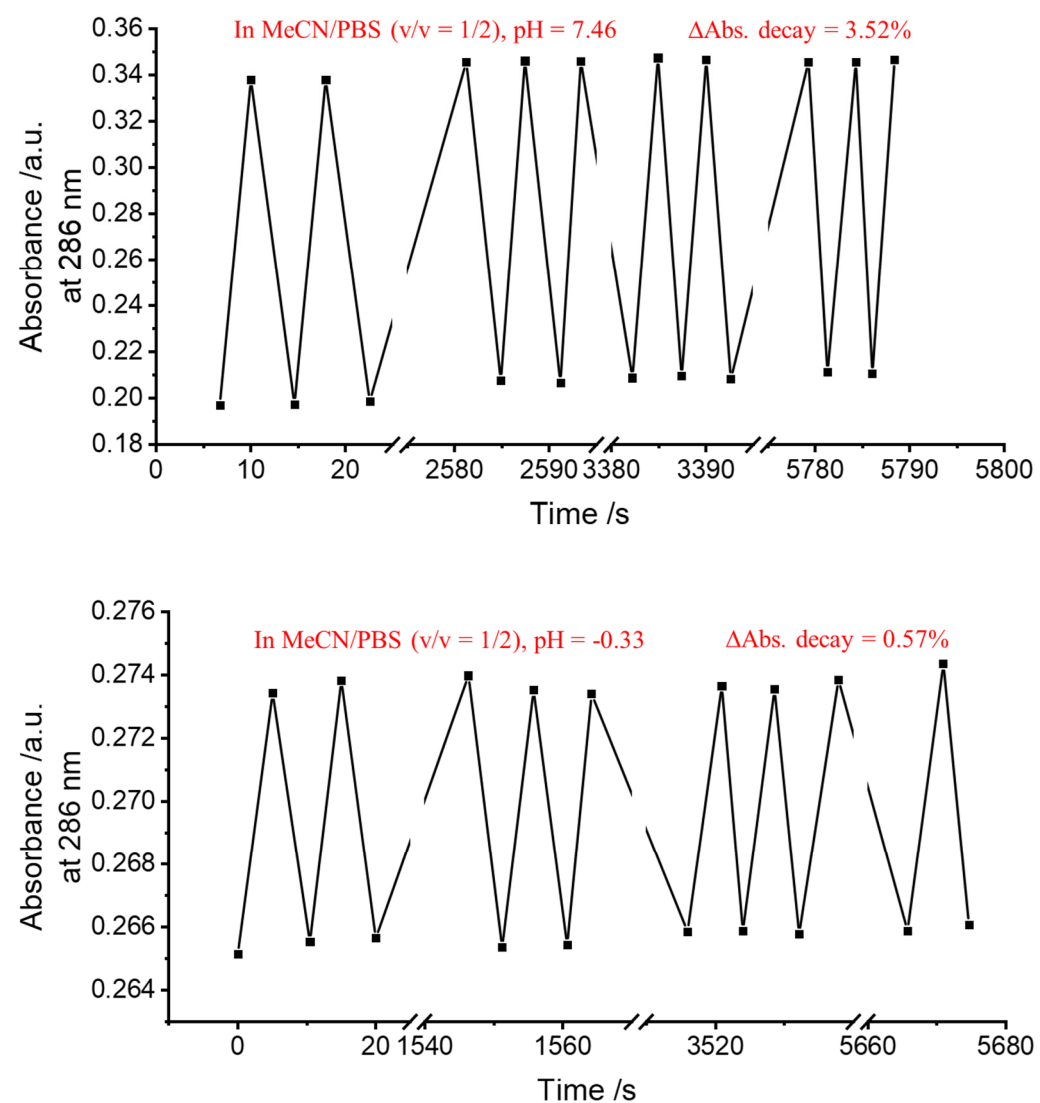
3.7 Photo-antifatigue studies for DBTD, **1a**, and **3a**. And photo-switching kinetic studies for DBTD, and **1a-4a**, under intermittent irradiation of 445 nm laser under various pH gradients.

The rate constants for the photo-isomerization (k_{light}) and thermal reversion (k_{relax}) processes of BPTDs and DPTD were determined through dynamic spectral tracking via a Sarspec optical fiber STD UV-Vis spectrophotometer. In a temperature-controlled fiber-optic cuvette holder, the optical path for photo-stimulating with a 445 nm laser and the absorbance detection optical path for ultraviolet-visible absorbance spectroscopy are arranged perpendicular and orthogonal to each other. This setup also involved intermittent illumination with the programmable 445 nm laser source (power density at 445 nm = 391 mW cm⁻²) at concentrations of either 50 μ M or 100 μ M in a mixed solvent of MeCN/PBS (v/v = 1/2, PBS = phosphate buffer saline at the indicated pH). A quartz beam expander was used to adjust the laser fiber output, ensuring an appropriate laser beam spot size as it traversed from the emitting surface of the solid-state laser to the cuvette, aiming for a uniform and even laser exposure spot on a quartz cuvette. BPTDs/DPTD stock solutions were diluted into the designated buffers to achieve the desired final concentration in sample vials, which were then transferred into the quartz cuvette with a 1.0 \times 1.0 cm optical path in a thermostatic controller. Absorbance evolution at the characteristic wavelength was dynamically monitored as

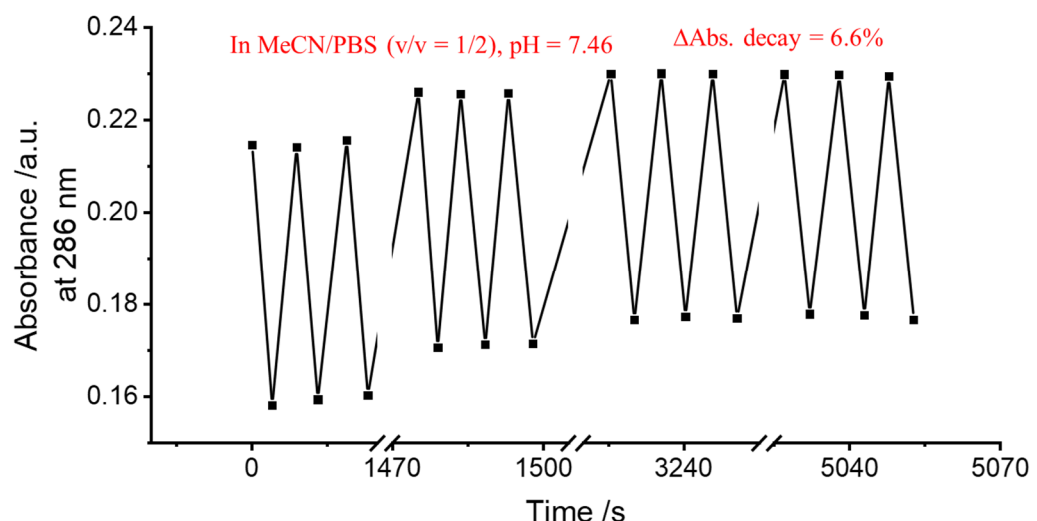
an indicator of the presence and dynamic conversion of the *E*-isomers, allowing us to capture the necessary data points for kinetic analysis. These datasets were subsequently recorded and analyzed using the Lightscan software package. During data processing, the "exponential" function within Origin Pro software was utilized to generate nonlinear fitting curves. Additionally, to further investigate the photo-stability of BPTDs and DPTD (concentration = 100 μ M) under acidic conditions, fatigue resistance tests were also performed on DBTD and **1a-4a** at pH = 7.46 and pH = -0.33, respectively, under intermittent 445 nm illumination.

3.7.1 The anti-fatigue tests were conducted during the back-and-forth photo-switching tests at pH values of -0.33 and 7.46.

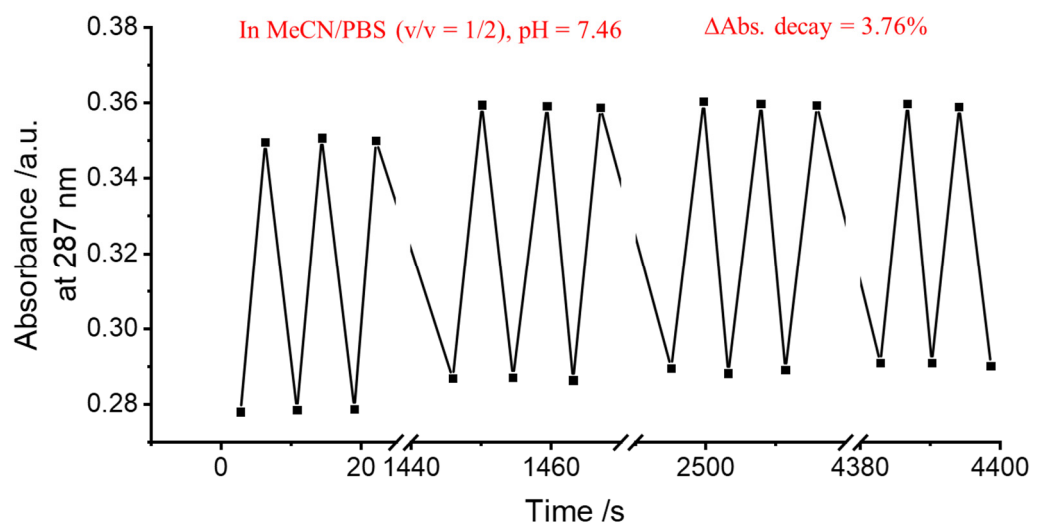
a) DBTD



b) **1a**



c) **3a**



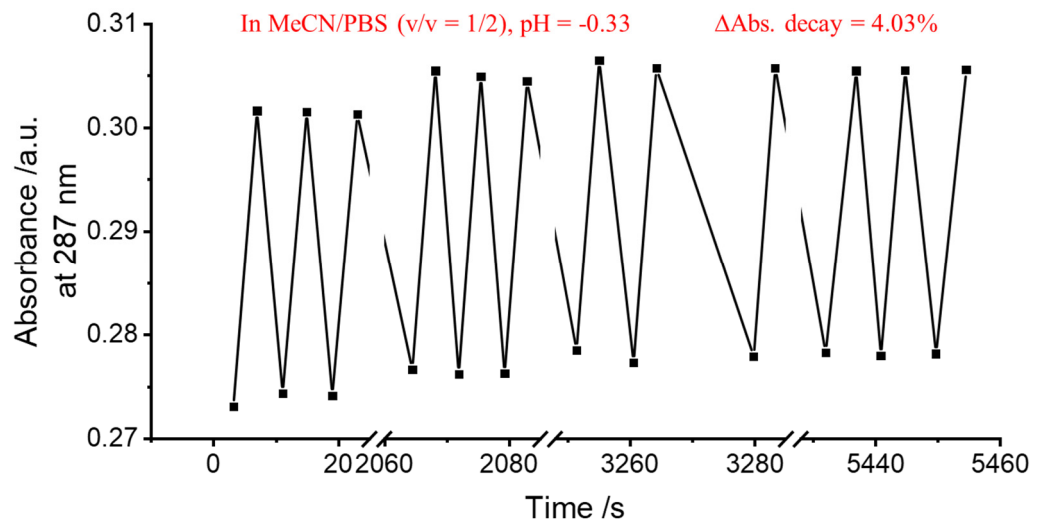
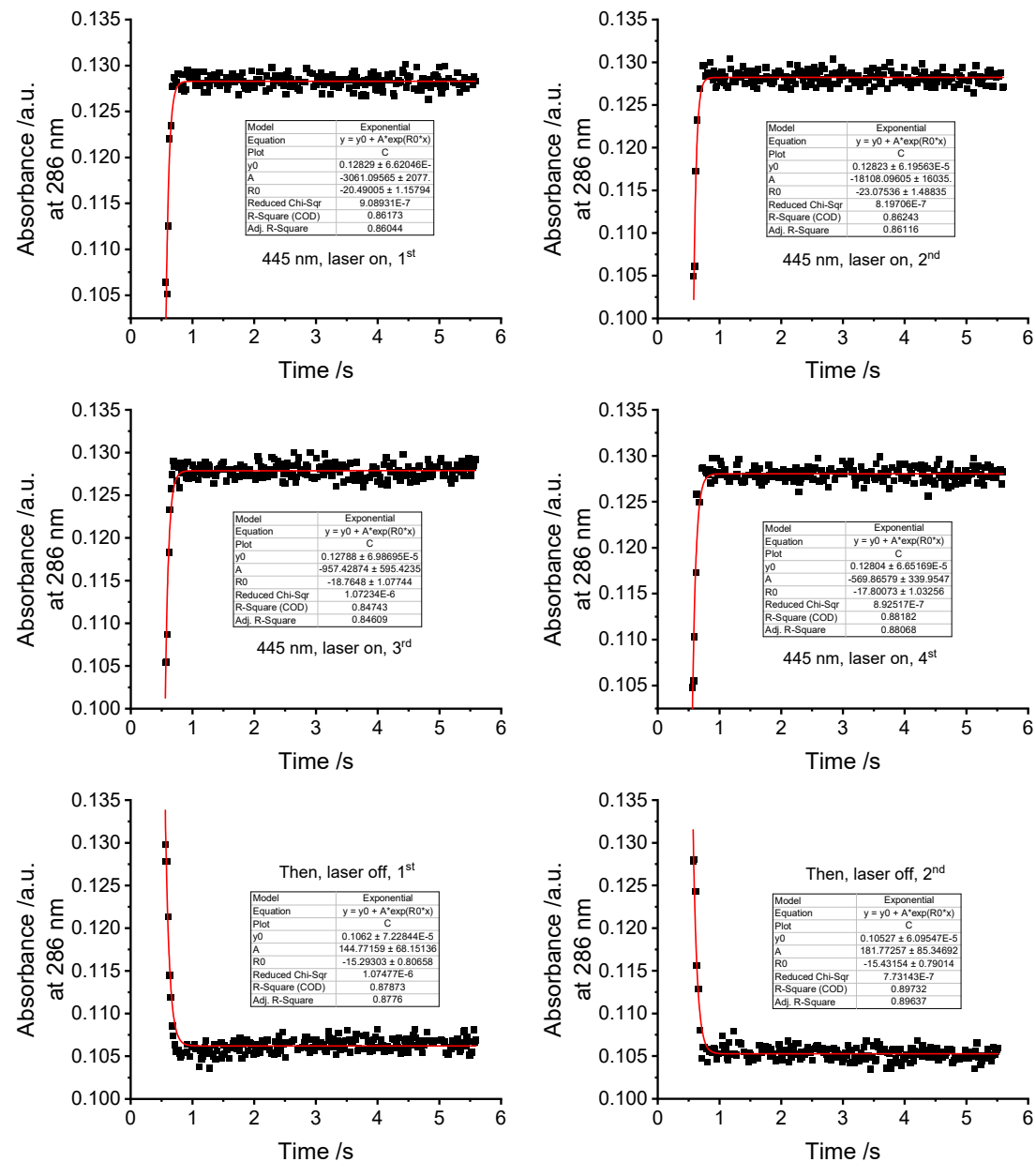
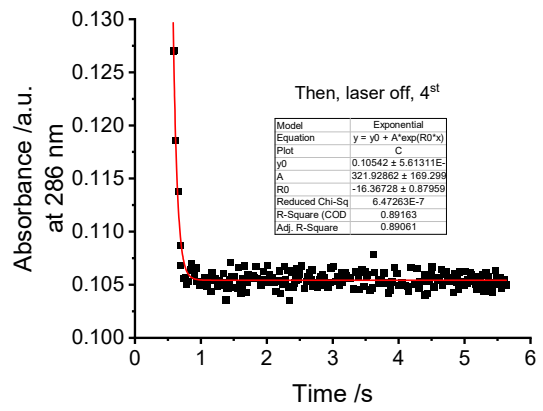
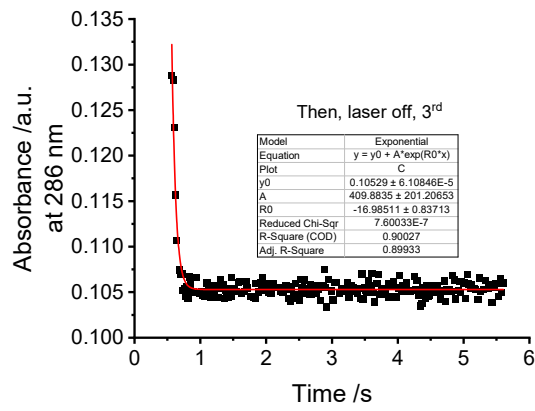


Figure S26. Investigation on the anti-fatigue performance of a) DBTD, b) **1a**, and c) **3a** after back-and-forth photoswitching process between the Z-isomer and the PSS induced by the 445 nm laser illumination via UV-Vis absorbance tracking at specified wavelength with the decay rate shown. Conditions: in PBS/MeCN, pH = -0.33 vs. 7.4, conc. = 100 μ M, T= 298 K, Power density of the 445 nm laser = 391 mW cm^{-2} .

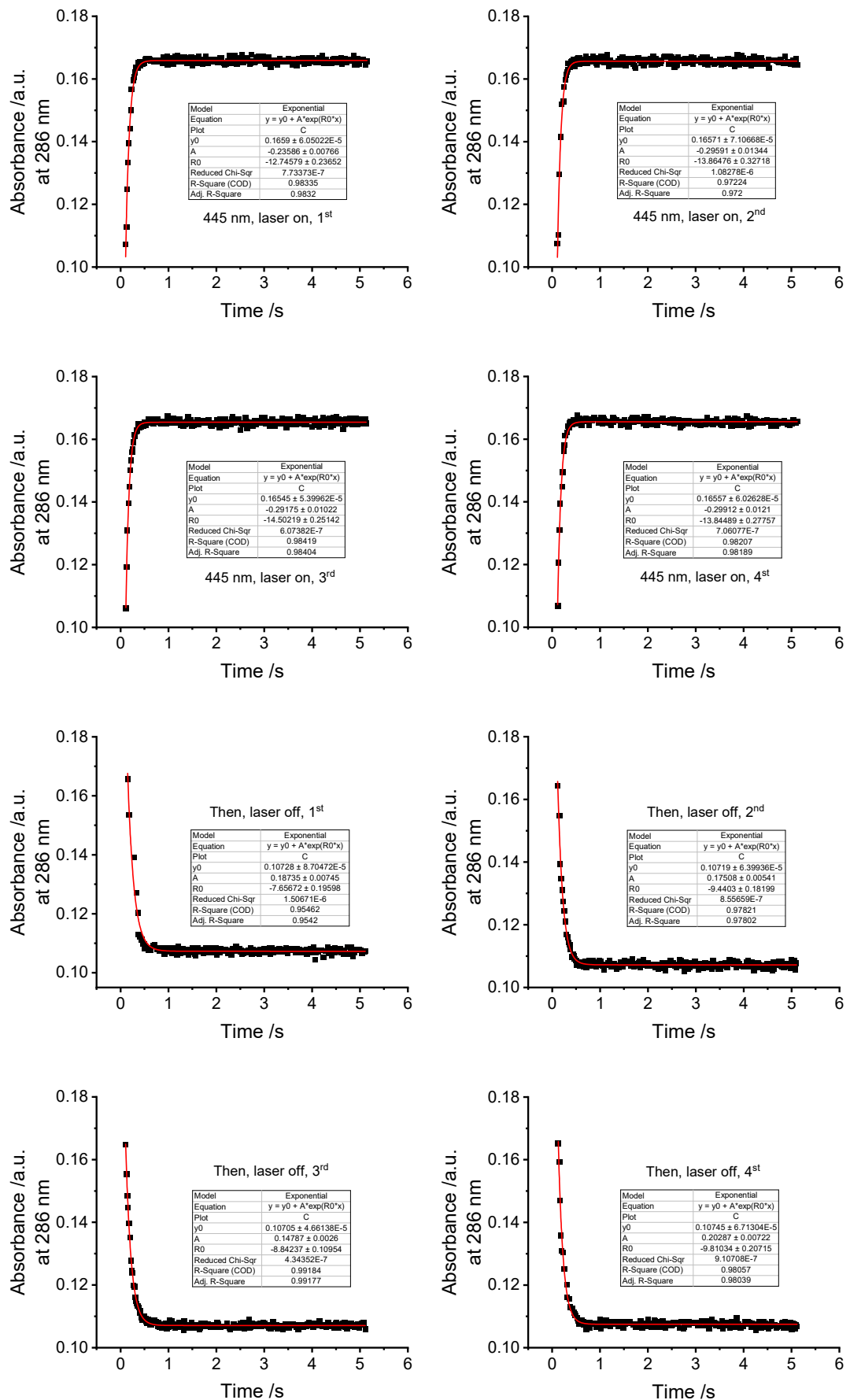
3.7.2 Photo-switching kinetics studies for DBTD and **1a-4a, under intermittent irradiation of 445 nm laser in various pH environment.**

a) DBTD, pH = 0.51

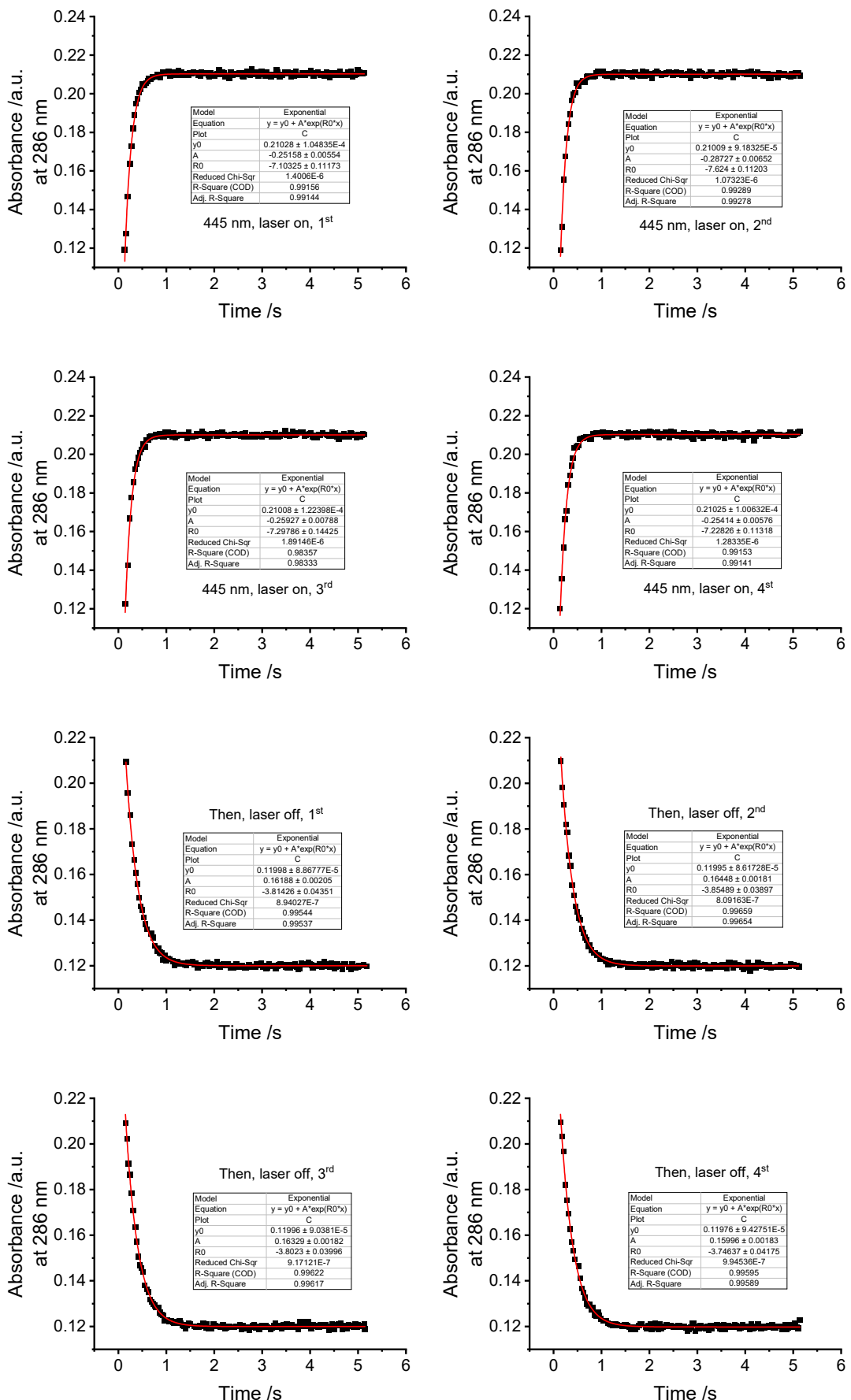




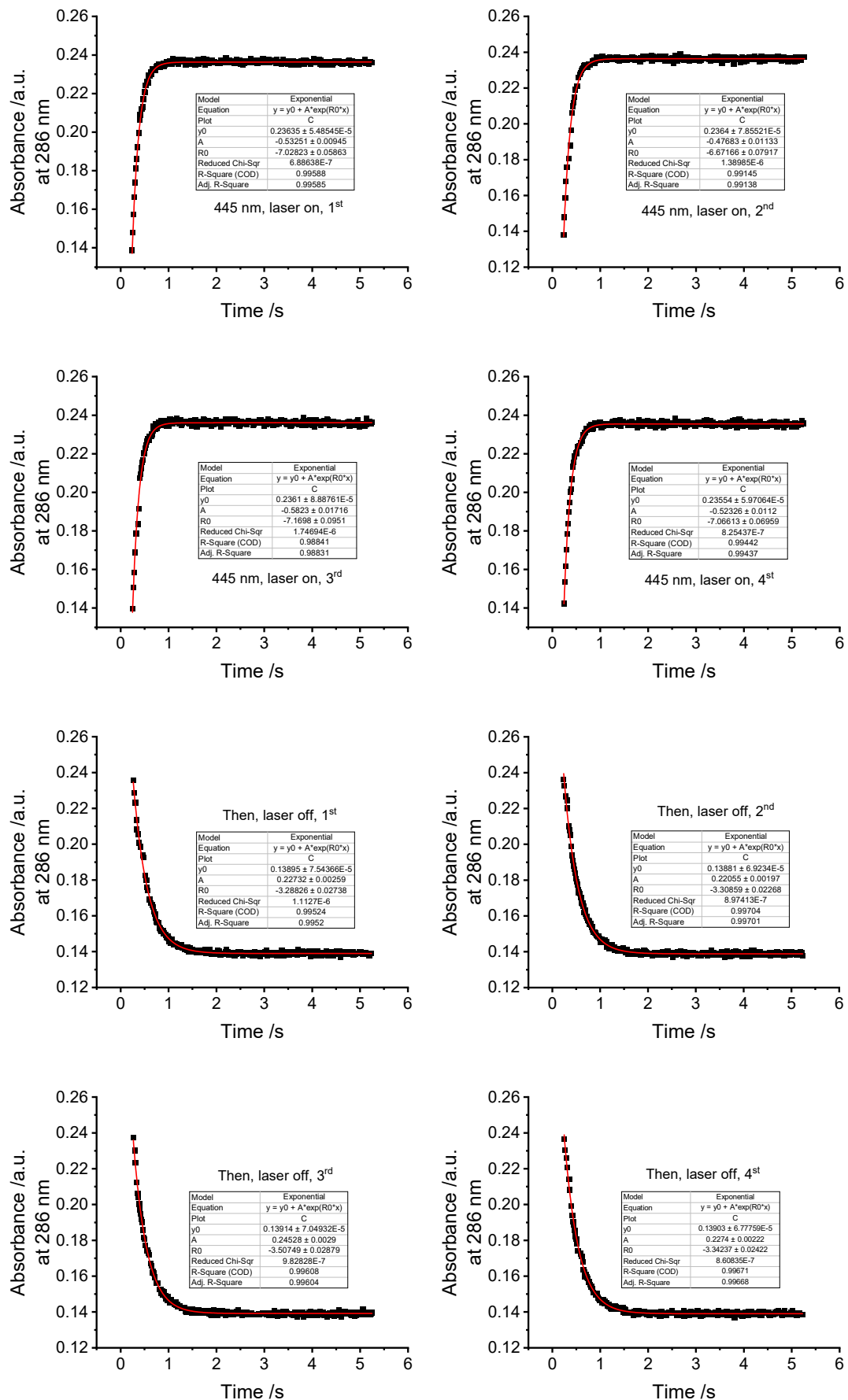
b) DBTD, pH = 1.11



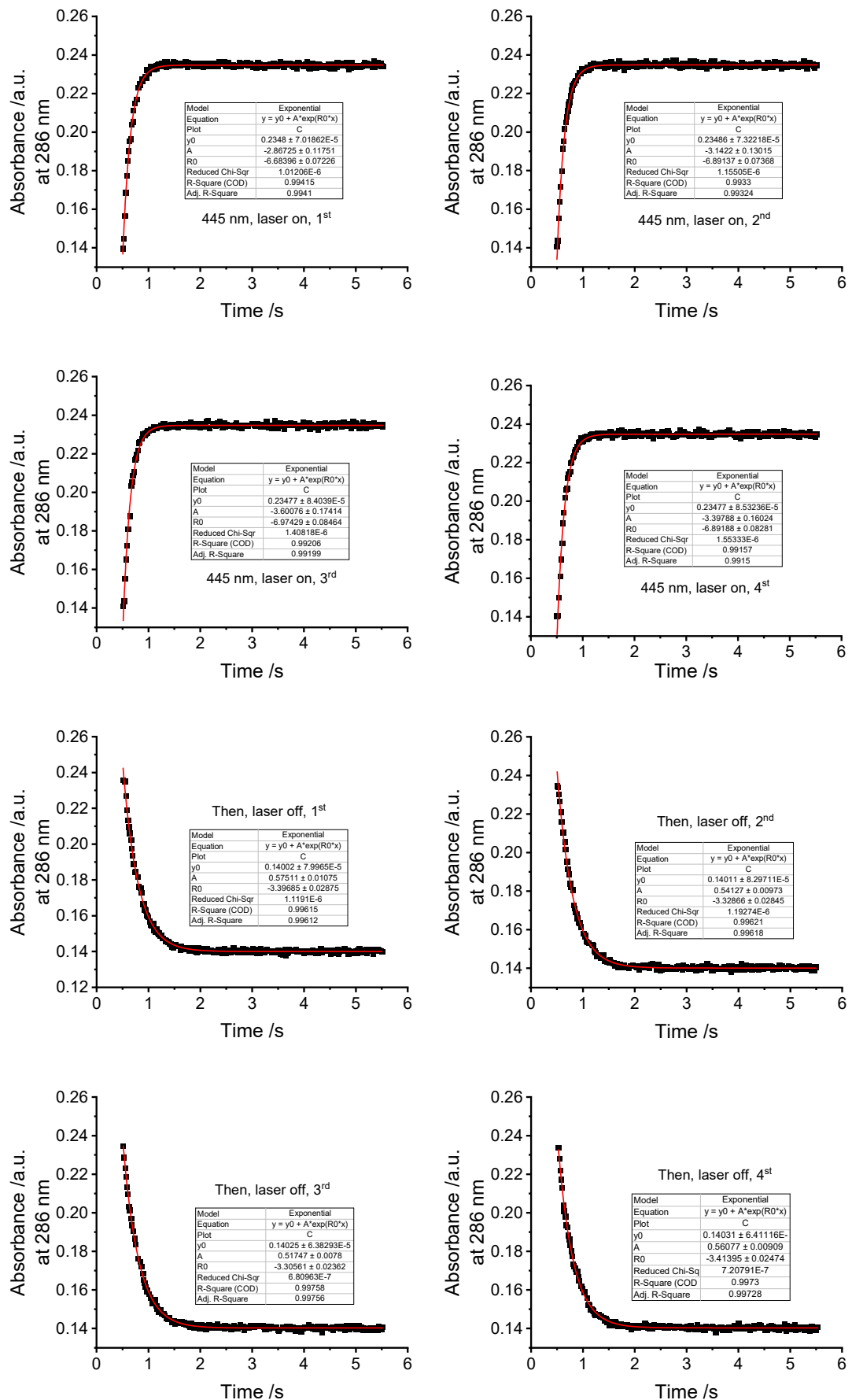
c) DBTD, pH = 2.00



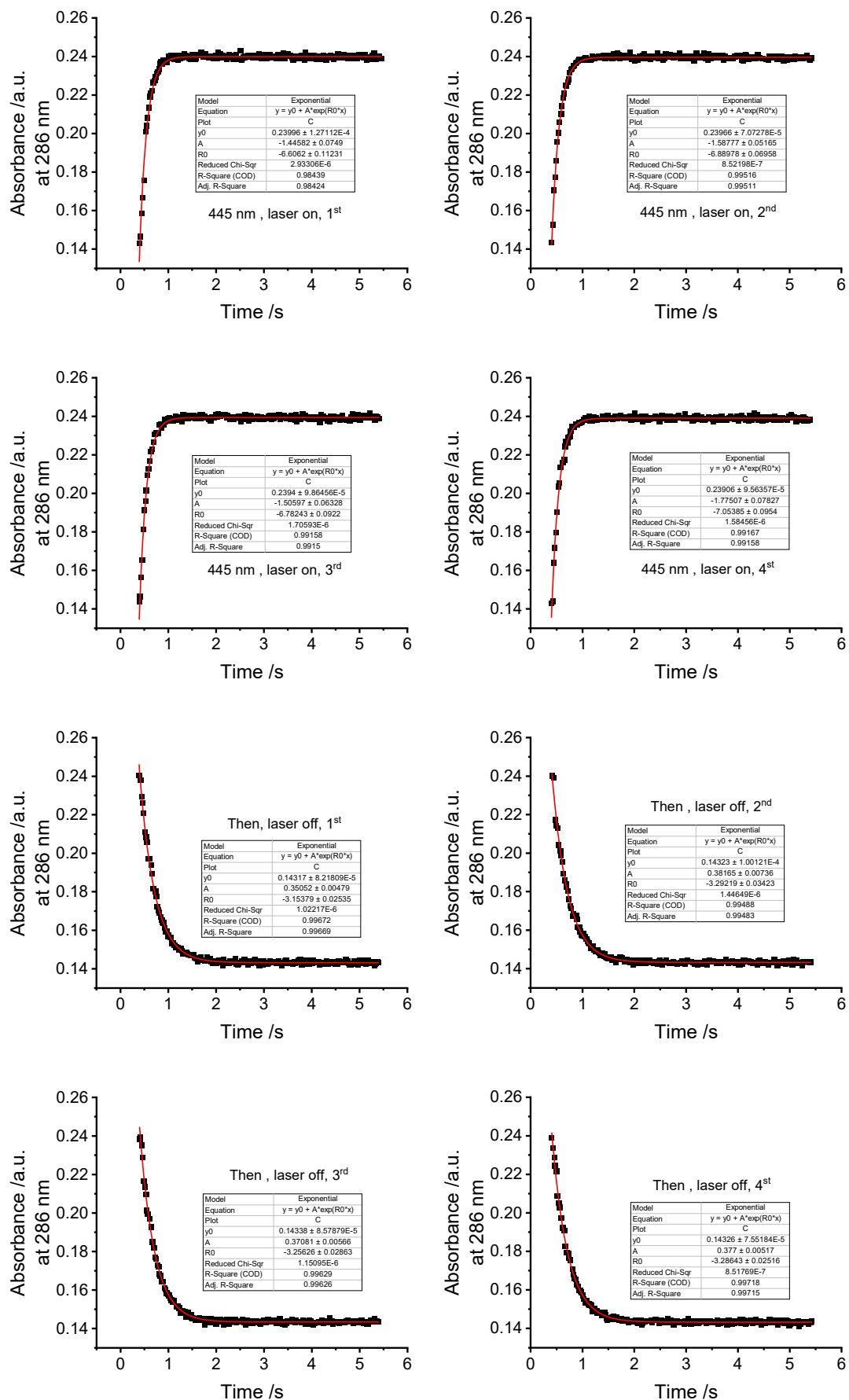
d) DBTD, pH = 3.02



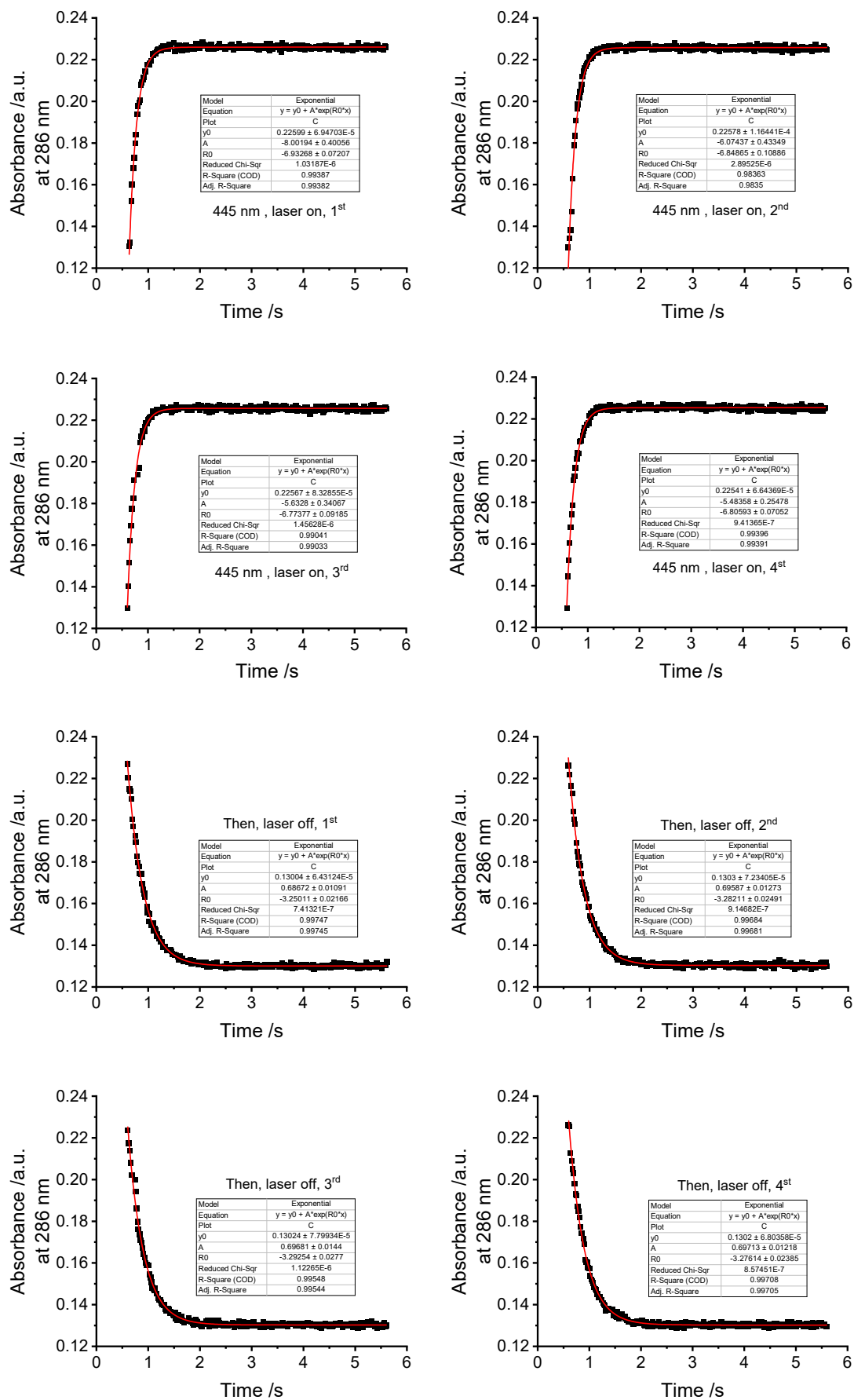
e) DBTD, pH = 4.02



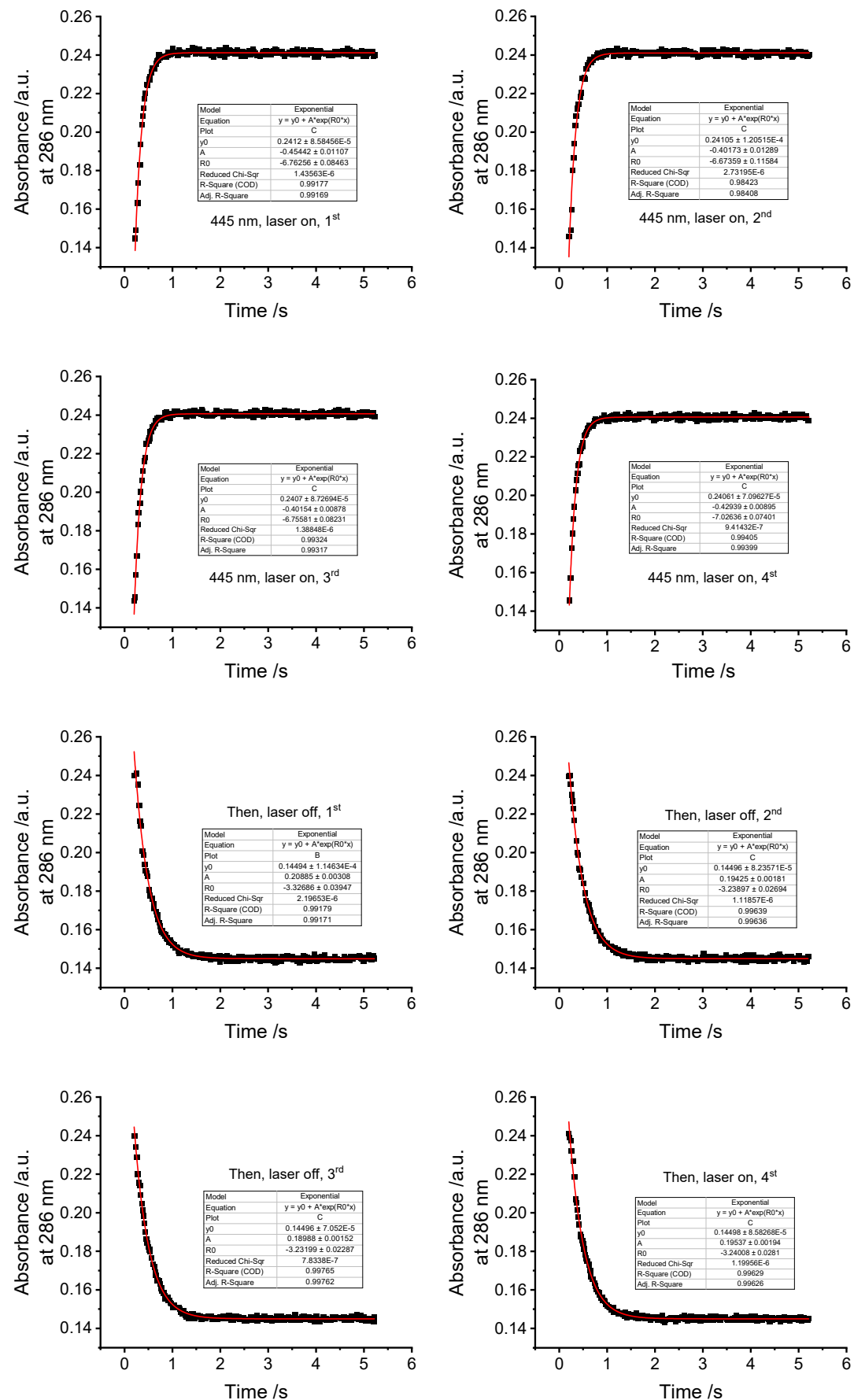
f) DBTD, pH = 5.19



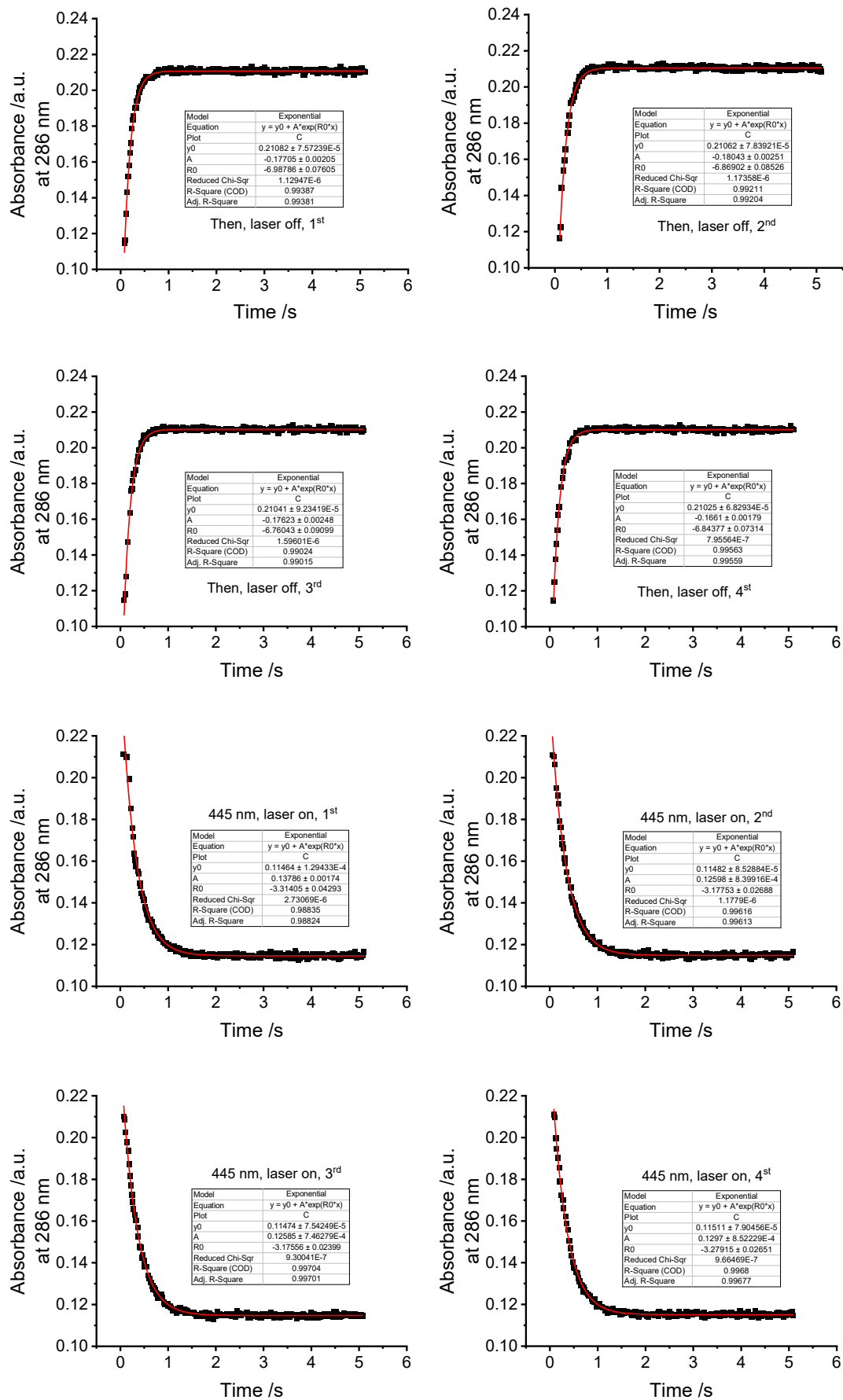
g) DBTD, pH = 6.01



h) DBTD, pH = 7.00



i) DBTD, pH = 7.46

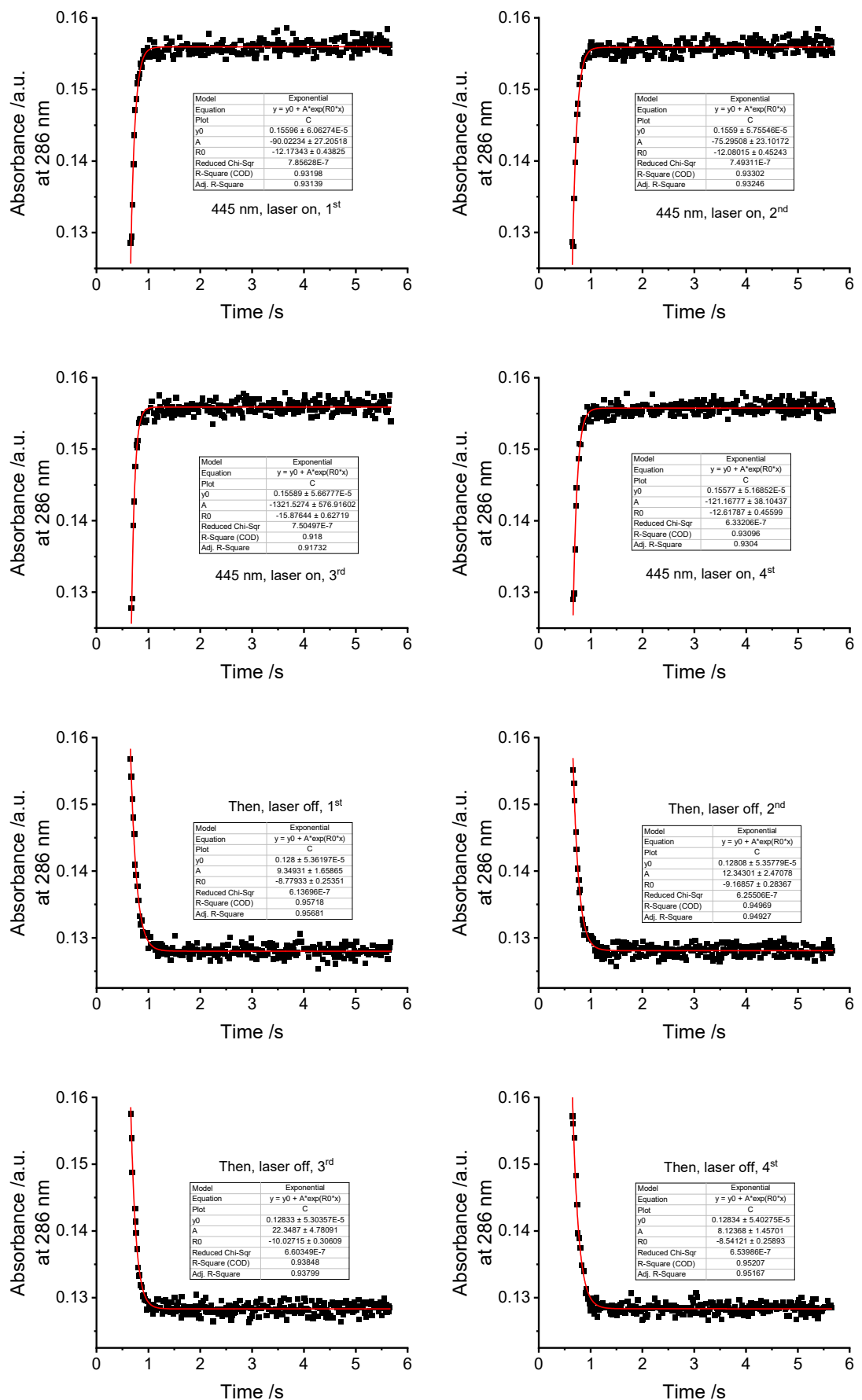


pH	k_{relax} /s⁻¹	k_{light}/s⁻¹	$t_{1/2}$ /ms	$\Delta \text{Abs.}$ /a.u.
-0.33	131.57848 ^a		5	0.0023
0.00	164.01756 ^a		4	0.0069
0.51	14.51924	20.03274	48	0.023
1.11	8.93743	13.73941	78	0.058
2.00	3.80445	7.31334	182	0.090
3.02	3.36168	6.98395	206	0.098
4.02	3.36127	6.86037	206	0.094
5.19	3.24717	6.83306	213	0.096
6.01	3.27522	6.84026	212	0.095
7.00	3.25947	6.80458	213	0.096
7.46	3.23657	6.86527	214	0.096

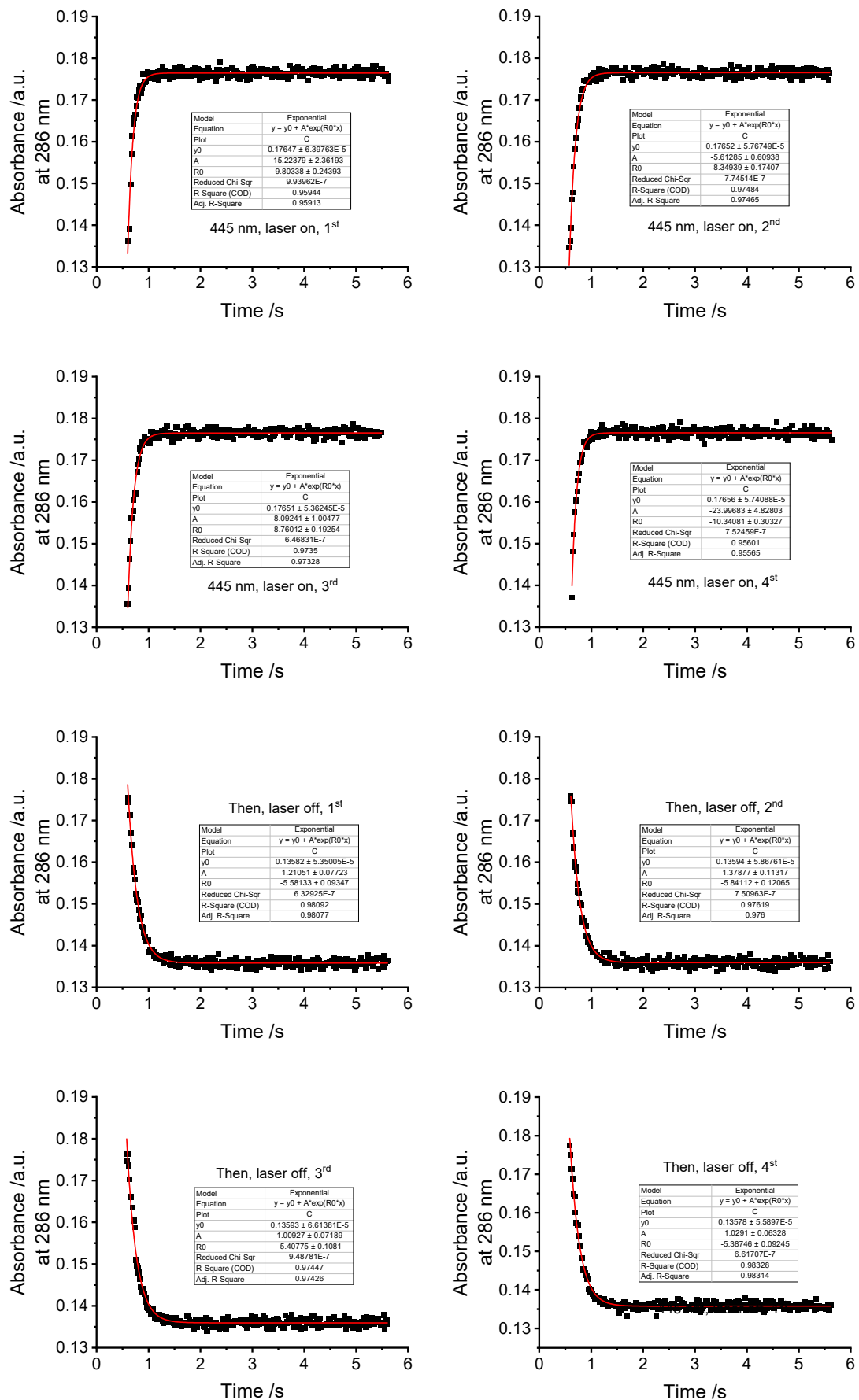
Table S1. Kinetics and half-life half-lives ($t_{1/2} = \frac{\ln 2}{k}$) of DBTD at pH = -0.33 to 7.46 in PBS/MeCN = 2/1, PBS = phosphate buffer saline at specified pH, pH ranging from -0.33 to 7.46, conc. = 50 μM , Power density_{445 nm} = 391 mW cm⁻² at room temperature (298 K).

^a. The room-temperature kinetic rate of DBTD at the indicated pH were extrapolated by using the Eyring equation.

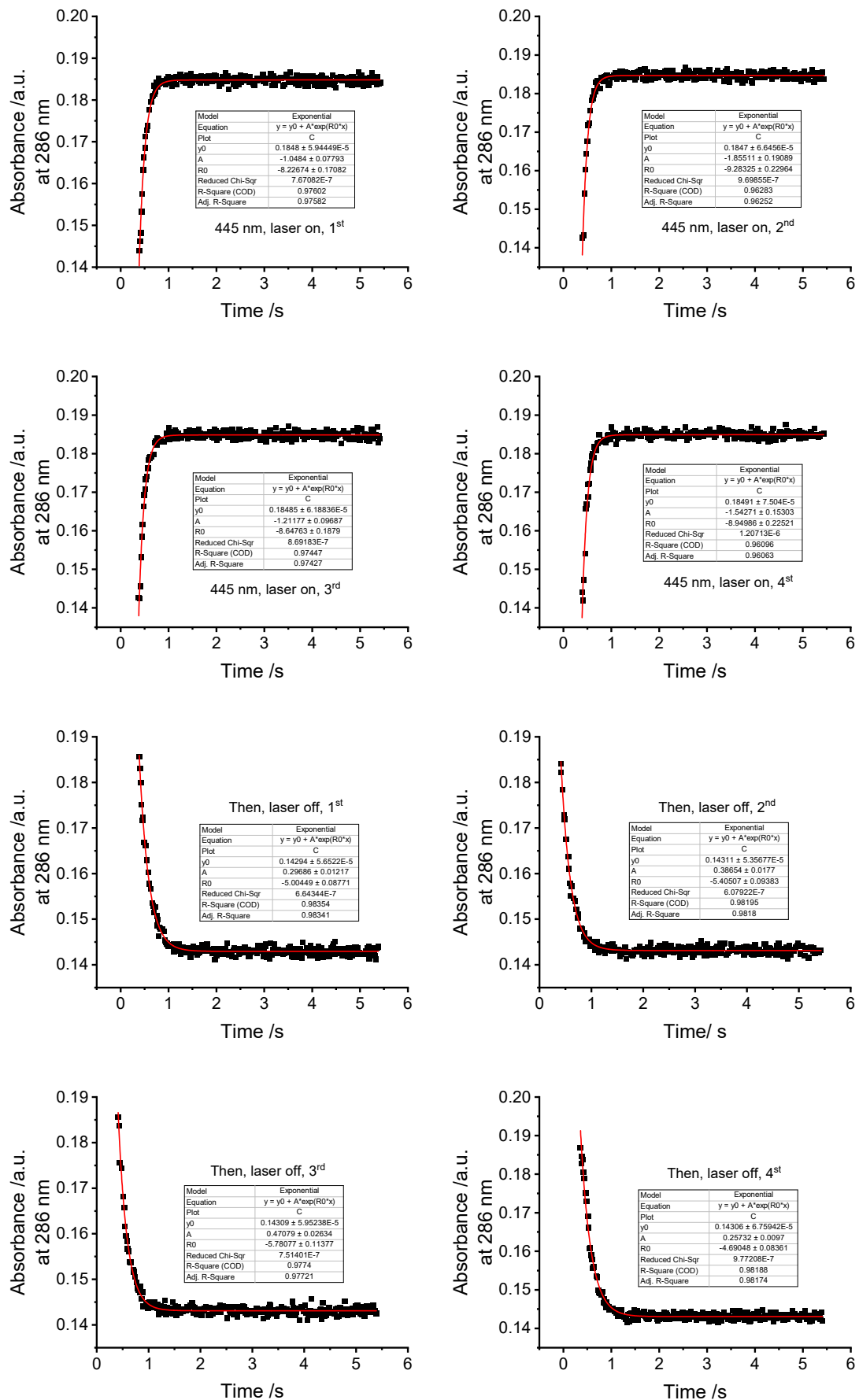
a) 1a, pH = 1.11



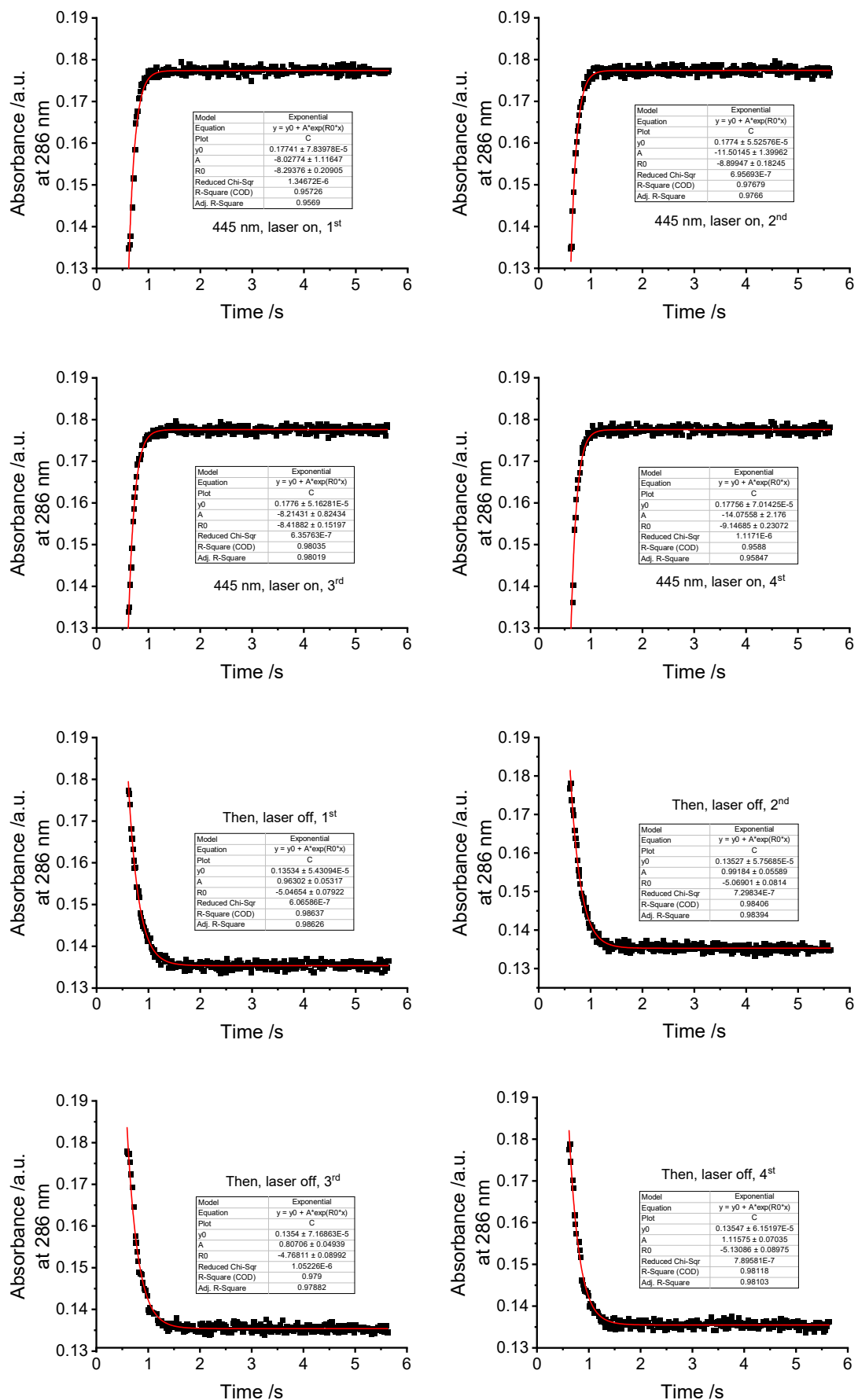
b) 1a, pH = 2.00



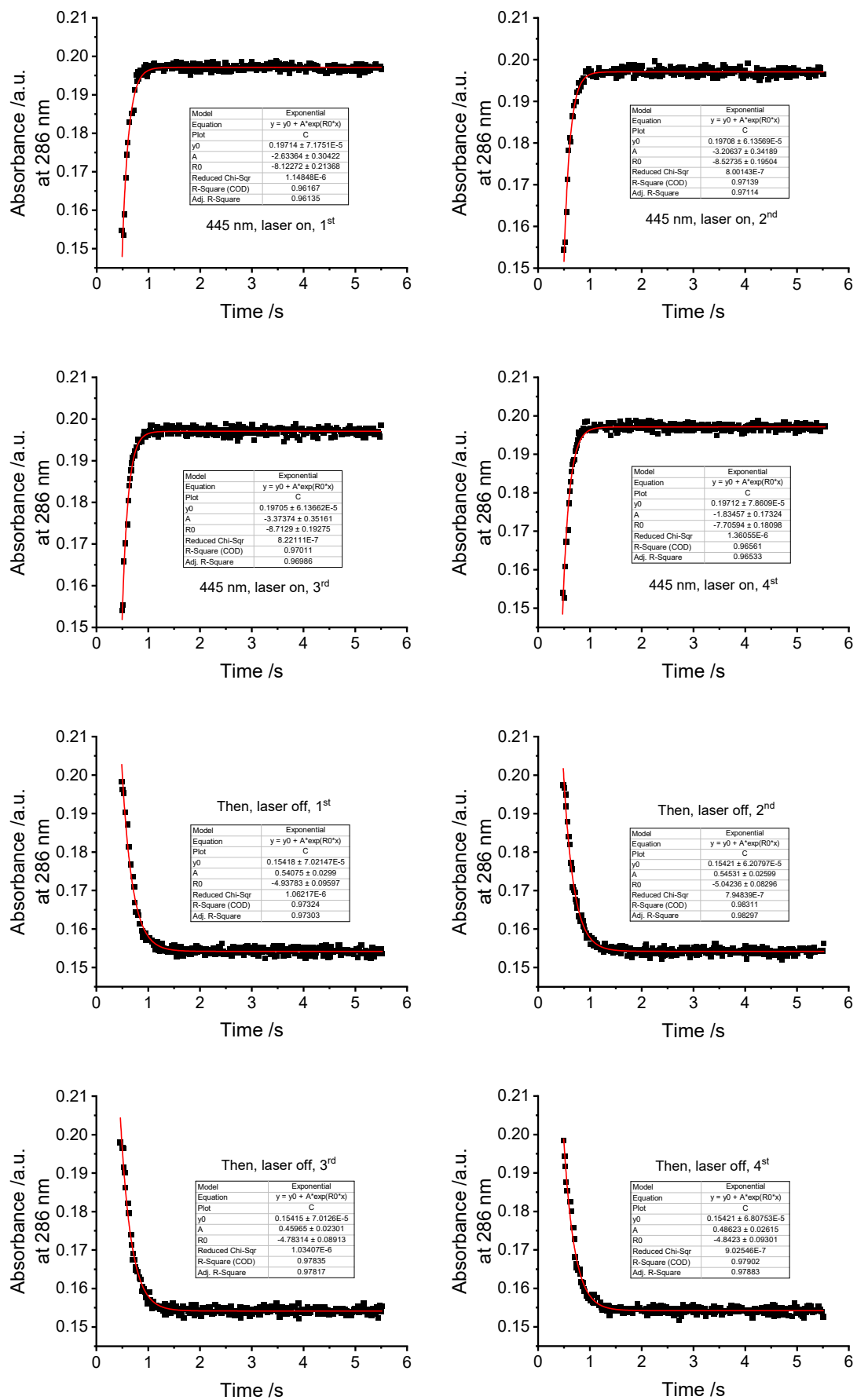
c) 1a, pH = 3.02



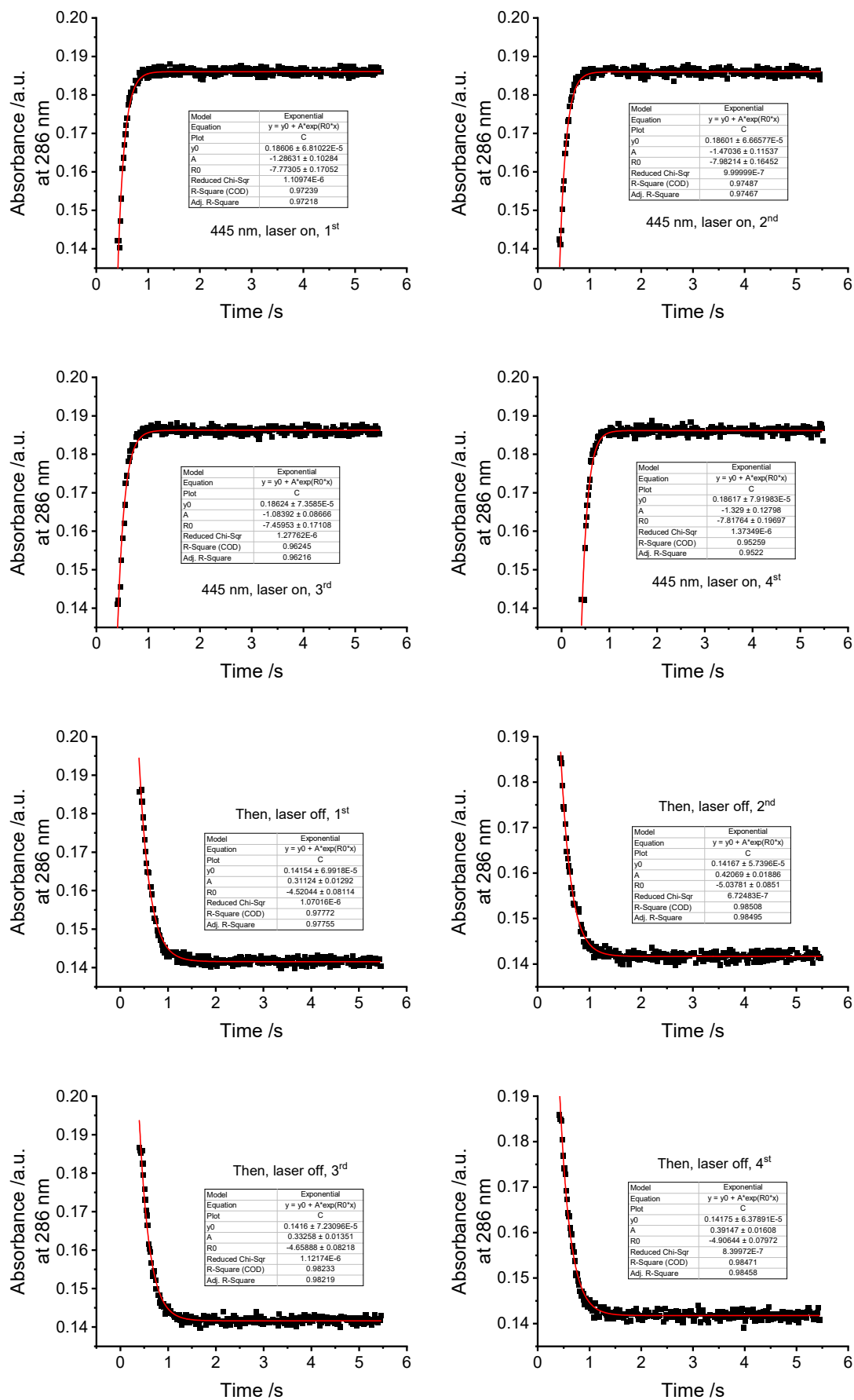
d) 1a, pH = 4.02



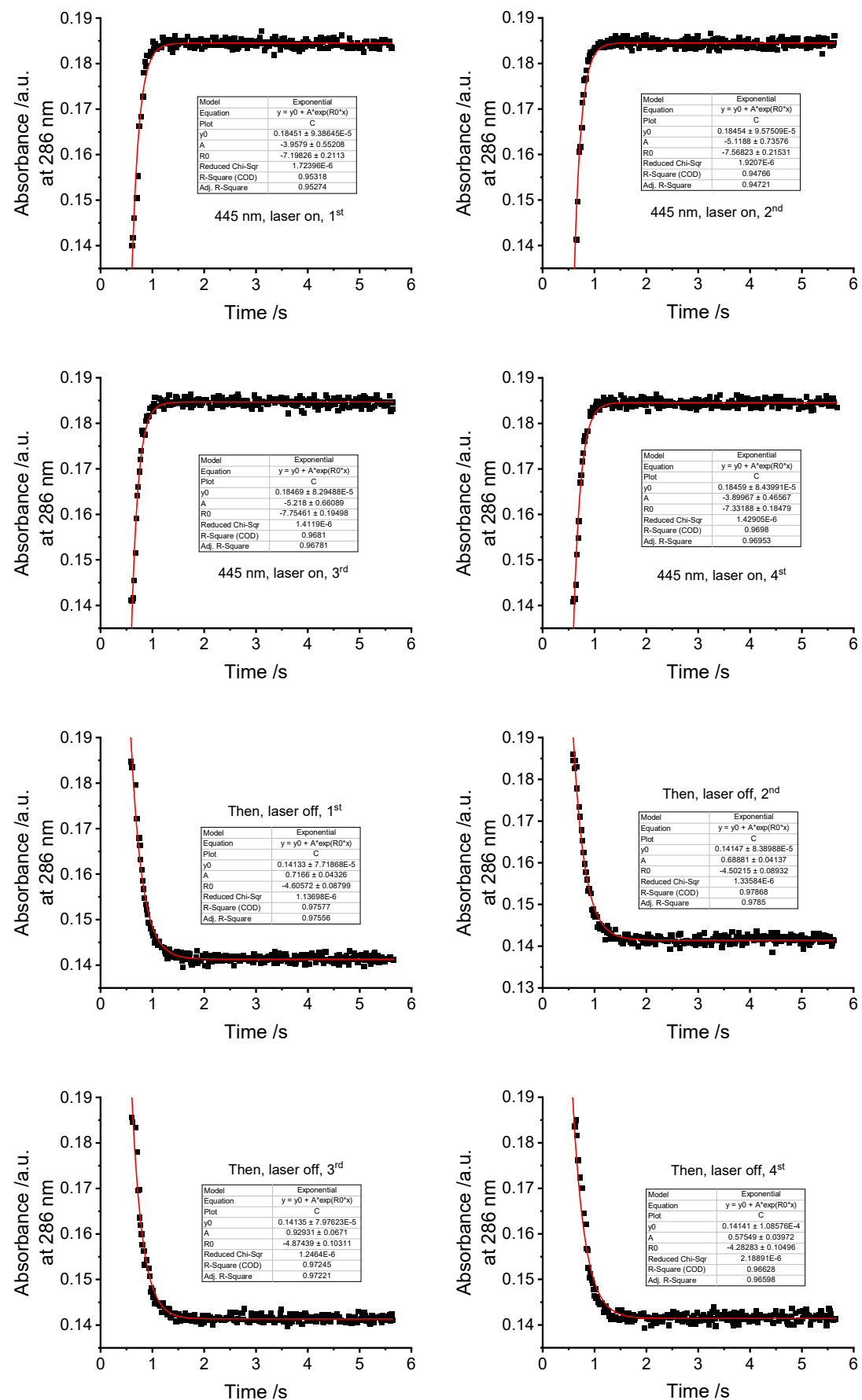
e) 1a, pH = 5.19



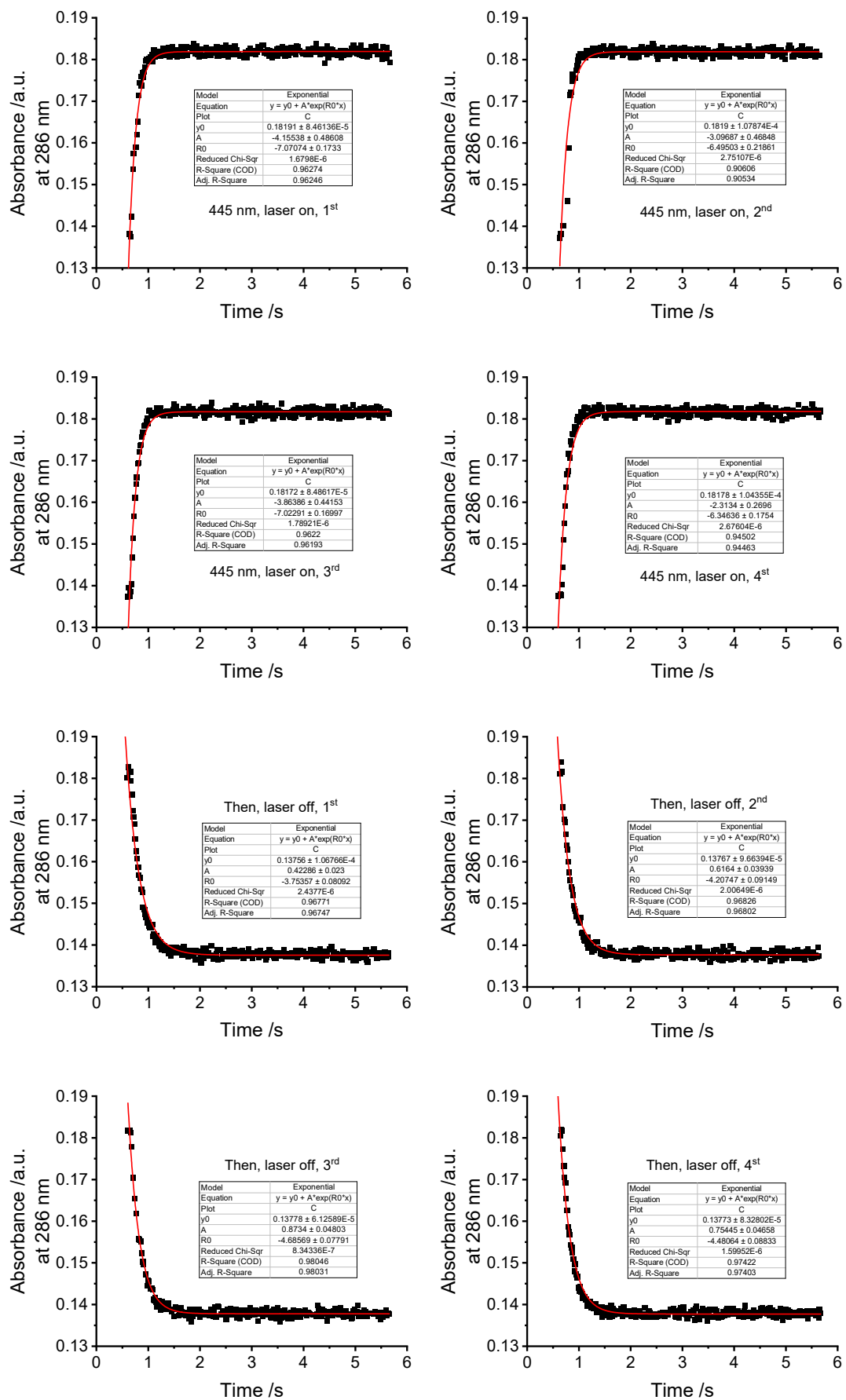
f) 1a, pH = 6.01



g) 1a, pH = 7.00



h) 1a, pH = 7.46

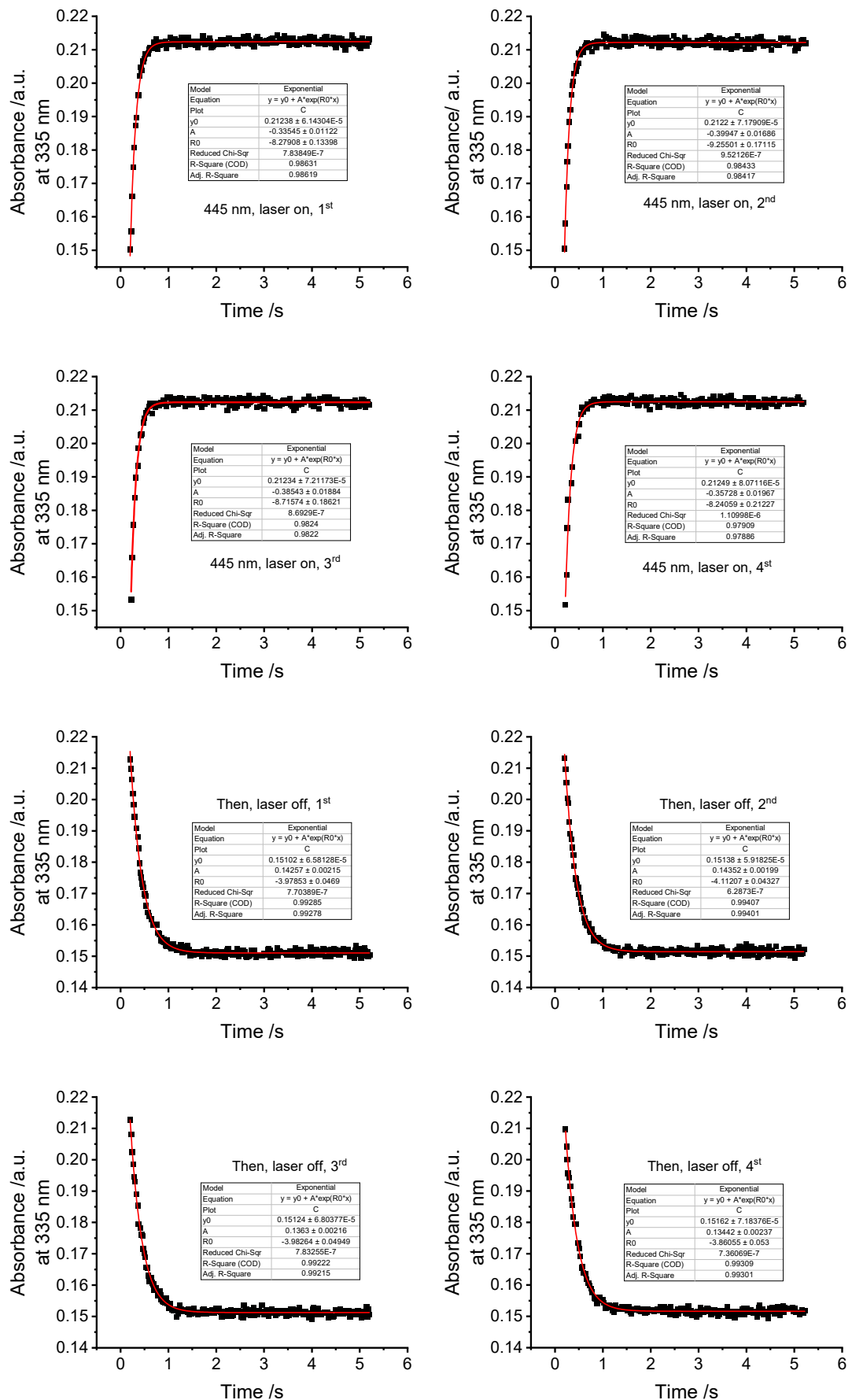


pH	<i>k</i>_{relax} /s⁻¹	<i>k</i>_{light}/s⁻¹	t_{1/2} /ms	ΔAbs. /a.u.
-0.33	51.72512 ^a		13	0.012
0.00	16.27326 ^a		43	0.02
0.51	4.62637 ^a		150	0.024
1.11	9.12906	13.18697	76	0.029
2.00	5.55441	9.31342	125	0.039
3.02	5.2202	8.77687	133	0.042
4.02	5.00363	8.68972	138	0.042
5.19	4.90141	8.26723	141	0.044
6.01	4.78089	7.75809	145	0.044
7.00	4.56627	7.46324	152	0.044
7.46	4.28184	6.73376	162	0.044

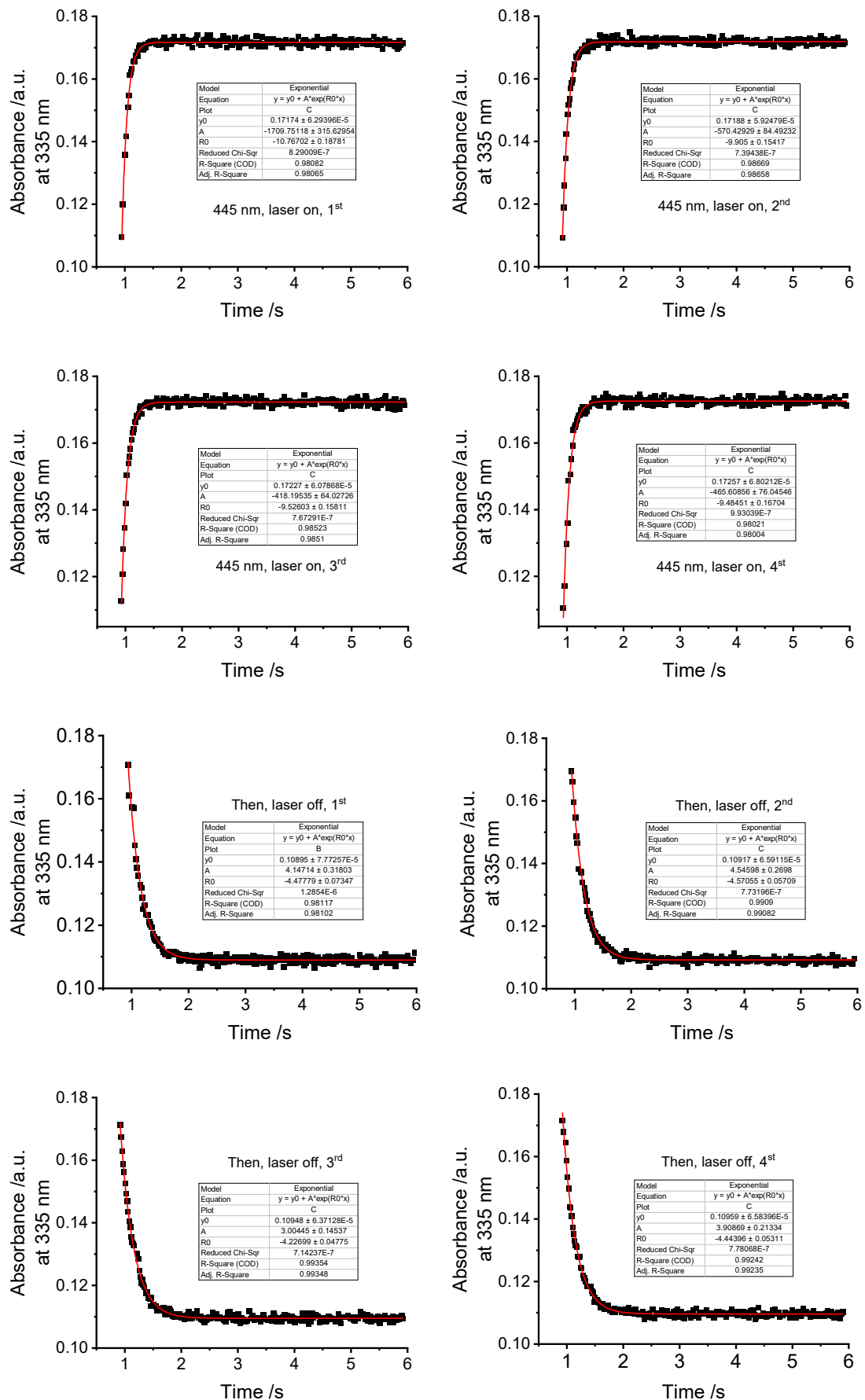
Table S2. Kinetics and half-life half-lives ($t_{1/2} = \frac{\ln 2}{k}$) of **1a** at pH = -0.33 to 7.46 in PBS/MeCN = 2/1, PBS = phosphate buffer saline at specified pH, pH ranging from -0.33 to 7.46, conc. = 50 μM, Power density_{445 nm} = 391 mW cm⁻² at room temperature (298 K).

^a. The room-temperature kinetic rate of **1a** at the indicated pH were extrapolated by using the Eyring equation.

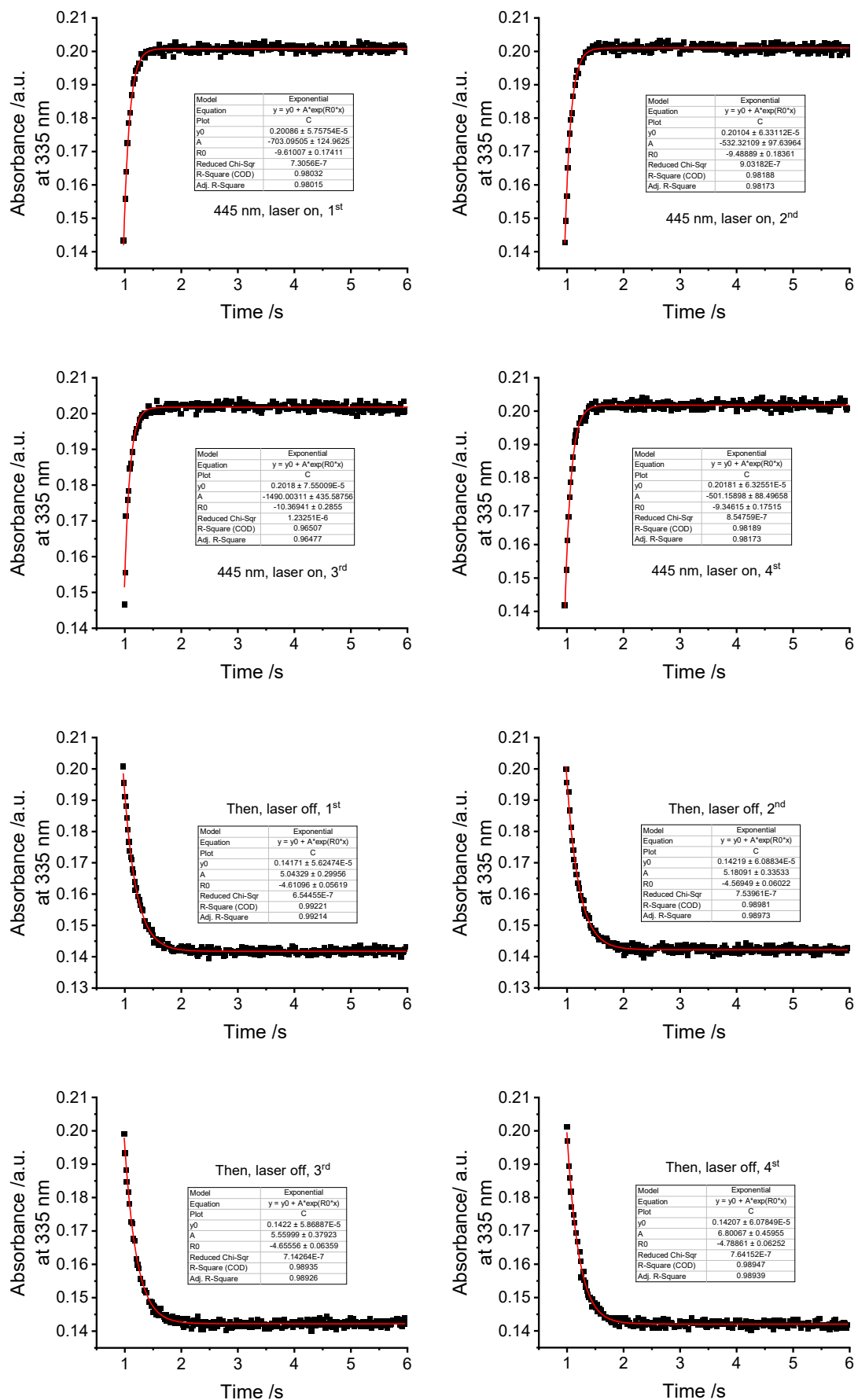
a) 2a, pH = -0.33



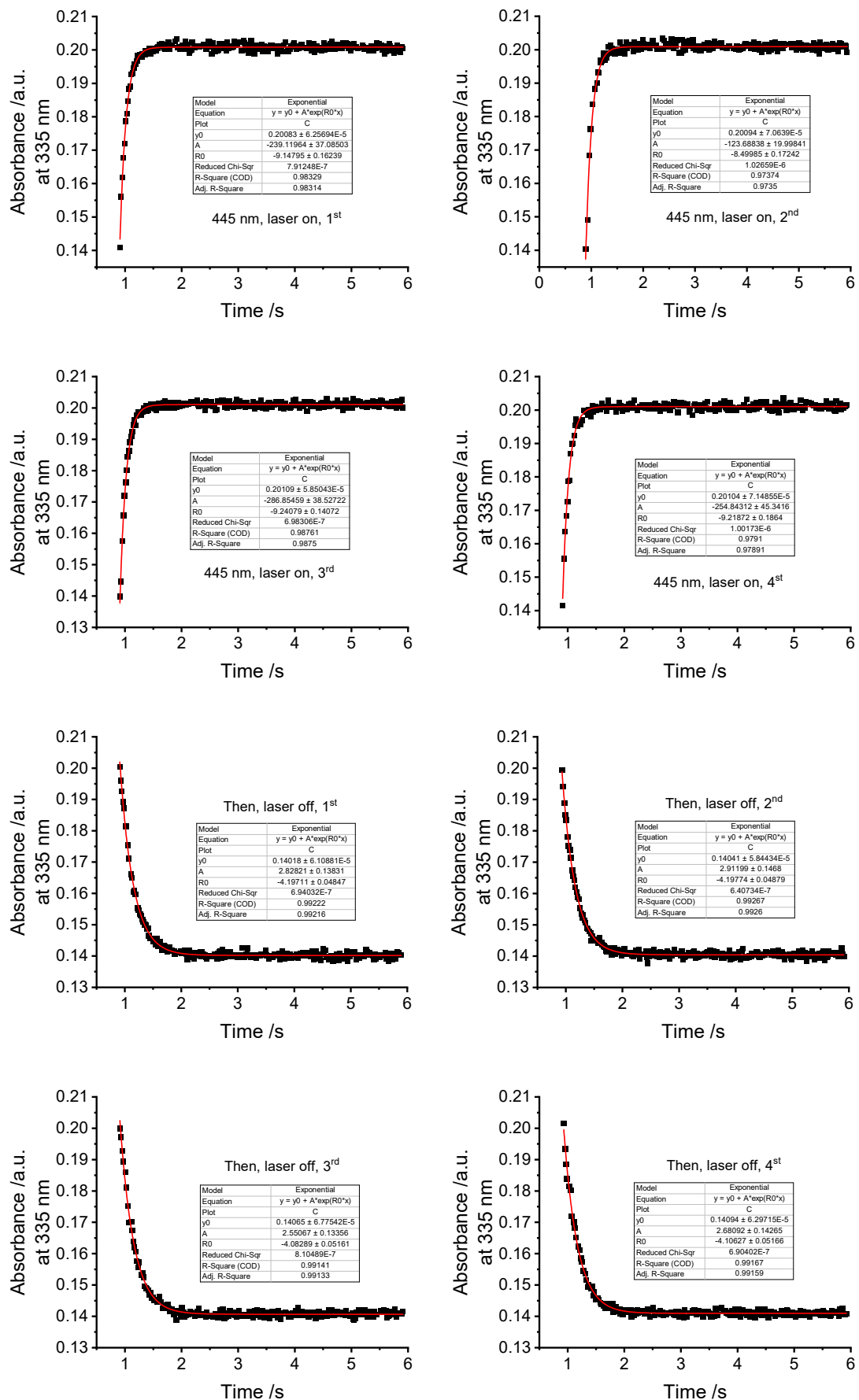
b) 2a, pH = 0.00



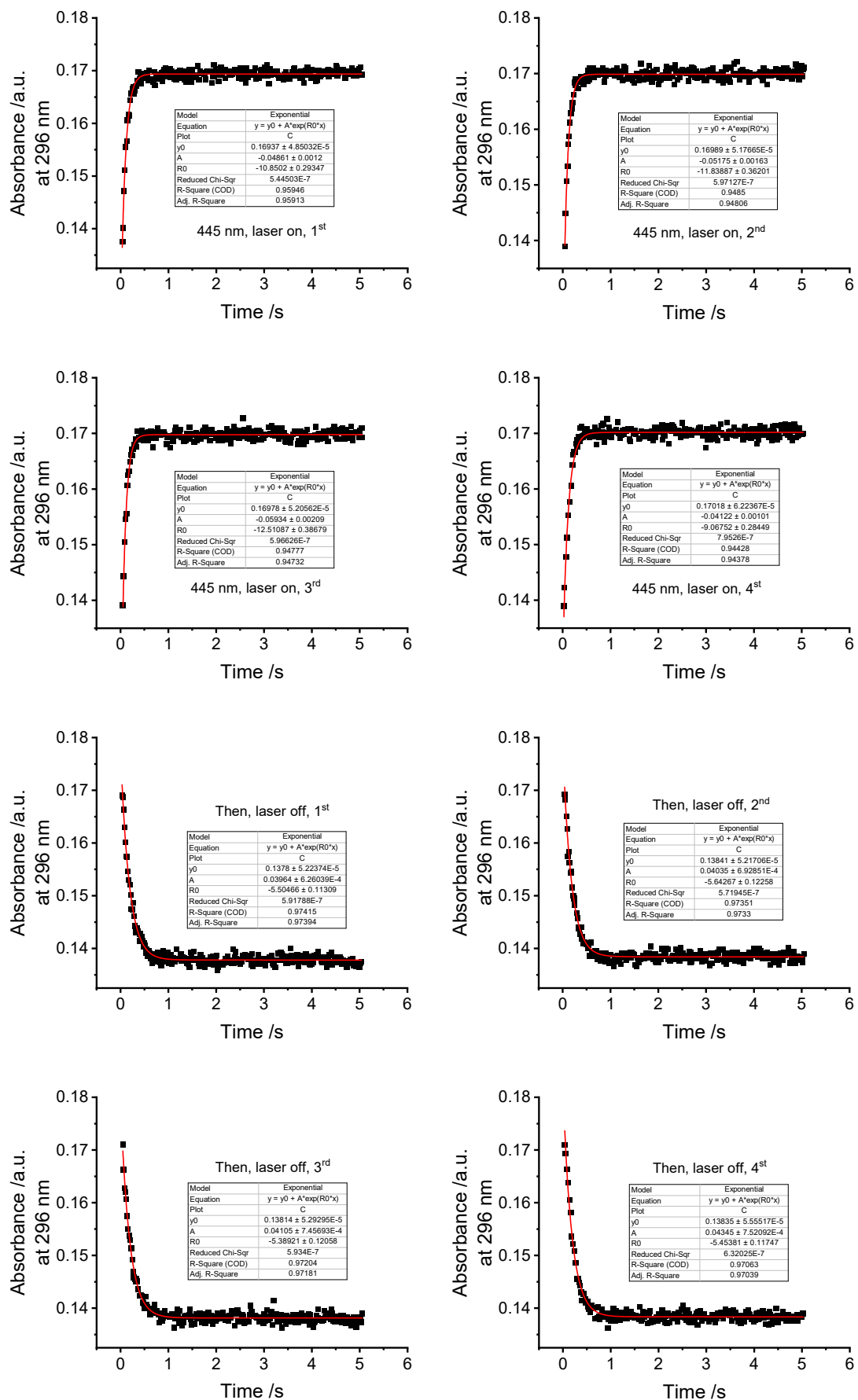
c) 2a, pH = 0.51



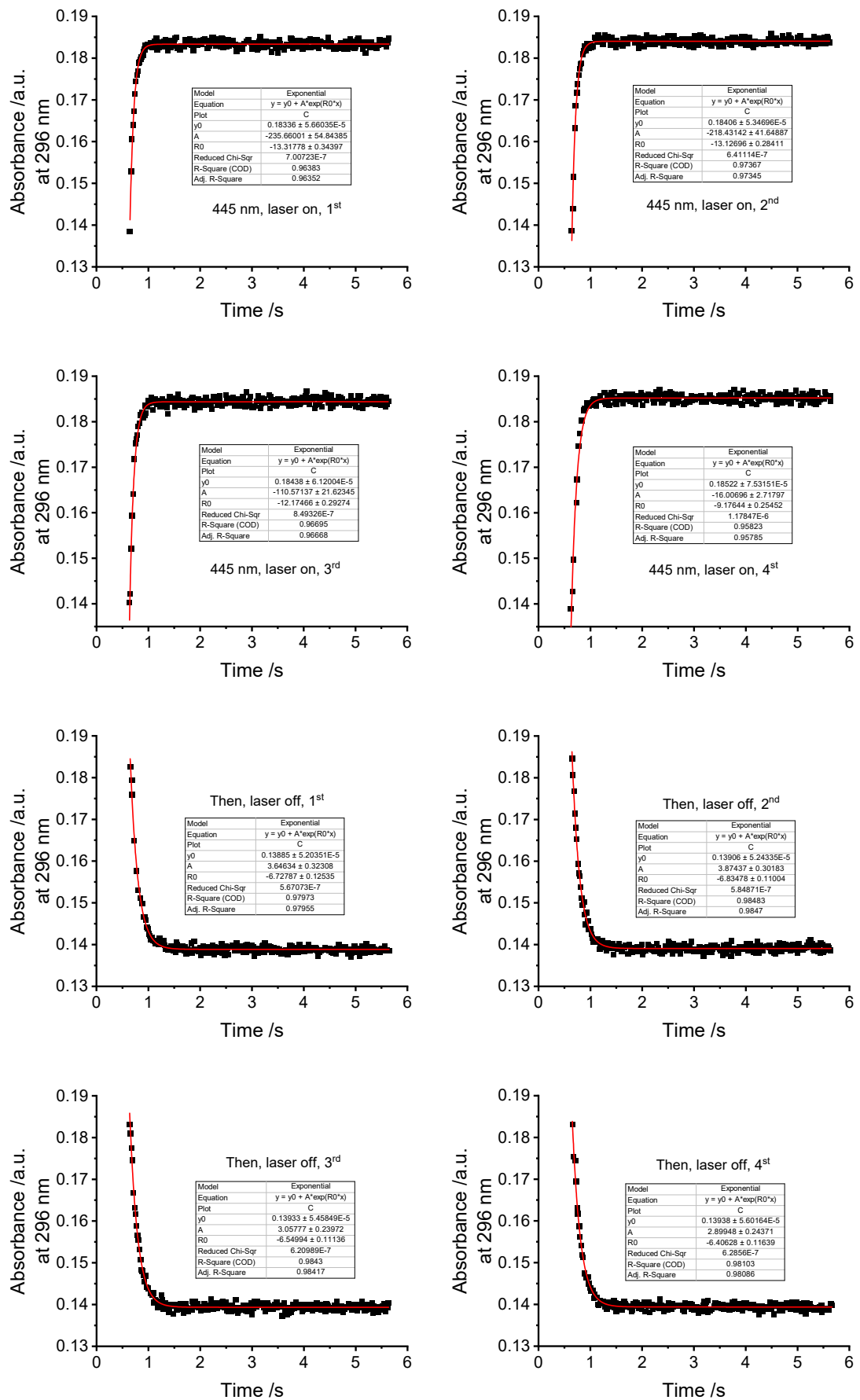
d) 2a, pH = 1.11



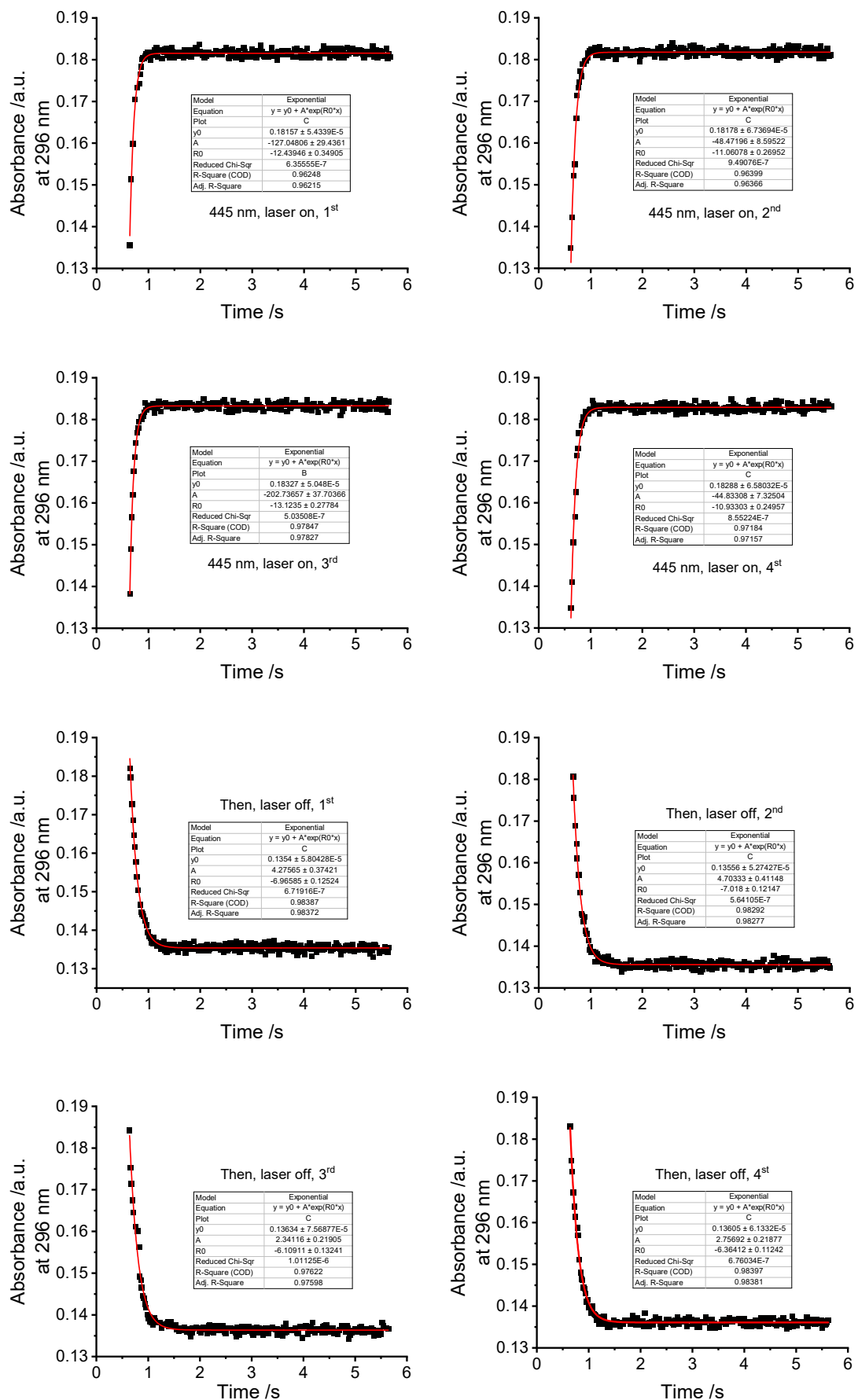
e) 2a, pH = 2.00



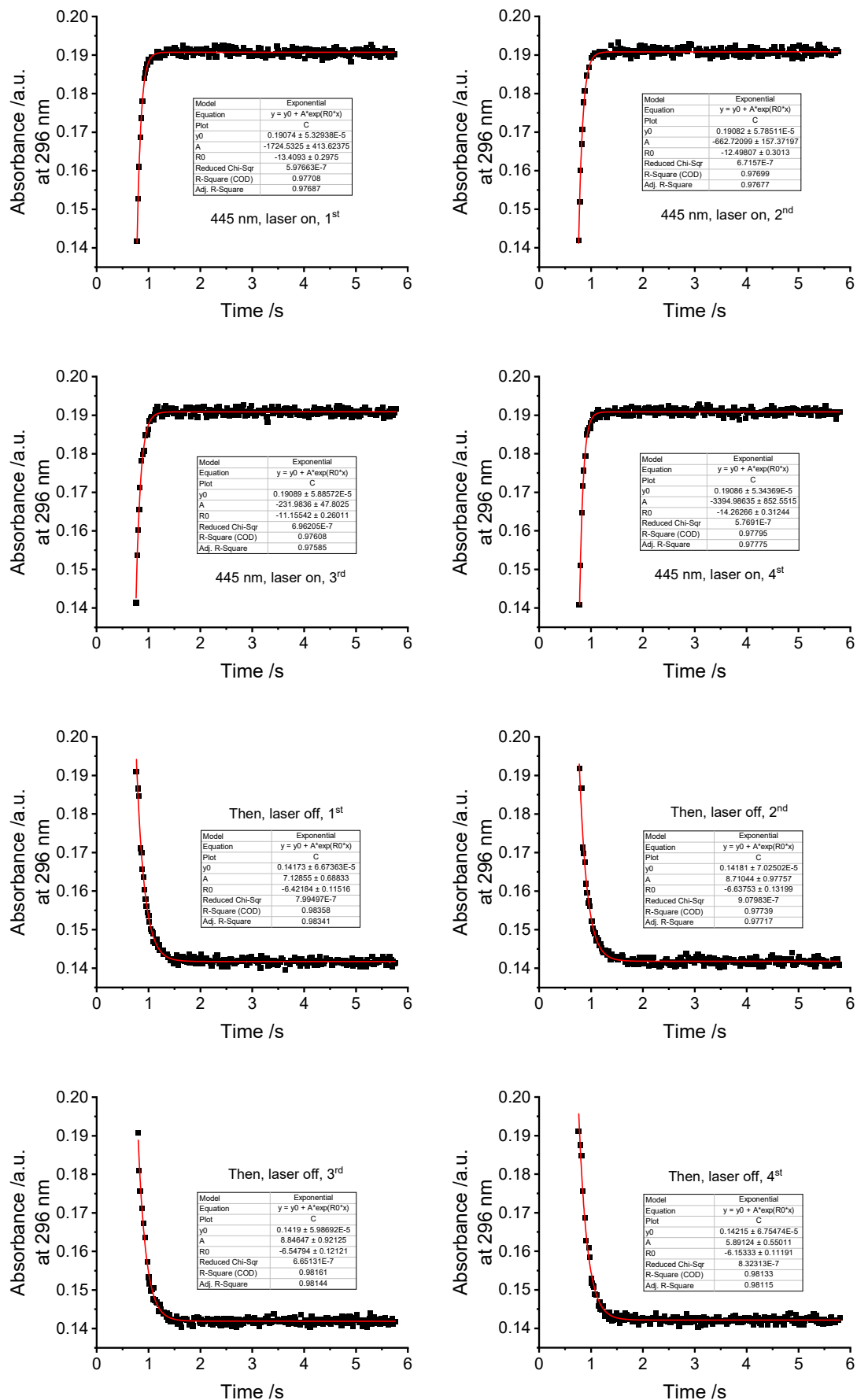
f) 2a, pH = 3.02



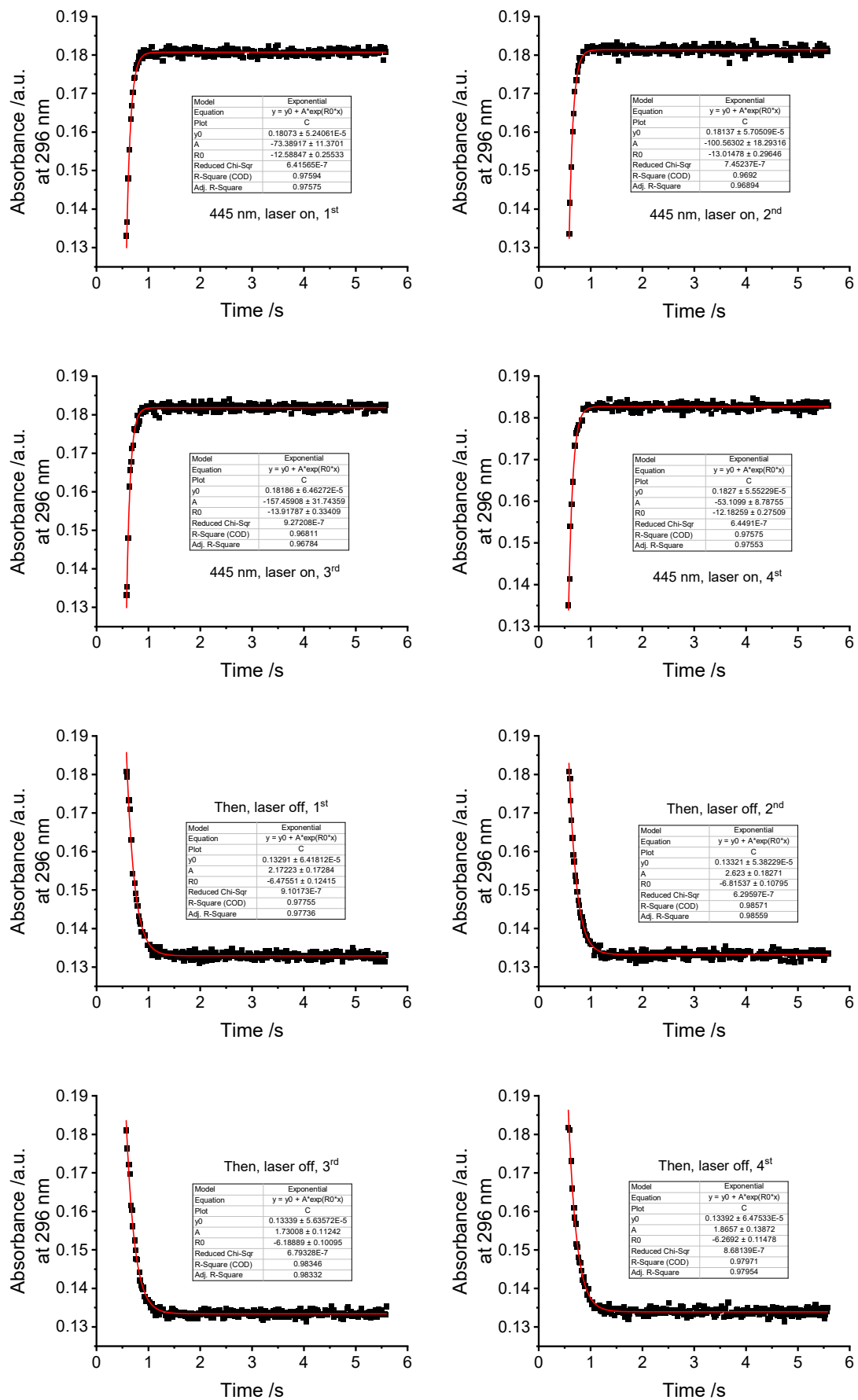
g) 2a, pH = 4.02



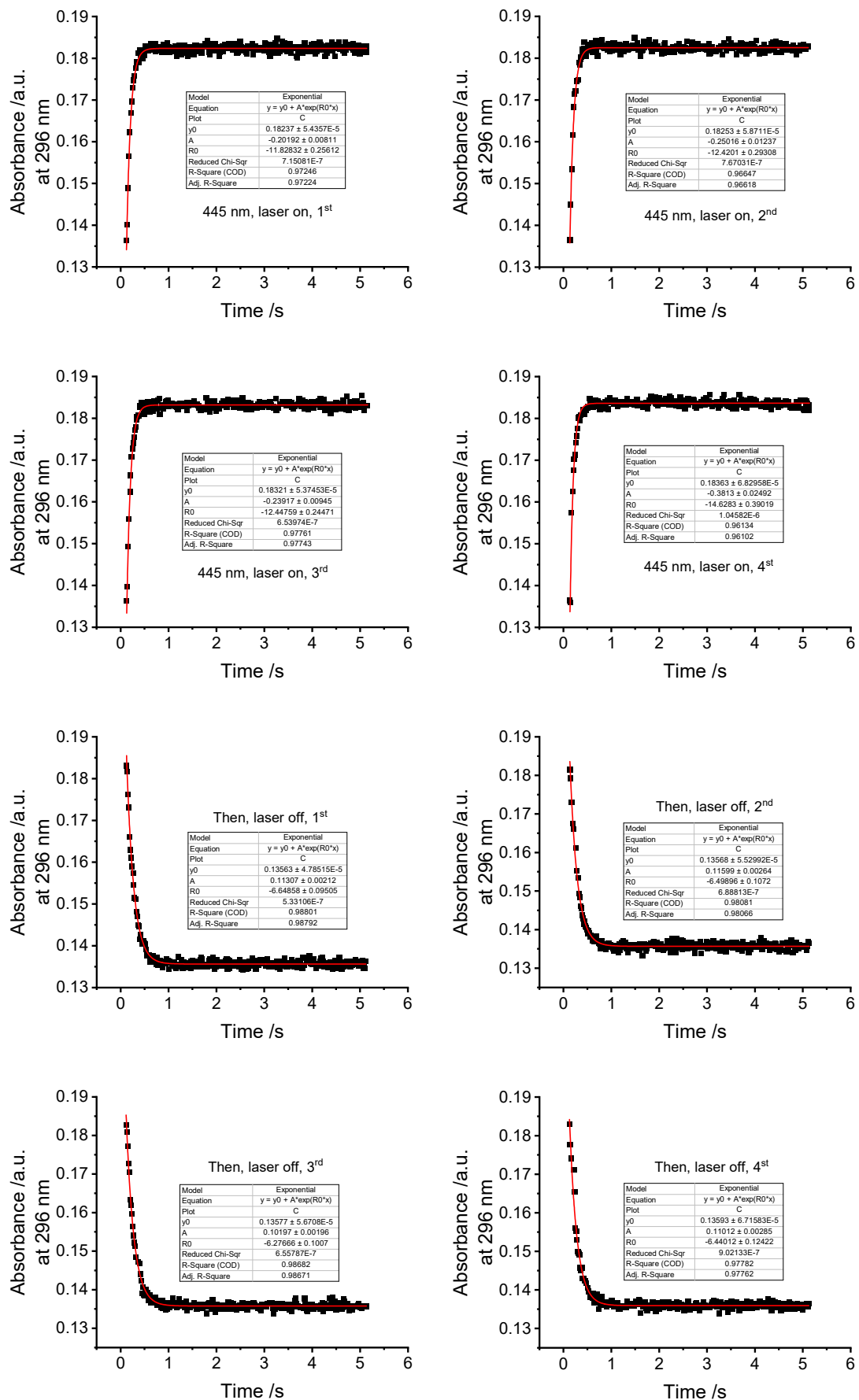
h) 2a, pH = 5.19



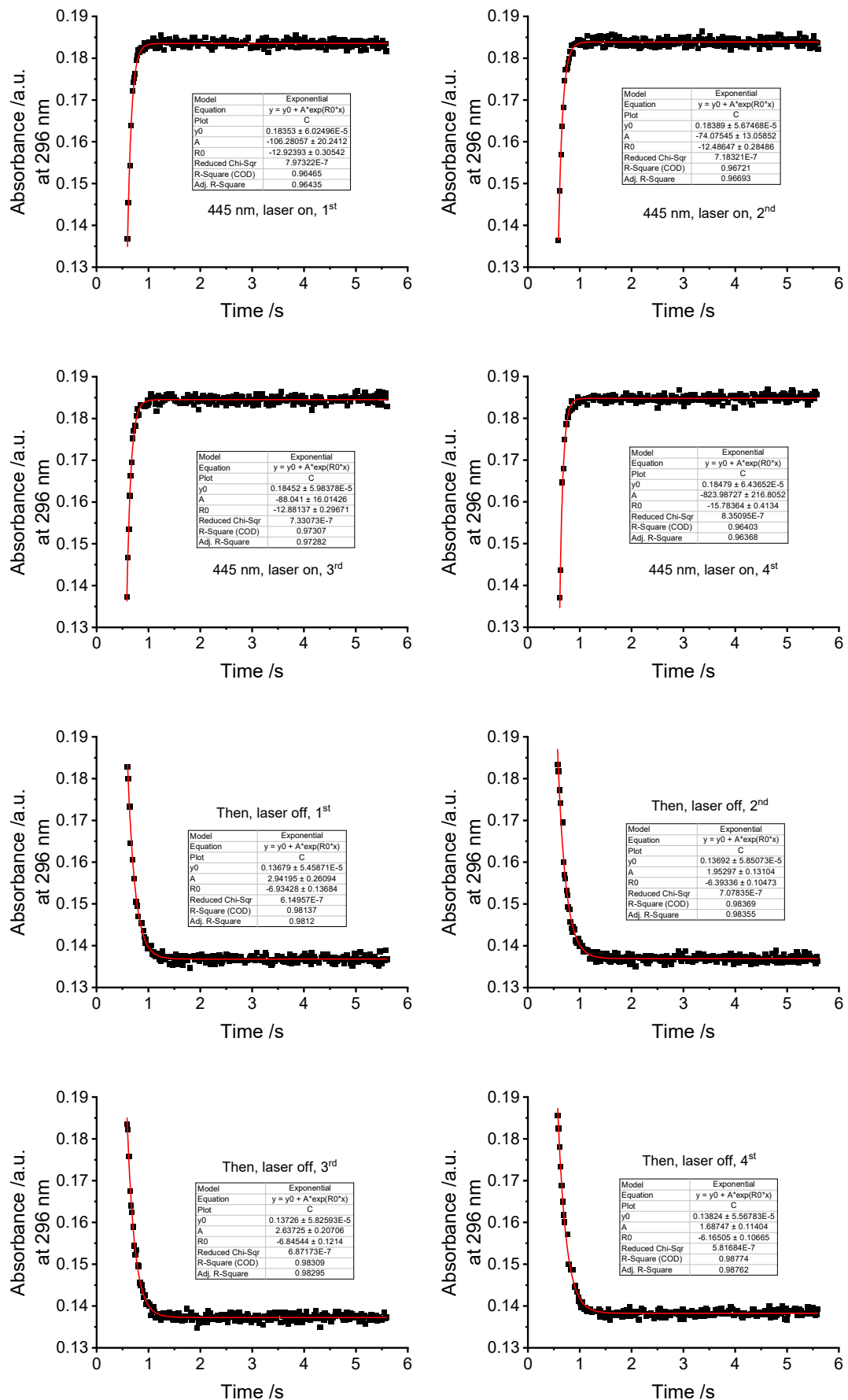
i) 2a, pH = 6.01



j) 2a, pH = 7.00



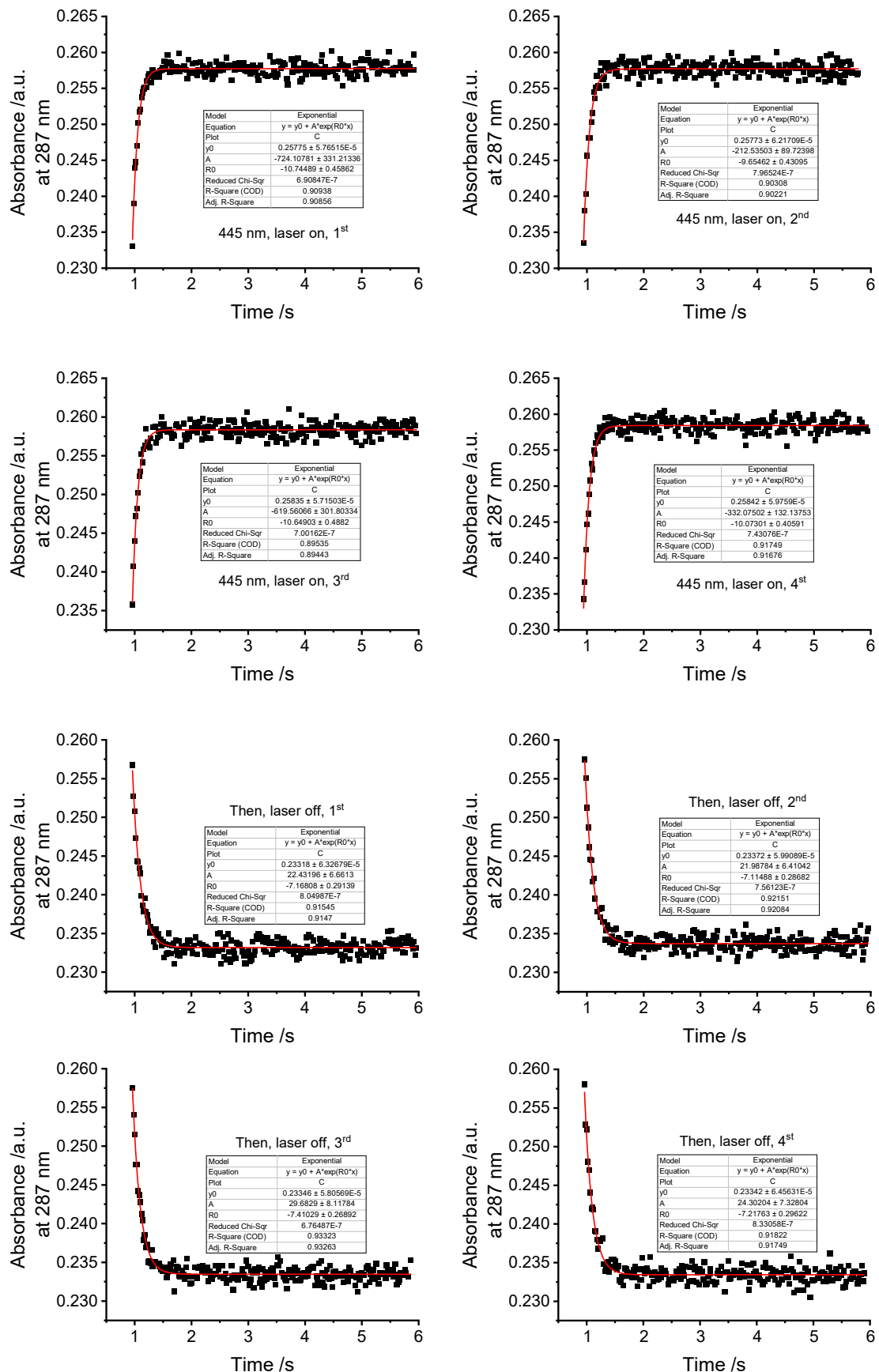
k) 2a, pH = 7.46



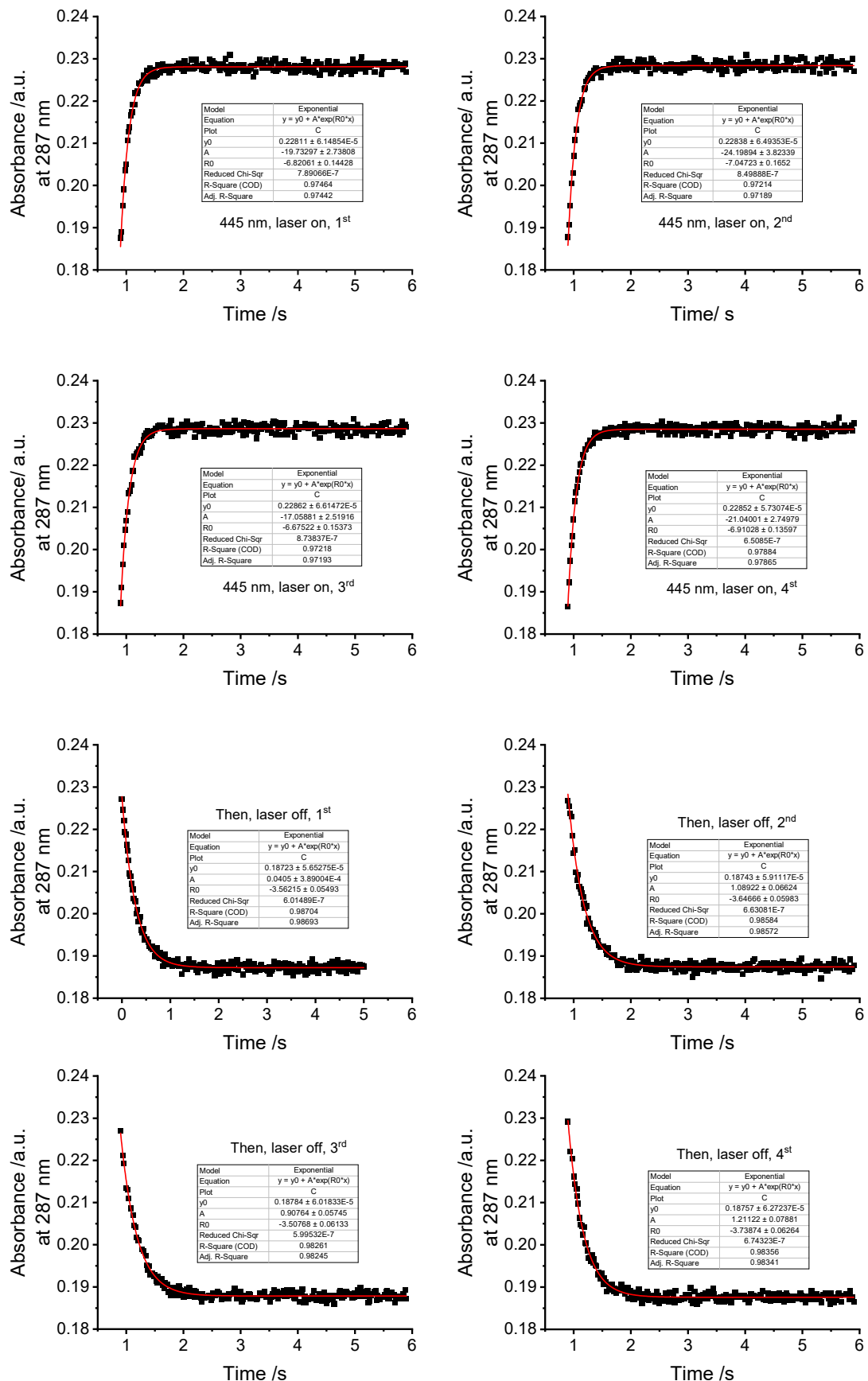
pH	<i>k</i>_{relax} /s⁻¹	<i>k</i>_{light}/s⁻¹	t_{1/2} /ms	ΔAbs. /a.u.
-0.33	4.18388	6.01393	166	0.044
0.00	3.84315	5.900043	180	0.044
0.51	4.06167	8.21844	171	0.07
1.11	4.01317	8.102408	173	0.071
2.00	4.32151	8.949758	160	0.036
3.02	5.46931	10.04589	127	0.055
4.02	5.646	8.921088	123	0.038
5.19	5.6501	9.027493	123	0.037
6.01	5.59934	9.220998	124	0.042
7.00	5.80261	9.266625	119	0.043
7.46	5.87945	9.511958	118	0.043

Table S3. Kinetics and half-life half-lives ($t_{1/2} = \frac{\ln 2}{k}$) of **2a** at pH = -0.33 to 7.46 in PBS/MeCN = 2/1, PBS = phosphate buffer saline at specified pH, pH ranging from -0.33 to 7.46, conc. = 50 μM, Power density_{445 nm} = 391 mW cm⁻² at room temperature (298 K).

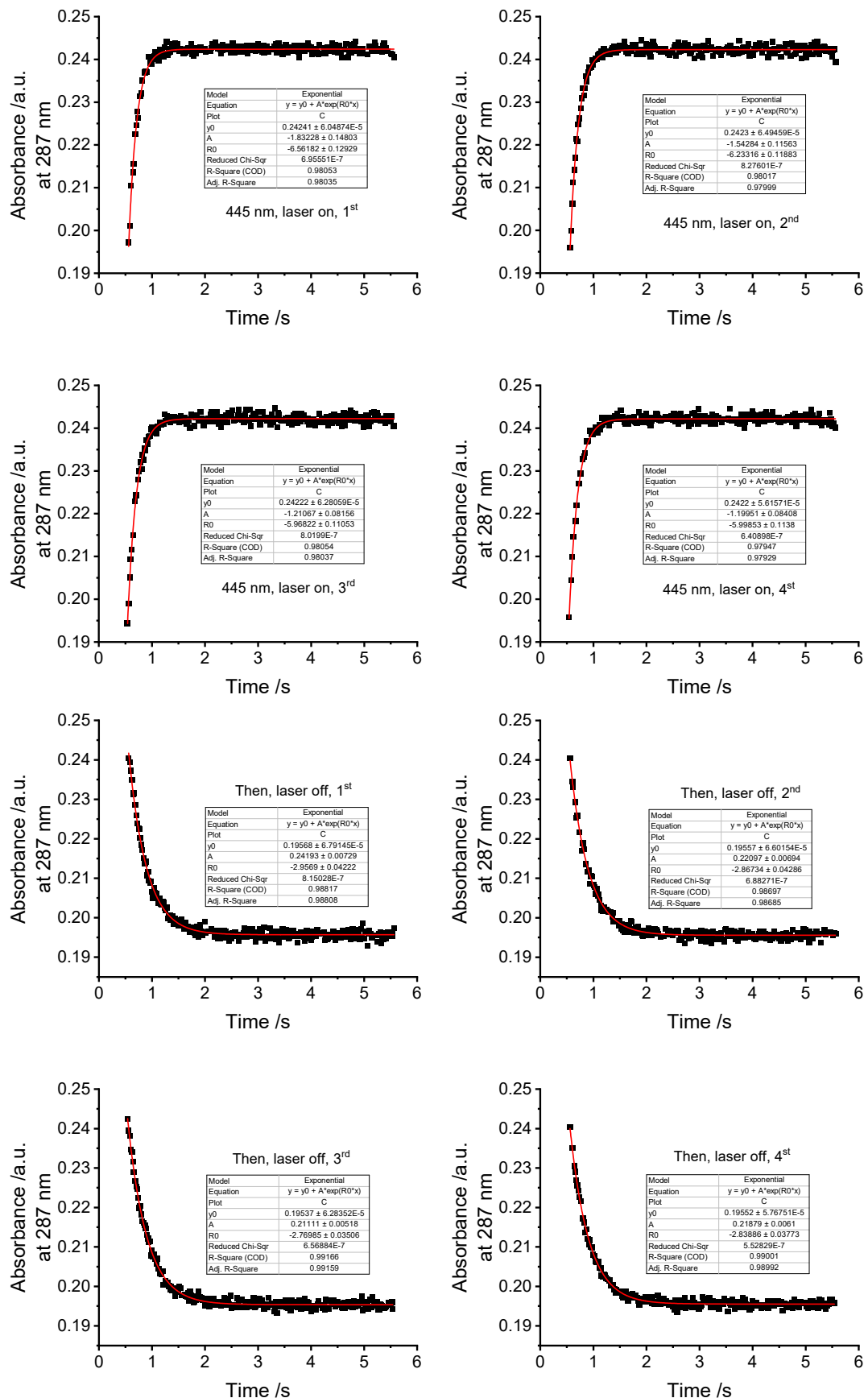
a) 3a, pH = 0.00



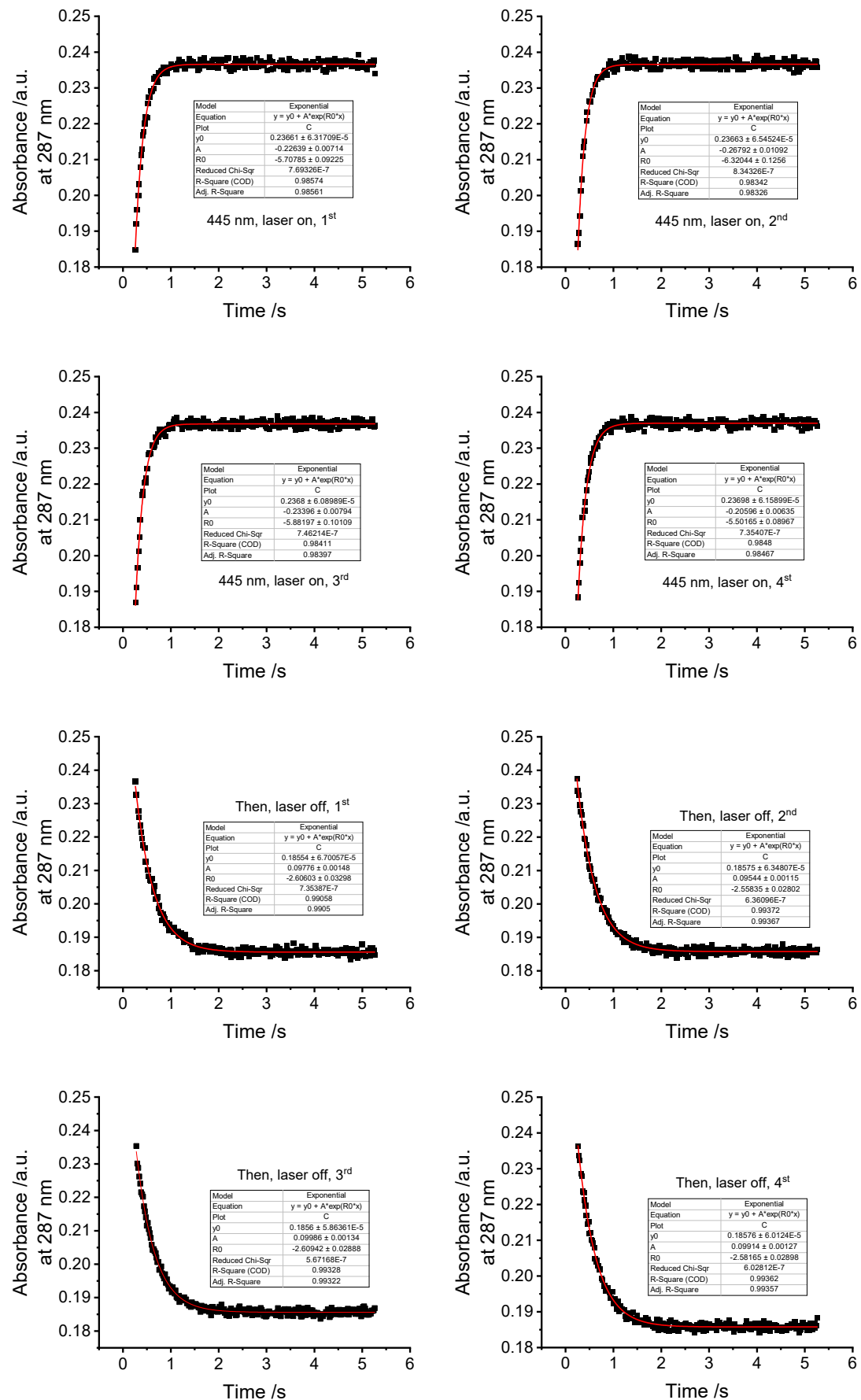
b) 3a, pH = 0.51



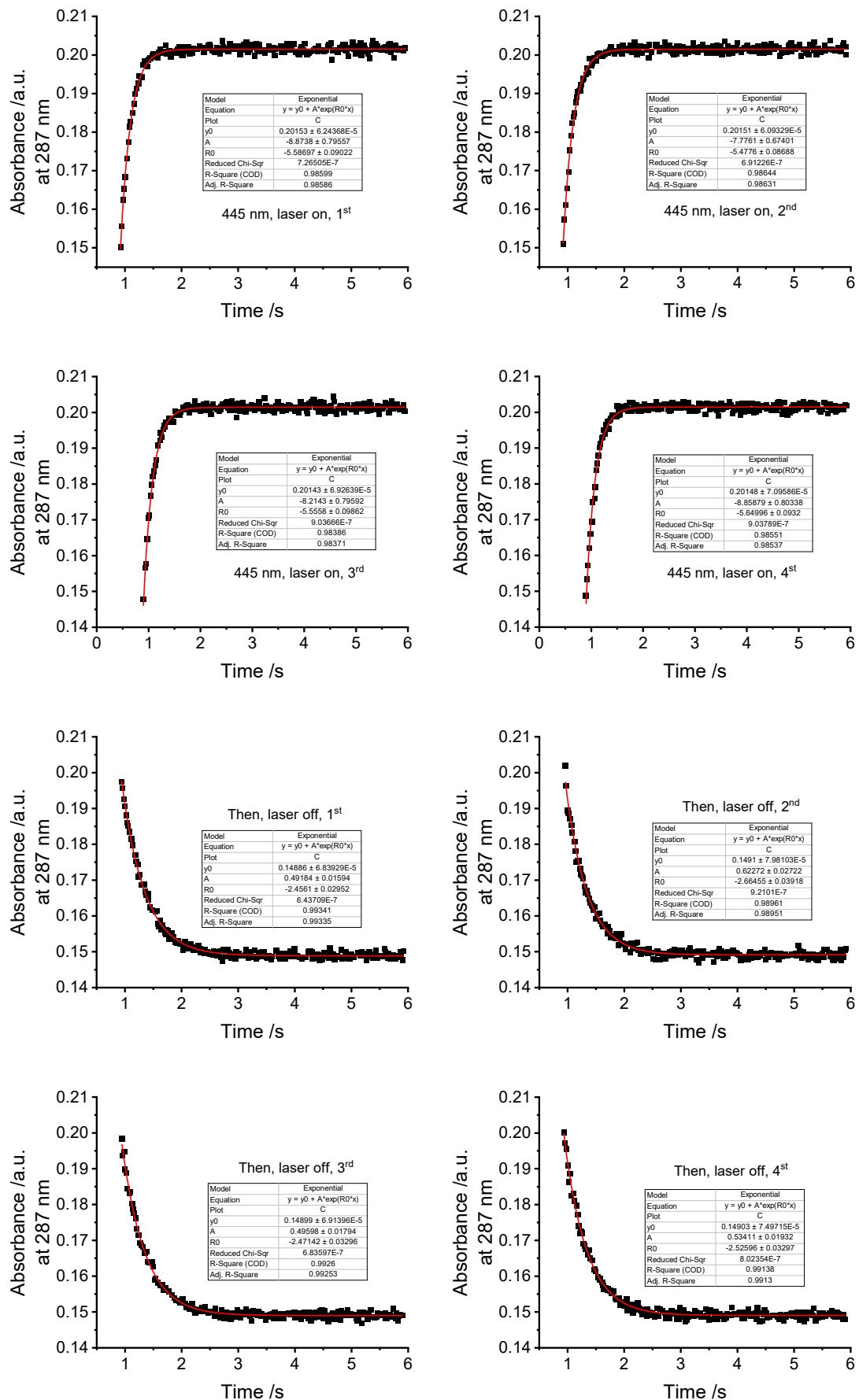
c) 3a, pH = 1.11



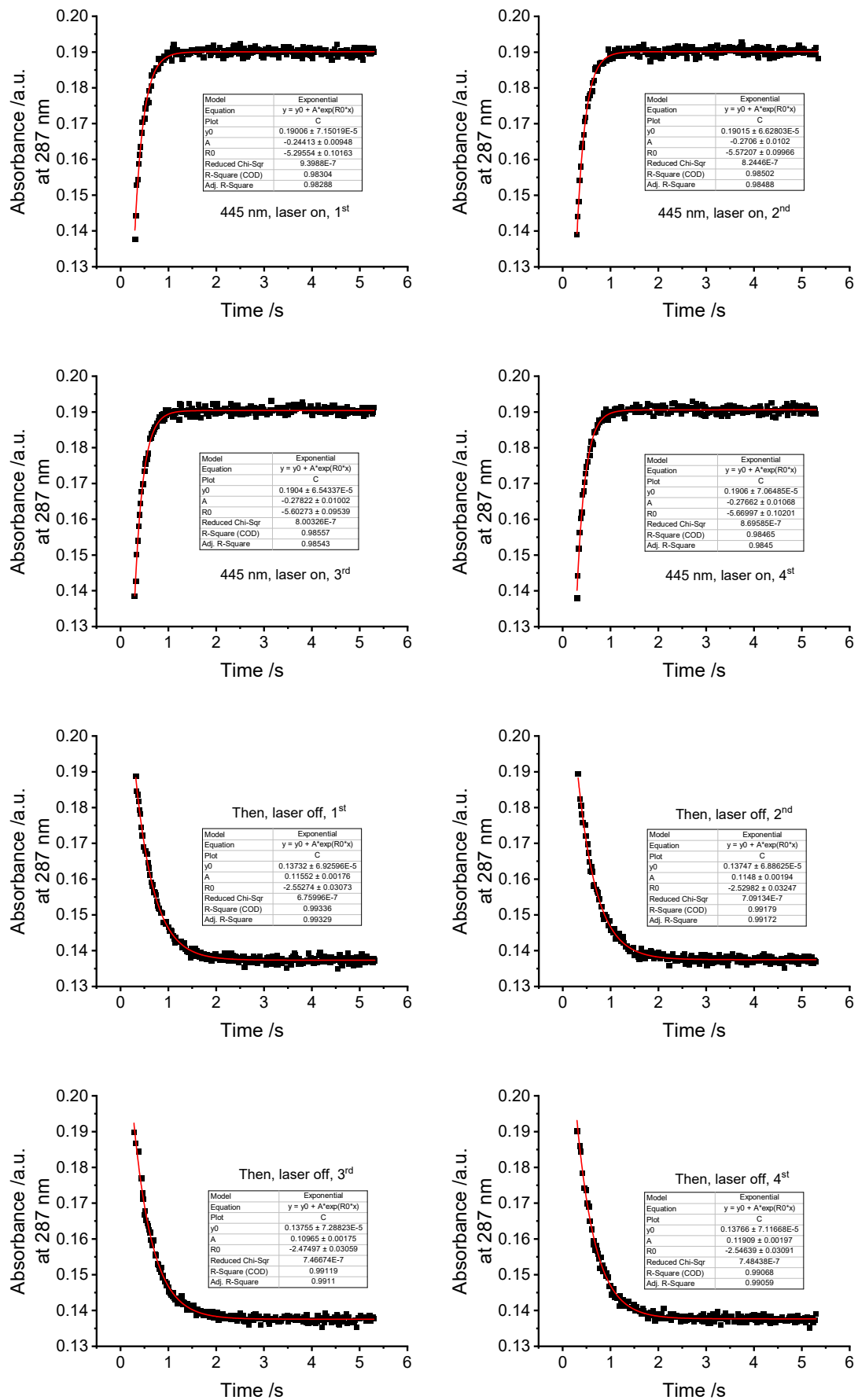
d) 3a, pH = 2.00



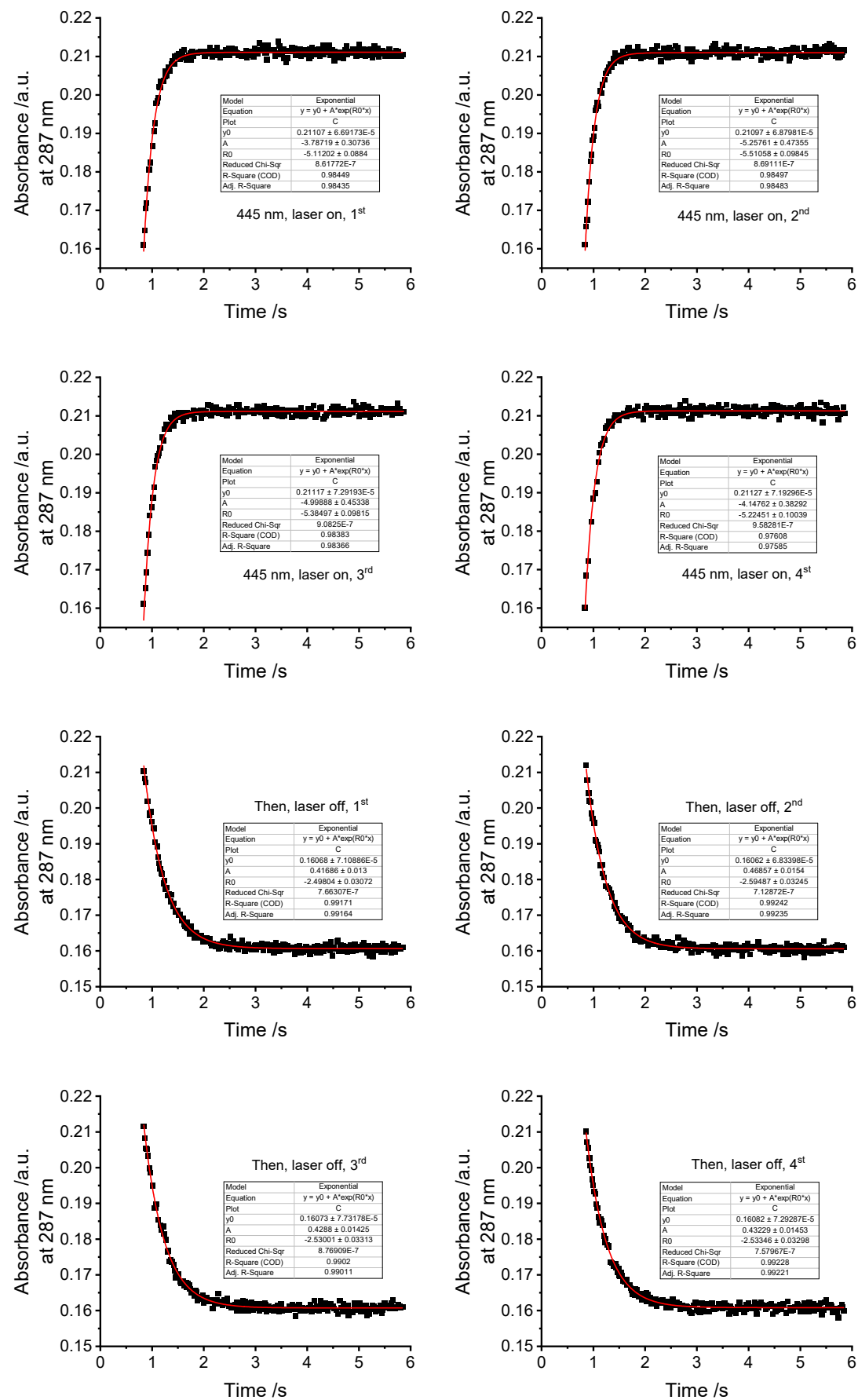
e) 3a, pH = 3.02



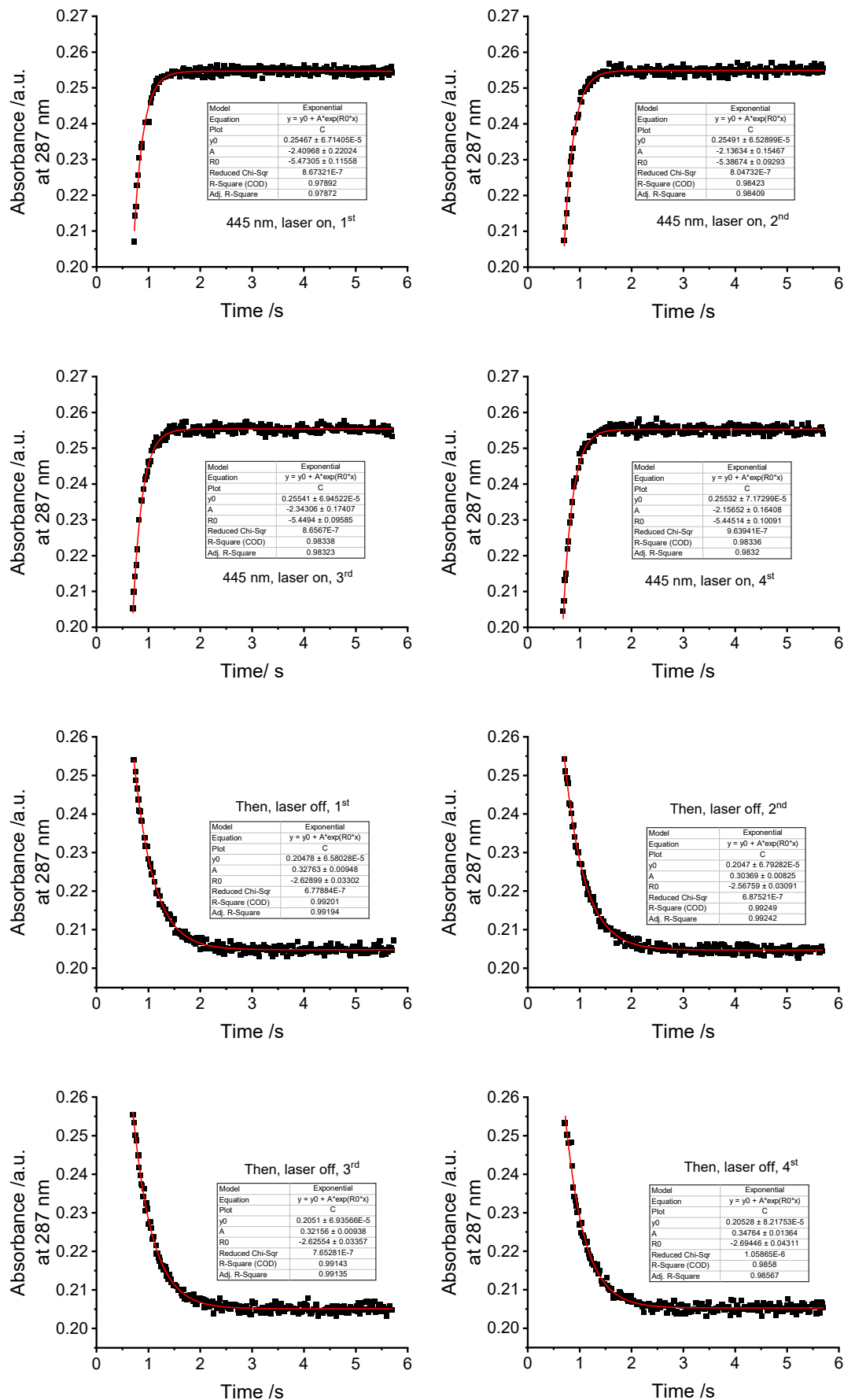
f) 3a, pH = 4.02



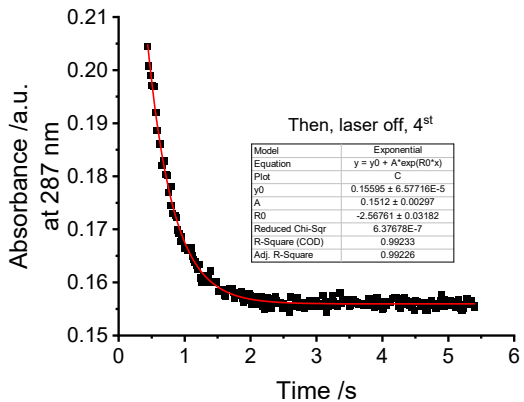
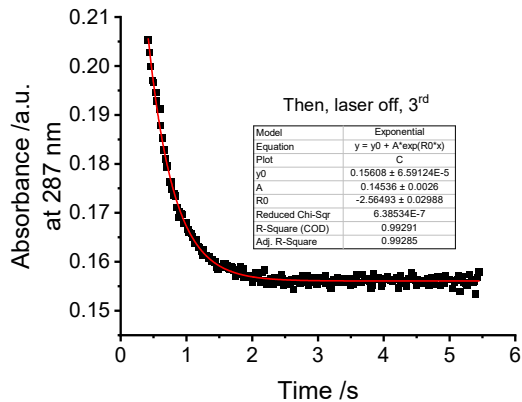
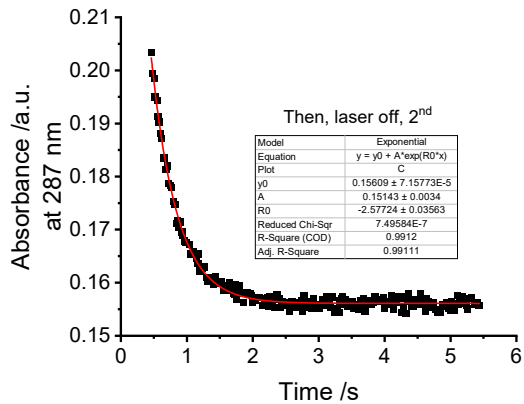
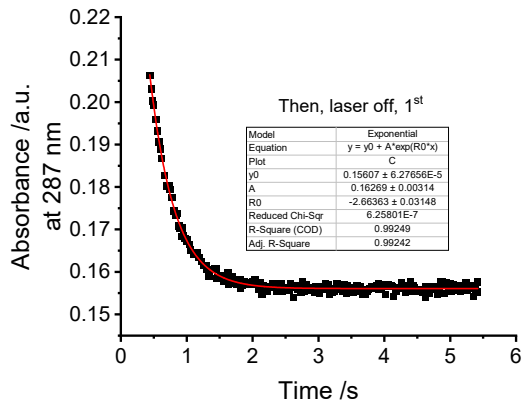
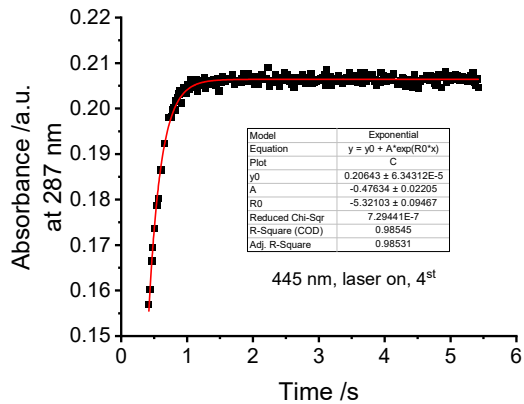
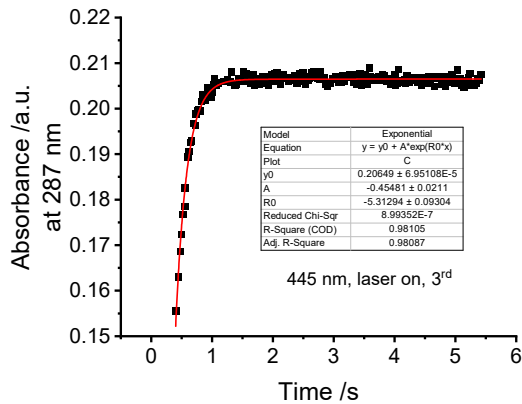
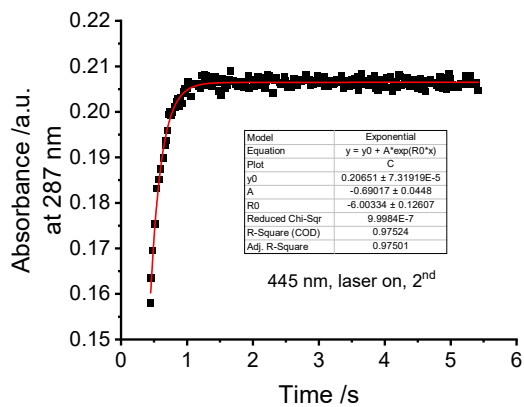
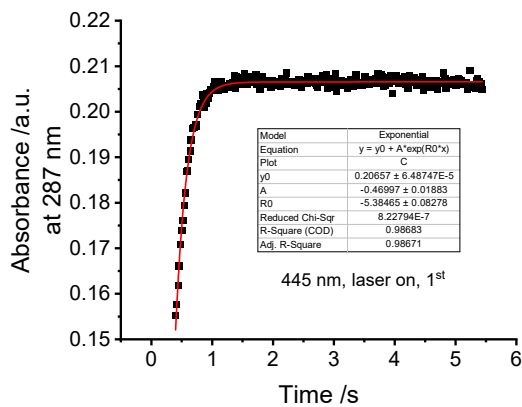
g) 3a, pH = 5.19



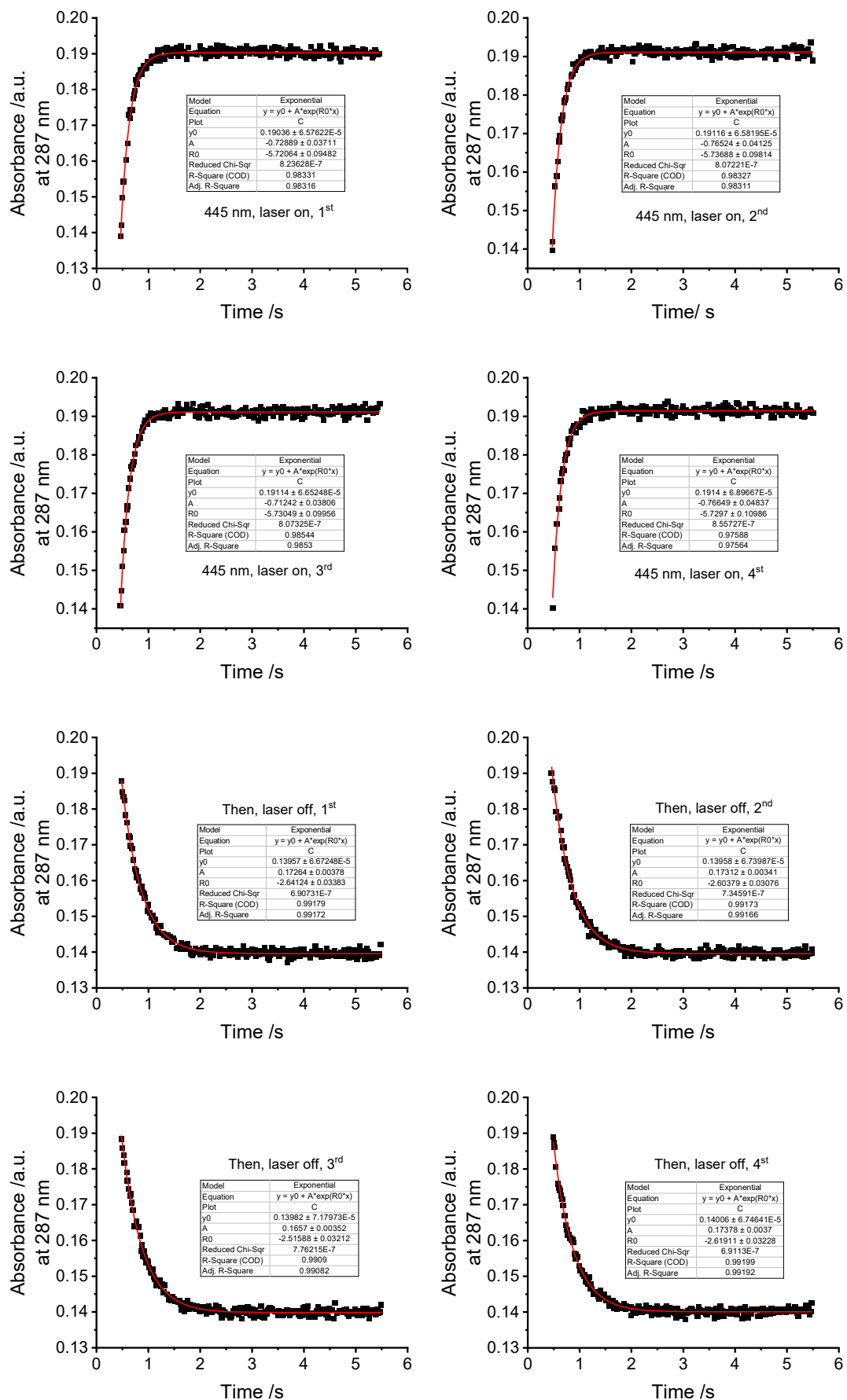
h) 3a, pH = 6.01



i) 3a, pH = 7.00



j) 3a, pH = 7.46

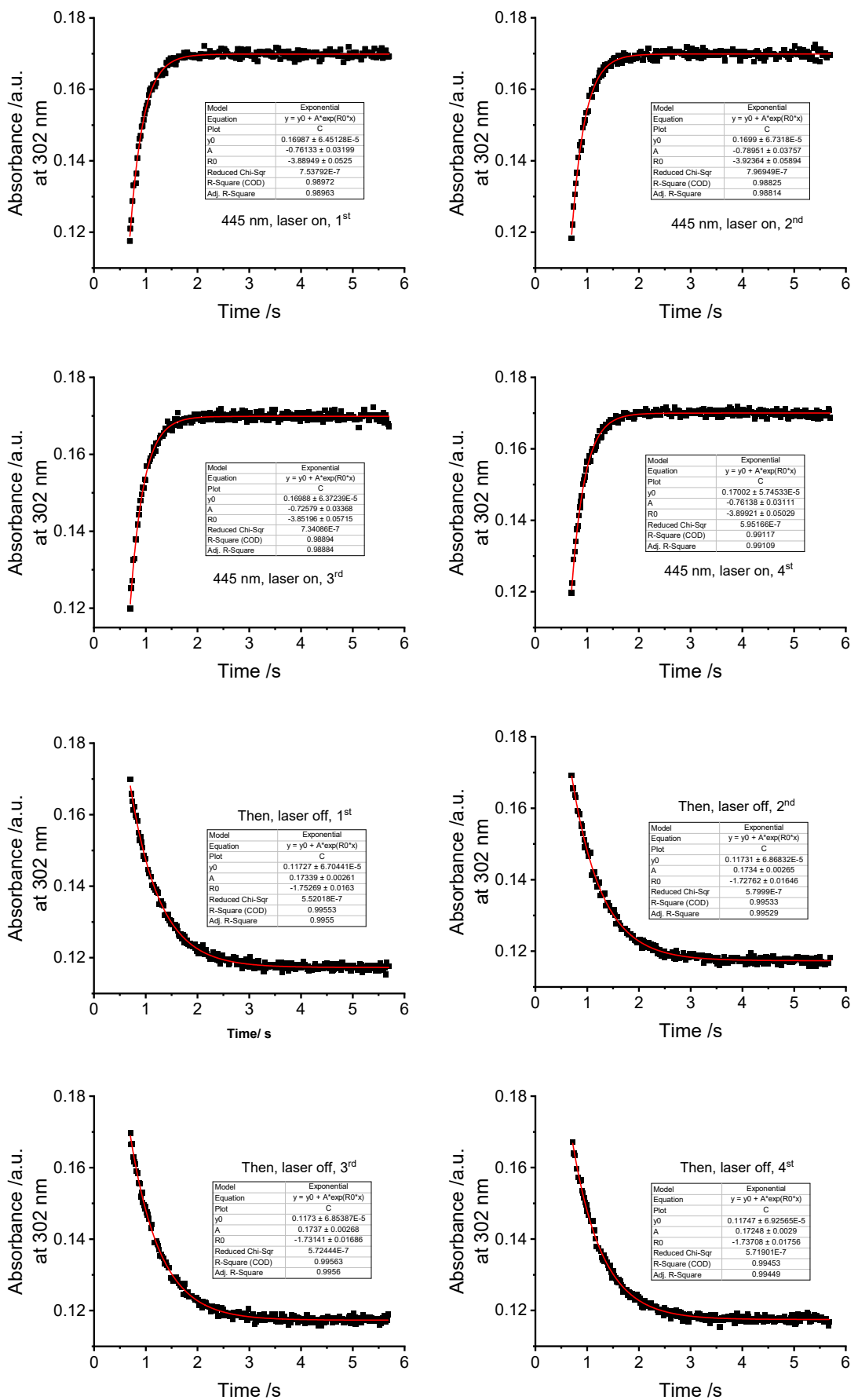


pH	<i>k</i>_{relax} /s⁻¹	<i>k</i>_{light}/s⁻¹	t_{1/2} /ms	ΔAbs. /a.u.
-0.33	8.54019 ^a	10.28039	81	0.011
0.00	7.22772	6.863335	96	0.024
0.51	3.61381	6.190433	192	0.039
1.11	2.85824	5.852978	242	0.045
2.00	2.58886	5.567583	268	0.05
3.02	2.52951	5.535078	274	0.05
4.02	2.52598	5.30802	274	0.052
5.19	2.53909	5.438583	273	0.051
6.01	2.62914	5.431815	264	0.05
7.00	2.59335	5.729428	267	0.05
7.46	2.59500	10.28039	267	0.05

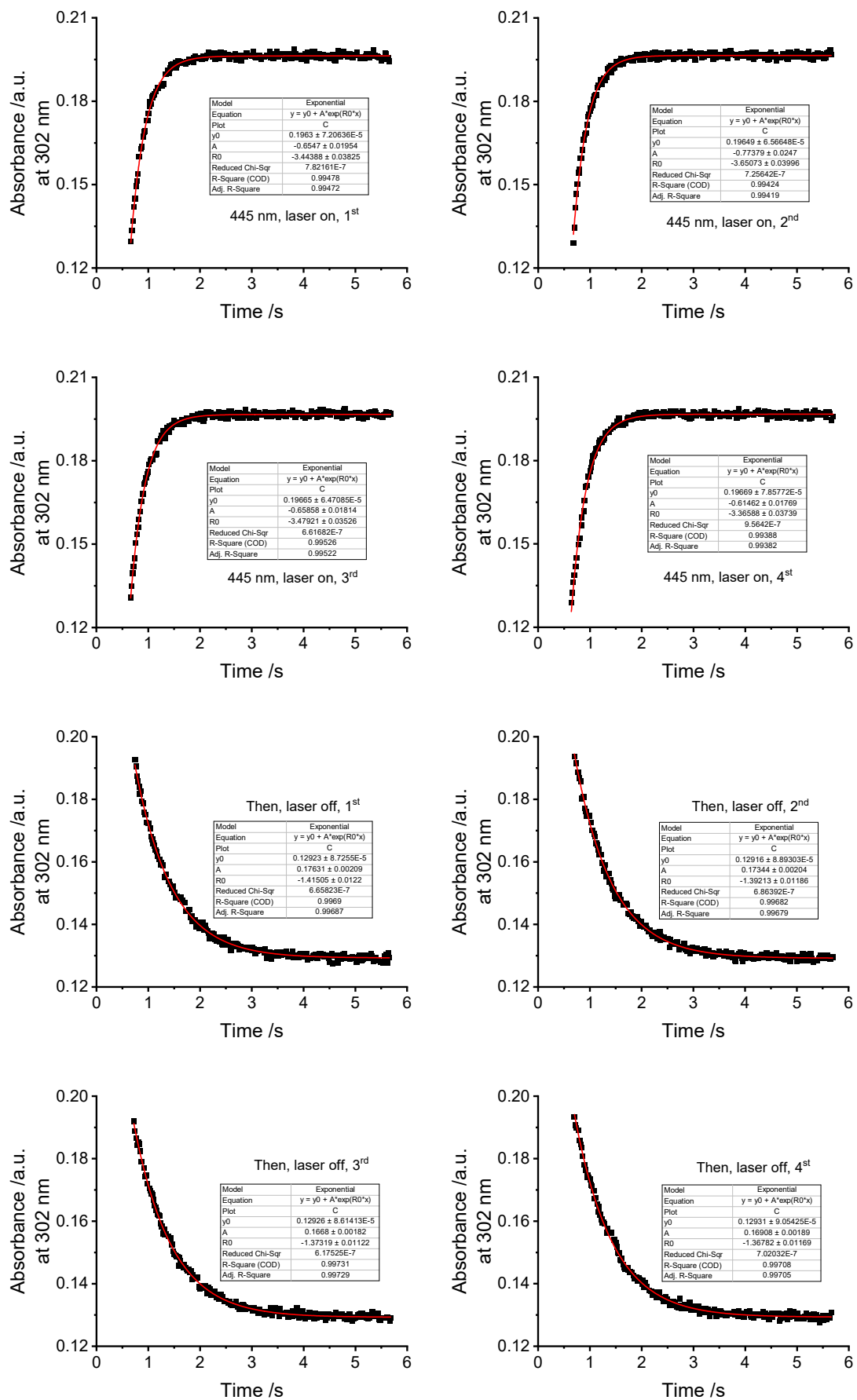
Table S4. Kinetics and half-life half-lives ($t_{1/2} = \frac{\ln 2}{k}$) of **3a** at pH = -0.33 to 7.46 in PBS/MeCN = 2/1, PBS = phosphate buffer saline at specified pH, pH ranging from -0.33 to 7.46, conc. = 50 μ M, Power density_{445 nm} = 391 mW cm⁻² at room temperature (298 K).

^a. The room-temperature kinetic rate of **3a** at the indicated pH were extrapolated by using the Eyring equation.

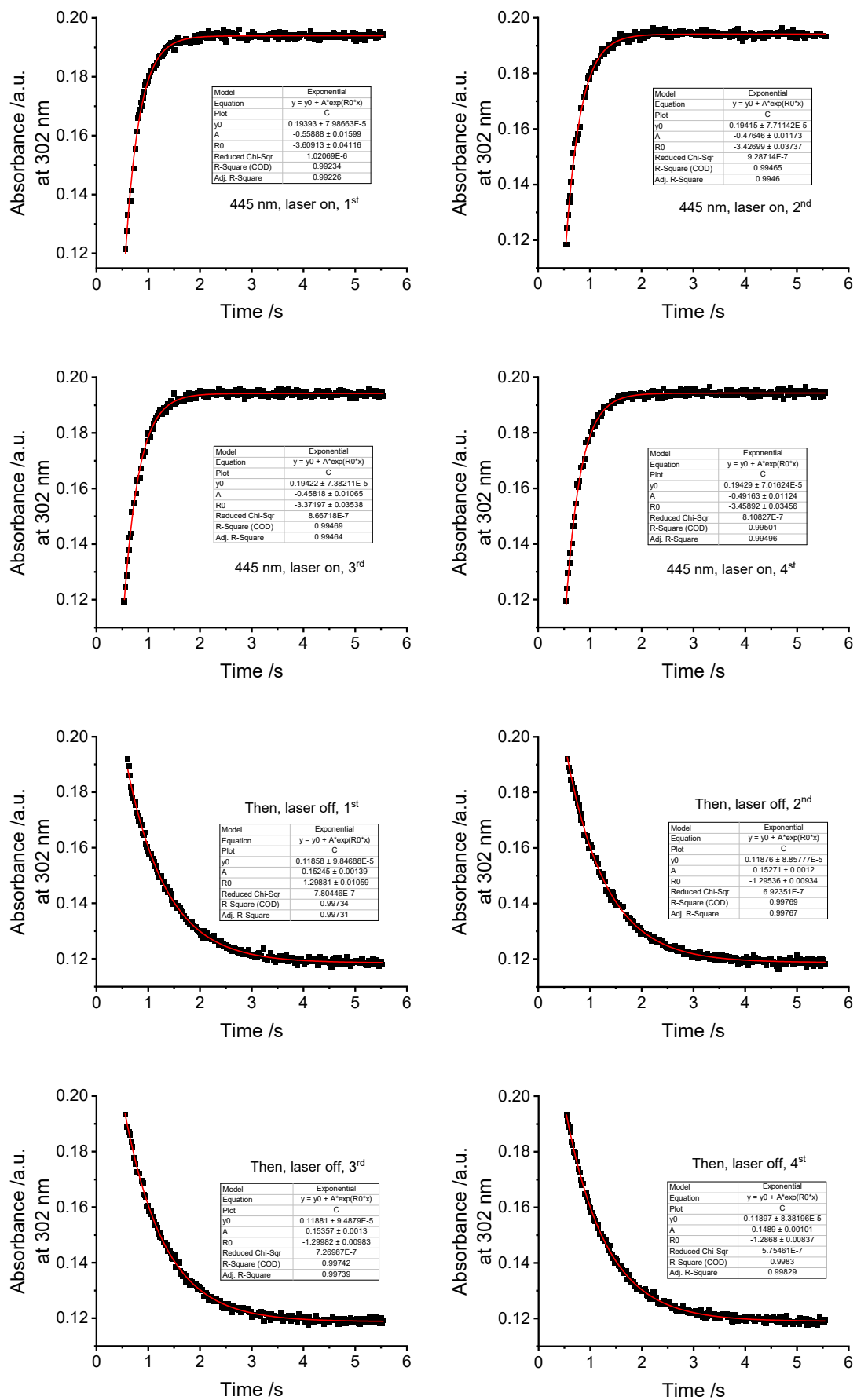
a) 4a, pH = -0.33



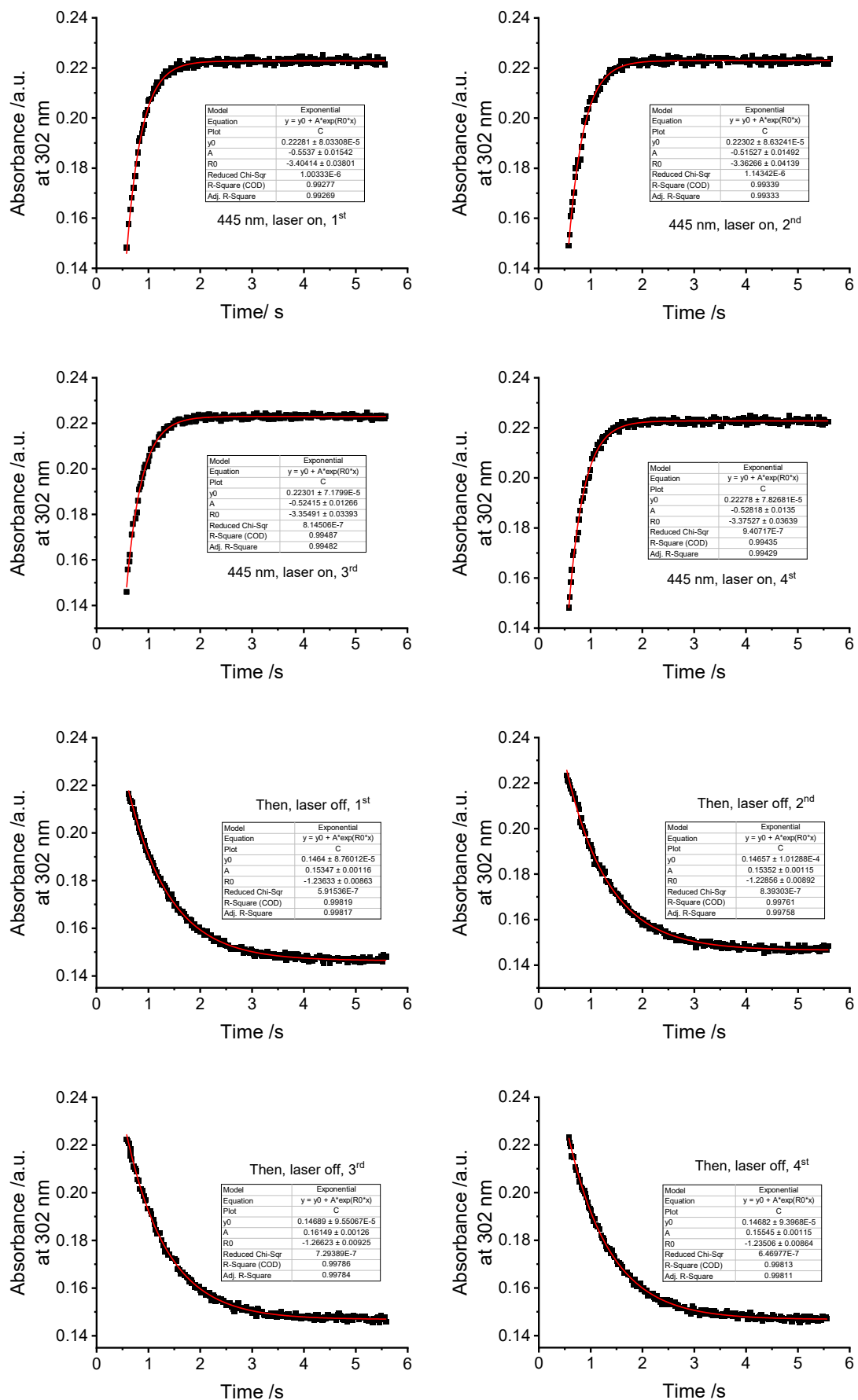
b) 4a, pH = 0.00



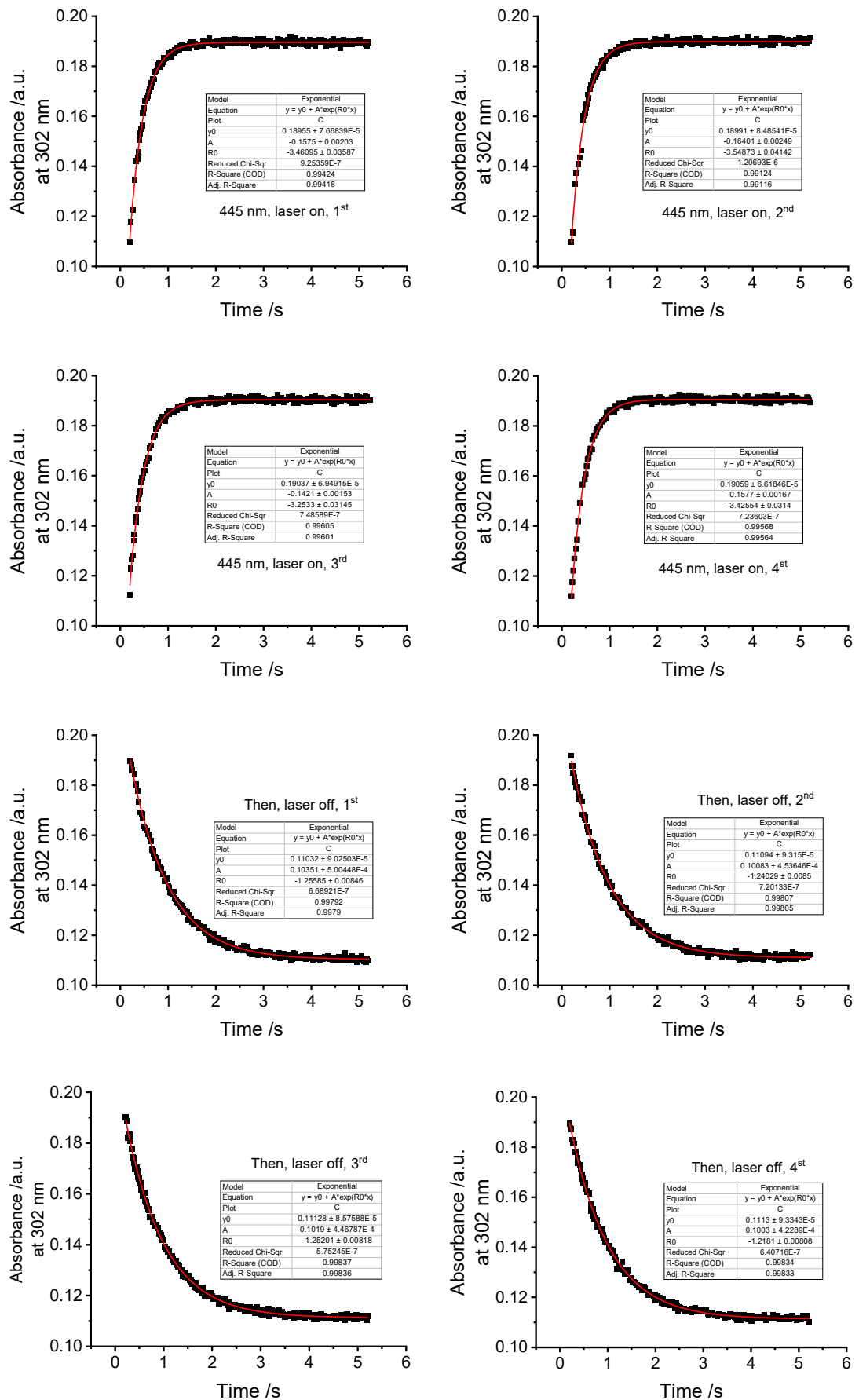
c) 4a, pH = 0.51



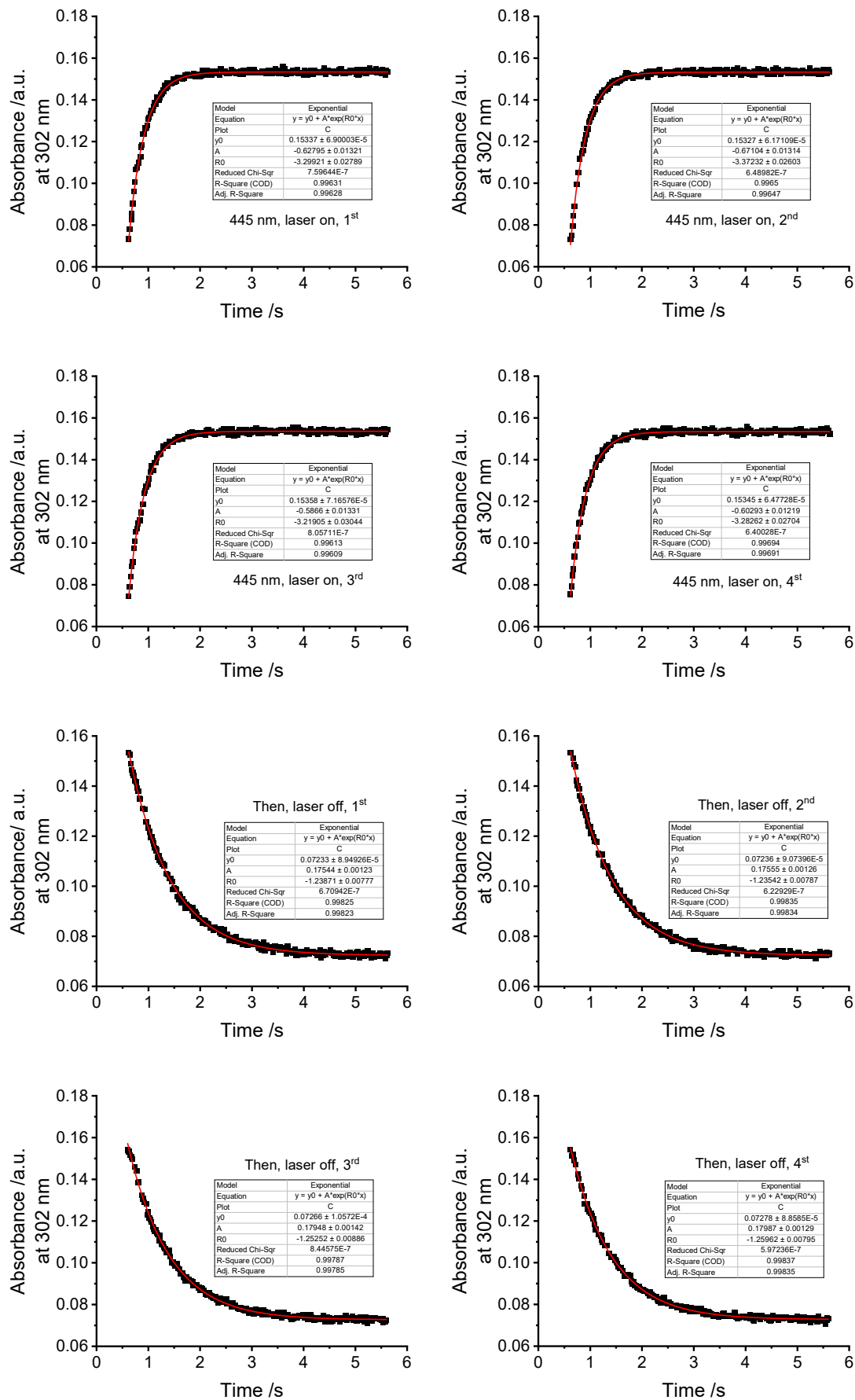
d) 4a, pH = 1.11



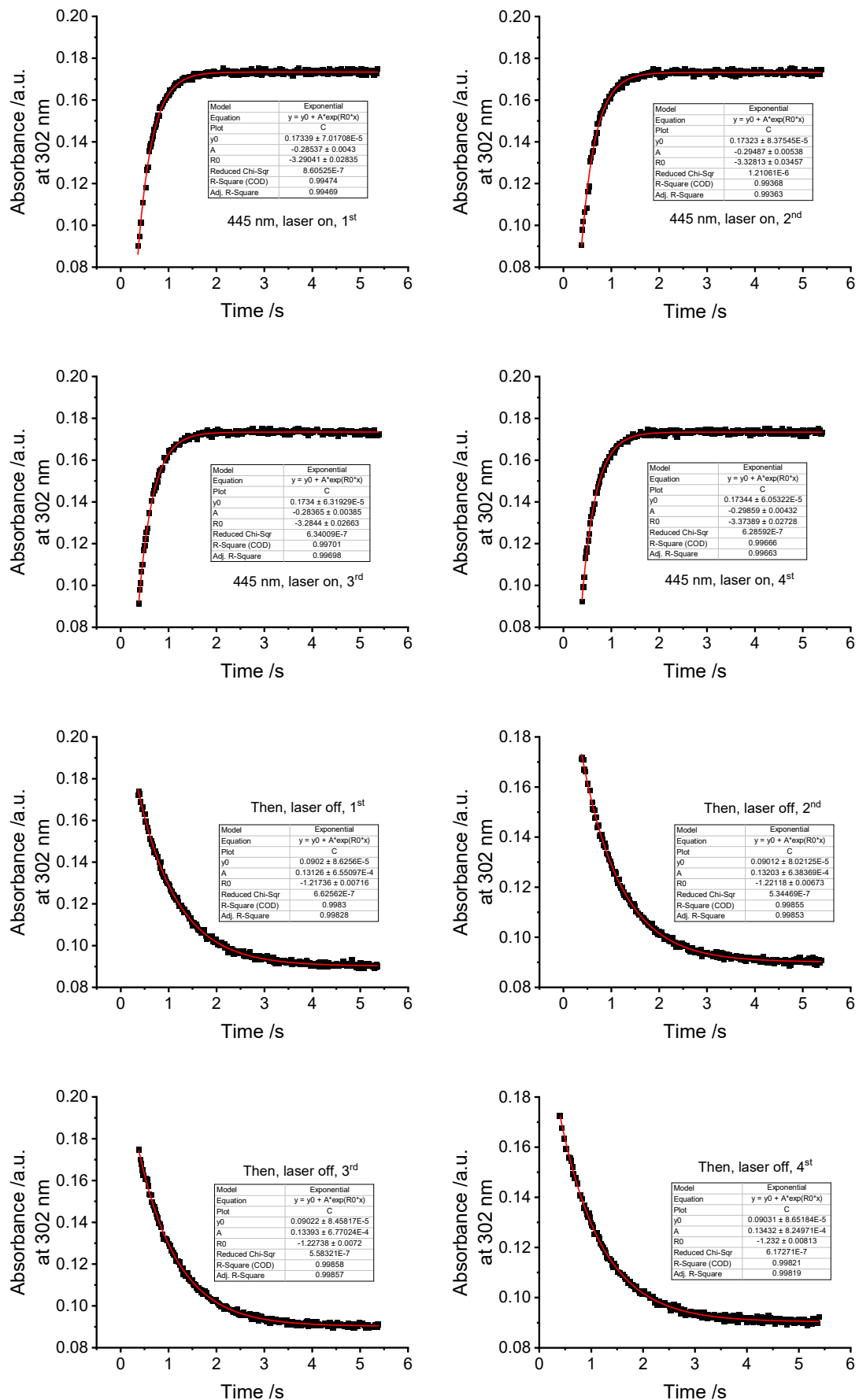
e) 4a, pH = 2.00



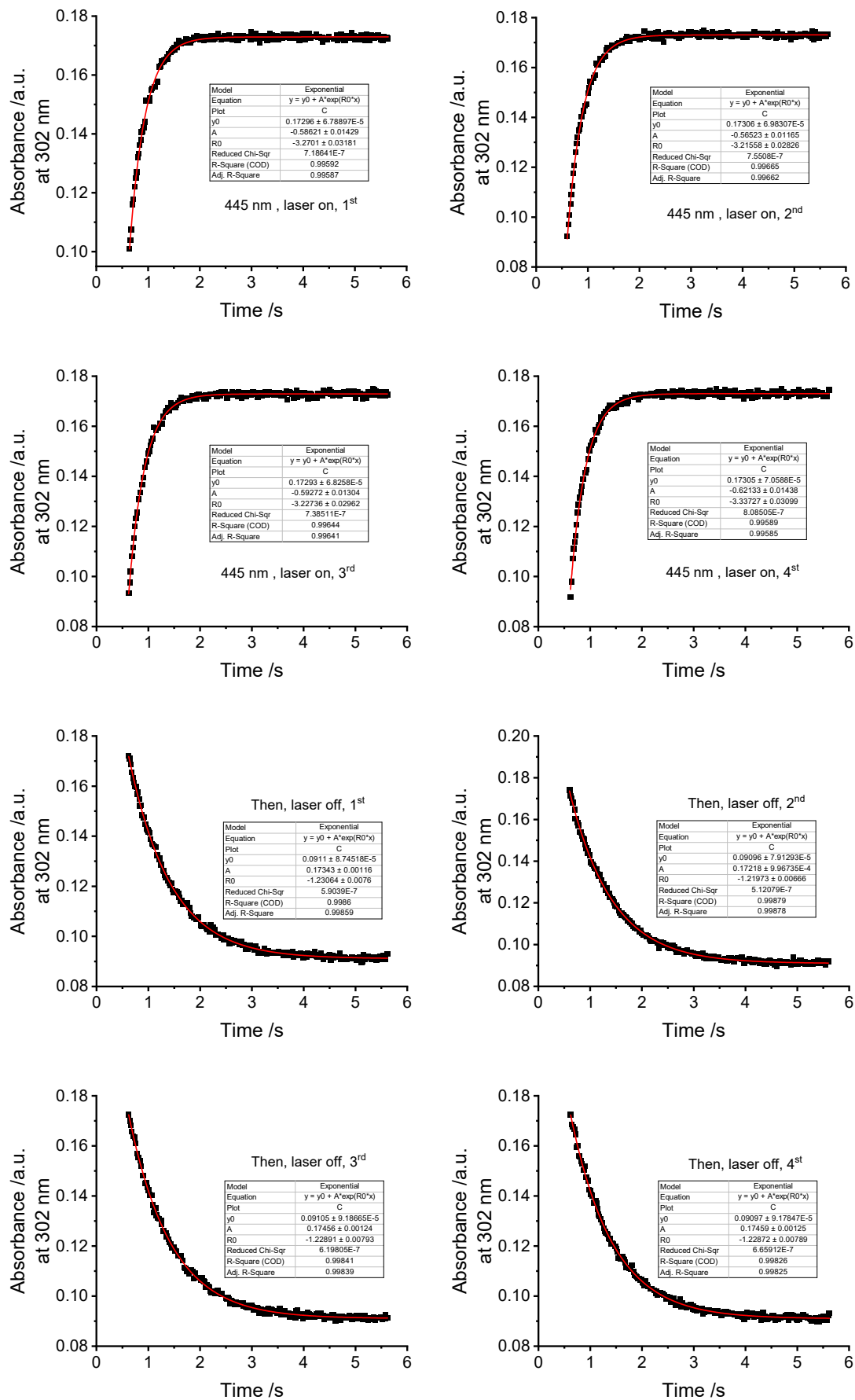
f) 4a, pH=3.02



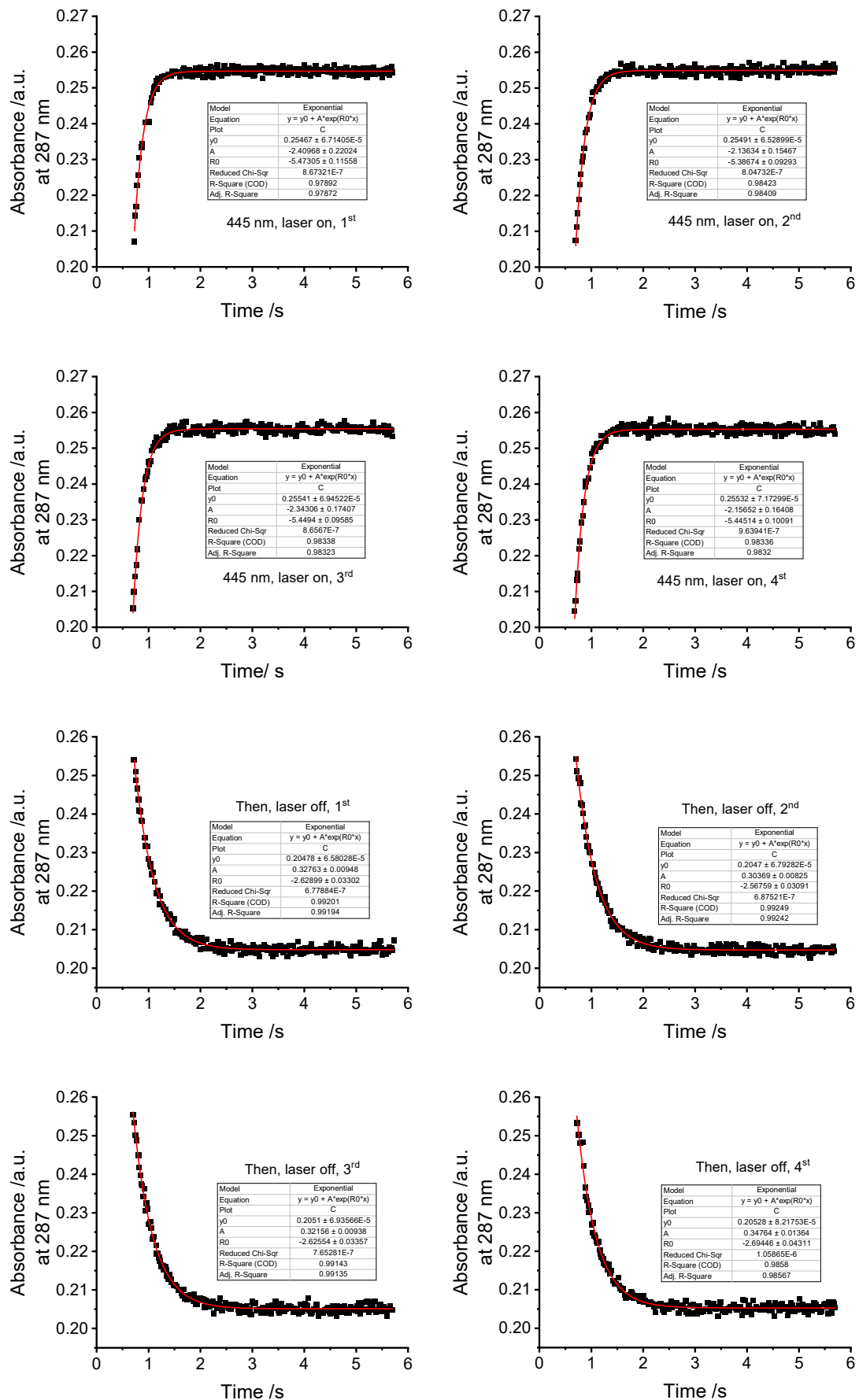
g) 4a, pH = 4.02



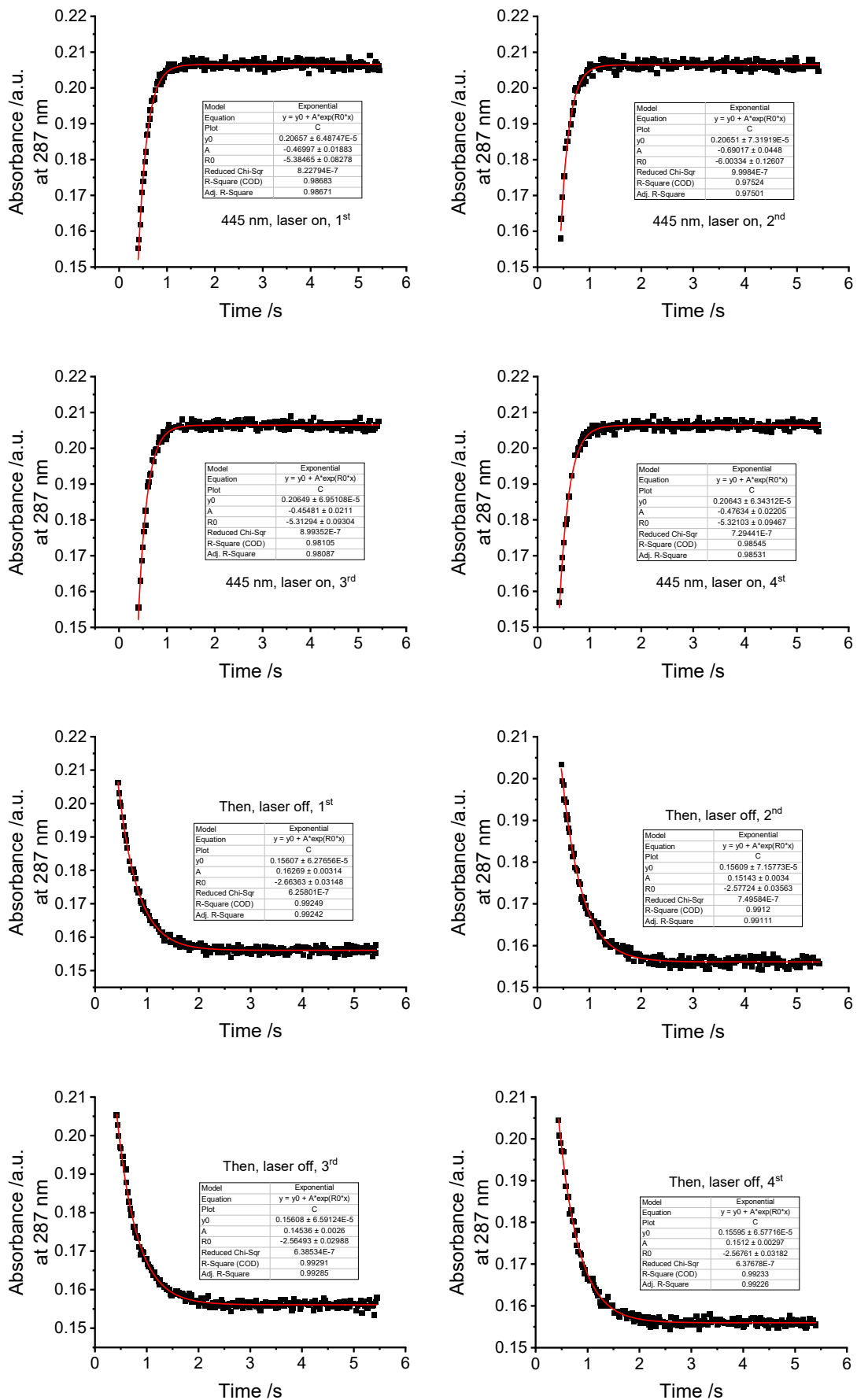
h) 4a, pH = 5.19



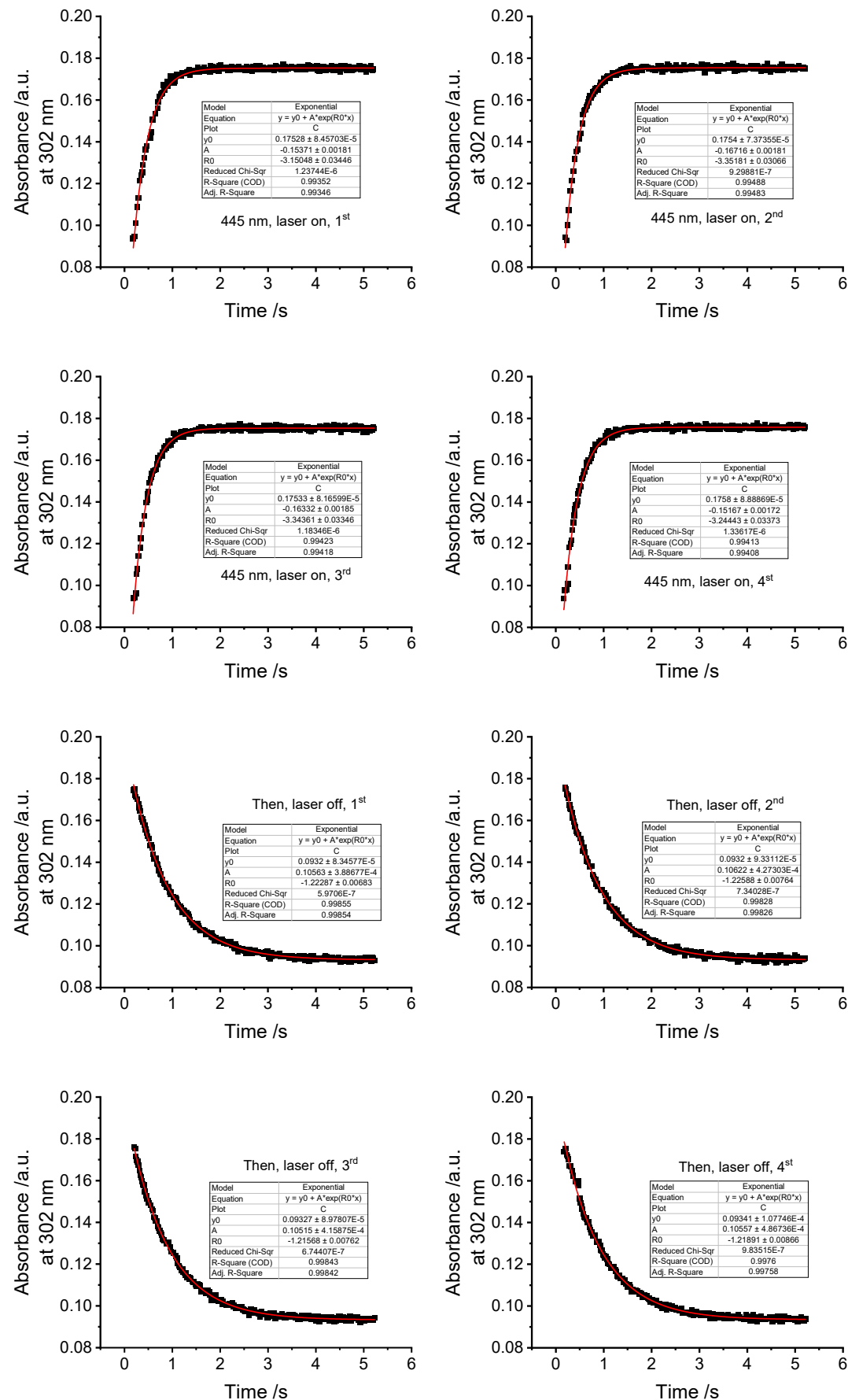
i) 4a, pH = 6.01



j) 4a, pH = 7.00



k) 4a, pH=7.46



pH	<i>k</i>_{relax} /s⁻¹	<i>k</i>_{light}/s⁻¹	t_{1/2} /ms	ΔAbs. /a.u.
-0.33	1.73720	3.89107	399	0.053
0.00	1.38705	3.48492	500	0.064
0.51	1.29520	3.46675	535	0.074
1.11	1.24154	3.37424	558	0.076
2.00	1.24156	3.42213	558	0.078
3.02	1.24657	3.2933	556	0.08
4.02	1.22448	3.31921	566	0.082
5.19	1.22700	3.26258	565	0.081
6.01	1.22868	3.26525	564	0.081
7.00	1.21539	3.30407	570	0.082
7.46	1.22083	3.27258	568	0.082

Table S5. Kinetics and half-life half-lives ($t_{1/2} = \frac{\ln 2}{k}$) of **4a** at pH = -0.33 to 7.46 in PBS/MeCN = 2/1, PBS = phosphate buffer saline at specified pH, pH ranging from -0.33 to 7.46, conc. = 50 μM, Power density_{445 nm} = 391 mW cm⁻² at room temperature (298 K).

3.8 Temperature-dependent thermodynamic decaying kinetics at different pHs and corresponding Eyring plots for 1a, 3a, and DBTD.

The thermodynamic $E \rightarrow Z$ isomerization kinetics was studied at various temperature (from 268 K to 273 K or 273K to 288K) and at various pH conditions in MeCN/PBS (v/v = 1/2) with a programmable thermostatic cuvette holder (Qpod 2eTM, American Quantum Northwest Ltd.). Kinetic parameters were acquired by plotting the absorbance evolution versus time in seconds at the chosen wavelength where there is a largest discrepancy in the absorbance between the Z -isomer and the PSS. All data processing was performed using the nonlinear-fitting ‘exponential’ and linear fitting function in Origin pro software. The Eyring equation was used to calculate the value of the thermodynamic variables (shown as follows).

$$\text{Eyring equation: } \ln \frac{k}{T} = -\frac{\Delta H^\ddagger}{RT} + \ln \frac{k_B}{h} + \frac{\Delta S^\ddagger}{R}$$

$$\text{Slope} = -\frac{\Delta H^\ddagger}{R}$$

$$\text{Y - intercept} = \ln \frac{k_B}{h} + \frac{\Delta S^\ddagger}{R}$$

where:

k = thermal reversion rate (s^{-1})

T = absolute temperature (K)

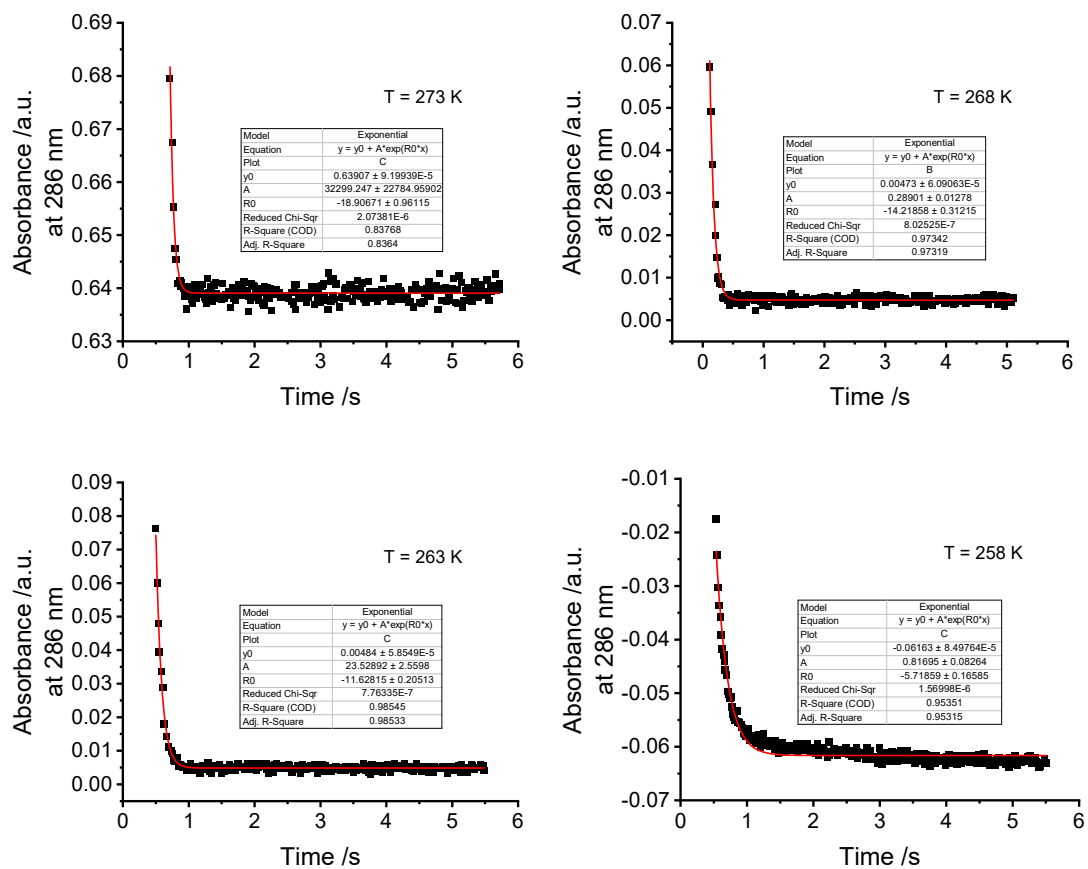
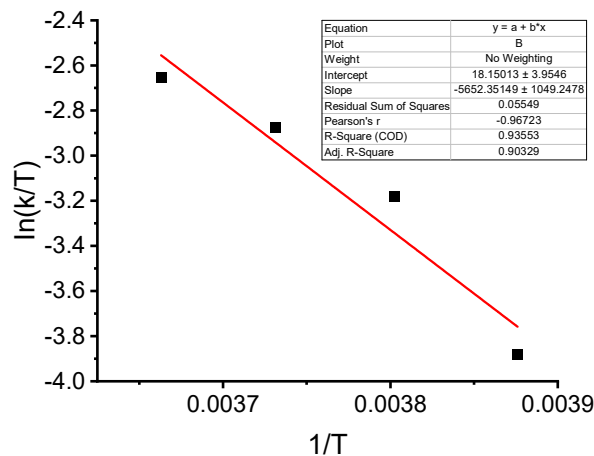
R = gas constant = $8.31446261815324 \text{ J}\cdot\text{K}^{-1}\cdot\text{mol}^{-1}$

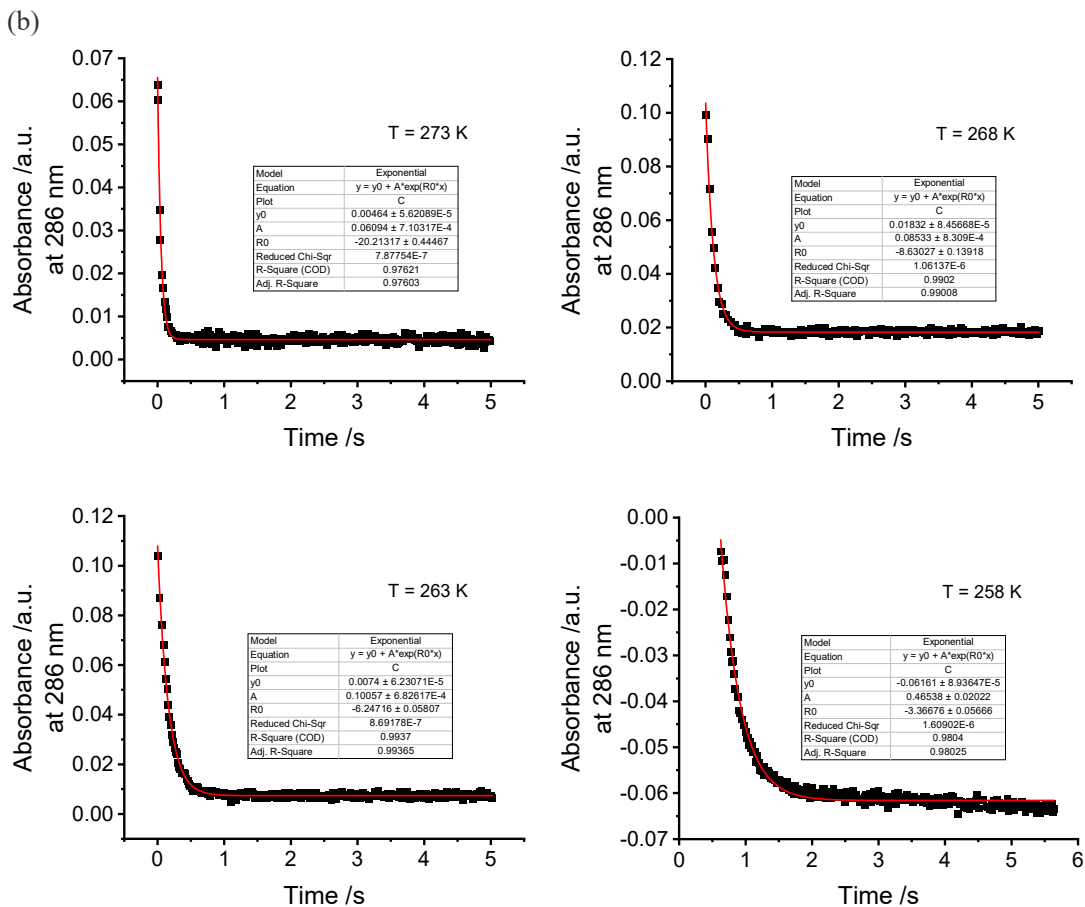
k_B = Boltzmann constant = $1.381 \times 10^{-23} \text{ J}\cdot\text{K}^{-1}$

h = Planck’s constant = $6.626070 \times 10^{-34} \text{ J}\cdot\text{s}$

Free energy of activation (free energy barrier) $\Delta G^\ddagger = \Delta H^\ddagger - T\Delta S^\ddagger$.

(a)

Eyring plot of $\ln(k/T)$ vs $1/T$ for DBTD at pH = -0.33. Linear fitting with Adjusted $R^2 = 0.903$.



Eyring plot of $\ln(k/T)$ vs $1/T$ for DBTD at $\text{pH} = 0.0$. Linear fitting with Adjusted $R^2 = 0.961$.

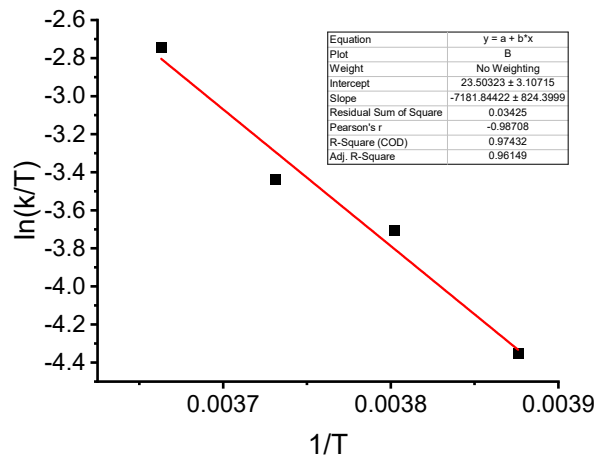
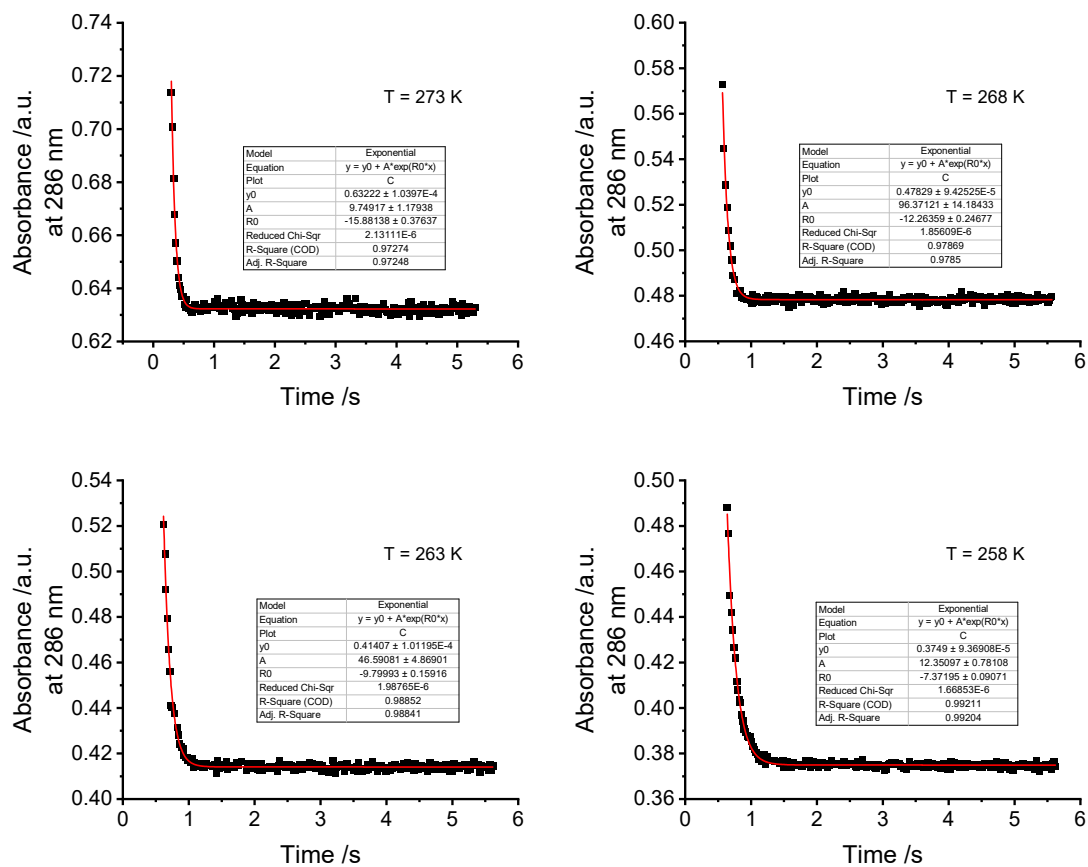
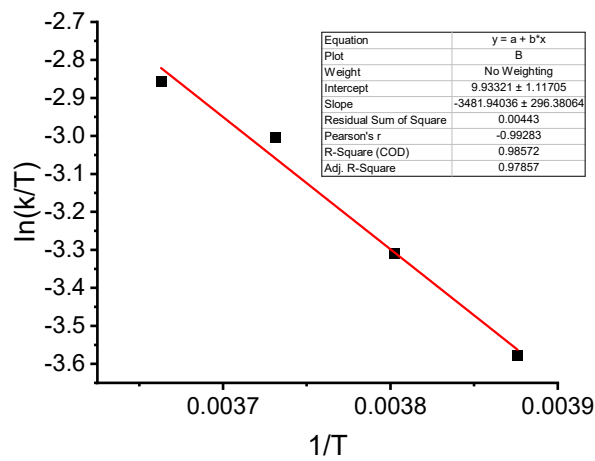
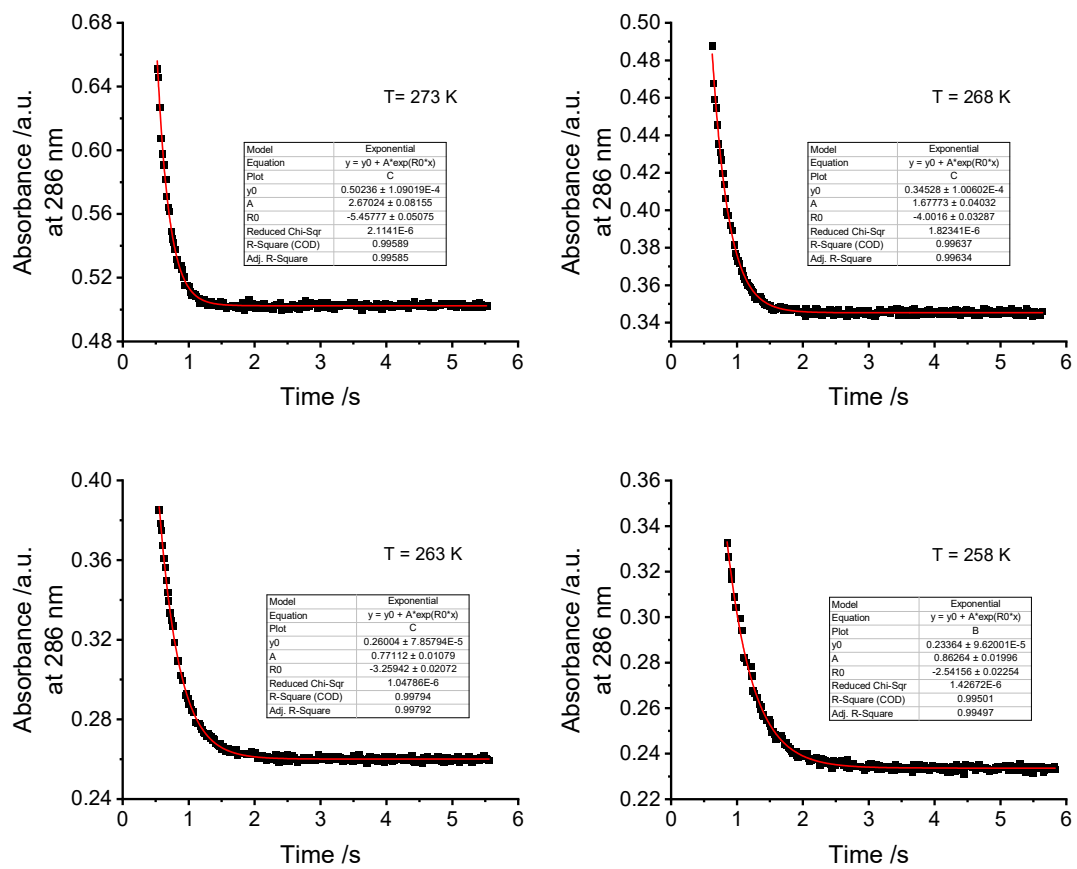


Figure S27. Temperature-dependent thermal decaying rates for *E*-DBTD in solution phase, in PBS/MeCN = 2/1, conc. = 50 μM , and corresponding Eyring plot of $\ln(k/T)$ versus $1/T$. (a) for DBTD, in $\text{pH} = -0.33$. (b) for DBTD, in $\text{pH} = 0.00$. Power density_{445nm} = 391 mW cm^{-2} .

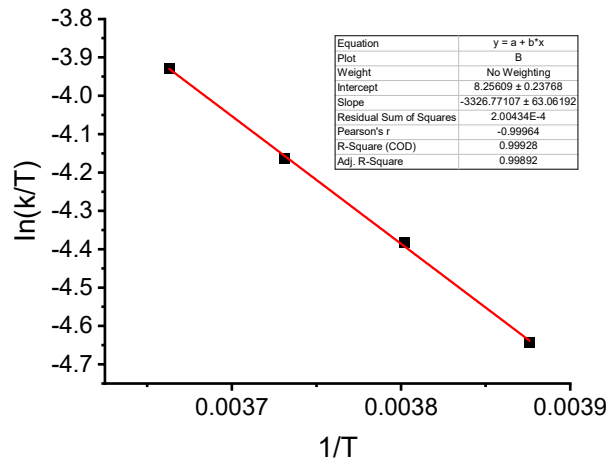
(c)

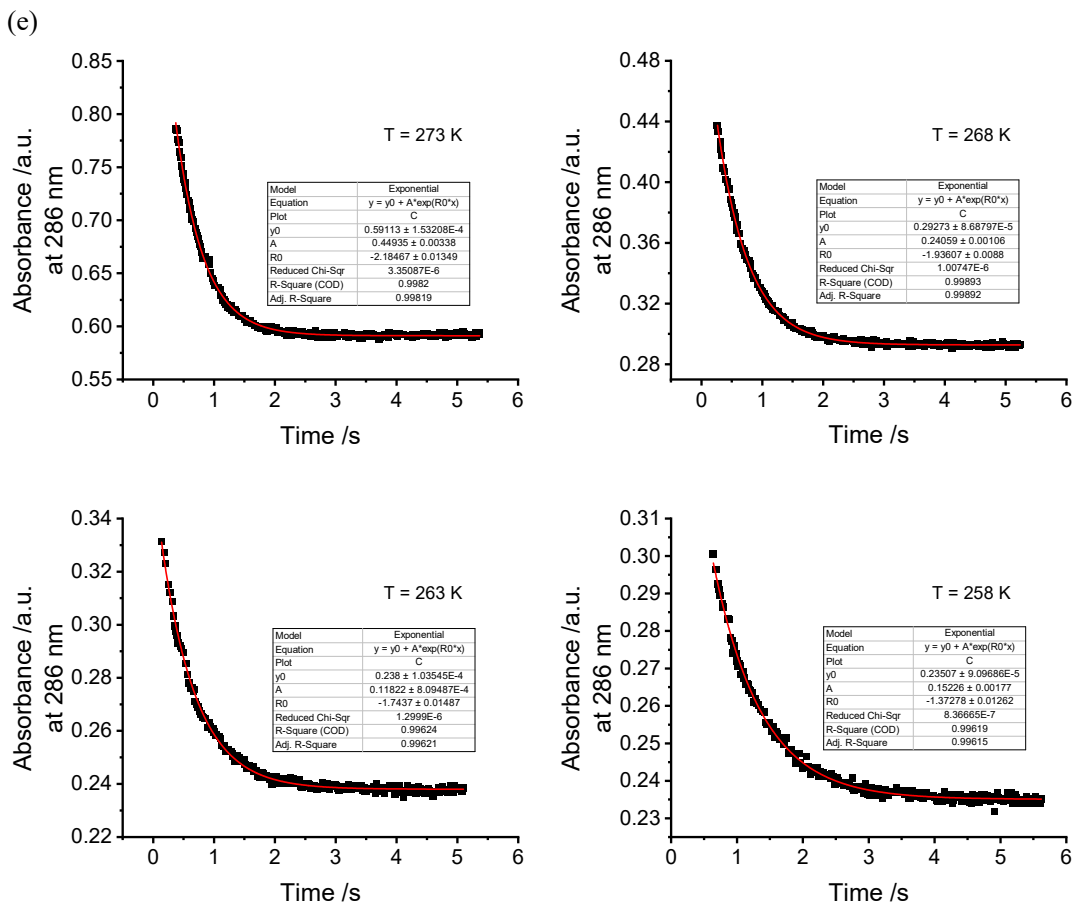
Eyring plot of $\ln(k/T)$ vs $1/T$ for **1a** at pH = -0.33. Linear fitting with Adjusted $R^2 = 0.979$.

(d)



Eyring plot of $\ln(k/T)$ vs $1/T$ for **1a** at pH = 0.0. Linear fitting with Adjusted $R^2 = 0.999$.





Eyring plot of $\ln(k/T)$ vs $1/T$ for **1a** at pH = 0.51. Linear fitting with Adjusted $R^2 = 0.993$.

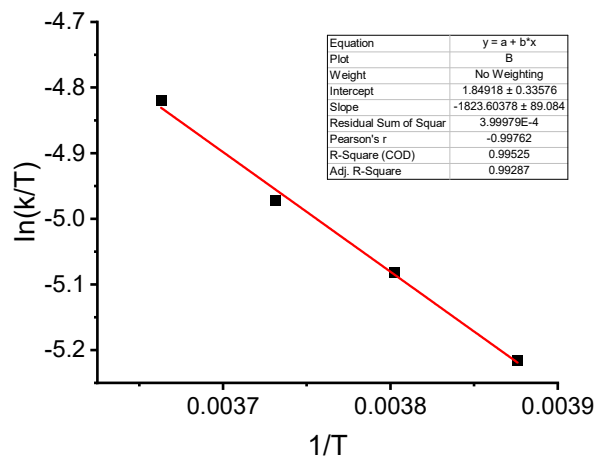
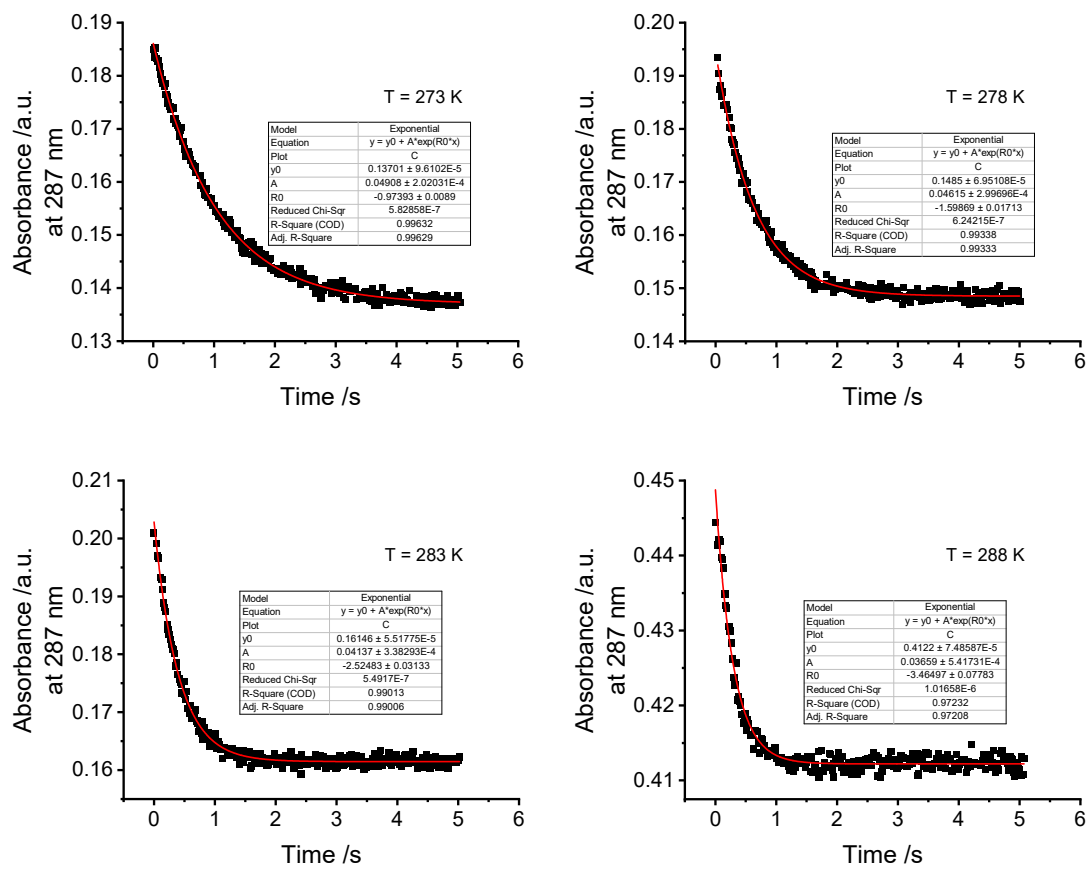


Figure S28. Temperature-dependent thermal decaying rates for *E*-isomers of **1a** in solution phase, in PBS/MeCN = 2/1, conc. = 50 μM , and corresponding Eyring plot of $\ln(k/T)$ versus $1/T$. (c) for **1a**, in pH = -0.33. (d) for **1a**, in pH = 0.00. (e) for **1a**, in pH = 0.51. Power density_{445nm} = 391 mW cm^{-2} .

(f)



Eyring plot of $\ln(k/T)$ vs. $1/T$ for **3a** at pH = -0.33. Linear fitting with Adjusted $R^2 = 0.997$.

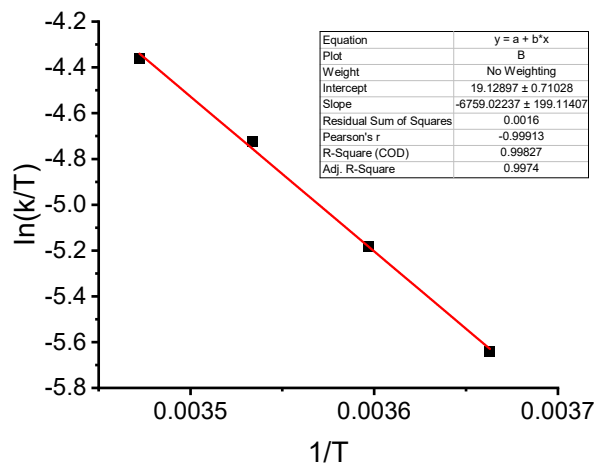
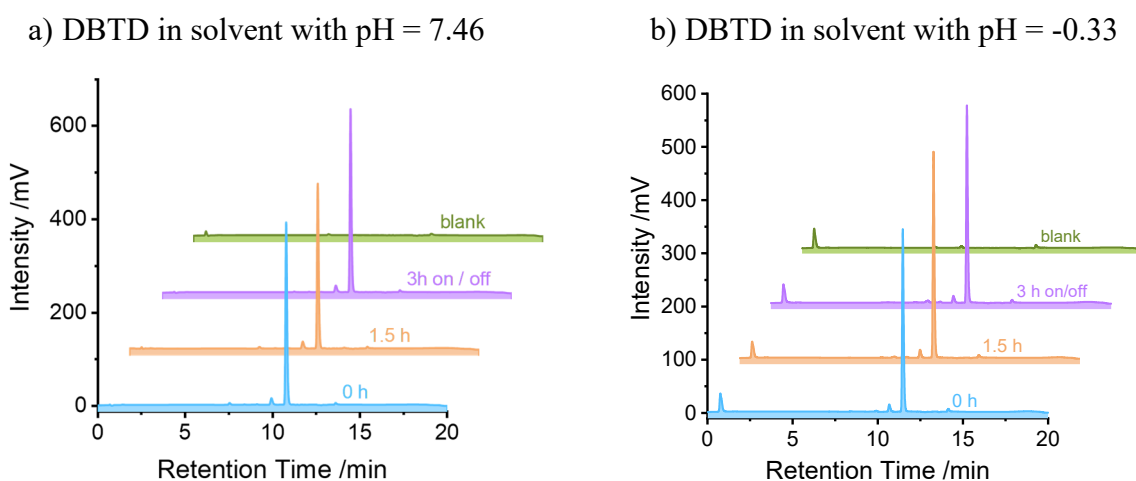


Figure S29. Temperature-dependent thermal decaying rates for *E*-isomers of **3a** in solution phase, in PBS/MeCN = 2/1, conc. = 50 μM , and corresponding Eyring plot of $\ln(k/T)$ versus $1/T$. (f) for **3a**, in pH = -0.33. Power density_{445nm} = 391 mW cm^{-2} .

4. HPLC-MS analysis to monitor the stability of DBTD and 1a-4a under neutral and acidic conditions.

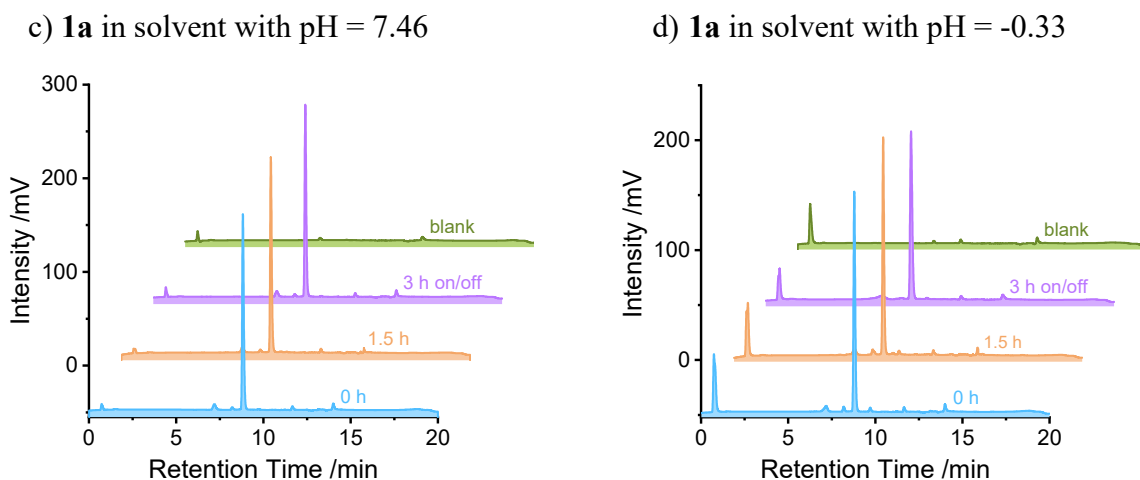
To further investigate the photo-stability of DBTD and **1a-4a**, HPLC experiments were conducted. Initially, DBTD and **1a-4a** were individually prepared as 1.0 mM stock solutions in MeCN. This step ensured accuracy and consistency in concentration during subsequent dilutions. Subsequently, these stock solutions were diluted in two different solvent systems to achieve the desired 100 μ M concentration for side-by-side comparison. The two solvent systems were PBS/MeCN (v/v = 2/1, pH = 7.4) and PBS/MeCN (v/v = 2/1, pH = -0.33). During the dilution process, precise measurements of solvents and stock solutions were crucial to guarantee the exactness of the final concentration. Following this, the prepared 100 μ M cycloazoarene solutions were transferred into 2.0 mL capped liquid chromatography vials, then the samples were exposed to the irradiation conditions or dedicated for sample storage in the dark as a reference. Finally, the vials containing the exposed cycloazoarene were subjected to the HPLC-MS resolving and analysis according to the predetermined analytical conditions.



Sample	Peak area	Remaining percentage
DBTD-pH = 7.46	2553003	
DBTD-pH = 7.46-1.5 h	2274866	89.1%
DBTD-pH = 7.46-3h on / off	2527767	99.0%

Sample	Peak area	Remaining percentage
DBTD-pH = -0.33	2350925	
DBTD-pH = -0.33-1.5 h	2350753	99.9%
DBTD-pH = -0.33-3h on / off	2350255	99.9%

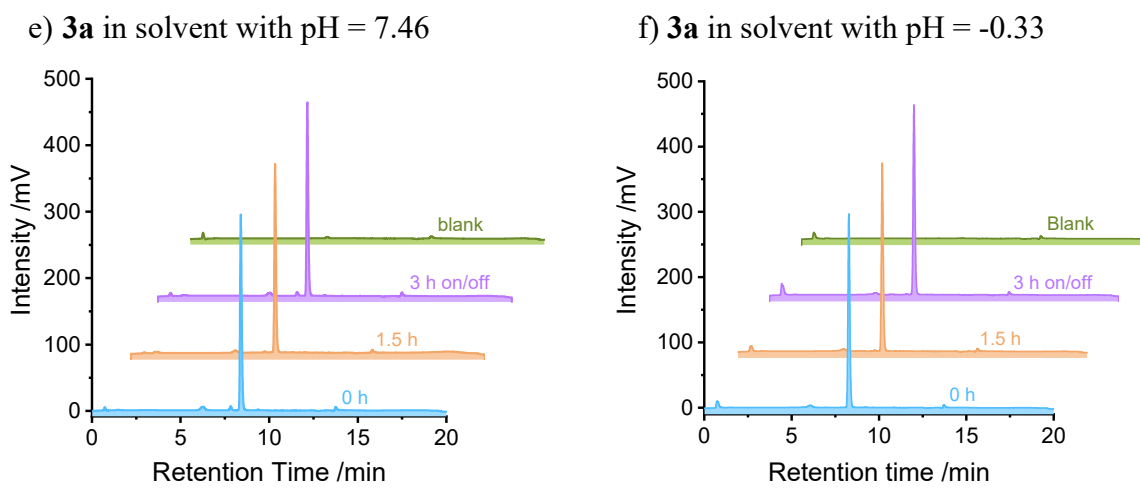
Figure S30. Stacked HPLC-MS traces for analyzing for the photo-stability of DBTD under the 445 nm irradiation. a) DBTD in pH = 7.46, b) DBTD in pH = -0.33. HPLC traces for sample stored in the dark, for sample after continuously exposure for 1.5 h, and for sample after intermittently exposure for 3 h (5s on, 5s off) were shown in cyan, orange, and purple colour, respectively. The integrated peak area and remaining percentage for DBTD are shown in the tables. Conditions: DBTD, in PBS/MeCN (v/v = 2/1) pH = 7.4 or in PBS/MeCN (v/v = 2/1) pH = -0.33, conc. = 100 μM , T = 298 K, Power density_{445 nm} = 391 mW cm⁻².



Sample	Peak area	Remaining percentage
1a -pH = 7.46	1372384	
1a -pH = 7.46-1.5 h	1339166	97.6%
1a -pH = 7.46-3h on / off	1349634	98.3%

Sample	Peak area	Remaining percentage
1a -pH = -0.33	1352553	
1a -pH = -0.33-1.5 h	1293541	95.6%
1a -pH = -0.33-3h on / off	1322112	97.7%

Figure S31. Stacked HPLC-MS traces for analyzing for the photo-stability of **1a** under the 445 nm irradiation. c) **1a** in pH = 7.46, d) **1a** in pH = -0.33. HPLC traces for sample stored in the dark, for sample after continuously exposure for 1.5 h, and for sample after intermittently exposure for 3 h (5s on, 5s off) were shown in cyan, orange, and purple colour, repectively. The integrated peak area and remaining percentage for **1a** are shown in the tables. Conditions: **1a**, in PBS/MeCN (v/v = 2/1) pH = 7.4 or in PBS/MeCN (v/v = 2/1) pH = -0.33, conc. = 100 μ M, T = 298 K, Power density_{445 nm} = 391 mW cm⁻².



Sample	Peak area	Remaining percentage
3a -pH = 7.46	1975951	
3a -pH = 7.46-1.5 h	1944842	98.4%
3a -pH = 7.46-3h on / off	1925238	97.4%

Sample	Peak area	Remaining percentage
3a -pH = -0.33	2170359	
3a -pH = -0.33-1.5 h	2099368	96.7%
3a -pH = -0.33-3h on / off	2159070	99.5%

Figure S32. Stacked HPLC-MS traces for analyzing for the photo-stability of **3a** under the 445 nm irradiation. e) **3a** in pH = 7.46, f) **3a** in pH = -0.33. HPLC traces for sample stored in the dark, for sample after continuously exposure for 1.5 h, and for sample after intermittently exposure for 3 h (5s on, 5s off) were shown in cyan, orange, and purple colour, repectively. The integrated peak area and remaining percentage for **3a** are shown in the tables. Conditions: **3a**, in PBS/MeCN (v/v = 2/1)

pH = 7.46 or in PBS/MeCN (v/v = 2/1) pH = -0.33, conc. = 100 μ M, T = 298 K, Power density_{445 nm} = 391 mW cm⁻².

g) **2a** in pH = 7.46 versus pH = -0.33

Sample	Peak area	Remaining percentage
2a -pH = 7.46	876067	
2a -pH = 7.46-1.5 h	839540	95.8%
2a -pH = 7.46-3h on / off	842218	96.1%

Sample	Peak area	Remaining percentage
2a -pH = -0.33	840237	
2a -pH = -0.33-1.5 h	813200	96.8%
2a -pH = -0.33-3h on / off	814736	97.0%

h) **4a** in pH = 7.46 versus pH = -0.33

Sample	Peak area	Remaining percentage
4a -pH = 7.46	1289848	
4a -pH = 7.46-1.5 h	1143545	88.7%
4a -pH = 7.46-3h on / off	1209017	93.7%

Sample	Peak area	Remaining percentage
4a -pH = -0.33	1271442	
4a -pH = -0.33-1.5 h	1157154	91.0%
4a -pH = -0.33-3h on / off	1205671	94.8%

Figure S33. HPLC-MS analysis results for the photo-stability of g) **2a** and h) **4a** under the 445 nm irradiation. The samples were either stored in the dark, or after continuously exposed for 1.5 h, or after intermittently exposed for 3 h (5s on, 5s off). The integrated peak area for **2a** and **4a**, and remaining percentage of these cycloazoarenes are shown in the tables. Conditions: **2a**, **4a** in PBS/MeCN (v/v = 2/1) pH = 7.46 or in PBS/MeCN (v/v = 2/1) pH = -0.33, conc. = 100 μ M, T = 298 K, Power density_{445 nm} = 391 mW cm⁻².

5. DFT calculation details

All geometry optimizations and frequency calculations were performed using Gaussian 09 program package.^[8] Geometry optimizations and frequency calculations in the mixture solvents (MeCN : H₂O = 1:1, volume ratio) were performed at the B3LYP(D3BJ)/def2-SVP level of theory.^[9-13] The self-consistent reaction field (SCRF) method based on the IEFPCM^[14] solvation model was adopted to evaluate the effect of solvent. The intrinsic reaction coordinate (IRC) path^[15] was traced to check the energy profiles connecting each transition state to two associated minima of the proposed mechanism. The single-point energies were computed at the ωB97M-V/def2-TZVPP/SMD(MeCN : H₂O=1:1) level of theory^[16-17] using ORCA 6.0.1 program,^[18-19] and Gibbs free energies were calculated by Shermo 2.6 program^[20] (Table S6). The theoretical pK_a value at the temperature of 298K was calculated by the following equation,^[21-22] where the conjugate base A was DBTD, **1a**, **2a**, **3a** or **4a** in this work:

$$pK_a = 0.733 \Delta G_{\text{aq}}$$

$$\Delta G_{\text{aq}} = G_{\text{gas}}(\text{A}) - G_{\text{gas}}(\text{HA}^+) + \Delta G_{\text{solv}}(\text{A}) - \Delta G_{\text{solv}}(\text{HA}^+) - 270.29$$

In the theoretical pK_a calculations, the high-accuracy single-point energies in gas phase were computed at the PWPB95(D3)/def2-QZVPP level of theory^[23] using ORCA 6.0.1 program and Gibbs free energies (G_{gas}) were also calculated by Shermo 2.6 program. And the Gibbs free energy of solvation (ΔG_{solv}) were computed at the M05-2X/6-31G*/SMD (MeCN : H₂O=1:1) level of theory^[24-25] using Gaussian 09 program.

TD-DFT calculations were performed at TD-PBE0/def2-TZVP/IEFPCM(MeCN:H₂O =1:1) level of theory.^[26] The natural transition orbitals (NTO)^[27] analysis was performed with Multiwfn3.8(dev) program^[28-29] and visualized by VMD1.9.3.^[30]

Table S6. Electronic energies (E_e), enthalpies (H) and Gibbs free energies (G) for key stationary points (in Hartree).

Structures	^a ZPE	E_e	^b H_{corr}	H	^c G_{corr}	G
<i>E</i> -DBTD	0.16996	-969.70493	0.18190	-969.52303	0.13407	-969.57086
<i>E</i> -DBTD-TS	0.16857	-969.66971	0.18033	-969.48939	0.13215	-969.53756
<i>E</i> -DBTD-H ⁺	0.18314	-970.12734	0.19518	-969.93216	0.14654	-969.98080
<i>E</i> -DBTD-H ⁺ -TS	0.18190	-970.10242	0.19369	-969.90873	0.14548	-969.95694
<i>E-1a</i>	0.15814	-985.75924	0.16996	-985.58928	0.12163	-985.63761
<i>E-1a</i> -TS	0.15686	-985.72821	0.16847	-985.55975	0.12050	-985.60771
<i>E-1a</i> -H ⁺	0.17149	-986.19256	0.18348	-986.00907	0.13489	-986.05766
<i>E-1a</i> -H ⁺ -TS	0.17031	-986.17189	0.18212	-985.98977	0.13383	-986.03806
<i>E-2a</i>	0.15820	-985.75555	0.17001	-985.58554	0.12171	-985.63384
<i>E-2a</i> -TS	0.15676	-985.72037	0.16838	-985.55199	0.12037	-985.60000
<i>E-2a</i> -H ⁺	0.17203	-986.20177	0.18395	-986.01782	0.13549	-986.06629
<i>E-2a</i> -H ⁺ -TS	0.17074	-986.16883	0.18248	-985.98635	0.13431	-986.03452
<i>E-3a</i>	0.15808	-985.63682	0.16990	-985.58852	0.12159	-985.63682
<i>E-3a</i> -TS	0.15662	-985.60380	0.16827	-985.55577	0.12024	-985.60380
<i>E-3a</i> -H ⁺	0.17175	-986.05963	0.18374	-986.01101	0.13512	-986.05963
<i>E-3a</i> -H ⁺ -TS	0.17050	-986.02906	0.18228	-985.98083	0.13404	-986.02906
<i>E-4a</i>	0.14622	-1001.81176	0.15790	-1001.65386	0.11044	-1001.70132
<i>E-4a</i> -TS	0.14465	-1001.77625	0.15622	-1001.62002	0.10823	-1001.66801
<i>E-4a</i> -H ⁺	0.15988	-1002.24727	0.17173	-1002.07554	0.12334	-1002.12393
<i>E-4a</i> -H ⁺ -TS	0.15858	-1002.21393	0.17028	-1002.04365	0.12210	-1002.09183

^a Zero-point correction energy;

^b Thermal correction to enthalpy obtained at the B3LYP(D3BJ)/def2-SVP/IEFPCM (ACN:H₂O = 1:1) level of theory;

^c Thermal correction to Gibbs free energy obtained at the B3LYP(D3BJ)/def2-SVP/IEFPCM (ACN:H₂O = 1:1) level of theory.

Cartesian coordinates of all stationary points in this work

E-DBTD

S	-0.83291400	0.00107700	0.08843200
N	0.07051500	0.06225900	-2.71447300
N	-1.12494200	0.45382900	-2.80732600
C	-1.30214600	1.70090600	-2.17925600
C	-1.11767600	1.55681900	-0.77934600
C	-1.33286100	2.67446900	0.04279900
C	-1.73754000	3.88583200	-0.52064800
C	-1.95173600	4.00064000	-1.90154000
C	-1.74828200	2.90022900	-2.73520900
C	0.13603000	-1.27922200	-2.29356300

C	-0.34052400	-1.38142000	-0.96061000
C	-0.27996000	-2.63034700	-0.32200700
C	0.25816600	-3.73005400	-0.99258100
C	0.75919300	-3.60290500	-2.29592700
C	0.71280300	-2.36916200	-2.94620800
H	-1.18784600	2.59323100	1.12259600
H	-1.89489700	4.74946200	0.12879500
H	-2.27233100	4.95310500	-2.32808800
H	-1.90100900	2.96656300	-3.81374500
H	-0.64944800	-2.73841900	0.70041900
H	0.29334700	-4.69737300	-0.48712700
H	1.18113200	-4.47055100	-2.80685900
H	1.08931700	-2.24660600	-3.96316900

E-DBTD-TS

C	1.43690200	-0.53136800	0.00493100
C	1.72799700	0.84210900	0.25232300
C	3.01992100	1.34685400	0.12184000
C	4.05154100	0.51392200	-0.32085600
C	3.77932000	-0.82867200	-0.59505600
C	2.48972700	-1.35004800	-0.42427200
C	-3.96448600	-0.66750100	-0.24241800
C	-3.97341600	0.70851700	-0.48502400
C	-2.80638600	1.46894500	-0.36118300
C	-1.60049700	0.82647000	-0.02270700
C	-1.57465700	-0.59746800	0.14203700
C	-2.76118600	-1.31925400	0.07947600
S	-0.03651700	-1.44957100	0.52905900
N	-0.37851000	1.35305500	0.09086900
N	0.64819900	1.66188000	0.70251600
H	3.19222800	2.40168200	0.34551000
H	5.05867200	0.91250400	-0.45627800
H	4.57808000	-1.48944700	-0.93878500
H	2.30304100	-2.40974000	-0.61060700
H	-4.88562400	-1.24773800	-0.32205700
H	-4.90657600	1.20769200	-0.75593100
H	-2.80795200	2.54668600	-0.52833600
H	-2.74688700	-2.40036900	0.23887200

E-DBTD-H⁺

S	-0.63496500	0.07316200	0.08997600
N	0.29410600	0.11014900	-2.75946700
N	-0.90101200	0.60607000	-3.02188400
C	-1.19893900	1.65386200	-2.23347300

C	-0.87981300	1.55561000	-0.81865500
C	-1.12368100	2.68554500	-0.00826300
C	-1.71428700	3.81528800	-0.54908000
C	-2.13671000	3.85728100	-1.90328500
C	-1.91782000	2.77959400	-2.72763400
C	0.26706000	-1.21851600	-2.26223200
C	-0.28438600	-1.30835600	-0.95836800
C	-0.37523100	-2.57455000	-0.35028800
C	0.08768300	-3.69569400	-1.03288300
C	0.66159100	-3.58217800	-2.30913300
C	0.76136700	-2.33615700	-2.92664800
H	-0.88680100	2.64908000	1.05683200
H	-1.89438500	4.67813200	0.09481700
H	-2.62716000	4.75229900	-2.28846600
H	-2.19307000	2.78785900	-3.78271500
H	-0.81342000	-2.67489600	0.64425800
H	0.00277500	-4.67699000	-0.56266300
H	1.02474500	-4.47272300	-2.82445100
H	1.19273300	-2.22006700	-3.92121500
H	0.98432500	0.73975300	-2.32376700

E-DBTD-H⁺-TS

C	1.46486300	-0.52660500	-0.41577300
C	1.71446500	0.84798600	-0.13448000
C	2.99031700	1.33581600	0.15790800
C	4.07474800	0.46155200	0.16002300
C	3.85853300	-0.89159500	-0.11291000
C	2.57207400	-1.37960600	-0.38067400
C	-3.91816500	-0.64795600	0.13506300
C	-4.00958900	0.75294900	0.08425900
C	-2.87930600	1.52036000	-0.18372300
C	-1.68228600	0.84394700	-0.46585700
C	-1.59021000	-0.58300100	-0.46931400
C	-2.70913000	-1.32308200	-0.09465100
S	-0.05337700	-1.40670100	-0.92233300
N	-0.41280800	1.27357400	-0.63139100
N	0.58093500	1.70526700	-0.04937100
H	3.11746500	2.39602100	0.38512600
H	5.07645500	0.83164900	0.38144100
H	4.69719200	-1.59044000	-0.10778200
H	2.43209900	-2.44678900	-0.56548300
H	-4.81023600	-1.23290200	0.36861500
H	-4.96479700	1.24156300	0.28166500
H	-2.90816600	2.61042000	-0.20046000

H	-2.65516800	-2.40925500	-0.00524600
H	0.57074000	2.48918900	0.63157600

E-1a

S	-0.84568500	0.00138600	0.11606100
N	0.06018600	0.02731500	-2.69696600
N	-1.12871600	0.43132700	-2.79856900
C	-1.29880700	1.68122500	-2.17515100
C	-1.11598200	1.54733100	-0.77400800
C	-1.32698400	2.67262900	0.03888200
C	-1.72402300	3.88142700	-0.53450900
C	-1.93701000	3.98614100	-1.91652200
C	-1.73963300	2.87824200	-2.74078900
C	0.11924800	-1.31089600	-2.26093100
C	-0.35747800	-1.38127100	-0.92021900
C	-0.29200200	-2.63784900	-0.30213900
C	0.25885000	-3.70736600	-1.00882500
H	-1.18433900	2.59912000	1.11951300
H	-1.87690400	4.75100900	0.10789400
H	-2.25249600	4.93674300	-2.35082100
H	-1.89196600	2.93569700	-3.81980800
H	-0.65961900	-2.77481000	0.71752400
H	0.32027500	-4.69728400	-0.55397400
C	0.74614000	-3.49533800	-2.30368300
H	1.20040800	-4.31725600	-2.86559800
N	0.68442000	-2.30826400	-2.91779500

E-1a-TS

C	1.42194700	-0.55120200	0.01606900
C	1.69876800	0.82152900	0.27531800
C	2.98109900	1.34848900	0.13107600
C	4.01279400	0.53465400	-0.34270800
C	3.75450500	-0.80932600	-0.62800600
C	2.47738200	-1.35238100	-0.43808300
C	-3.92874300	-0.64306700	-0.23591800
C	-1.61890400	0.79951600	-0.00429800
C	-1.56067200	-0.62478400	0.19761100
C	-2.75101700	-1.32871200	0.11957400
S	-0.02781800	-1.47744200	0.57691300
N	-0.41191500	1.36129700	0.12649900
N	0.61393200	1.59982300	0.76829400
H	3.14506000	2.40188500	0.36634000
H	5.01193000	0.94807900	-0.49129800
H	4.55643700	-1.45345800	-0.99478100

H	2.30165800	-2.41282800	-0.63004300
H	-4.87600700	-1.17504200	-0.33174500
H	-2.76222500	-2.40945600	0.28160800
C	-3.84690100	0.71830900	-0.50937900
H	-4.73582400	1.26748800	-0.83808900
N	-2.72222900	1.44170300	-0.38480000

E-1a-H⁺

S	-0.91197900	-0.01657700	0.08570900
N	0.00727500	0.00831300	-2.72086200
N	-1.16255200	0.47045700	-2.87043300
C	-1.29731900	1.69519600	-2.21383400
C	-1.09647700	1.53493500	-0.81243600
C	-1.29637400	2.64908700	0.01999800
C	-1.68740800	3.86753700	-0.53142000
C	-1.92383500	3.99582500	-1.91013600
C	-1.75241600	2.90297600	-2.75311700
C	0.05245000	-1.28628300	-2.25908600
C	-0.41005400	-1.39344500	-0.92419600
C	-0.31246600	-2.65118200	-0.31224100
C	0.28960500	-3.71764300	-0.98903500
H	-1.15134700	2.55780200	1.09861500
H	-1.82366300	4.72849900	0.12561100
H	-2.23904100	4.95572000	-2.32267300
H	-1.92090500	2.97551600	-3.82834300
H	-0.68848800	-2.79557500	0.70286400
H	0.38200800	-4.69422600	-0.51517500
H	1.00115800	-2.19728400	-3.81455100
H	1.28446600	-4.30932300	-2.84756400
N	0.66143300	-2.32363900	-2.85903000
C	0.79155000	-3.53132900	-2.26660900

E-1a-H⁺-TS

C	1.40281700	-0.53760700	-0.05576100
C	1.68793000	0.83869700	0.22605700
C	2.99001100	1.35365000	0.15070300
C	4.02136000	0.53701700	-0.29793000
C	3.75434900	-0.80245500	-0.61550900
C	2.47095400	-1.34101800	-0.47423600
C	-3.95157100	-0.63719400	-0.20205700
C	-1.57691600	0.79954700	0.00516000
C	-1.56117300	-0.62061100	0.22668000
C	-2.75260500	-1.30926700	0.15317700
S	-0.02368400	-1.48899900	0.49867100

N	-0.41625600	1.40036600	0.04819300
N	0.61906900	1.58769100	0.71113900
H	3.15370000	2.40240500	0.40298400
H	5.03093900	0.93652600	-0.40314700
H	4.56212900	-1.44859400	-0.96463300
H	2.30159100	-2.40046200	-0.67523900
H	-4.89026400	-1.18307900	-0.28355700
H	-2.72522300	2.38930600	-0.58137300
H	-2.76459100	-2.39005900	0.31153900
H	-4.76801200	1.27676200	-0.83677000
N	-2.73392600	1.38814100	-0.39084500
C	-3.90819700	0.69688800	-0.50457500

E-2a

S	-0.87137200	-0.00098800	0.09565600
N	0.05521200	0.05592700	-2.70829000
N	-1.13751500	0.45102000	-2.80377300
C	-1.30849700	1.70250300	-2.18167500
C	-1.12796300	1.55947600	-0.78153100
C	-1.33780200	2.67696400	0.04073600
C	-1.73103500	3.89104200	-0.52541200
C	-1.94024900	4.00591300	-1.90689100
C	-1.74357100	2.90411800	-2.74041300
C	0.11743100	-1.27823400	-2.27006100
C	-0.35174100	-1.37108200	-0.93576000
C	-0.27334600	-2.62953400	-0.32240200
C	0.28160200	-3.68883900	-1.04328000
C	0.68784000	-2.39249300	-2.88840900
H	-1.19783000	2.59495000	1.12107000
H	-1.88333700	4.75649800	0.12260200
H	-2.25185600	4.96072900	-2.33469900
H	-1.89257700	2.97079400	-3.81929500
H	-0.62635500	-2.78437900	0.69896100
H	0.34793600	-4.67592000	-0.57350100
H	1.07135400	-2.30303300	-3.91018300
N	0.75893100	-3.58251700	-2.29123000

E-2a-TS

C	1.44235800	-0.53657400	-0.01134800
C	1.72383800	0.83622700	0.24809000
C	3.01569600	1.34760900	0.13369800
C	4.05386600	0.52313300	-0.30635400
C	3.78990900	-0.81880900	-0.59337200
C	2.50214500	-1.34787500	-0.43655800

C	-3.93565200	-0.60242400	-0.21821200
C	-2.82285600	1.40507600	-0.36973400
C	-1.59279900	0.80229900	-0.02609100
C	-1.56058100	-0.61916800	0.14167700
C	-2.76248300	-1.31230500	0.09338900
S	-0.02803000	-1.48136400	0.47834000
N	-0.38475400	1.34799000	0.07979300
N	0.64107500	1.64513900	0.69972000
H	3.18085800	2.40136900	0.36695400
H	5.06039000	0.92684400	-0.42960600
H	4.59431700	-1.47337300	-0.93546000
H	2.32321600	-2.40740100	-0.63133500
H	-4.89010300	-1.13637500	-0.27120400
H	-2.84986400	2.47719700	-0.58771200
H	-2.79610100	-2.39285900	0.24859900
N	-3.95493500	0.70709100	-0.47342200

E-2a-H⁺

S	-0.84624400	-0.00917700	0.07270800
N	0.06449000	0.06301400	-2.70123000
N	-1.11708300	0.46761800	-2.84337200
C	-1.29250800	1.70820900	-2.20482000
C	-1.10053700	1.55516700	-0.80714000
C	-1.32426000	2.65516500	0.03239400
C	-1.73111700	3.87066500	-0.52068800
C	-1.94938100	3.99749600	-1.89987500
C	-1.74885900	2.90887800	-2.74816700
C	0.12735500	-1.27181400	-2.28044500
C	-0.33268100	-1.36561100	-0.93121200
C	-0.27663900	-2.62946800	-0.31025800
C	0.26215300	-3.69973700	-0.99652300
C	0.68638900	-2.36201100	-2.91178500
H	-1.18652200	2.56149200	1.11180100
H	-1.89115600	4.72707500	0.13687900
H	-2.27502300	4.95323100	-2.31438000
H	-1.90704400	2.98525900	-3.82474600
H	-0.64090700	-2.77753900	0.70668200
H	0.33877700	-4.69813100	-0.56802500
H	1.07906400	-2.32813700	-3.92714000
N	0.73074900	-3.53909500	-2.25403800
H	1.12660400	-4.34719200	-2.73456500

E-2a-H⁺-TS

C	1.42712600	-0.52986800	-0.04028600
---	------------	-------------	-------------

C	1.71343500	0.83587300	0.24309200
C	3.01141900	1.34332700	0.15294700
C	4.04308200	0.51889900	-0.29473700
C	3.77266200	-0.81802400	-0.60423400
C	2.48316400	-1.34553100	-0.46123400
C	-3.93494200	-0.64525500	-0.19822000
C	-2.79044200	1.43350300	-0.39744000
C	-1.58164100	0.83017600	-0.02986300
C	-1.55516600	-0.59990600	0.16055200
C	-2.75681500	-1.30420600	0.14213900
S	-0.04431200	-1.48109900	0.42197500
N	-0.39424800	1.39637700	0.08137500
N	0.63923700	1.62136600	0.71751600
H	3.18187700	2.39128300	0.40557800
H	5.05349800	0.91607200	-0.40326000
H	4.57596600	-1.47157100	-0.94984000
H	2.30332700	-2.40316100	-0.66443400
H	-4.89781100	-1.14602100	-0.28096700
H	-2.88166200	2.49398100	-0.62124000
H	-2.78051200	-2.38063600	0.31625000
N	-3.89856400	0.66742900	-0.48356800
H	-4.76624600	1.12464300	-0.76342800

E-3a

S	-0.90364600	-0.05057500	0.04904900
N	0.03283800	0.06488300	-2.76117500
N	-1.16579400	0.45426300	-2.82963200
C	-1.33121700	1.69452100	-2.18552000
C	-1.13316900	1.53307000	-0.78859700
C	-1.31803600	2.64459100	0.04753400
C	-1.71122300	3.86814100	-0.49863400
C	-1.94113300	3.99994400	-1.87513900
C	-1.76468900	2.90589300	-2.72390400
C	0.12186900	-1.27038800	-2.35330300
C	-0.35277600	-1.40851500	-1.01810800
C	0.24576500	-3.61850100	-0.97428200
H	-1.16151900	2.54864000	1.12446000
H	-1.84706900	4.72762700	0.16100900
H	-2.25119000	4.96196100	-2.28781900
H	-1.92628700	2.98734100	-3.80001600
H	0.25129000	-4.55753000	-0.41183900
C	0.79443300	-3.56198200	-2.26105200
H	1.24257900	-4.45137300	-2.70630100
H	1.14440000	-2.26172900	-3.97443400

C	0.74300200	-2.35693500	-2.96396200
N	-0.29883800	-2.56002900	-0.36526200

E-3a-TS

C	1.42177300	-0.53673600	-0.00642600
C	1.72296300	0.82897900	0.26716100
C	3.02257300	1.32463000	0.15547200
C	4.04620100	0.49204200	-0.29956900
C	3.76226000	-0.84302200	-0.60545700
C	2.46902300	-1.35583700	-0.45172000
C	-3.85977900	-0.67088800	-0.21120100
C	-1.58953600	0.88593500	-0.04600100
C	-1.59574700	-0.54663000	0.11793800
S	-0.06343300	-1.44426100	0.48348200
N	-0.37581000	1.40274600	0.09361500
N	0.65509600	1.64483400	0.73048900
H	3.20345800	2.37315200	0.40031000
H	5.05807200	0.88289200	-0.42077200
H	4.55727000	-1.50347100	-0.95818000
H	2.27307400	-2.40968100	-0.66035400
H	-4.74129000	-1.31576000	-0.26355200
C	-3.94604700	0.69290800	-0.48665400
H	-4.90707200	1.13587700	-0.75492600
H	-2.83954800	2.57014100	-0.59231700
N	-2.68698500	-1.26637000	0.08692400
C	-2.80444100	1.49732400	-0.40018800

E-3a-H⁺

S	-0.82631400	-0.02210600	0.06973400
N	0.05894400	0.06328100	-2.73263000
N	-1.13261000	0.45453900	-2.83325100
C	-1.30666200	1.69540000	-2.19543900
C	-1.10285700	1.54358300	-0.80054400
C	-1.31481000	2.63900700	0.04629000
C	-1.72761000	3.85537600	-0.50089100
C	-1.95835700	3.98471300	-1.87745700
C	-1.76607800	2.89826300	-2.73080700
C	0.13921000	-1.27293400	-2.32013000
C	-0.33281600	-1.35744400	-0.98365000
C	0.24137900	-3.67310000	-0.97711500
H	-1.16508600	2.54327800	1.12383900
H	-1.88133100	4.71001100	0.16034600
H	-2.28663000	4.94169000	-2.28687800
H	-1.93189000	2.97801400	-3.80591600

H	-0.62813700	-2.66537000	0.56908800
H	0.22189200	-4.58803100	-0.38629300
H	1.11393900	-2.27590700	-3.95177400
H	1.17747000	-4.48727100	-2.72249100
C	0.75821400	-3.59581600	-2.25771100
N	-0.27486500	-2.57189700	-0.38549900
C	0.72062500	-2.37192200	-2.93876500

E-3a-H⁺-TS

C	1.40583000	-0.52480000	-0.00702400
C	1.71210400	0.83583500	0.29004500
C	3.01132700	1.32841200	0.17469200
C	4.02068800	0.49341800	-0.30903300
C	3.72748600	-0.83364800	-0.63428500
C	2.43419500	-1.34955700	-0.46832800
C	-3.89132900	-0.68284300	-0.22439000
C	-1.58207500	0.86514600	-0.01565800
C	-1.54444600	-0.55560300	0.17352600
S	-0.05813900	-1.44329100	0.55103600
N	-0.37848400	1.39939400	0.10879100
N	0.63835600	1.62272000	0.77191500
H	3.20293700	2.37195100	0.43004500
H	5.03332000	0.87945500	-0.43593300
H	4.51473900	-1.49061100	-1.00883300
H	2.23544700	-2.40178700	-0.68012800
H	-4.74754400	-1.35328100	-0.25166700
H	-2.82200200	2.52921100	-0.63066100
H	-2.66937900	-2.24778200	0.26593100
H	-4.89100100	1.11541600	-0.81140100
C	-3.93952300	0.66895700	-0.52277900
C	-2.79323100	1.45973100	-0.42264300
N	-2.69684500	-1.23879200	0.10545300

E-4a

S	-0.82479200	0.00681900	0.03421200
N	0.07845700	0.06459300	-2.77859100
N	-1.11674400	0.46361600	-2.87106200
C	-1.29664000	1.70122300	-2.24526900
C	-1.10022800	1.57414200	-0.83995400
C	-1.68907300	3.76084100	-0.50204900
C	-1.97071100	3.96116100	-1.85863900
C	-1.78128800	2.90439900	-2.75134400
C	0.14634400	-1.26733800	-2.35778000
C	-0.34249900	-1.38676900	-1.02501800

C	0.20316800	-3.60954200	-0.96299600
C	0.76642200	-3.57244200	-2.24408600
C	0.74850900	-2.37122600	-2.95559300
H	-1.80369000	4.58109300	0.21348200
H	-2.31868400	4.93395700	-2.20883200
H	-1.97065400	3.01256300	-3.82067500
H	0.18056400	-4.54540500	-0.39588300
H	1.19800000	-4.47460100	-2.67984200
H	1.15946800	-2.29265200	-3.96355300
N	-0.32249400	-2.53422500	-0.36620700
N	-1.27975000	2.58734400	-0.00797800

E-4a-TS

C	1.46051800	-0.49240800	-0.05202000
C	1.72334000	0.88323700	0.22079800
C	3.03185100	1.35341200	0.14698800
C	4.03686200	0.47934200	-0.26947400
C	3.68076000	-0.83951200	-0.56104100
C	-3.84614300	-0.69087400	-0.19451500
C	-2.82404500	1.49176800	-0.38629400
C	-1.59299100	0.89146400	-0.06753000
C	-1.57718100	-0.54104300	0.08288300
S	-0.03204800	-1.44495700	0.35654900
N	-0.38847800	1.42884600	0.06878200
N	0.65113000	1.68794500	0.68219200
H	3.23674800	2.39673300	0.39568800
H	5.07040700	0.81166200	-0.37421500
H	4.43518000	-1.55313500	-0.90759000
H	-4.72075100	-1.34606000	-0.23344900
H	-2.87541400	2.56577300	-0.56802300
N	-2.66112500	-1.27398600	0.07062800
N	2.43340400	-1.30901300	-0.43332800
C	-3.95665200	0.67527700	-0.45491000
H	-4.92909300	1.10805700	-0.69693900

E-4a-H⁺

S	-0.91823500	-0.02547600	0.03103600
N	0.03482200	0.06064100	-2.79591000
N	-1.16197200	0.44885200	-2.84864100
C	-1.33373000	1.68878400	-2.21982500
C	-1.13968700	1.51423600	-0.82420100
C	-1.68690500	3.81324800	-0.50715800
C	-1.93957400	3.98606500	-1.85622900
C	-1.77440200	2.90313000	-2.72963300

C	0.11867500	-1.26957900	-2.37642500
C	-0.36756800	-1.39755900	-1.04847600
C	0.22809300	-3.59712500	-0.95253000
C	0.79002200	-3.55755500	-2.23537600
C	0.74951100	-2.36694100	-2.96055800
H	-1.77939800	4.60810100	0.23204400
H	-2.25199700	4.96297800	-2.22313000
H	-1.95784300	3.00562700	-3.80014600
H	0.22470200	-4.52500600	-0.37373400
H	1.24332600	-4.45358800	-2.66105500
H	1.16182700	-2.28962900	-3.96764500
N	-0.31848100	-2.52405000	-0.37076100
N	-1.30609300	2.60375000	-0.03710800
H	-1.14778900	2.51143600	0.96865100

E-4a-H⁺-TS

C	1.44986500	-0.47575600	-0.05963300
C	1.71586800	0.89216400	0.23736700
C	3.02836300	1.35392400	0.16400800
C	4.01886600	0.47532400	-0.27586800
C	3.65340900	-0.83641600	-0.58820000
C	-3.88967100	-0.68249400	-0.20024100
C	-2.80942300	1.46613600	-0.40813100
C	-1.58625000	0.87435700	-0.03544200
C	-1.53305000	-0.54792000	0.13451400
S	-0.03408600	-1.45366600	0.39289400
N	-0.39034900	1.42344800	0.08992600
N	0.63907700	1.66880900	0.72025000
H	3.24636800	2.39130200	0.42433100
H	5.05433800	0.80032600	-0.38194000
H	4.39644300	-1.55019100	-0.95541000
H	-4.74401200	-1.35603200	-0.20717600
H	-2.84727700	2.53697200	-0.60770600
N	-2.68634900	-1.23541100	0.09703200
N	2.40153900	-1.29659700	-0.45025400
C	-3.95336700	0.67057500	-0.49027800
H	-4.91373600	1.11344400	-0.75349700
H	-2.65355400	-2.24473800	0.25484700

Z-1a-H⁺ + 2H₂O

S	0.77157500	-1.60719300	1.18508500
N	-0.48216100	1.29715500	0.93837500
N	0.73648200	1.57028000	0.87573000
C	-0.73802800	-1.15005600	0.37097700

C	-1.12522800	0.19563600	0.32560500
C	-3.12795100	-0.37852800	-0.78681600
H	-4.04781400	0.00601300	-1.22879000
C	-2.79902600	-1.72910000	-0.76382000
H	-3.47797900	-2.46243300	-1.19822600
C	-1.59209900	-2.11419300	-0.18220300
H	-1.29615200	-3.16445000	-0.15683000
C	1.86197300	-0.57908100	0.21122000
C	1.72236800	0.82944700	0.20244100
C	2.69436500	1.61576900	-0.44474600
H	2.58828900	2.70076300	-0.40340400
C	3.74653700	1.01492700	-1.12969500
H	4.48012400	1.63367200	-1.64922000
C	3.87478500	-0.37766800	-1.12392100
H	4.71302200	-0.85412900	-1.63592500
C	2.94261500	-1.16955900	-0.44541900
H	3.05264500	-2.25485600	-0.41860900
N	-2.30469600	0.52683600	-0.24371700

E-1a-H⁺ + 2H₂O

S	-0.94353800	-0.00236100	0.22164100
N	-0.16281100	0.00803400	-2.65252000
N	-1.35094400	0.45199700	-2.69333800
C	-1.44002200	1.69366000	-2.05848500
C	-1.15659400	1.54775500	-0.66987600
C	-1.29061400	2.67410500	0.15937100
C	-1.70007100	3.89062900	-0.38290300
C	-2.01698400	4.00469200	-1.74626600
C	-1.90986300	2.89971300	-2.58556000
C	-0.09567300	-1.28930900	-2.16720000
C	-0.50725100	-1.38031800	-0.81714200
C	-0.39637900	-2.64316300	-0.20791200
C	0.16222600	-3.70931900	-0.91304600
H	-1.07838100	2.59354200	1.22765100
H	-1.78498900	4.76169100	0.26942000
H	-2.34362100	4.96384200	-2.15172100
H	-2.14114500	2.96285400	-3.64959400
H	-0.73081300	-2.78544200	0.82191500
H	0.25988700	-4.69025400	-0.44871800
H	0.87230100	-2.11659600	-3.80562100
H	1.09788000	-4.29803000	-2.80414700
N	0.48865300	-2.31539200	-2.79835700

Z-3a-H⁺ + 2H₂O

S	-0.08251000	-1.04322200	1.51620900
N	-0.59476800	1.97333500	0.76271000
N	0.65229500	1.94001000	0.77967000
C	-1.35778500	-0.39517400	0.47380800
C	-1.43666300	0.97846700	0.19918200
C	-2.51451700	1.44059100	-0.57293600
H	-2.60282500	2.51348300	-0.75307600
C	-3.45123000	0.54313200	-1.08065600
H	-4.28808400	0.88278700	-1.69014000
C	-3.31559700	-0.80544700	-0.77788500
H	-4.00858300	-1.57275300	-1.12469300
C	1.26784200	-0.48059900	0.48438700
C	1.45546500	0.89867200	0.25294100
C	2.58415900	1.31944500	-0.47074000
H	2.73704300	2.39071600	-0.61082100
C	3.47243900	0.38558400	-0.99903500
H	4.33412500	0.72493800	-1.57673300
C	3.27308100	-0.98037900	-0.77058500
H	3.97856100	-1.71361300	-1.16579300
C	2.17453900	-1.41330900	-0.02403600
H	2.01143100	-2.47492500	0.16634400
N	-2.29059100	-1.22840600	-0.02027100

E-3a-H⁺ + 2H₂O

S	-0.35467500	0.03259000	0.08681700
N	-0.13099800	-0.04041000	-2.84880300
N	-1.31500900	0.35597900	-2.69026600
C	-1.34423600	1.63115500	-2.09779300
C	-0.83175400	1.55235200	-0.77869800
C	-0.85332200	2.69422300	0.03252100
C	-1.38489300	3.88260100	-0.47179900
C	-1.91937000	3.93956900	-1.76641700
C	-1.91731200	2.80730400	-2.58098700
C	0.03997800	-1.35459200	-2.39396000
C	-0.12046700	-1.37481000	-0.98523400
C	0.42493800	-3.67289700	-0.97542900
H	-0.46473500	2.65488900	1.05250300
H	-1.39097900	4.77244100	0.16030200
H	-2.33654100	4.87534200	-2.14275500
H	-2.32118200	2.83037800	-3.59401700
H	-0.08804100	-2.57877600	0.73966600
H	0.53109200	-4.55862800	-0.34874700
H	0.62200700	-2.45757900	-4.14722600

H	0.95074700	-4.59931000	-2.84083700
C	0.64821800	-3.67763800	-2.34493600
N	0.06240300	-2.54322300	-0.33965400

Z-4a-H⁺ + 2H₂O

S	-0.14064500	-1.11814100	1.51249100
N	-0.62664100	1.93302400	0.84563600
N	0.61925100	1.88414000	0.88338300
C	-1.37356400	-0.41773000	0.45233300
C	-1.45629100	0.96399700	0.22677100
C	-2.51233900	1.44654700	-0.56378100
H	-2.60838100	2.52437000	-0.70624000
C	-3.41188600	0.55704900	-1.14543100
H	-4.22883800	0.91018500	-1.77397000
C	-3.26226300	-0.80392800	-0.90247800
H	-3.92350900	-1.56280500	-1.32226700
C	1.22302600	-0.52782700	0.49901400
C	1.41036200	0.85664800	0.31396700
C	2.55129900	1.26130300	-0.39699400
H	2.74520500	2.32817100	-0.52048800
C	3.39971300	0.29593200	-0.92978500
H	4.28352700	0.57970300	-1.50215600
C	3.10640800	-1.05240400	-0.70820200
H	3.74437600	-1.84395100	-1.10958900
N	-2.26632300	-1.24553200	-0.11983200
N	2.04110000	-1.44324800	0.00085800
H	-2.09743800	-2.33324000	-0.00733800

E-4a-H⁺ + 2H₂O

S	-1.29395700	-0.09597600	-0.06450800
N	0.14847700	0.10332400	-2.67038300
N	-1.00334000	0.55547200	-2.90644700
C	-1.22951800	1.76639000	-2.23789700
C	-1.29110200	1.51327000	-0.84401000
C	-1.78153300	3.79138400	-0.46878800
C	-1.78834100	4.06526400	-1.82922500
C	-1.51998000	3.03233300	-2.73415600
C	0.10503700	-1.25115400	-2.32686300
C	-0.60856400	-1.42877700	-1.11236900
C	-0.11518600	-3.65599200	-1.05294700
C	0.66066800	-3.57213500	-2.21638200
C	0.78785100	-2.34241100	-2.86214100
H	-1.96547300	4.54775500	0.29463100
H	-1.98955900	5.07843000	-2.17571200

H	-1.50595000	3.20908400	-3.81058300
H	-0.24948200	-4.61307200	-0.54085200
H	1.14933700	-4.46302300	-2.61276400
H	1.37199100	-2.22778700	-3.77643900
N	-0.71660600	-2.59333100	-0.50751500
N	-1.54624800	2.54515200	-0.01780700
H	-1.56517100	2.36915700	1.05976300

6. References

- [1] Paudler, W. W., Zeiler, A. G., Diazocine Chemistry. VI. An Inquiry into the Aromaticity of 5,6-Dihydridobenzo[b,f] [1,2] diazocine, *J. Org. Chem.* 1969, **43**, 3237.
- [2] W. Moormann, D. Langbehn, R. Herges, Solvent-Free Synthesis of Diazocine, *Synthesis*. 2017, **49**, 3471–3475.
- [3] M. Sacerdoti, V. Bertolasi, V. Ferretti and C. A. Accorsi, *Zeitschrift für Kristallographie-Crystalline Materials*, 1990, **192**, 111-118.
- [4] M. Jang, T. Lim, B. Y. Park, and M. S. Han, Metal-Free, Rapid, and Highly Chemoselective Reduction of Aromatic Nitro Compounds at Room Temperature, *J. Org. Chem.*, 2022, **87**, 910–919.
- [5] M. F. G. Stevens, D. Shi and A. Castro, Antitumour benzothiazoles. Part 2.¹ Formation of 2,2'-diaminobiphenyls from the decomposition of 2-(4-azido-phenyl)benzazoles in trifluoromethanesulfonic acid, *J. Chem. Soc., Perkin Transactions I.*, 1996, 83-93.
- [6] F. A. Bottino, A. Marno and A. Recca and J. Brady, A. C. Street and P. T. McGrail, Synthesis and characterization of pendantly amine functionalized poly (arylene ether sulfone), *POLYMER*., 1993, **34**, 2901-2902.
- [7] S. Zhang, G. Chen, Y. Wang, Q. Wang, Y. Zhong, X. Yang, Z. Li, and H. Li, Far-Red Fluorescent Probe for Imaging of Vicinal Dithiol-Containing Proteins in Living Cells Based on a pK_a Shift Mechanism, *Anal. Chem.*, 2018, **90**, 2946–2953.
- [8] M. J. Frisch, G. W. Trucks, H. B. Schlegel, G. E. Scuseria, M. A. Robb, J. R. Cheeseman, G. Scalmani, V. Barone, B. Mennucci, G. A. Petersson, H. Nakatsuji, M. Caricato, X. Li, H. P. Hratchian, A. F. Izmaylov, J. Bloino, G. Zheng, J. L. Sonnenberg, M. Hada, M. Ehara, K. Toyota, R. Fukuda, J. Hasegawa, M. Ishida, T. Nakajima, Y. Honda, O. Kitao, H. Nakai, T. Vreven, J. A. Montgomery, J. J. E. Peralta, F. Ogliaro, M. Bearpark, J. J. Heyd, E. Brothers, K. N. Kudin, V. N. Taroverov, T. Keith, R. Kobayashi, J. Normand, K. Raghavachari, A. Rendell, J. C. Burant, S. S. Iyengar, J. Tomasi, M. Cossi, N. Rega, J. M. Millam, M. Klene, J. E. Knox, J. B. Cross, V. Bakken, C. Adamo, J. Jaramillo, R. Gomperts, R. E. Stratmann, O. Yazyev, A. J. Austin, R. Cammi, C. Pomelli, J. W. Ochterski, R. L. Martin, K. Morokuma, V. G. Zakrzewski, G. A. Voth, P. Salvador, J. J. Dannenberg, S. Dapprich, A. D. Daniels, O. Farkas, J. B. Foresman, J. V. Ortiz, J. Cioslowski, D. J. Fox. Gaussian 09 (Revision D.01) I. *Gaussian*, Wallingford, CT, 2013.
- [9] P. J. Stephens, F. J. Devlin, C. F. Chabalowski, M. J. Frisch, Ab Initio Calculation of Vibrational Absorption and Circular Dichroism Spectra Using Density Functional Force Fields. *J. Phys. Chem.* 1994, **98**, 11623–11627.
- [10] F. Weigend and R. Ahlrichs, Balanced basis sets of split valence, triple zeta valence and quadruple zeta valence quality for H to Rn: Design and assessment of accuracy. *Phys. Chem. Chem.*

- Phys.* 2005, **7**, 3297–3305.
- [11] F. Weigend, Accurate Coulomb-fitting basis sets for H to Rn. *Phys. Chem. Chem. Phys.* 2006, **8**, 1057–1065.
- [12] S. Grimmea, J. Antony, S. Ehrlich, and H. Krieg, A consistent and accurate ab initio parametrization of density functional dispersion correction (DFT-D) for the 94 elements H-Pu. *J. Chem. Phys.* 2010, **132**, 154104.
- [13] S. Grimme, S. Ehrlich, L. Goerigk, Effect of the Damping Function in Dispersion Corrected Density Functional Theory. *J. Comput. Chem.* 2011, **32**, 1456–1465.
- [14] G. Scalmani and M. J. Frisch, Continuous surface charge polarizable continuum models of solvation. I. General formalism. *J. Chem. Phys.* 2010, **132**, 114110.
- [15] C. Gonzalez, H. B. Schlegel, An improved algorithm for reaction path following. *J. Chem. Phys.* 1989, **90**, 2154–2161.
- [16] N. Mardirossian and M. Head-Gordon, ω B97M-V: A combinatorially optimized, range-separated hybrid, meta-GGA density functional with VV10 nonlocal correlation. *J. Chem. Phys.* 2016, **144**, 214110.
- [17] A. V. Marenich, C. J. Cramer, and D. G. Truhlar, Universal solvation model based on solute electron density and on a continuum model of the solvent defined by the bulk dielectric constant and atomic surface tensions. *J. Phys. Chem. B.* 2009, **113**, 6378–6396.
- [18] F. Neese, The ORCA program system. *WIREs Comput. Mol. Sci.* 2012, **2**, 73–78.
- [19] F. Neese, Software update: The ORCA program system—Version 5.0. *WIREs Comput. Mol. Sci.* 2022, **12**, e1606.
- [20] Tian Lu, Qinxue Chen, Shermo: A general code for calculating molecular thermochemistry properties, *Comput. Theor. Chem.* 2021, **1200**, 113249.
- [21] M. D. Liptak and G. C. Shields, Accurate pKa Calculations for Carboxylic Acids Using Complete Basis Set and Gaussian-n Models Combined with CPCM Continuum Solvation Methods. *J. Am. Chem. Soc.* 2001, **123**, 7314–7319.
- [22] C. C. R. Sutton, G. V. Franks, and G. da Silva, First Principles pKa Calculations on Carboxylic Acids Using the SMD Solvation Model: Effect of Thermodynamic Cycle, Model Chemistry, and Explicit Solvent Molecules. *J. Phys. Chem. B* 2012, **116**, 11999–12006.
- [23] L. Goerigk and S. Grimme, Efficient and Accurate Double-Hybrid-Meta-GGA Density Functionals—Evaluation with the Extended GMTKN30 Database for General Main Group Thermochemistry, Kinetics, and Noncovalent Interactions. *J. Chem. Theory Comput.* 2011, **7**, 291–309.
- [24] Y. Zhao, N. E. Schultz, and D. G. Truhlar, Design of density functionals by combining the

- method of constraint satisfaction with parametrization for thermochemistry, thermochemical kinetics, and noncovalent interactions. *J. Chem. Theory and Comput.* 2006, **2**, 364–382.
- [25] M. M. Frantl, W. J. Pietro, W. J. Hehre, J. S. Binkley, D. J. DeFrees, J. A. Pople, and M. S. Gordon, Self-Consistent Molecular Orbital Methods. 23. A polarization-type basis set for 2nd-row elements. *J. Chem. Phys.* 1982, **77**, 3654–3665.
- [26] C. Adamo, V. Barone, Toward Reliable Density Functional Methods Without Adjustable Parameters: The PBE0 Model. *J. Chem. Phys.* 1999, **110**, 6158–6170.
- [27] R. L. Martin. Natural transition orbitals. *J. Chem. Phys.* 2003, **118**, 4775.
- [28] T. Lu, F. Chen. Multiwfn: A multifunctional wavefunction analyzer. *J. Comput. Chem.* 2012, **33**, 580–592.
- [29] T. Lu. A comprehensive electron wavefunction analysis toolbox for chemists, Multiwfn. *J. Chem. Phys.* 2024, **161**, 082503.
- [30] W. Humphrey, A. Dalke, K. Schulten. VMD: Visual molecular dynamics. *Journal of molecular graphics*. 1996, **14**, 33–38.